Reviews in Mineralogy & Geochemistry
Vol. 88 pp. 1–118, 2022

A Review of the Geology of Global Diamond Mines and Deposits

Bruce A. Kjarsgaard
Geological Survey of Canada
Natural Resources Canada
Ottawa, Ontario, K1A0E8
Canada
bruce.kjarsgaard@NRCan-RNCan.gc.ca

Mike de Wit
Department of Earth Sciences
Stellenbosch Unviversity
Stellenbosch
South Africa
dewit@icon.co.za

Larry M. Heaman, D. Graham Pearson
Department of Earth and Atmospheric Sciences
University of Alberta
Edmonton, Alberta
T6G 2E3
Canada
gdpearso@ualberta.ca

Johann Stiefenhofer
Anglo American
Johannesburg
South Africa
Johann.Stiefenhofer@angloamerican.com

Nicole Janusczcak
BHP
Toronto, Ontario
Canada
nicole.januszczak@bhp.com

Steven B. Shirey
Earth and Planets Laboratory
Carnegie Institution for Science
5241 Broad Branch Road NW
Washington DC 20015, U.S.A.
sshirey@carnegiescience.edu

1529-6466/22/0088-0001$15.00 (print)
1943-2666/22/0088-0001$15.00 (online)
http://dx.doi.org/10.2138/rmg.2022.88.01

INTRODUCTION

Diamond is not a common rock-forming mineral (an exception being "diamondite"; see Jacob and Mikhail 2022, this volume) nor a common crustal mineral (the exceptions being "UHP diamonds"; see Dobrzhinetskaya et al. 2022, this volume); it is a scarce or minor mantle mineral whose rarity belies its importance in understanding mantle geochemistry and dynamics, as the numerous chapters in this volume attest. A complete understanding of natural diamond formation and the mantle geology it reveals, starts with an understanding of the magmas that deliver diamonds many hundreds of kilometers upward from the mantle to the upper crust. There, at Earth's surface, diamonds are found in primary magmatic deposits of kimberlite and olivine lamproite, or secondary deposits weathered from these primary sources. The goal of this chapter is to summarise the important geological aspects of primary and secondary diamond deposits found at the Earth's surface.

This chapter covers both primary and secondary diamond deposits because both have played an important role in the science of diamond geology, and in the gem diamond trade. A significant scientific research focus since the 1980's has been on lithospheric diamonds, sourced from kimberlite mines; however, some of the first and most important discoveries of sublithospheric diamonds were made from the alluvial diamond fields of Australia (Ororoo), Brazil (Juina) and West Africa (Kan Kan) as described in Stachel et al. (2022, this volume). Africa, where the beneficiation of both primary and secondary diamond deposits has been substantial, provides a ready comparison of the importance of both of these types of deposit. Since the discovery of diamonds in Africa in 1854 until the end of 2019, Africa has produced almost 3.6 billion carats (Bct) of diamonds out of a total global production of some 5.9 Bct (updated from de Wit et al. 2016). Of the 3.6 Bct African production it is estimated that 1.3 Bct have been mined out of placer and paleo-placer (including marine) deposits, which represents 22% of total global production. With the combined production of placers and paleo-placers from South America, India, Australia and Siberia it is estimated that close to 1.5 Bct (or just over 25% of the global production), have come from these deposits. Furthermore, these diamonds are typically better quality having survived erosion from a primary source, subsequent transport and deposition and hence are of higher carat value.

Despite the importance of alluvial diamonds produced with respect to total diamond production in terms of their values, the alluvial deposits themselves have little to teach us directly about the mantle aside from providing isolated diamond research specimens. In this respect, an overview of the magmas that host primary diamond deposits, with specific aspects such as geochemistry, mineralogy, and age of these rocks, along with diamond grade and value data is provided herein for four important reasons.

First, kimberlites, carbonate-rich olivine lamproites (CROL—see *Magmatic Source Rocks: General Background and Historical Perspectives*) and olivine lamproites (see Table 1 for the mineralogy of these three rock types) are samples of magmas and their fluids moving through the lithospheric mantle precisely where the vast majority (>90%) of all diamonds have formed. While the nature of diamonds as xenocrysts imply that they are typically derived from an older generation of melt/fluid than their magmatic host rocks, they also bear some broad similarities to younger generations of diamond-forming fluids. In the case of fibrous diamonds (Harris et al. 2022, this volume), epitaxial overgrowth of a second generation of diamond suggests some kimberlites (or kimberlite-related melts), are diamond-forming magmas.

Second, as most kimberlites are diamond-poor or are barren of diamonds, with only ~1% proving to be economic, understanding the key aspects of the magmatic host rock–diamond relationship and the geological occurrences of these deep-seated magmas are critical factors in establishing that newly discovered kimberlites, CROLs, or olivine lamproites contain sufficient quantities of diamonds of a size and quality that permits economically viable mining.

Table 1. Mineralogy of kimberlite, carbonate-rich olivine lamproite (CROL), and olivine lamproite.

Minerals present	Kimberlite	Carbonate-rich olivine lamproite (CROL)	Olivine lamproite
Megacryst suite (> 1 cm)	Common to absent	Absent, rare	Absent, ?very rare?
	Cognate and antecryst minerals		
Olivine	Common to absent	Rare to absent	Rare to absent
Phlogopite	Minor to absent	Common to minor	Common, minor, rare
Spinel	Common to rare (spinel cores)	Minor to absent (spinel cores)	Minor to absent (spinel cores)
Diopside	Absent	Rare to absent	Rare to absent (Minor)
	Phenocryst /Microphenocrysts (0.2–1.0 mm)		
Olivine phenocrysts	Common	Common	Common
Olivine microphenocrysts	Common	Minor to rare	Minor to rare
Phlogopite phenocrysts	Minor, rare, absent	Common	Common
Phlogopite microphenocrysts	Minor, rare (poikilitic)	Common	Common (poikilitic)
Spinel phenocrysts	Common to minor	Minor to rare	Minor to rare
Diopside microphenocrysts	Absent	Variable: Common to absent	Minor to absent
	Groundmass (<0.2 mm)		
Olivine	Common	Minor to rare	Rare, absent
Phlogopite	Common, laths (poikilitic)	Common (poikilitic)	Common (poikilitic)
Spinel	Common to minor	Minor to rare	Minor to rare
Glass	Absent, exceptionally rare?	Absent (not reported)	Common, minor, rare
Apatite	Common to rare	Common to minor	Minor to rare
Perovskite	Common to minor, rare	Minor to rare	Minor to rare
Carbonate (calcite, dolomite)	Common to minor	Common to minor	Rare, absent
Monticellite	Common to absent	Absent, very rare	Absent
Diopside	Absent	Variable: Minor to absent	Rare to absent
Leucite	Absent	Rare to absent	Minor to rare
Sanidine—K Feldspar	Absent	Rare to absent	Rare to absent
Ti-K-richterite	Absent	Rare to absent	Minor to rare
Ilmenite	Minor, rare to absent	Minor to rare	Rare to absent
Zr-silicates	Rare to absent	Rare to absent	Rare to absent
Hollandite, priderite	Rare to absent	Rare to absent	Rare to absent
Brucite	Rare to absent	Absent	Absent
Periclase	Rare to absent	Absent	Absent

Minerals present	Kimberlite	Carbonate-rich olivine lamproite (CROL)	Olivine lamproite
		Mineral chemistry zoning trends	
Spinel	Trend 1; Trend 2; Trend 1–2; Trend 3	Trend 2; Trend 1–2	Trend 2
Phlogopite	Phlogopite–eastonite; phlogopite–tetraferri-phlogopite	Phlogopite–tetrafer-riphlogopite; phlogopite–Al-poor phlogopite	Phlogopite–Al-poor phlogopite; Al-poor phlogopite–tetraferriphlogopite
		Alteration	
Serpentine	Common to rare	Common to rare	Common to minor
Talc	Rare	Rare	Common to minor
Calcite, dolomite	Common to absent	Common to absent	Rare to absent
Magnetite	Common to absent	Common to absent	Rare to absent
Diopside	Common to absent		

Third, kimberlites, CROLs and olivine lamproites are the dominant magma types that actually deliver the deepest-derived samples of mantle lithologies in the form of xenoliths of peridotite and eclogite. The geologic history of these samples, and studies of diamondiferous xenoliths and diamond inclusions, has become essential knowledge in understanding how diamonds, especially lithospheric diamonds, form.

Fourth, kimberlite-derived diamonds are known to contain sublithospheric mantle mineral inclusions. These mineral inclusions and the kimberlite magmas that carry them inform us about the deep Earth, such as when and how deep slabs devolatilize, how these deep supercritical fluids react with mantle lithologies, what is the nature of this fugitive mantle fluid reservoir, and what is the relationship to mantle convection. There is a substantive quantity of literature on this currently active field of research and the reader is directed to early work (e.g., Sobolev 1977; Nixon 1987), and chapters in the *Treatise on Geochemistry* (Pearson et al. 2003, 2018; Pearson and Wittig 2014), as well as the chapters in this volume and references therein.

Brief historical overview of the key diamond discoveries

There have been numerous descriptions of the history of diamond discovery and mining, from its inception to present day and we shall not attempt to replicate this history. The interested reader is referred to reviews by Balfour (1987), Kirkley et al. (1992), Harlow (1998), Erlich and Hausel (2002) and Wilson et al. (2007a).

The first known mining of diamonds on an economic scale occurred in the Indian alluvial deposits, in the region of the Godavari and Krishna rivers, exploited since ~ 2000 B.C., but first described in western literature by Gaveia de Orta in 1565 and later by Tavernier in 1676 (cited in Balfour 1987). For over 2000 years, the main recognised source of the world's diamonds was from India. The second significant discovery of diamonds that led to economic mining occurred in Brazil in 1725 when Bernardo Francisco Lobo purchased diamonds from locals, prompting a "rush" to exploit alluvial diamonds that established the city now known as Diamantina (Erlich and Hausel 2002). This discovery was followed, in 1844, by the discovery of rich alluvial deposits in Bahia State (Brazil).

The subsequent identification of diamonds in South Africa led to a third global source of diamonds. The first diamond discovery in South Africa, which prompted the exploration rush that ultimately led to the finding of diamond in a primary source rock, took place in 1866 or 1867 when a diamond was discovered on the banks of the Orange River at the farm "De Kalk"

(Janse 1995). After numerous other diamond finds, including an 83.5 carat (ct) alluvial stone in 1869, a 50 ct diamond was extracted by a farmer named De Klerk from what was to be recognised as the Jagersfontein kimberlite pipe (Wilson et al. 2007a). This discovery is usually credited as the first diamond find from a "primary" deposit, although it is now evident that diamonds had been mined in India well before that time, from what was later recognised as the Majhgawan olivine lamproite (Wilson et al. 2007a). Discoveries of primary diamond deposits in South Africa that became major mines include Jagersfontein (1869 or 1870) Dutoitspan and Bultfontein (1869), Koffiefontein (1870), De Beers and Kimberley (1871), Wesselton (1890), and Cullinan (aka, also known as, Premier) in 1903, Letšeng-la-Terai (1957), Finsch, (1963) and lastly Venetia (1979), as documented by Janse (1995) and Wilson et al. (2007a).

Following these initial discoveries, mainly in the 1800s, large scale commercial diamond mining was slow to develop in other areas of the world. A detailed broader history of the development of diamond mining across Africa is given by Janse (1995, 1996) who noted the inception of alluvial mining in Zaire (now the Democratic Republic of Congo, DRC) in 1903 and the Mbuji Mayi area in 1918, and in Angola in 1912. The Colossus kimberlite was discovered in Zimbabwe in 1907, along with the richly diamondiferous kimberlites at Mbuji Mayi (DRC) in 1946, and many diamondiferous kimberlites in the Lunda Norte region of Angola in 1952, with the Catoca kimberlite discovered in 1985 (Janse 1996, 2007). Key discoveries elsewhere in Africa include the Mwadui (Williamson) diamond mine in Tanzania, discovered in 1940, and the Koidu area kimberlites in Sierra Leone in 1948 (Janse 1996).

Though diamonds had been reported in Russia since 1829 from the Ural Mountains, mining primary deposits on a large scale only commenced following the discovery of Siberian (southern Yakutia) kimberlites by Larisa Popugayeva in 1954—a discovery that was to lead to the establishment of the major diamond mines of Mir (1954) and its associated placers (1957); Sytykanskaya (1955); Udachnaya (1957), 23rd Party Congress (1959); Aikhal (1960); Internationalaya (1969) and Jubileinaya (1975), establishing Russia as the world's largest producer for a time (Janse 2007).

In global terms, three other highly significant discoveries of diamonds are of note. Firstly, exploration by De Beers in the Kalahari desert led to the discovery, in 1967, of the vast Orapa kimberlite in Botswana, followed in 1972 by the discovery of the Jwaneng kimberlite (Brook 2012). The development of these two kimberlite-hosted diamond mines alone placed Botswana as the world's leading diamond producer for the decades that followed, with other significant developments being the opening of the Letlhakane, Damtshaa, Lerala mines and Karowe mines (Janse 1995, 1996, 2007; Brook 2012), and more recently the Ghaghoo mine (2014–2017).

Although alluvial diamonds had been found in Australia in 1861, and small-scale extraction from placers occurred in the Copeton area of New South Wales since 1884, large scale production from a primary deposit commenced only with the discovery in 1979 of the richly diamondiferous Argyle olivine lamproite pipe, whose exploration and discovery history is documented by Smith et al. (2018).

The establishment of large-scale commercial diamond mining in North America took much longer. Despite diamonds being found in the eastern USA in the 1840s and in glacial tills in the Great Lakes region since 1876 (Kjarsgaard and Levinson 2002), exploration success was slow to materialise. The Prairie Creek (Arkansas, USA) olivine lamproite was discovered in 1906, although it did not prove to be economic. However, the discovery of diamondiferous kimberlite in the Lac de Gras region of the Northwest Territories in 1990 (Kjarsgaard and Levinson 2002) led to one of the greatest staking rushes in Canadian history and the commencement of large-scale diamond mining at the Ekati Mine in 1998 and Diavik Mine in 2002 (Kjarsgaard and Levinson 2002; Janse 2007).

Classification of mined diamond deposits

Primary magmatic deposits classified by rock type. Three rock types host primary magmatic diamond mines and include kimberlite, olivine lamproite, and carbonate-rich olivine lamproite (CROL; formerly termed micaceous kimberlite, or Group II kimberlite, or orangeite). The mineralogy of these rocks types are defined in Table 1, and described in more detail in this Chapter. Kimberlites occur on stable cratonic continental crust; there are no known kimberlites on oceanic crust or young orogenic belts (Fig. 1). These deep-seated magmas are derived from hundreds of kilometers beneath Earth's surface and due to their affinity with thick continental lithospheric mantle are intimately associated with cratons. Olivine lamproite and carbonate-rich olivine lamproite also occur on stable cratonic continental crust (Fig. 2). All primary magmatic-hosted diamond mines are intimately associated with cratons. Cratons, as defined by Pearson et al. (2021) have thick lithospheric roots (>150 km) and have not been disturbed tectonically since ~1 Ga.

Secondary diamond deposits classified by geologic setting and age. Three categories of placer diamond deposits have been recognised: retained placers, transient placers, and terminal placers (Bluck et al. 2005). These three different types of placer deposits are decribed in more detail in *Review of Secondary Global Diamond Deposits.*

Tiered classification system of primary magmatic-hosted diamond mines

Diamonds mined in primary magmatic source rocks are found in magmatic rocks classified as kimberlite, olivine lamproite and carbonate-rich olivine lamproite (previously referred to as micaceous kimberlite, or Group II kimberlites, or orangeites)—see Table 1 for details. Diamonds in these rocks occur as sparsely dispersed diamond xenocrysts, both micro- and macro-diamonds. A macrodiamond is defined (using Canadian National Instrument 43-101 reporting standards) as diamonds that do not pass through a 0.85 mm square mesh screen. However, it is also relevant to include a definition of the term "macrodiamond", which from a diamond sale point of view includes diamonds that do not pass through a +1 Diamond Trading Company (DTC) screen, which has a round aperture of 1.092 mm.

In total, there are globally ~7,000 known occurrences of these three rock types, dominantly kimberlite (~6,500; Giuliani and Pearson 2019), with subordinate numbers of olivine lamproite (Bergman 1987) and carbonate-rich olivine lamproite (Skinner 1989). However, only ~1000 kimberlites (~15%) contain macrodiamonds (de Wit et al. 2016), and are of potential economic interest. A similar (or lower) percentage of macrodiamond bearing olivine lamproites are also known. In contrast, from the available data, if taken as representative, it appears that significantly more than 15% of CROL are macrodiamond-bearing, given the high number of macrodiamond-bearing CROL in southern Africa (Table 2). In total, there are < 100 producing or past producing diamond mines globally (Table 2)—an amazingly small number that has supplied humanity's demand for diamonds.

Key parameters of global diamond mines include diamond grade (carat/tonne), diamond value (US$/carat), mine size (hectare), and ore value (US$/tonne), as listed in Table 2. Together these parameters can be utilized to determine the potential value and economic viability of the deposit. Note that carats per hundred tonnes (cpht) is also widely used as diamond deposit grades are often less than 1 carat per tonne (Table 2) As noted by Field et al. (2008), these four key parameters do not define "large" versus "small" mines. Instead, the key features that define the "scale" of a mine are the rate of diamond production (carats per year) and the lifespan of the mining operation, the latter not necessarily being directly related to size (area) and/or tonnes of contained ore. Simply stated, the economic viability of a diamond mine, or any mine for that matter, requires that the value of the ore (US$/tonne) needs to exceed the mining, processing and other affiliated costs, while factoring in the initial capital outlay of the project. A number of these costs are a strong function of the geographic location of the mine and the available infrastructure. For instance, the exploration and operating costs for diamond mines in southern

African, northern Russian or Canadian diamond deposits vary greatly. de Wit et al. (2016) refined the "size" concept of diamond mines of Field et al. (2008), introducing a four-Tier diamond mine classification system. In their definition, diamond mines are characterized by their yearly carat production, as well as the in-situ value of diamonds produced over the life of the mine. Here, we further modify the "Tier Structure", defining a total of five tiers, Tier 1 being the most valuable and Tier 5 being the least valuable, using the following rationale:

- **Tier 1.** World Class Mine. US$13B or greater in-situ diamond value produced up to 2019/20. Twelve mines.
- **Tier 2.** Large Mine. Produce >1 million carats/per year for 5 years minimum, but has not exceeded US$13B in value to date. Some Tier 2 mines, with continued (future) mining, may achieve Tier 1 status. Twenty-three mines.
- **Tier 3.** Medium Mine. Produce >0.4–1 million carats/per year for 5 years minimum. Fifteen Mines
- **Tier 4.** Small Mine. Produce 50,000– 400,000 carats/per year for 5 years minimum. Twenty-seven mines.
- **Tier 5.** Very Small Mine. 5,000 –50,000 carats/year/per year for 5 years minimum. Five mines.

The US$B13B cut-off for Tier 1 mines is approximately one-third lower than that suggested by De Beers (2014) and de Wit et al. (2016), who placed the cut-off for Tier 1 diamond mines at US$20B. Our division at US$13B was selected based on a clear-cut break on a cumulative probability plot (Fig. 3; derived from data in Table 2) of mine value. It could be argued that the ~US$50B Jwaneng deposit should be in a Tier of its own, being a clear outlier at the top of the global deposit value list (Fig. 3; Table 2). Importantly, note that the data in Table 2 is derived from a wide variety of public sources and may not be as robust as the confidential or difficult to obtain data held by large diamond mining companies—especially with respect to data for tonnes of ore mined, diamond grade, and diamond value—as determined on a yearly basis. Furthermore, the reader should note there are a number of past-producing diamond mines that are not listed in Table 2, either because they did not meet the 5-year mine life criteria, or simply because, there is limited or no data available to classify them. This is especially true for diamond mines that operated >100 years ago, for example many of the kimberlite or carbonate-rich olivine lamproite (CROL) diamond mines in South Africa. However, these former mines, as well as current advanced diamond exploration projects, are shown on global, and continent or craton-scale maps throughout this Chapter, for completeness. The "Tier Structure" established above underpins the following sections of this Chapter as context for categorising or discussing the different aspects of diamond deposits.

MAGMATIC SOURCE ROCKS

General background and historical perspective

The primary magmatic host rocks for diamond mines include kimberlite, olivine lamproite, and carbonate-rich olivine lamproite (CROL). Additional rock types such as ultramafic lamprophyre (variety aillikite) are known to be diamond-bearing (Hutchison and Frei 2009; Nielsen et al. 2009), as well as some possible kamafugite localities, but these have not as yet been proven to be mineable resources. The nomenclature, terminology and classification of magmatic diamond source rocks, specifically kimberlite, CROL and olivine lamproite, has been the source of much contention, fueling numerous debates and sowing significant confusion. We attempt to provide some clarity by briefly reviewing this issue below, though we acknowledge that in such inherently variable and complex magmatic systems, a degree of subjectivity remains.

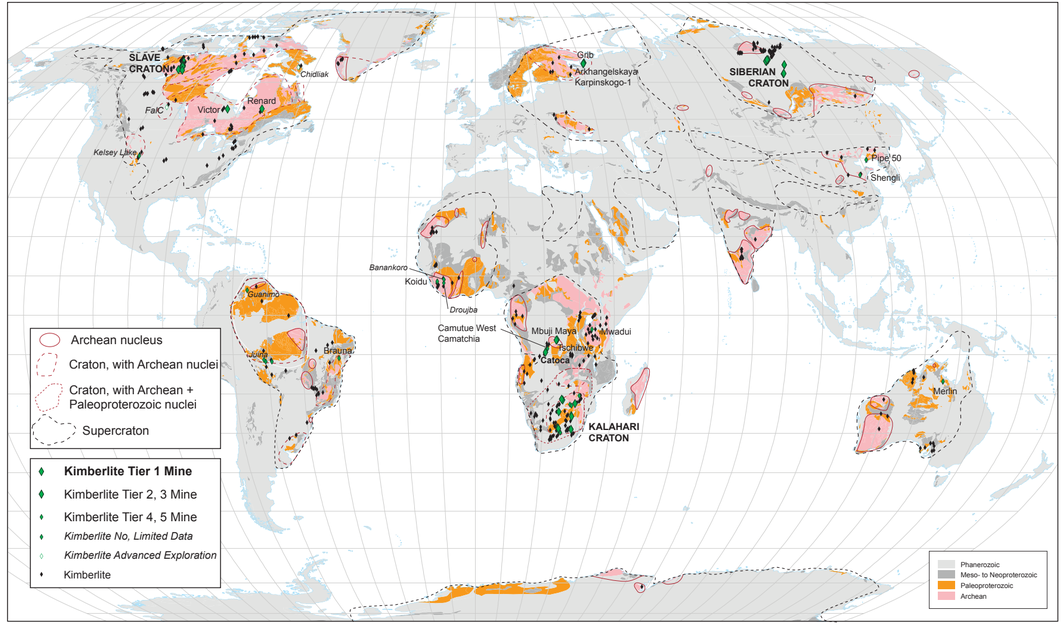

Figure 1. Global distribution of kimberlite and kimberlite-hosted diamond mines, past producing mines and advanced exploration projects. Additional kimberlite locations show the main fields and clusters globally. Bedrock geology backdrop from Chorlton (2007); note the dominant bedrock geology is that at the surface; i.e., Phanerozoic rocks that overlie Archean or Proterozoic rocks are shown on this map as Phanerozoic. Craton outlines from Pearson et al. (2021). Robinson map projection.

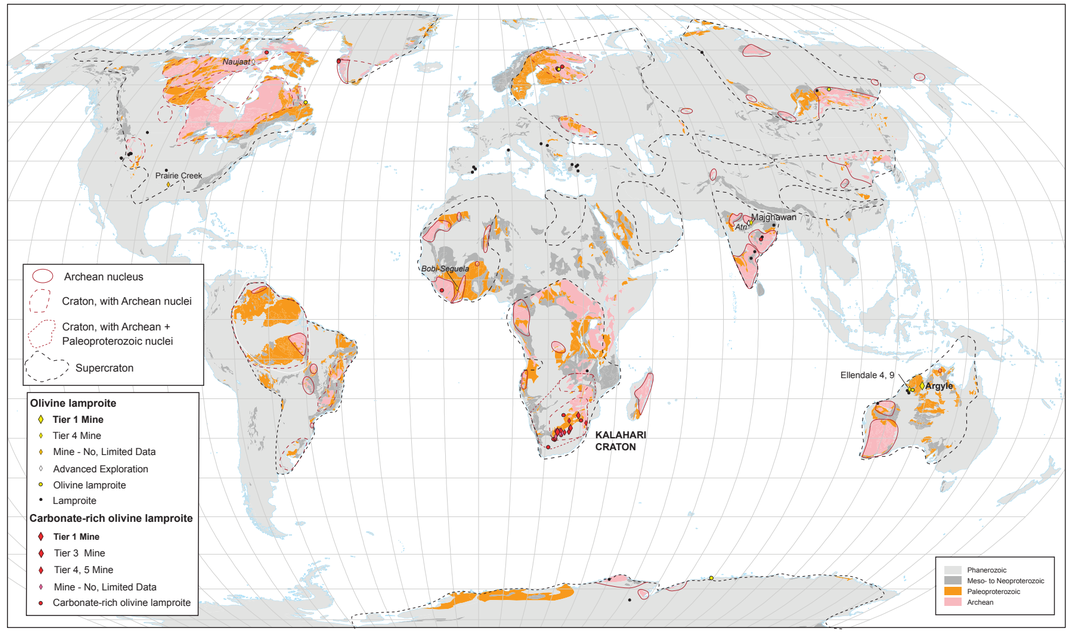

Figure 2. Global distribution of CROL- and olivine lamproite-hosted diamond mines, past producing mines and advanced exploration projects. Additional CROLs, olivine lamproites and lamproites (e.g., leucite lamproites, Mediterranean lamproites) locations show the main fields and clusters globally. Bedrock geology backdrop from Chorlton (2007); note the dominant bedrock geology is that at the surface i.e., Phanerozoic rocks that overlie Archean or Proterozoic rocks are shown on this map as Phanerozoic. Craton outlines from Pearson et al. (2021). Robinson map projection.

Table 2. Eighty-two producing or past producing magmatic-hosted global diamond mines, and their key parameters.

Mine	Field	Country	Rock Type	Grade (ct/t)	Stone Value (US$/ct)	Ore Value (US$/t)	Area (ha)	US$B to 2019/20	Mine Tier	Age (Ma)
Catoca	Lunda South	Angola	K	0.645	86	63.6	63.6	14.654	1	117.9
Camutue West	Lunda North	Angola	K	0.096	59	57.12	9	0.91	4	*120*
Camatchia (Luo)	Lunda North	Angola	K	0.17	200	34	29.4	0.93	4	*120*
Ellendale 9	Ellendale	Australia	OL	0.049	220	10.78	46	0.387	4	22
Ellendale 4	Ellendale	Australia	OL	0.14	220	30.8	76	0.079	4	22
Merlin	EMU	Australia	K	0.2	150	30	small pipes	0.076	4	382
Argyle	East Kimberley	Australia	OL	3.5	20	70	47	17.92	1	1126
Orapa (AK1)	Orapa	Botswana	K	0.95	70	66.5	118	29.54	1	92
Karowe (AK6)	Orapa	Botswana	K	0.153	690	105.57	9.5	0.966	4	93
Letlhakane	Orapa	Botswana	K	0.284	200	56.8	15.2	7.436	2	92.1
Damtshaa	Orapa	Botswana	K	0.215	200	43	13.5	0.86	4	94
Jwaneng	Jwaneng	Botswana	K	1.56	110	171.6	54	52.58	1	235
Lerala	Martin's Drift	Botswana	K	0.255	55	14.03	small pipes	n.d.	4	1364
Brauna	Brauna	Brazil	K	0.29	338	98.02	2	0.358	4	682
Beartooth	Lac de Gras	Canada	K	1.1	100	110	0.5	0.28	3	53
Koala North	Lac de Gras	Canada	K	0.5	143	71.5	0.5	0.24	4	53.3
Panda	Lac de Gras	Canada	K	1.11	168	186.48	3.3	4.03	2	53.3
Koala	Lac de Gras	Canada	K	1.26	200	252	4.5	5.17	2	53.3
Pigeon	Lac de Gras	Canada	K	0.41	150	61.5	1	0.17	3	*54*
Sable	Lac de Gras	Canada	K	0.9	128	115.2	2.4	0	2	*54*
Misery	Lac de Gras	Canada	K	4.17	50	208.5	1.1	2.06	2	*55*
A-154 North	Lac de Gras	Canada	K	3.021	166	501.54	1.2	5.014	2	55.2
A-154 South	Lac de Gras	Canada	K	4.778	126	602.08	2.6	7.003	2	55.5

Mine	Field	Country	Rock Type	Grade (ct/t)	Stone Value (US$/ct)	Ore Value (US$/t)	Area (ha)	US$B to 2019/20	Mine Tier	Age (Ma)
Fox	Lac de Gras	Canada	K	0.37	241	89.17	11	2.14	2	56
Lynx	Lac de Gras	Canada	K	0.8	230	184	0.6	0.07	4	56
A-21	Lac de Gras	Canada	K	2.7	126	340.2	1	1.286	2	56
A-418	Lac de Gras	Canada	K	3.426	90	308.32	1.4	2.957	2	56
Victor	Lac de Gras	Canada	K	0.25	458	114.5	15	3.708	3	177
Snap Lake	SE Slave	Canada	K	1.46	144	210.24	dike	1.21	2	523
Tuzo	SE Slave	Canada	K	1.23	57	70.11	1.4	0	2	530
Hearne	SE Slave	Canada	K	2.08	70	145.6	1.5	0.665	2	534
GK503-4	SE Slave	Canada	K	1.84	82	150.88	2	1.51	2	542
Renard-2	Orish Mts	Canada	K	0.84	85	71.4	1	1.836	2	643.4
Pipe 50	Fuxian	China	K	1	20	20	0.9	0.14	4	464
Shengli	Mengyin	China	K	0.5	20	20	0.4	0.14	4	476
Mbuji Mayi M1	Mbuji-Mayi	DRC	K	1.3	13	16.9	22.6	0.71	3	69.9
Tshibwe	Bena-Baya	DRC	K	0.381	16	6.1	60	0.98	2	85
Dokolwayo	Dokolwayo	Eswatini	CROL	0.4	100	40	2.8	0.072	4	203
Majhgawan	Hinota	India	OL	0.13	220	28.6	6.5	0.22	4	1072
Mothae	Lesotho	Lesotho	K	0.027	931	25.14	8.8	0	5	87
Kao	Lesotho	Lesotho	K	0.054	350	18.9	19.8	0.476	4	89
Liqhobong	Lesotho	Lesotho	K	0.27	80	21.6	8.6	0.38	3	91
Letšeng Satellite	Lesotho	Lesotho	K	0.023	2750	63.25	4.7	n.d.	4	91
Letšeng Main	Lesotho	Lesotho	K	0.023	1650	37.95	17.2	2.805	4	94
Syrykanskaya	Alakit	Russia	K	0.6	85	51	6	0.842	3	344

Mine	Field	Country	Rock Type	Grade (ct/t)	Stone Value (US$/ct)	Ore Value (US$/t)	Area (ha)	US$B to 2019/20	Mine Tier	Age (Ma)
Komsomolskaya	Alakit	Russia	K	0.38	20	76	4	1.4	4	357
Jubileinaya	Alakit	Russia	K	0.84	100	84	59	17.227	1	358
Aikhal	Alakit	Russia	K	5.35	100	535	3	14.493	1	378
Udachnaya	Daldyn	Russia	K	1.5	80	120	25	18.055	1	360
Zarnitsa	Daldyn	Russia	K	0.21	185	38.85	21.5	3.511	2	362.3
Internationalnaya	Malo-Botuobiya	Russia	K	8.73	160	1396.8	1.7	26.397	1	360
Mir	Malo-Botuobiya	Russia	K	5.55	130	721.5	6.9	17.639	1	363
23rd Party Congress	Malo-Botuobiya	Russia	K	4	120	480	1.5	2.4	2	433
Botuobinskaya	Nakyn	Russia	K	5.19	55	285.45	2.9	0.213	3	365
Nyurbinskaya	Nakyn	Russia	K	4.13	55	227.15	2.4	3.912	2	366
Grib	Verkhotina	Russia	K	0.7	105	73.5	14.2	2.661	2	374
Arkhangelskaya	Lomonosov	Russia	K	0.86	100	86	19	0.861	2	375
Karpinskogo-1	Lomonosov	Russia	K	1.14	100	114	14	1.368	2	380
Koidu K1	Koidu	Sierra Leone	K	0.67	350	234.5	0.5	0.642	4	143
Koidu K2	Koidu	Sierra Leone	K	0.33	350	115.5	0.5	0.583	4	146
Jagersfontein	Jagersfontein	South Africa	K	0.12	200	24	12	1.9	4	85.8
Dutoitspan	Kimberley	South Africa	K	0.32	140	44.8	10.8	2.8	3	86.5
De Beers	Kimberley	South Africa	K	0.64	100	64	5.1	2.3	3	86.5
Kimberley	Kimberley	South Africa	K	1.5	100	150	3.7	2.2	3	87
Bultfontein	Kimberley	South Africa	K	0.54	75	40.5	9.7	1.838	3	88.3
Wesselton	Kimberley	South Africa	K	0.37	75	27.75	8.7	2.138	3	89.6
Koffiefontein	Koffiefontein	South Africa	K	0.08	510	40.8	11.1	6.12	4	93.9
Finsch	Lime Acres	South Africa	CROL	0.36	99	35.64	17.9	12.989	1	118

Mine	Field	Country	Rock Type	Grade (ct/t)	Stone Value (US$/ct)	Ore Value (US$/t)	Area (ha)	US$B to 2019/20	Mine Tier	Age (Ma)
Frank Smith	Barkley West	South Africa	K	0.05	500	25	7.4	n.d.	5	114
Main, Bobbejaan	Bellsbank	South Africa	CROL	0.5	250	125	dike	n.d.	5	118
Star	Theunissen	South Africa	CROL	0.62	323	200.26	dike	n.d.	5	124
Roberts Victor	Boschof	South Africa	CROL	0.45	100	45	2	0.044	4	126
Voorspoed	Kroonstad	South Africa	CROL	0.24	150	36	12	1.062	3	132
Lace/Crown	Kroonstad	South Africa	CROL	0.41	180	73.8	2.9	0.135	3	133.2
Helam	Swartruggens	South Africa	CROL	2	100	200	dike	n.d.	5	145.1
Marsfontein	Klipspringer	South Africa	CROL	1.73	142	245.66	0.4	0.256	3	155
The Oaks	Marnitz	South Africa	K	0.34	105	35.7	1	0.103	4	505
Venetia	Venetia	South Africa	K	1.22	125	152.5	23.3	19.55	1	521
Cullinan	Pretoria	South Africa	K	0.466	185	86.21	32.2	29.415	1	1153.3
Mwadui	Shinyanga	Tanzania	K	0.07	307	21.49	146	6.831	4	52
Murowa	Murowa	Zimbabwe	K	0.9	65	58.5	4.5	0.215	4	527

Notes: K = kimberlite, OL = olivine lamproite, CROL = carbonate-rich olivine lamproite. Mine area, for example in twin or triple pipes is the total area; for dikes, or mines consisting of multiple small bodies (dike enlargements/blows/diatreme buds) the area is not determined (n.d), or termed small pipes. The emplacement age data for each mine is listed when known; if unknown the geochronology data is inferred and shown in italics, based on data from other bodies in that field (see Geochronology section for further details). Sources of diamond mine data: Janse (1993, 1995, 1996, 2007), De Beers (2004), Kjarsgaard (2007a), Read and Janse (2009) and references therein. Post-2000 data is mainly based on public domain National Instrument 43-101 and JORC compliant reports, and company reports e.g., ALROSA, Anglo American plc, BHP Billiton Limited, Rio Tinto plc, etc.; Roffey et al. (2018) provide a detailed listing of these sources.

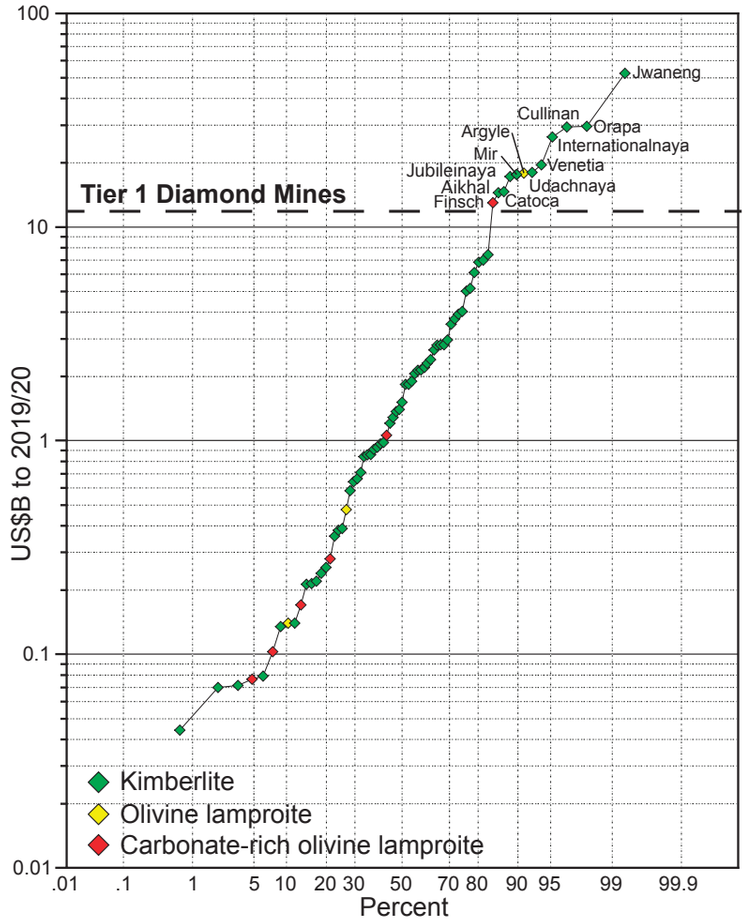

Figure 3. Cumulative probability plot for the value of individual diamonds mined up to 2019/20 (data from Table 2). The Tier 1 versus Tier 2 division is defined by the break between the Finsch Mine (US$13B—Tier 1) and the Letlhakane Mine (US$7.4B—Tier 2). All primary magmatic hosted diamond mines are color coded by rock type (Kimberlite, CROL, olivine lamproite). All Tier 1 mines are labeled by locality.

The term kimberlite (following type-locality nomenclature rules of the day) was introduced by Lewis (1888) for the distinctive volcanic rocks being mined for diamonds at Kimberley, South Africa, which he described as "porphyritic volcanic peridotite of basaltic structure". Importantly, Lewis (1888) recognized distinctions between kimberlite, kimberlite breccia and kimberlite tuff. Subsequently, the landmark monograph of Wagner (1914) subdivided kimberlites into two distinct petrographic types, a "basaltic" variety, being poor in mica and equivalent to the kimberlite described by Lewis (1988), and a "lamprophyric" or "micaceous" variety, rich in phlogopite mica. Wagner (1914) further described the "basaltic" variety as being exceptionally rich in large and small olivine crystals (50–75 modal%), with the "lamprophyric" variety as having up to 50% phlogopite, with less olivine. The terms "basaltic" and "lamprophyric" were used by Wagner to emphasize the structure/texture/habit/fabric of these diamondiferous volcanic and intrusive rocks, but his term "basaltic" did not imply the presence of plagioclase (cf. Dawson 1980; Mitchell 1986, 1995).

The hallmark paper of Smith (1983) on Late Jurassic–Cretaceous age southern African kimberlites utilized Sr–Nd–Pb isotope systematics to subdivide the studied sample suite into two distinct rock types, which he termed Group I (Gp I) and Group II (Gp II) kimberlites. Smith (1983) specifically stated that his Group I and II kimberlites corresponded to the "basaltic" and "micaceous" varieties of kimberlite as defined by Wagner (1914) and also by Dawson (1967, 1980). However, Mitchell (1986; p. 6 and 7) noted that contemporary advances in kimberlite petrology from 1970-1985 resulted in the final overthrow of the Lewis–Wagner classification, in favour of a scheme (Clement and Skinner 1979, 1985) based on the modal abundance of primary kimberlite minerals. However, the publications of Clement and Skinner (1979, 1985), Clement et al. (1984), and subsequently by Mitchell (1986) did not distinguish, but instead lumped all kimberlite types together, including the petrographic (Wagner 1914) and isotopically distinctive (Smith 1983) Group I and Group II kimberlite types.

Dawson (1980, 1987) stated that southern African micaceous/Group II kimberlites are the Kaapvaal craton's variant of globally observed lamproites, based on similarities in mineralogy and geochemistry. Later, Mitchell and Bergmann (1991) suggested a few southern African micaceous/Group II kimberlite localities could be lamproites. Tainton and Browning (1991), Tainton (1992), and Tainton and McKenzie (1994) examined the Kaapvaal lamproite versus micaceous/Group II kimberlite problem in detail, concluding all these rocks are a variety of lamproite. Mitchell (1995) subsequently re-named micaceous/Group II kimberlites with the term "orangeite", following on the original suggestion by Wagner (1928), with these rocks deemed to occur only in southern Africa. However, studies by Mahotkin (1998) and O'Brien and Tyni (1999) described and classified rocks from Finland and western Russia as Gp II kimberlite, and also as olivine lamproite. Sarkar et al. (2018) described and classified kimberlite pipes and orangeite sills, and kimberlite dikes and olivine lamproites from northern and southern Melville Peninsula (Arctic Canada), respectively; the olivine lamproites have similarities in mineralogy, bulk composition and age to the lamprophyric rocks of Sisimiut, Greenland studied by (Scott 1979, 1981) and Thy et al. (1987). However, the Sisimiut rocks are better described as carbonate-bearing olivine lamproites, due to their calcite contents. Carbonate-bearing and carbonate-rich olivine lamproites have also been documented from e.g., Kodomali and Behradih in India (Lehmannn et al. 2010; Rao et al. 2011). Therefore, the rocks variably termed micaceous kimberlite/Gp II kimberlite/orangeite are not globally restricted to southern Africa.

More recently, Pearson et al. (2019) clarified and revised these nomenclature issues by (1) utilizing the term kimberlite instead of Group I kimberlite or archetypal kimberlite; and; (2) introducing the term carbonate-rich olivine lamproite (CROL) for global occurrences of rocks formerly known as micaceous kimberlite or Group II kimberlite or orangeite. Simply put, CROL are carbonate-bearing or carbonate-rich modal variants of olivine lamproite. This terminology is used herein, and key aspects of the mineralogy and geochemistry of kimberlite, carbonate-rich olivine lamproite, and olivine lamproite are described in the following subsections of this chapter.

The diamond-bearing volcano

The volcanology terms employed in this chapter are common to all three magma types (i.e., kimberlite, carbonate-rich olivine lamproite and olivine lamproite), which form intrusive and extrusive rocks that host diamond mines, These different magma types all form volcanic landforms and volcanic structures that are similar to those observed in small-volume alkali basalt systems, as previously suggested for kimberlites (Lorenz 1975, 1987; Kjarsgaard 2003, 2007a,b) and olivine lamproites (e.g., Atkinson et al. 1984; Smith and Lorenz 1989; Boxer et al. 1989; Stachel et al. 1994). These are termed maar-diatreme volcanoes (Wagner 1914; Mannard 1962; Lorenz 1975), or "small volcanoes" (White and Ross 2011). That these three different magmas can generate similar styles of volcanism and volcanic products is not a new idea (e.g., see Harris 1984; Atkinson et al. 1984; Atkinson 1989; Nixon 1995). Kimberlite geologists

have been—and to some extent still are—under the mistaken belief that exceptionally volatile-rich "kimberlite" (i.e., kimberlite and carbonate-rich olivine lamproite) magmas are unique and thus do not have to conform to the basic tenets of magma physics and volcanology, such that standard volcanological nomenclature and terminology, (e.g., Fisher 1961, 1966; Schmid 1981; McPhie et al. 1993), have not been applied. Recent, revised kimberlite nomenclature and terminology (compare Cas et al. 2008a,b, 2009 with Scott Smith et al. 2013, 2018) is highly problematic and contradictory and cannot be construed as improvements to this situation; see also Field et al. (2008) for further discussion on this topic. In contrast, studies of olivine lamproite (and lamproite) have followed standard volcanology terminology and nomenclature (e.g., Jaques et al. 1986; Rayner et al. 2018a,b).

Terminology. The key geomorphological/structural elements of maar-diatreme volcanoes associated with diamond mines are illustrated in Figure 4 (modified after S. Kurszlaukis, written communication 2003, 2020; Kjarsgaard 2007a,b; White and Ross 2011). These elements include: (1) the paleo-eruptive land surface (aka pre-eruptive land surface); (2) positive relief, with respect to the paleo-eruptive land surface (and rarely preserved), tuff cone and/or tuff ring; (3) crater, crater wall, crater floor; (4) diatreme (upper and lower), diatreme wall, diatreme fill; (5) root zone, and; (6) feeder dike. Note that root zones are neither defined by their size or shape, nor by their consituent rocks types (see *lithofacies nomenclature)*.

A maar-diatreme volcano is defined by the crater floor lying below the paleo-eruptive land surface and is formed by the eruption of magma (Lorenz 1973); the maar crater is surrounded by a tuff ring when preserved. Tuff cones (aka cinder cones, scoria cones) may overlie a maar, thus obscuring an older maar crater and tuff ring plus underlying diatreme. Tuff rings and tuff cones are differentiated on the basis of their morphometric parameters (Wood 1980; Vespermann and Schminke 2000). These include the crater rim height (HCR), the crater rim diameter (DCR), the HCR/DCR ratio, maximum bedding dips, and the crater floor depth below the paleo-eruptive land surface for tuff rings; tuff cones use the cone height (HCO), the crater rim diameter (DCR), the cone basal diameter (DCO), and HCO/DCO and DCR/DCO ratios. Note that for kimberlite, CROL and olivine lamproite magmatic systems, the volcanic edifice (when observed) is typically consolidated/lithified and hence tuff cone or tuff ring is preferred terminology instead of tephra (i.e., loose, unconsolidated).

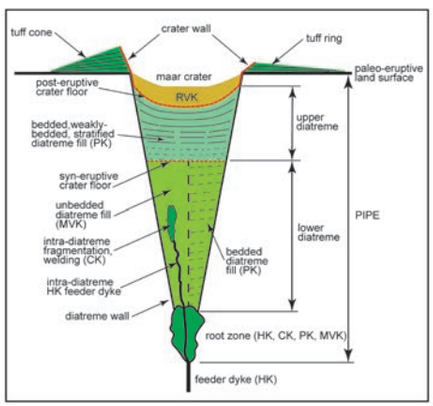

Figure 4. Cross-section (highly schematic composite, no scale implied) of a kimberlite maar-diatreme volcano, at the post eruptive stage in which the maar-crater has been partially in-filled, illustrating the key terms used in this chapter. RVK = resedimented volcaniclastic kimberlite; PK = pyroclastic kimberlite; MVK = massive volcaniclastic kimberlite; HK = hypabyssal kimberlite; CK = coherent kimberlite. The terminology of this non-genetic maar-diatreme volcano as well as the associated lithofacies can be equally applied to olivine lamproite or CROL. Modified after Kurszlaukis (written communication 2003, 2020), Kjarsgaard (2007a,b) and White and Ross (2011).

The root zone plus the diatreme is termed a pipe (alternately, the diatreme structure; White and Ross 2011); importantly, note that a pipe can consist of multiple, discrete and individual diatremes. The root zone and the diatreme can be in-filled with an exceptionally wide array of different rock types (lithofacies), derived from magmas that are extrusive (typically fragmental), or, are intrusions (non-fragmental) such as dikes, sills, and feeder conduits for tephra jets. As well, resedimented material that can include large blocks of wall rock that are not in-situ can constitute part of the pipe in-fill. Upper diatreme deposits are more typically bedded, diffusely bedded or stratified; lower diatreme deposits are more typically massive in nature. However, bedded pyroclastic rocks, or blocks of this material can be observed in the lower diatreme (e.g., Clement 1982). The crater, an open hole with a bottom or base, can be syn-eruptive and in-filled by primary pyroclastic, volcaniclastic and resedimented material, or post-eruptive when volcanic activity has ceased and the crater is open to air, or filled with water, or, infilled by younger resedimented ("epiclastic") material.

Lithofacies nomenclature. A key aspect of the description of rocks in kimberlite (and also CROL and olivine lamproite) volcanoes is the use and application of non-genetic terminology (Kjarsgaard 2003, 2007a,b; Sparks et al. 2006; Field et al. 2008); this is certainly not a new idea with respect to volcanic systems in general (e.g., McPhie et al. 1993). A very simple, non-genetic nomenclature system (Kjarsgaard 2003, 2007a,b; Sparks et al. 2006; Field et al. 2008) to describe rocks from kimberlite (and also from CROL and olivine lamproite) magmatic systems is preferred. Here kimberlite is used as an example of the subdivisions: (1) volcaniclastic kimberlite (VK), i.e., fragmental rocks, and (2) coherent kimberlite (CK), typically, non-fragmental intrusive rocks. With more detailed information, these two fundamental root rock names can be further subdivided: massive volcaniclastic kimberlite (MVK), which were formerly termed tuffisitic kimberlite or tuffisitic kimberlite breccia (TK/TKB; Clement 1982); pyroclastic kimberlite (PK), and; resedimented volcaniclastic kimberlite (RVK), which were formerly and variably termed epiclastic kimberlite. MVK, PK and RVK are all varieties of VK. Introduction of type-locality lithofacies terms such as "Kimberley-type pyroclastic—KPK" (Mitchell et al. 2009, 2012) and "Fort à la Corne-type pyroclastic—FPK" (Scott Smith et al. 2013, 2018), when the fragmentation and depositional processes are not or are very poorly understood, represents the nadir of kimberlite lithofacies classification.

Coherent kimberlites (CK) are typically 1–3 m in width and manifest as either dikes or sills, and more rarely as dike enlargements termed blows, or as small plugs. If the rock is demonstrably an intrusion, the use of the term hypabyssal, as in hypabyssal kimberlite (HK) is perfectly acceptable, for example HK dike or HK sill. These hypabyssal intrusions can be associated with a pipe, and include: precursor (aka antecedent), contemporaneous, and consequent (aka subsequent) dikes and sills (Wagner 1914; Clement 1982). The most important and key application of the term CK is when the rock is not obviously fragmental, nor obviously an intrusion, based on the available information. Examples of bonafide CK are rare, but would include pyroclastic rocks that have welded or agglutinated in the root zone or within the diatreme and appear dike- or sill-like in nature (Sparks et al. 2006). At the Victor Diamond mine (Canada), detailed studies led van Straaten et al. (2011) to interpret that lava fountaining and welding generated clastogenic coherent kimberlite that in appearance resembled intrusive hypabyssal kimberlite sills. Additional possible examples of bonafide CK include rootless lava flows, or lava lakes in which the magma has fragmented (via fire fountaining) and subsequently welded. While kimberlite (and CROL) lava lakes and lava flows are rare (or rarely preserved), they are quite common in olivine lamproite and lamproite magmatic systems (Jaques et al. 1986; Mitchell and Bergman 1991). Furthermore, note that the existence of a lava lake or lava flow, while extrusive, is not synonymous with magma fragmentation and welding, as these rocks could simply be related to flows from very passive fissure eruptions. At the Igwisi Hills, Brown et al. (2012) could find no evidence that the kimberlite lavas formed by welding of spatter.

Pipe formation and preservation. Our understanding of diamondiferous volcanoes is derived from "temporal snapshots" of individual volcanoes, which includes: rocks at the present-day erosional surface, rocks observed in open pit and underground mining exposures, and rocks from drill cores. Hawthorne (1975) astutely observed that South Africa kimberlites had experienced significant erosion, in contrast to kimberlites in Angola, Botswana, Tanzania and the Democratic Republic of Congo (DRC), which preserved RVK and/or "epiclastic kimberlite" that infilled a basin (i.e., a syn- or post-eruptive crater) above the diatreme. The preservation of a kimberlite volcano and its surficial edifice is dependent on the age and degree of cementation of the rocks; however, the regional-scale post-volcanic depositional and/or erosional environment is key. Importantly, variably preserved and intact tuff rings and tuff cones are rare, but known from mid-Cretaceous age kimberlites at Fort à la Corne (Canada) due to post-eruptive sedimentation and burial (e.g., Zonneveld et al. 2004), and the Holocene age Igwisi Hills kimberlites (Tanzania) that are preserved due to minimal erosion (Reid et al. 1975; Dawson 1994; Brown et al. 2012). In contrast, kimberlite pipes in the Kimberley area of South Africa area have been subjected to ~850 m of erosion (Hanson et al. 2006, 2009; Stanley et al. 2015), with original (ca. 1870's) surface exposures at mid-diatreme depths. The observation that near surface hypabyssal dikes, sills, blows, plugs and root zones exist without any fragmental rocks (i.e., a diatreme consisting of fragmental rocks at the same stratigraphic level) does not imply there was significant erosion and removal of the diatreme. Rather, this is simply a reflection of near-surface magma fragmentation (or not!), i.e., how the magma degassed, and/or interacted with ground and/or surface water.

As emphasized by Nixon (1995), no single example of a diamondiferous volcano is known that has an exposed feeder dike, plus root zone, plus diatreme, plus tuff ring or cone, and crater (as per Fig. 4). Nixon (1995) further underscored the notion that no single example of a diamondiferous volcano would be definitive, due to the exceptionally wide variations that are known in pipe geometry and internal morphology, and pipe or crater size and shape (see Figs. 5 through 12). This simple statement of Nixon (1995) is true for kimberlite, CROL and olivine lamproite pipes. The notion that there are three highly distinctive classes/types of kimberlite pipes globally (Field and Scott Smith 1999; Skinner and Marsh 2004; Scott Smith 2006, 2008) is inconsistent with known observations. These tripartite endmembers serve little if any purpose, because each individual model is highly oversimplified, to the point of being misleading, especially from an exploration perspective (Kjarsgaard 2007a,b). Volcanological studies at the Murowa mine (Zimbabwe) led Moss et al. (2013) to arrive at a similar conclusion; he noted that in general, kimberlites cannot be easily or completely described by any single class/type of pipe and its implied emplacement model.

Juvenile magmatic degassing versus phreatomagmatic eruption styles. The volcanology, volcanic architecture and volcanic deposits of olivine lamproites (and lamproites) in terms of their modes of formation are not controversial—there is general agreement that phreatomagmatic processes, in which a hot magma interacts with ground or surface water in a highly explosive manner—is key to understanding magma fragmentation (e.g., Zimanowski et al. 1991, 2015; Büttner et al. 2002). In contrast, two kimberlite pipe formation models are actively debated: the exsolution of juvenile magmatic CO_2 dominant (due to near-surface lowering of the confining pressure) volatile driven pipe formation model, and the phreatomagmatic pipe formation model; compare Scott Smith (1999) with Lorenz et al. (1999), but see also Lorenz and Kurszlaukis (2007), Kurszlaukis and Lorenz (2008), and Field et al. (2008) and their contained references for further discussion. For example, diametrically opposed pipe formation models are described for two nearby (<1 km distance) kimberlite pipes from the Diavik Mine (Lac de Gras, Canada) that are of identical age (within uncertainty). The A418 pipe is considered to be of phreatomagmatic origin (Porritt et al. 2013), while the A154 North and A154 South pipes are considered to be driven by exsolution of magmatic volatiles (Moss et al. 2009, 2018). More recently, the Diavik A154 North and A154 South pipes were reinvestigated by Tovey et al. (2020), who interpreted that groundwater availability and phreatomagmatism controlled kimberlite fragmentation processes.

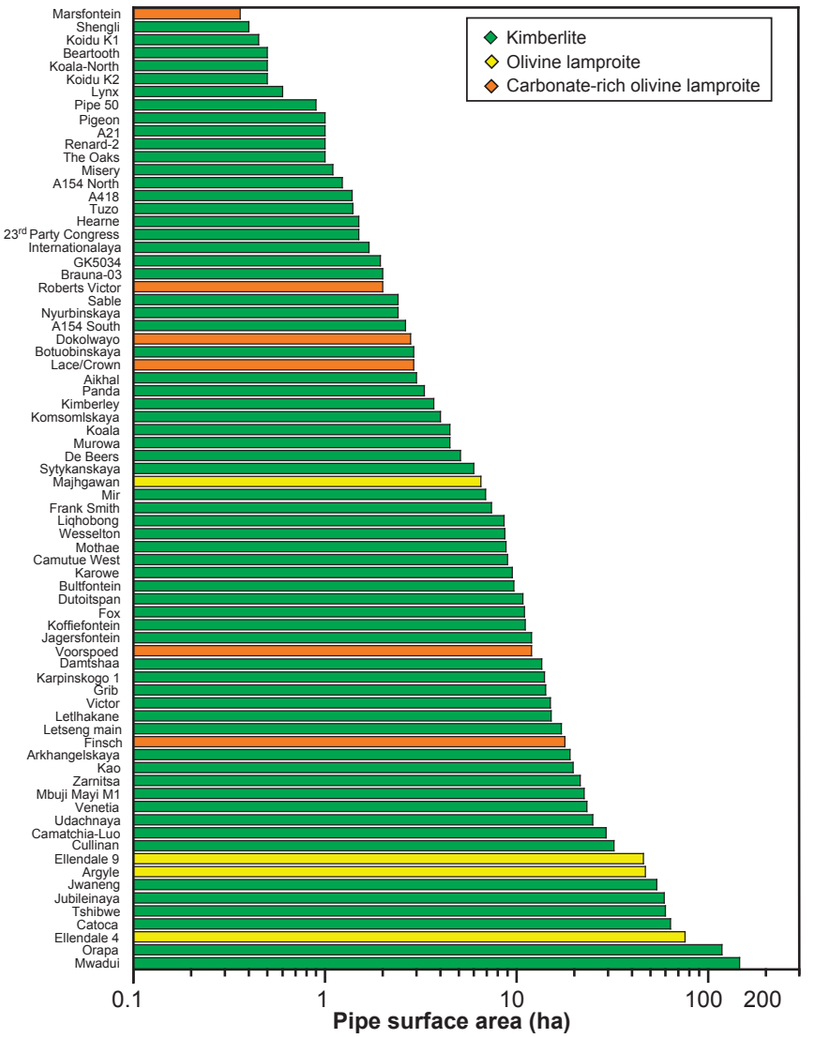

Figure 5. Pipe surface area (ha) of global diamond mines, log histogram plot (data from Table 2). All primary magmatic hosted diamond mines are color coded by rock type (Kimberlite, CROL, olivine lamproite). Note that the area can either represent the surface area of the pipe, or represent the surface area of the volcanic edifice (e.g., the tuff ring or "apron" deposits surrounding the diatreme) at the start of mining.

Given that carbonate-rich olivine lamproites have high whole rock CO_2 concentration levels (see *Whole Rock Geochemistry*), the debate regarding kimberlite pipe formation models is thus equally applicable to CROL pipe formation. Of course, a multitude of pipe formation models, which variably combine aspects of both magmatic and phreatomagmatic processes are entirely feasible. In this respect, the induced phreatomagmatic explosion experiment of a volatile-rich (CO_2 and H_2O) kimberlite melt generated very high energy shock waves, and produced pyroclasts with exceptional ejecta speeds of >400 m/s (Kurszlaukis et al. 1998). Specific features of diamondiferous volcanoes, such as exceptionally large pipes, are perhaps

resultant from such processes. One could speculate further that the huge size of the olivine lamproite-hosted Tier 1 Argyle mine resulted from higher magmatic CO_2 contents than is the "norm" for an olivine lamproite magma (see Abersteiner et al. 2022).

Diamond mine volcanoes. Examples of kimberlite, CROL and olivine lamproite diamond mines, advanced exploration projects, and non-economic maar-diatreme volcanoes are utilized to illustrate key basic concepts via plan views, cross sections, isometric views, and 3-D solids images in Figures 6–12.

A variety of variably intact tuff cones, tuff rings and maar craters are known from Fort à la Corne (Canada), and the Igwisi Hills (Tanzania) kimberlites. The ca. 105–95 Ma kimberlites at the Fort à la Corne advanced exploration project have typically well preserved volcanic edifices due to burial by subsequent kimberlite volcanic events, but mainly by rapid deposition of contemporaneous and younger mid-Cretaceous deltaic, and near-shore and deeper marine sediments (Leckie et al. 1997; Kjarsgaard 2003, 2007a,b; Zonneveld et al. 2004; Kjarsgaard et al. 2009). The Fort à la Corne kimberlite volcanoes are typically multiphase, as has been established for many kimberlites, but they are also polygenetic (cf. Fulop and Kurszlaukis 2016; see also *Geochronology*, this chapter).

From drill intersections and 2-D seismic imaging, the early Joli Fou (EJF) eruptive phase at the #169 kimberlite forms a cone-like volcanic edifice with ~100 m of relief above the paleo-eruptive land surface (the JF shale), and overlies an older, small, flared (~45°) diatreme; (Leckie et al. 1997; Kjarsgaard et al. 2007). The top of the EJF tuff cone is flattened and has a reduced height due to marine shoreface reworking and slumping (Leckie et al. 1997). The Pense P2 eruptive phase at the Orion South kimberlite also has ~100 m of relief above the paleo-eruptive land surface (the Pense shale), with a truncated and irregular cone-like form; the top of the P2 kimberlite is in direct contact with Quaternary till, a glacial erosion surface (Kjarsgaard et al. 2009). The P2 edifice overlies a >150 m deep, 500 m wide and flared (~45°) P2 diatreme. At the Star kimberlite, the EJF eruptive phase forms a ~400 m diameter tuff ring with the rim having 44 m of elevation above the paleo-eruptive land surface (the JF shale); the EJF crater floor is ~49 m below the paleo-eruptive surface (Fig. 6a) and together they define a tuff ring–maar crater (Zonneveld et al. 2004). The EJF crater is underlain by a flared (~45°) diatreme that extends ~100 m below the EJF crater floor (Fig. 6a). The EJF crater itself is filled by RVK, and then subsequently by a younger phase of kimberlite volcanism from an adjacent diatreme (the Mid-JF), which has partially cut into the EJF diatreme and tuff ring (see Fig. 10 in Zonneveld et al. 2004). The Tokapal kimberlite (India) has a wide pyroclastic apron around a central feeder vent (Mainkar et al. 2004), similar to some of the Fort à la Corne kimberlites.

For the Igwisi Hills (Tanzania), erosion of these young Holocene, ca. 12,000 to 6,000 years old kimberlites are negligible, with good preservation of the three adjacent volcanic edifices (Sampson 1953; Reid et al. 1975; Dawson 1994; Brown et al. 2012), with the following adapted from Brown et al. (2012). The NW volcano has pyroclastic kimberlite deposits with bedding dips of 8–32° and the crater floor is at or below the paleo-surface, i.e., a tuff ring and maar crater. A significant lava flow breaches the east side of the tuff ring; the crater is interpreted to be filled by a lava lake. The SW volcano is a tuff cone, with beds dipping at 6–31°. A lava flow breaches the east side, fed by a perched lava lake. The central volcano has pyroclastic beds dipping at 6–31°, the volcanic edifice has an angle of repose of 24° and is suggested to be a tuff (scoria) cone, although interpretation is problematic due to the significant lava coulee that obscures the morphology of the east side of the central volcano. The Igwisi Hills and the Fort à la Corne examples each illustrate substantive variations in styles of volcanism and volcanic architecture for kimberlites that are in close proximity within a cluster or field, and are of similar age. These kimberlites have deposits consistent with volcanic formation processes ranging from fire fountaining (magmatic degassing driven) at the Igwisi Hills (Brown et al. 2012) and at Fort à la Corne (welded PK; Leckie et al. 1997), to tephra jets associated with phreatomagmatic processes at Fort à la Corne (McClintock et al. 2009; Kjarsgaard et al. 2009).

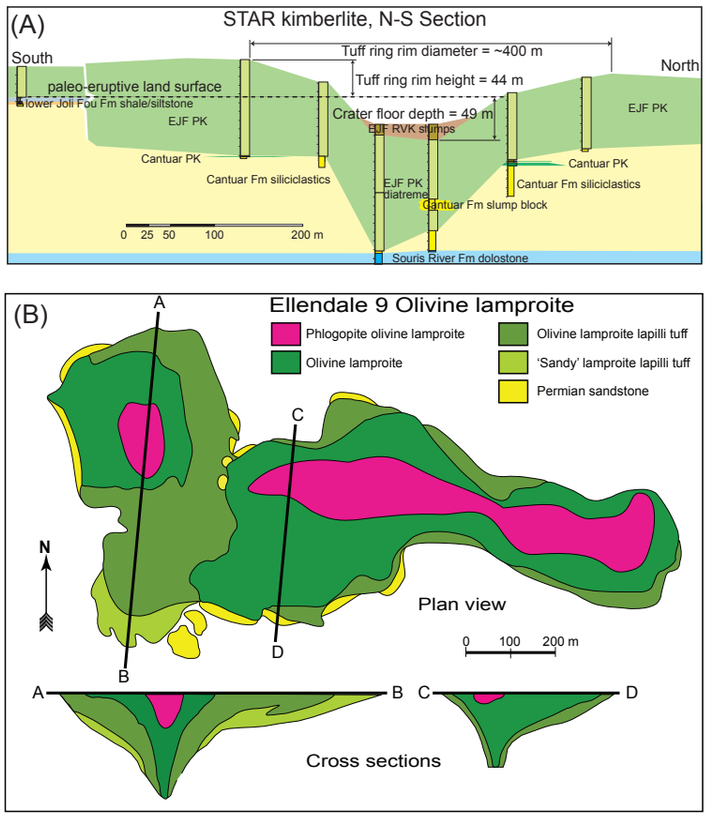

Figure 6. (**A**) North–South simplified cross section (partial, not the full N-S extent) of the Star kimberlite pipe and its host rock geology (Fort à la Corne, SK, Canada), showing only the early Joli Fou (EJF) tuff ring, and the partially in-filled maar crater that overlies the EJF diatreme. Adapted from B.A. Kjarsgaard (unpublished); see also Harvey et al. (2009). (**B**) Simplified plan and section views of the Ellendale 9 (Australia) olivine lamproite pipe. Note the occurrence of at least two distinct diatremes in this pipe. Area of phlogopite olivine lamproite constitutes a lava lake. Adapted from Smith and Lorenz (1989).

A number of other kimberlite pipes actively mined for diamonds (or past producers) are known that resemble the deposits described above, with specific similarities such as pipes with significant PK and RVK deposits that are preserved both external and internal to the pipe/maar crater. These include the 22 ha Tier 2 Mbuji Mayi (M1) mine, DRC (Fieremans 1953; Meyer de Stadelhofen 1963), the 60 ha Tier 2 Tshibwe mine, DRC (de Wit et al. 2016) and possibly quite a number of other examples in Angola (e.g., Camafuca-Camazamba). The olivine lamproite pipes in the Ellendale field (Jaques et al. 1986) also bear some morphological similarities to the kimberlite volcanoes in the DRC and Angola listed above. The geology of the 76 ha Tier 4 Ellendale 4 and 46 ha Tier 4 Ellendale 9 olivine lamproite-hosted past producing diamond mines are well documented by Jaques et al. (1986), Smith and Lorenz (1989) and Stachel et al. (1994). Plan and section views of Ellendale 9 (in which the tuff ring is not preserved due to erosion), are shown in Figure 6b. The E-W elongated Ellendale 9 pipe is interpreted to be the product of two (or more) flared diatremes, each >200 m deep, filled with well-bedded "sandy" quartz-rich olivine lamproite base surge deposits of phreatomagmatic origin, pyroclastic mass flow deposits, and variably welded spatter deposits (Jaques et al. 1986; Smith and Lorenz 1989;

Stachel et al. 1994). Coherent olivine lamproite and coarser-grained madupitic phlogopite olivine lamproite lava lakes overlie these rocks. There are certainly other known olivine lamproites with similarities to Ellendale 4 and 9, with the pipes filled by fragmental lamproite, and then by overlying spatter deposits and/or lava lakes of coherent lamproite. Examples would include the weakly diamondiferous Prairie Creek, Arkansas (Bolivar 1984; Mitchell and Bergmann 1991) and the Kapamba, Zambia olivine lamproite pipes (Scott Smith et al. 1989).

Since the important and influential observations of Hawthorne (1975) on minimally eroded kimberlite pipes that preserve crater in-fill deposits in central and southern Africa, a number of significant new studies have been published. New geology and volcanology data and interpretations have been generated as a result of greater exposures of these kimberlite pipes from decades of diamond mining since the 1970's. The geology of the 118 ha Orapa (Botswana) Tier 1 diamond mine, a kimberlite twin pipe that coalesced at the surface, is described by Field et al. (1997) and Kilham et al. (1998), with more recent studies and overviews in Field and Stiefenhofer (2006), Field et al. (2008), Gernon et al. (2009), de Wit et al (2016) and Kruger and Maphane (2017). The 54 ha Tier 1 Jwaneng (Botswana) diamond mine, a kimberlite triple pipe (Fig. 7) that coalesced at the surface, was noted to be quite different as compared to a typical South African kimberlite, due to the pipes being dominantly in-filled with VK, bedded VK, PK and RVK, but not massive volcaniclastic kimberlite (MVK) as is typical of a Kimberley cluster pipe (Field and Scott Smith 1999; Webb et al. 2003; Skinner and Marsh 2004). More recent geological studies on Jwaneng include the work of Mmualefe (2017) and the overviews presented by Field et al. (2008), and de Wit et al. (2016). A cross section of the geology of the Jwaneng pipe is shown in Figure 7. The Koffiefontein mine kimberlite (South Africa) contains bedded PK at depth in the diatreme, in what was originally described as TK/TKB (Naidoo et al. 2004). The Tier 4 Mwadui (Tanzania) diamond mine is the world's largest (146 ha) kimberlite-hosted diamond mine, but with low diamond grades (Table 2). The geology at Mwadui was initially described by Tremblay (1956), Mannard (1962) and Edwards and Howkins (1966). More recent studies were undertaken by Stiefenhofer and Farrow (2004), who concluded it is an almost perfectly preserved example of a post-eruptive kimberlite crater that is in-filled by a wide variety of types of RVK to ~600 m depth, with the tuff ring surrounding the crater having been eroded away. Interestingly, these RVK crater in-fill deposits are interpreted to be underlain by diatreme-filling PK (and not MVK). The Tier 1 Catoca (Angola) kimberlite-hosted diamond mine is quite large (63.6 ha; Table 2) and has ~250 m of preserved post-eruptive crater in-fill (Pervov et al. 2011). These RVK deposits and their geometry appear to bear a number of similarities to those at Mwadui. Another very large (59 ha; Table 2) and complex multiphase kimberlite is the Tier 1 Jubileinaya (Russia) diamond mine (Kurszlaukis et al. 2009, 2015). Here a number of smaller pre-cursor pipes are cut by a younger and much larger main pipe comprised dominantly of MVK, which itself is overlain by PK, and in turn overlain by a variety of post-eruptive crater in-fill RVK (Kurszlaukis et al. 2009).

More highly eroded examples of diamondiferous volcanoes, with no preserved volcanic edifice or post-eruptive crater in-fill are much more common in the geological record. The Tier 1 Argyle diamond mine (Fig. 8) is a large (47 ha, Table 2) steep sided and elongated olivine lamproite pipe that is interpreted to have formed from several distinct individual diatremes that have coalesced, and are aligned along a fault (Rayner et al. 2018a,b; Fig. 8), with the fault presumably coincident with an olivine lamproite feeder dike. The Argyle mine is interpreted to have formed by numerous phreatomagmatic eruptions (Rayner et al. 2018a,b). At the Argyle mine, the steep-walled individual diatremes (and collectively, as a larger elongated pipe structure) resemble classic steep-walled kimberlite diatremes, as observed in the Kimberley area (Clement 1982; Clement et al. 1986) and at many other global kimberlite localities. The 6.5 ha Tier 4 Majghawan olivine lamproite-hosted mine is also a steep sided diatreme, being circular–elliptical in plan-view (Rao 2007). The Atri (Bunder) twin pipe is also a steep-walled olivine

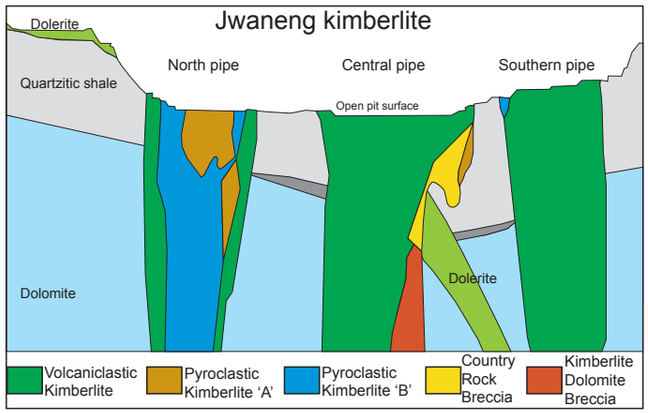

Figure 7. Simplified cross section of the Jwaneng (Botswana) triple kimberlite pipe mine and its host-rock geology. This section shows the three pipes that coalesced at the surface and are currently mined; the fourth pipe (not mined) has been omitted for clarity. Adapted from de Wit et al. (2016).

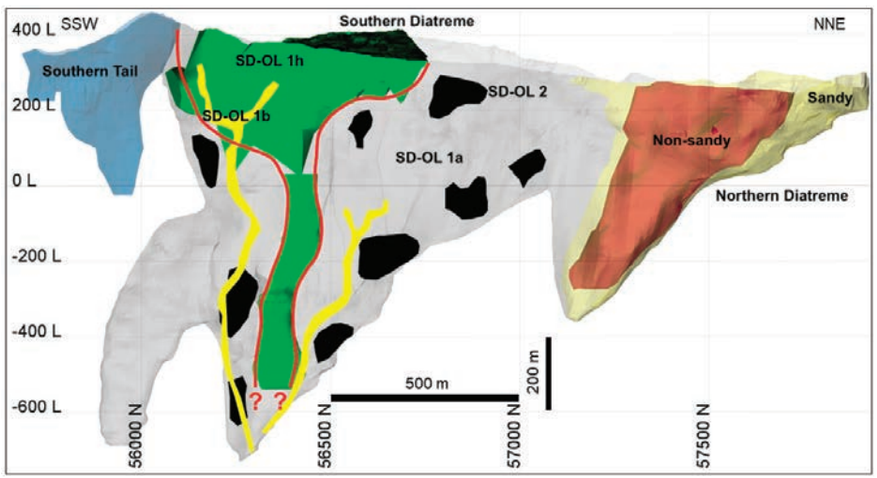

Figure 8. 3-D view of the elongated, steep-walled olivine lamproite pipe that hosts the Argyle Mine, Australia. Note the multiple olivine lamproite diatremes that make up this this pipe. The northern diatreme consists of two main sub-units, a sandy and a non-sandy phase. The southern diatreme consists of unit SD-OL 1a (**grey**), a well-bedded to massive to chaotic pyrclastic olivine lamproite; unit SD-OL 2 (**black**), a massive to crudely bedded olivine and juvenile pyroclast poor olivine lamproite; unit SD-OL 1h (**green**), a bedded to well-bedded pyroclastic olivine lamproite, and; unit SD-OL 1b (**yellow**), a massive to chaotic textured pyroclastic olivine lamproite interpreted as feeder conduits or fragments thereof. After Rayner et al. (2017, 2018b), with permission.

lamproite pipe (Das et al. 2018). The Argyle, Majghawan and Atri olivine lamproite pipes closely resemble steep-walled kimberlite diatremes i.e., they do not have "champagne-bowl shaped" or a flared diatreme (e.g., Mitchell 2020b), as per Ellendale 4 or 9 (see Fig. 6b), or Prairie Creek. The kimberlite-hosted Tier 1 Aikhal (Russia) diamond mine (Kostrovitsky et al. 2015) has a number of similarities in terms of overall pipe morphology with Argyle, including a strongly elongated (in plan-view), steep-walled pipe, which consists of multiple discrete individual diatremes.

The Tier 1, CROL-hosted 18 ha Finsch diamond mine (Fig. 9; Clement 1982), which along with the Tier 4 CROL-hosted12 ha Voorspoed mine, is somewhat unusual as many CROL in southern Africa and globally tend to form smaller-sized pipes, and/or dike and blow systems (Table 2). However, the Finsch mine has numerous similarities to South African kimberlite pipes, having a steep-walled diatreme and the pipe being in-filled by a variety of lithofacies including massive volcaniclastic, hypabyssal, and bedded/diffusely bedded volcaniclastic CROL (Clement 1982; Ekkerd et al. 2003; Field et al. 2008). Another steep-walled pipe is the 25 ha Tier 1 Udachnaya (Russia) diamond mine, a kimberlite twin pipe (Kostrovitsky et al. 2105). Plan and cross section views of the Udachnaya East and West pipes are shown in Figure 10. The 32 ha Tier 1 Cullinan (South Africa) diamond mine is another kimberlite twin pipe, with multiple discrete kimberlite phases. The geology of Cullinan mine is described by Wagner (1914), Bartlett (1998), Field et al. (2008) and de Wit et al. (2016). Other excellent examples of steep-walled kimberlite diatremes would have to include the five diamond mines in the Kimberley cluster, South Africa (Kimberley, De Beers, Dutoitspan, Bultfontein and Wesselton). The studies of Clement (Clement 1982; Clement et al. 1986) are seminal with respect to our fundamental understanding of these pipes, and kimberlite geology in general. More recent work on the Kimberley cluster pipes is summarized in Field et al. (2008) and de Wit et al. (2016).

Much smaller area pipes (<3 ha) that host economic diamond deposits include multiple Tier 2 mines at both the Ekati and Diavik mines (Canada) in the Lac de Gras kimberlite field, and the Tier 1 Internationalaya and Tier 2 23rd Party Congress mines (Russia) in the Malo-Botuoba kimberlite field (Fig. 11b; Table 2). At Lac de Gras, the A154 North and A154 South pipes of the Diavik mine (Fig. 11a) have very small surface areas (1.2 and 2.6 ha, respectively), which increase with depth (Moss et al. 2018). Multiple different kimberlite lithofacies are observed in the Diavik kimberlites, as illustrated in Figure 11a for the A154 North pipe. Moss et al. (2018) demonstrated that A154 South pyroclastic kimberlite (PK) eruptions in-filled the top of the adjacent A154 North crater (PK4-N in Fig. 11a). The observation that a kimberlite eruptive event from a nearby pipe can in-fill a crater in an older adjacent kimberlite was also described by Zonneveld et al. (2004) for the Star kimberlite, Fort à la Corne (Canada). The Internationalaya mine (Fig. 11b) is also a small (1.7 ha) steep-walled, but irregular shaped pipe that expands and contracts with depth (Kostrovitksy et al. 2015). The CROL-hosted 0.4 ha, Tier 3 Marsfontein M1 mine, and the kimberlite-hosted Tier 4 Koidu K1 and K2 pipes (both ~0.5 ha) in Sierra Leone, plus the ~1 ha The Oaks (South Africa) diamond mines are additional examples of very small pipes that have been mined (Table 2). These Tier 3 and 4 examples from Africa are further described by Field et al. (2008) and de Wit et al (2016).

In terms of surface area, the smallest diamond mines are hosted by dikes, sills, and blows, and these are typically Tier 4 or Tier 5 mines. Classic localities include the CROL-hosted Tier 4 Roberts Victor mine (Fig. 12a), which consists of two dikes with three affiliated blows and two small pipes (Wagner 1914; Field et al. 2008; de Wit et al. 2016) and the CROL dikes and blows that host diamond mines in the Bellsbank area (Fig. 12b) of South Africa (Clement 1973; Mitchell 1995; Field et al. 2008; de Wit et al. 2016).

Summary of diamond mine volcanology. Magmatic-hosted diamond deposits are quite variable in surface area (Fig. 5), 3-D geometry, morphology and volcanic architecture (dikes, sills, blows, root zones, pipes, tuff rings, tuff cones, apron deposits; Figs. 6 to 12). A 1:1 correlation does not exist between these parameters and the primary magma type (kimberlite, CROL, olivine lamproite).

Notwithstanding active or past producing diamond mines or advanced exploration projects, a paucity 3-D solids models and ore tonnage data exist for most kimberlites, CROLs and olivine lamproites. Due to the highly variable geometry and geology of these deposits, even when the surface area is known, a significant amount of drilling and drill core is required to generate

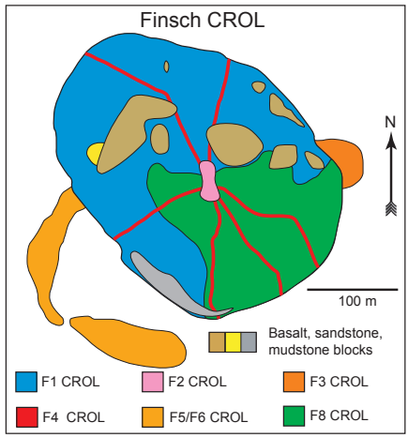

Figure 9. Simplified plan view of the Finsch (South Africa) CROL-hosted diamond mine, at the 610 m level. Note the individual CROL phases in and adjacent to the pipe, as well as the blocks of host-rock basalt, sandstone and mudstone in the pipe. Re-drawn from Field et al. (2008), after Clement (1982) and Ekkerd et al. (2003).

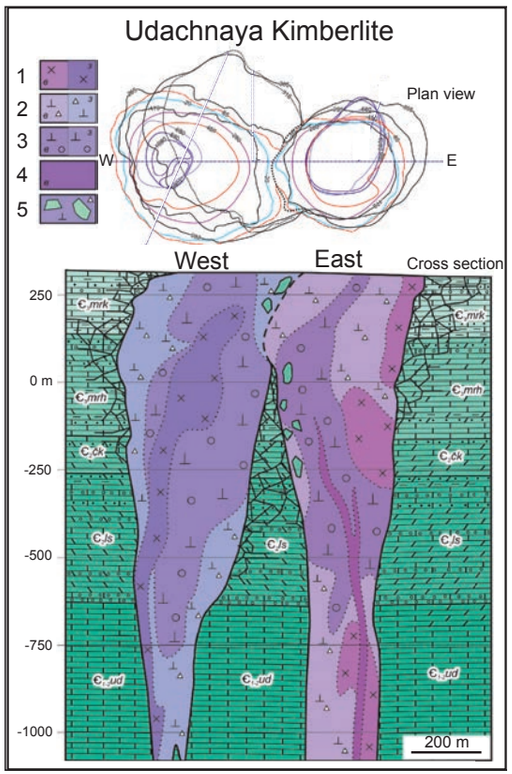

Figure 10. Udachnaya kimberlite twin pipe mine and its host rock geology. Plan and section views. Note the multiple individual phases of kimberlite in each pipe. Geology units as follows: 1 = phase 1, pyroclastic kimberlite; 2 = phase 2, kimberlite breccia; 3 = phase 3, autolithic kimberlite breccia; 4 = phase 4, pyroclastic kimberlite; 5 = sedimentary xenoliths in kimberlite. Note geology legend units 1, 2, and 3 are divided in half with the left side the east diatreme and the right side the west diatreme. After Kostrovitsky et al. (2015), with permission.

these 3-D models and calculate ore tonnages. This is further complicated by the fact that these diamondiferous volcanoes all have distinctive and discrete lithofacies, formed by differing processes that can have exceptionally variable diamond grades (e.g., Clement 1982; Clement et al. 1986; Kjarsgaard 2007a,b; Field et al. 2008). From an economic perspective (i.e., the determination of ore reserve or resource tonnage) this is an exceptionally challenging task, as not all of a diamondiferous volcano may contain economically viable ore (Wagner 1914; Nowicki 2014; Kjarsgaard et al. 2019). In other words, only part or parts of a diamondiferous volcano could be of economic interest, with the rest being low diamond grade, or waste rock.

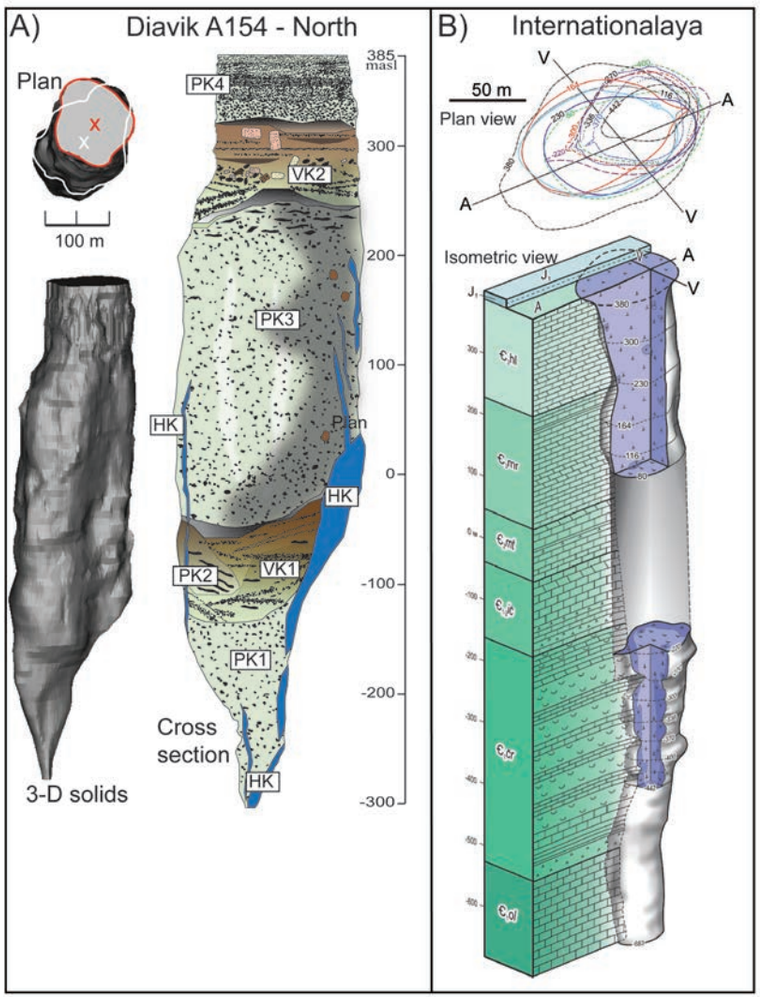

Figure 11. (**A**) Plan and 3-D solids and cross section of the A154—North kimberlite, Diavik Mine, Lac de Gras kimberlite field, NT, Canada. Note the multiple phases of kimberlite in the A154 North cross section. HK = hypabyssal kimberlite; PK1, PK2, PK3 = pyroclastic kimberlite phases 1, 2, 3; VK1, VK2 = volcaniclastic kimberlite phases 1 and 2. After Moss et al. (2018), with permission. (**B**) The steep-walled Internationalaya, Russia kimberlite, plan and isometric views. After Kostrovitsky et al. (2015), with permission.

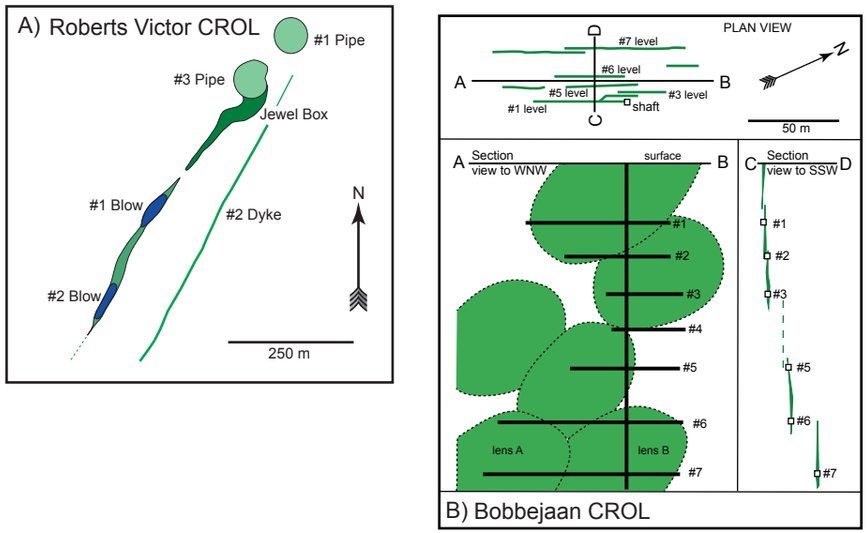

Figure 12. (**A**) Roberts Victor Mine (South Africa) CROL dike—blow—pipe system. Re-drawn after Wagner (1914), Gurney and Kirkley (1996) and de Wit et al. (2016). Bobbejaan Mine (Bellsbank area, South Africa), CROL en-echelon dike system. Adapted and re-drawn from Clement et al. (1973). Note there is diamond grade and rough diamond value variation between the pipes, blows and dikes in (**A**) and the dike lenses shown in (**B**).

Mineralogy and mineral chemistry

Comparative mineralogy of magmatic rocks that host diamond mines. Kimberlite, CROL and olivine lamproite contain a widely variable load of xenocrysts, including macrodiamonds. A summary and comparison of the mineralogy of kimberlite, carbonate-rich olivine lamproite (CROL) and olivine lamproite is listed in Table 1. The petrography of ultramafic lamprophyres (UMLs, variety aillikite), which have some similarities with kimberlite and CROL, is compared to and described and discussed in detail by Tappe et al. (2005). A first order observation from Table 1 is that the mineral assemblages (and the modal abundances of these minerals) for these three rock types can be overlapping, and/or similar (see also Tappe et al. 2005). Olivine, spinel, phlogopite, apatite and perovskite are common minerals to all three rock types. The application of mineral chemistry—specifically mineral zoning trends—has been previously utilized by Mitchell (1986) to classify, distinguish and discriminate "kimberlites" (i.e., historically combined kimberlite plus CROL), lamproites, and UMLs. A number of important observations concerning the mineralogy and mineral chemistry of these "lamprophyre clan rocks" was reviewed by Rock (1988). Subsequently, Mitchell and Bergman (1991) and Mitchell (1995) re-visited these mineralogical and mineral chemistry discriminant classifications with respect to "archetypal kimberlites", "orangeites", lamproites, and UML.

Here, we re-examine the suites of minerals observed in kimberlite, CROL and olivine lamproite, and scrutinise the mineral chemistry zoning trends for groundmass phlogopite and spinel for these three primary diamond-bearing magma types. Our focus is on the primary mineralogy of little altered, hypabyssal or coherent examples of cratonic kimberlite, CROL and olivine lamproite. Note that we do not examine in detail "evolved" CROL, or "evolved" olivine lamproites, or primary leucite lamproites, or Mediterranean lamproites, for which we use the generic term lamproite, even though some of these rocks may be diamond-bearing.

Incorporation of lithospheric mantle and crustal xenoliths and xenocrysts is commonly observed in kimberlite, CROL and olivine lamproite, more so in volcaniclastic (fragmental) rocks. The incorporation of mantle and crustal materials, and their partial or complete digestion or assimilation into the melt can result in the formation of a variety of "new" minerals, or magmatic overgrowths on existing minerals (Caro et al. 2004; Gaudet et al. 2018; Dalton et al. 2019). Due to the volatile-rich nature of kimberlite and CROL (both CO_2- and H_2O-rich) and olivine lamproite (H_2O-dominant) as detailed in *Whole Rock Geochemistry, this chapter*, there can be significant carbohydrothermal and hydrothermal alteration with concomitant precipitation of subsolidus mineral phases and suites of these minerals (e.g. serpentine plus magnetite, serpentine plus magnetite plus calcite, etc) as described in more detail below. The magmatic crystallization of, versus the fluid precipitation of, e.g., calcite or magnetite certainly can complicate the classification of these three rock types.

Kimberlite—General and petrographical aspects. Macrodiamonds in kimberlite are xenocrysts. Hypabyssal kimberlite is typically rich in macrocrysts (large crystals), which includes mineral grains from 0.5–10 mm in size. Note that the 0.5 mm size break is completely arbitrary, as macrocryst minerals can form part of a continuum with similar minerals < 0.5 mm and > 10 mm in size; as an example, see the discussions in Moss et al. (2010) and Moore et al. (2021) regarding olivine grain size in kimberlites. Macrocrysts have varied origins, and can be comprised of mantle xenocrysts such as olivine, Cr-diopside, enstatite and Cr-pyrope garnet derived from the dis-aggregation of peridotite xenoliths (dunite, harzburgite, lherzolite and wehrlite), omphacite and pyrope-almandine garnet derived from dis-aggregated eclogite xenoliths, and Mg-ilmenite and phlogopite plus amphibole xenocrysts from metasomatized peridotites (e.g., Dawson 1980; Nixon 1987). Macrocrysts in kimberlite also include bonafide cognate high pressure kimberlite magma-derived phenocrysts, with olivine being the classic example. More recently, the term antecryst (high pressure phenocrysts crystallized from an earlier-formed and "allied" proto-kimberlite or kimberlite magma) has also been applied to a subset of olivine macrocrysts (Sobolev et al. 2015; Soltys et al. 2020). An additional complexity of kimberlite mineralogy is the occurrence of the megacryst suite of minerals (olivine, phlogopite, Cr–Ti-pyrope, Cr-diopside, enstatite, Mg-ilmenite, zircon, baddelyite), which are large (>1 cm) single grains (or fragments thereof) up to ~30 cm in size. Both a Cr-poor (Boyd and Nixon 1973) and Cr-rich (Eggler et al. 1979) suite are known, but the distinction between them in kimberlites globally is somewhat poorly defined. Megacryst suite mineral(s) occur in variable modal proportions in kimberlite. The Cr-poor suite of megacryst minerals was interpreted as high pressure (cognate) minerals crystallized from a kimberlite or proto-kimberlite magma (e.g., Gurney et al. 1979; Schulze 1987). More recent studies suggest the Cr-rich suite represents greater mantle lithosphere interaction with kimberlite magma, whereas the Cr-poor suite has a less dominant lithosphere interaction with kimberlite magma (e.g., Pivin et al. 2009; Bussweiler et al. 2016, 2018).

In a kimberlite, the coarser-grained minerals (megacrysts, macrocryts, antecrysts and cognate phenocrysts) are set in a finer-grained matrix, which imparts a distinctive inequigranular texture to these rocks—prominent in outcrop, drill core and thin section. Kimberlite matrix mineralogy, often viewed as complex, is in fact relatively simple (Table 1). Olivine, spinel and phlogopite phenocrysts and microphenocrysts (typically < 0.2–1 mm) are observed in quite variable modal proportions; these grains can have xenocrystic or antecrystic cores. Importantly, in kimberlite, phlogopite can be rare or absent (e.g., Nielsen and Sand 2008; Tovey et al. 2021), but may also be very abundant (e.g., Taylor and Kingdom 1999; Howarth and Giuiani 2020). The olivine, spinel and phlogopite (when present) phenocrysts are set in a very fine-grained (< 0.2 mm) groundmass assemblage consisting of a suite of minerals of magmatic origin, including: olivine, spinel, phlogopite–kinoshitalite and phlogopite–tetraferriphlogopite mica, apatite, perovskite, monticellite, calcite, dolomite and ilmenite, with less common rutile and sulfides. Any given kimberlite groundmass contains only a subset (i.e., not all) of these

minerals. Additional minor, rare minerals are also observed in kimberlite, but these can often only be identified by electron beam methods via back scattered electron images (BSEI) on a scanning electron microscope (SEM) or electron microprobe (EMP) with energy dispersive spectrometry (EDS) or wavelength dispersive (WDS) analysis, due to their small size (<10 μm). Glass (not a mineral) is present only as exceptionally rare melt inclusions (Howarth and Büttner 2019), but Skinner and Marsh (2004) have suggested that groundmass antigorite in kimberlite represents devitrified glass. These findings require further study, however. Combinations of calcite, dolomite, serpentine, magnetite and rare talc (plus other minerals) are precipitated at sub-solidus temperatures from fluids, which variably overprint the macrocrysts and magmatic crystallized phenocryst/microphenocryst/groundmass mineral phases and can constitute significant modal proportions of a kimberlite. In Lac de Gras, C–O isotopic analyses of precipitated calcite (with serpentine) and dolomite coupled with modelling determined the fluids to be of deuteric origin (Wilson et al. 2007b). Based on analyses of serpentine minerals and modelling, Mitchell (2013) proposed a deuteric origin for serpentinizing fluids. In contrast, Sparks (2013) has advocated a crustal origin for serpentinizing fluids in kimberlites, while Giuliani et al. (2014) has modelled that serpentinizing fluids could have either a meteoric, or a mixed deuteric–meteoric origin.

Crustal contamination of kimberlite can be quite common; granitoid contamination of kimberlite magma results in higher Si-, Al-, alkali-contents and the potential for crystallization of non-diagnostic kimberlite minerals such as diopside (e.g., Fulop et al. 2018; Gaudet 2018). For example, diopside, titanite and amphibole are not observed in uncontaminated kimberlite, as the silica activity is too low in these ultrabasic melts for these minerals to crystallize (Mitchell 1986, 1995, 2020a). Similarly, alkali- and plagioclase feldspars and the feldspathoid minerals kalsilite and nepheline are not observed due to the low Na, K and Al-activities in the kimberlite melt; the absence of melilite is interpreted to be due to low Na- and/or Al-activities (Mitchell 1995; Kjarsgaard et al. 2009; Foley et al. 2019).

Carbonate-Rich Olivine Lamproite (CROL)—General and petrographical aspects. Macrodiamonds in CROL are xenocrysts. Similar to kimberlite, a wide array of macrocryst minerals occur in CROLs, consisting dominantly of xenocrysts derived from a variety of mantle xenoliths (see *Kimberlite—General and petrographical aspects*). As with kimberlites, olivine xenocrysts are observed in variable quantities in CROL. Mantle peridotite and eclogite xenoliths, plus minerals derived from their disaggregation can be very common in some CROL (e.g., Roberts Victor eclogites). Megacryst suite minerals are not characteristic of CROL, but are observed at a few localities (Skinner et al. 1994; Moore and Gurney 1991). In CROL, cognate (high pressure) phlogopite phenocrysts (and thus potentially also antecrysts) can be common. In contrast, phlogopite antecrysts, cognate phenocrysts and phenocrysts in kimberlites are a minor to rare phase, and of potentially have cryptogenic origin (Mitchell 1995). The mineralogy of CROL is characterized by the occurrence of olivine and phlogopite (macrocrysts, phenocrysts, microphenocrysts), and spinel phenocrysts/microphenocrysts set in a groundmass of apatite, calcite (or dolomite), spinel, perovskite and phlogopite. Note that diopside microphenocrysts and groundmass diopside may be present, or absent (Wagner 1914; Mitchell 1995). The occurrence of magmatic calcite in CROL is consistent with the observation that there is a statistical correlation between measured wholerock CaO and CO_2 concentrations (as per kimberlites; see *Whole Rock Geochemistry*). CROL are both CO_2- and H_2O-rich (as per kimberlite), and similar to kimberlite they contain subsolidus low temperature fluid-precipitated minerals that can include calcite, dolomite, serpentine, talc and magnetite. A distinctive subset of "evolved CROL" occur at Pniel and Postmasburg (South Africa) that originally were suggested to be lamproites by Tainton and Browning (1991). These rocks, as well as other "evolved CROL" localities in South Africa identified by Mitchell (1995) have petrographic similarities to lamproites with respect to the presence of sanidine and potassium richterite in the groundmass and more rarely as microphenocryts. In evolved CROL, olivine

macrocrysts and phenocrysts may be mantled/overgrown by parallel olivine aggregates ("dog tooth habit") as observed at Postmasburg and Sover North (Mitchell 1995). Plagioclase feldspars, the feldspathoid minerals kalsilite and nepheline, and melilite are absent in CROL.

Olivine Lamproite—General and petrographical aspects. Macrodiamonds in olivine lamproite are xenocrysts; leucite lamproite can be diamondiferous, but these rocks have lower diamond tenor and have not been proven to be economically viable thus far (Mitchell and Bergman 1991; Mitchell 2020b). Similar to kimberlite and CROL, a suite of macrocryst minerals are present in olivine lamproites, that can include, for example, olivine and phlogopite, plus xenocrysts derived from a variety of mantle xenoliths (see *Kimberlite—General and petrographical aspects*). However, mantle xenoliths and xenocrysts derived from their disaggregation are typically rare in olivine lamproite and even less so in lamproite, as compared to kimberlite or CROL. The megacryst suite of minerals (typical of many kimberlites) is completely absent (or possibly exceptionally rare) in olivine lamproite. However, high pressure cognate phenocrysts (and thus potentially also antecrysts) such as phlogopite, diopside, richterite and olivine, as well as cognate xenoliths (e.g., phlogopite clinopyroxenite, glimmerite), are observed in both olivine lamproite and lamproite, but these are perhaps more common in lamproite (Mitchell and Bergman 1991).

The mineralogy of olivine lamproite is characterized by the occurrence of olivine (macrocrysts, phenocrysts, microphenocrysts; Jaques et al. 1986; Jaques and Foley 2018), plus spinel and phlogopite phenocrysts/microphenocrysts that are set in a groundmass of glass, often altered. Fine-grained (<50 µm) apatite, perovskite and leucite are variably observed, but may be rare or absent (Jacques et al. 1986). In coarser-grained coherent or hypabyssal (aka "magmatic") olivine lamproite, poikilitic phlogopite plates can be common, and in the very coarsest-grained examples interstitial or poikilitic K-richterite is also observed (Jaques et al. 1986). Olivine macrocrysts with "dog-tooth habit" overgrowths occur in some olivine lamproites (e.g., Prairie Creek; Scott Smith and Skinner 1984). In leucite lamproite and more evolved lamproites, apatite, perovskite, leucite, sanidine, diopside, wadeite and ilmenite occur in the groundmass (Jaques et al. 1986; Mitchell and Bergman 1991); however, only a subset of these minerals may be present in any given sample. These minerals, if present, are far more common and typically of larger grain size than compared to what is observed in olivine lamproite. Additional accessory minerals of lamproite include rutile, hollandite–priderite, jeppeite, and Ti–Zr garnets, but these are rare or absent in olivine lamproites (Mitchell and Bergman 1991). Crustal contamination can also be quite common in volcaniclastic lamproite, for example the high quartz contents at Argyle and Ellendale (Australia) and Prairie Creek (Arkansas, USA), derived from their siliciclastic host-rock sediments. Alteration products of serpentine and talc are typical of olivine lamproites; secondary carbonate minerals are observed. Minor modal amounts of calcite, interpreted as primary have also been observed in olivine lamproites, providing a potential link between olivine lamproites and CROLs. The feldspathoid minerals kalsilite and nepheline are not observed in olivine lamproites, nor are melilite or plagioclase.

Mineral chemistry—General aspects of kimberlites, CROLs and olivine lamproites. The compositions of the various minerals observed in kimberlites, CROLs and olivine lamproites can be quite distinct as compared to other rock types/magmatic lineages. For example, in olivine lamproite, lamproite and evolved CROL, amphiboles are K-, Ti-rich richterites (e.g., Mitchell 1985, 1995); in lamproites, sanidine (if present) is often iron-bearing, with Fe_2O_3 substituting for Al_2O_3 (e.g., Carmichael 1967). Comparing kimberlites, CROLs and olivine lamproites, a mineral phase can have near-identical, or conversely quite disparate compositions and zoning trends. A significant amount of major- and minor-element mineral chemistry data determined by EMP (+/- trace elements determined by laser ICP-MS) exists for olivine, spinel, phlogopite, diopside, monticellite and more recently for apatite, perovskite and carbonates. Spinel and phlogopite are considered to have unique compositions and zoning trends that are diagnostic with respect to kimberlite, CROL and olivine lamproite/lamproite

(Mitchell 1986, 1995; Mitchell and Bergman 1991; Mitchell et al. 2019). Our understanding of the compositional range of olivine and its paragenetic significance (xenocrystal or magmatic in origin) in kimberlite, CROL and olivine lamproite has advanced significantly, but is still imperfectly understood and debated (e.g., Bussweiler et al. 2015; Giuliani 2018, Jaques and Foley 2018; Howarth and Nembambula 2021; Moore et al. 2021). However, identification of xenocrystic olivine versus magmatic formed olivine, provides insight to lithospheric mantle sampling, and thus potentially macrodiamond sampling.

Spinel zoning trends. Two different plots—the "reduced" and "oxidized" spinel prisms (Irvine 1965; Haggerty 1976; Mitchell 1986)—are typically used to examine compositional trends of spinel in kimberlite, CROL, olivine lamproite, and many other basic or ultrabasic rock types. A projection to the front face of the reduced or oxidized spinel prism is often utilized to generate a bivariate plot. The oxidized prism projection (Fig. 13) has axes of Mg# (using a stoichiometric calculation for Fe^{2+}) versus $Fe^{3+}/(Fe^{3+} + Cr + Al)$, while the reduced prism projection (Fig. 14) has axes of Mg# (using Fe_{total}) versus $Ti/(Ti + Cr + Al)$. The use of Fe_{total} instead of Fe^{2+} to determine Mg# in spinel shifts the Mg# to lower values, as discussed by Pasteris (1982). The reduced and oxidized spinel prism plots (or the projected bivariate plots) have been suggested to provide diagnostic discrimination between spinel from kimberlite, CROL, and olivine lamproite.

Kimberlite spinel "Trend 1" compositions (the magnesian ulvöspinel trend; Mitchell 1986) are defined by spinel evolution at a high, and near constant Mg# (Figs. 13, 14). "Trend 2" spinel compositions (the titanomagnetite trend; Mitchell 1986) observed in olivine lamproite, lamproite, CROL and also some kimberlites are defined by spinel zoning with decreasing Mg#, followed by subsequent evolution at constant and low Mg# (Figs. 13, 14). While many kimberlites have spinel compositions that fall into the Trend 1 field, this however, is an oversimplification. A number of kimberlites have spinel compositions that fall into Trend 2, such as those at the Koidu mine (Tompkins and Haggerty 1984), the Jagersfontein mine (Taylor and Kingdom 1999), the Renard mine (Birkett et al. 2004), De Beers peripheral (Pasteris 1983), Rich (Roeder and Schulze 2008), Buffalo Hills K6 (Eccles et al. 2004), Tunraq and Elwin Bay (Mitchell 1986, 1995) and Zagodachnaya and Marushkaya (Rozova et al. 1982).

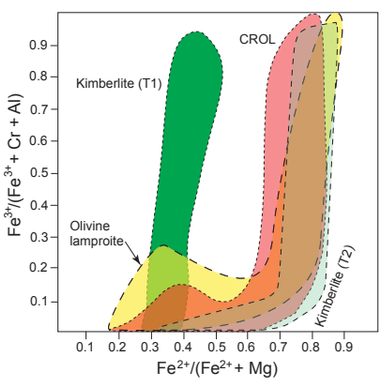

Figure 13. Spinel "oxidized" bivariate plot; Mg# (using a stoichiometric calculation for Fe^{2+}) versus $Fe^{3+}/(Fe^{3+} + Cr + Al)$, outlining the region of kimberlite Trend 1 and Trend 2 spinel compositions, and olivine lamproite and CROL Trend 2 spinel compositions. See text for details and data sources.

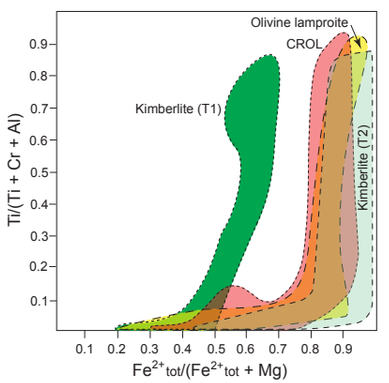

Figure 14. Spinel "reduced" bivariate plot; Mg# (using Fe_{total}) versus $Ti/(Ti + Cr + Al)$, outlining the region of kimberlite Trend 1 and Trend 2 spinel compositions, and olivine lamproite and CROL Trend 2 spinel compositions. See text for details and data sources.

Furthermore, some kimberlites (e.g. Jagersfontein, De Beers, Tunraq, Elwin Bay) have both Trend 1 and Trend 2 spinels, which are observed in distinct phases of kimberlite. The situation is additionally complicated by kimberlites with spinel compositions that lie intermediate between Trend 1 and Trend 2 (T1–2), such as those from the Jericho mine (Roeder and Schulze 2008), Tonguma in Sierra Leone (Howarth and Giuliani 2020) and Maniitsoq in Greenland (Nielsen et al. 2009). The Maniitsoq kimberlite is also of additional interest as it contains spinel compositions with higher Mg# than typical for Trend 1 spinels. Of additional intrigue is the recognition of Trend 1 spinels in some carbonatites (Roeder and Schulze 2008).

CROL and olivine lamproite contain spinel grains with compositions consistent with Trend 2 (Figs. 13, 14); an exception being the New Elands CROL with spinel compositions that are intermediate between Trend 1 and Trend 2 (Roeder and Schulze 2008). Because a variety of non-unique spinel chemistry trends are known, Roeder and Schulze (2008) emphasized the application of a molar Cr^{3+}–Al^{3+}–Fe^{3+} spinel ternary plot (Fig. 15). They described eight spinel zoning trends for kimberlites (and CROLs). The three main types of spinel zoning trends in kimberlites include Trend 1 and Trend 2, together with a third trend, in which spinel zones from chromite to pleonaste. Roeder and Schulze (2008) also noted that pleonaste can further evolve to Trend 1 spinel compositions (see also Abersteiner et al. 2019; Tovey et al. 2020), and that Trend 1 spinel can evolve to pleonaste.

Phlogopite zoning trends. Application of two bivariate plots (Al_2O_3 versus FeO_{tot} and Al_2O_3 versus TiO_2) for micas have been suggested to permit discrimination between kimberlite, CROL, olivine lamproite, and other rock types (Figs. 16, 17; e.g., Mitchell 1995). Compositionally zoned groundmass phlogopite micas in kimberlite have previously been noted to have an Al-enrichment trend (phlogopite-eastonite trend), whereas phlogopite in CROL and olivine lamproite exhibit decreasing Al with increasing Fe and variable (increasing; constant or decreasing) Ti contents (e.g., Mitchell and Bergman 1991; Mitchell 1995; Mitchell et al. 2019). The typical kimberlite groundmass phlogopite zoning trend is one of Al-enrichment (often with Ba-enrichment; Spriggs 1988), with decreasing Ti and constant or decreasing Fe (Figs. 16, 17). However, this phlogopite Al-enrichment trend, while typical of kimberlite does not describe all kimberlite micas. A zoning trend of decreasing Al, and decreasing or constant Ti, with Fe-enrichment is also known (i.e., a phlogopite-tetraferriphlogopite zoning trend; Figs. 16, 17). Moreover, this tetraferriphlogopite (TFP) trend is observed in a number of kimberlites globally, such as: Jagersfontein mine, South Africa (Taylor and Kingdom 1999); Renard mine, Canada (Birkett et al. 2004); Koidu mine and Tonguma, Sierra Leone (Mitchell 1995; Howarth and Giuliani 2020); Ororoo, Australia (Scott Smith et al. 1984); Mayeng, South Africa (Apter et al. 1984); Skinners sill, South Africa (Mitchell 1984); Antochka, Guinea (Mitchell 1995); K4 Buffalo Hills, Canada (Eccles et al. 2004); Porpoise, Lac de Gras, Canada (Armstrong et al. 2004); Guaniamo, Venezuela (Kaminsky et al. 2004) and Adamantin, Quebec, Canada (Barnett and Laroulandie 2017). An Al–Fe–Mg ternary plot is also useful for examining phlogopite mica Al-enrichment and Al-depletion trends (Rock 1988; Mitchell 1995).

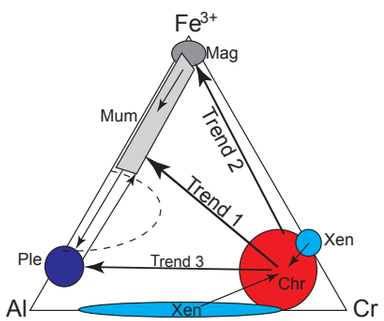

Figure 15. Spinel molar Cr^{3+}–Al^{3+}–Fe^{3+} ternary plot, showing the spinel xenocryst–chromite zoning trends, and the chromite–spinel Trend 1, chromite–spinel Trend 2, and chromite–spinel Trend 3 (pleonaste trend), as well as additional, less common zoning trends. Xen = xenocryst spinel; Chr = chromite; Ple = pleonaste; Mag = magnetite; Mum = magnesian ulvöspinel magnetite. Modified and adapted from Roeder and Schulze (2008).

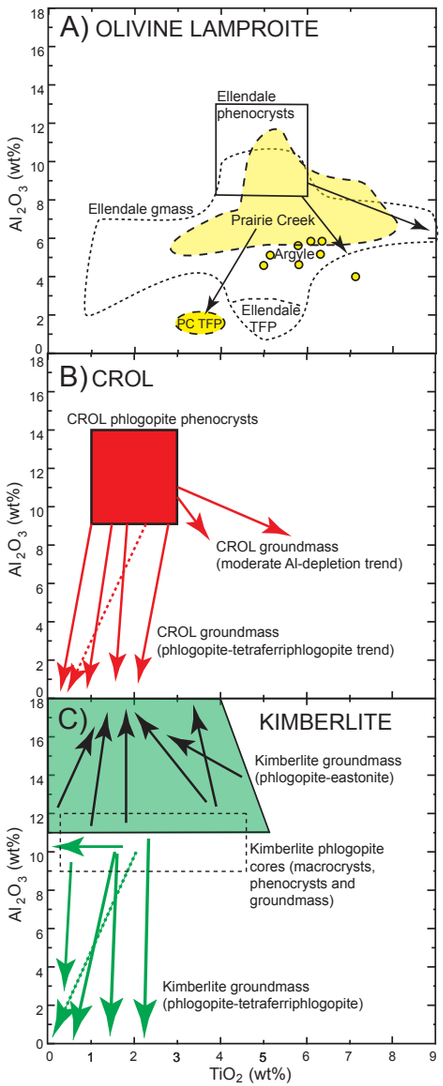

Figure 16. Bivariate plot of Al_2O_3 versus TiO_2 for phlogopite mica from (**A**) olivine lamproites, (**B**) CROL, and (**C**) kimberlites. For olivine lamproites and CROLs, zoning trends are from phenocryst cores to rims and groundmass grains; both these rock types contain phlogopite that exhibit moderate- and/or extreme-Al depletion trends. Kimberlite zoning trends can be observed within groundmass grains, and as phlogopite cores (macrocrysts, phenocrysts, microphenocrysts) with compositional zoning to the margins. In kimberlites, phlogopite Al-enrichment and Al-depletion trends are observed. See text for details and data sources.

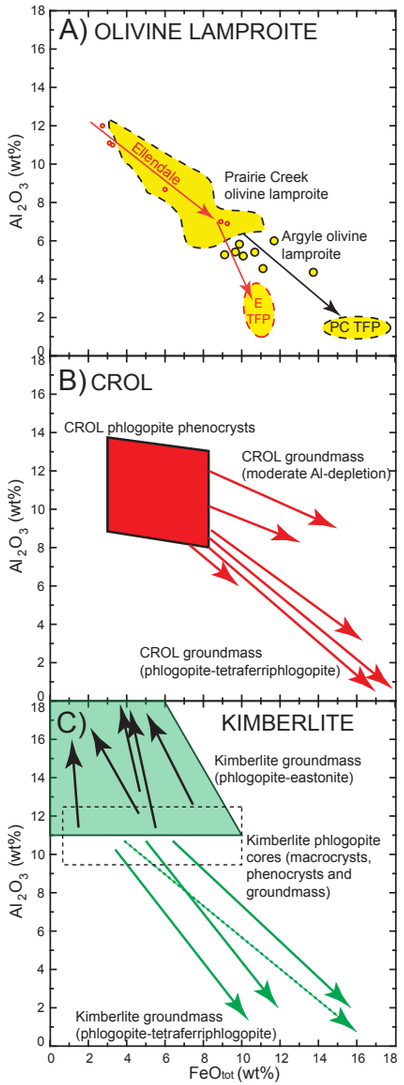

Figure 17. Bivariate plot of Al_2O_3 versus FeO_{total}, for phlogopite mica from (**A**) olivine lamproites, (**B**) CROL, and (**C**) kimberlites. For olivine lamproites and CROLs, zoning trends are from phenocryst cores to rims and groundmass grains; both these rock types exhibit phlogopite with moderate-Al depletion- and extreme-Al depletion (to TFP) trends. Kimberlite zoning trends can be observed within only groundmass grains, and as phlogopite cores (macrocrysts, phenocrysts, microphenocrysts) with compositional zoning to the margins. See text for details and data sources

CROL micas exhibit a trend of phlogopite zoning towards Al-depleted tetraferriphlogopite. These micas typically have an extreme Al-depletion trend, with very low Al_2O_3 concentrations (to <2 wt% Al_2O_3) and concomitant decreasing or constant TiO_2 (< 2 wt%), with FeO-enrichment (Figs. 16, 17). Examples include the Sover, Lace, New Elands, Finsch, Helam (Swartruggens) and Star (Theunissen) CROL-hosted diamond mines (Figs. 16, 17; data of Mitchell 1995). However, a "moderate" phlogopite Al-depletion trend (to 8–9 wt% Al_2O_3) is noted at the Voorspoed CROL-hosted diamond mine, and from a CROL dike in the Postmasburg area (Figs. 16, 17; data of Mitchell 1995). Tetraferriphlogopite is also reported from Sisimiut, Greenland (Thy et al. 1987). A subtle difference between the phlogopite—tetraferriphlogopite zoning trends for CROL and kimberlite is observed: CROL mica tend to have slightly higher FeOt concentrations (14–18 wt%) as compared to kimberlite mica (11–16 wt%) at the lowest Al_2O_3 concentrations (Figs. 16, 17). Thus, these kimberlite TFP micas have comparatively higher Mg# as compared to CROL TFP micas.

Olivine lamproite micas typically exhibit a phenocryst–microphenocryst—groundmass Al-depletion trend that is quite variable depending upon the locality. In general, there are a limited number of studies with detailed core to rim mica zoning trends. At the Argyle olivine lamproite, with increasing Fe, alumina decreases from 6 to 4 wt% Al_2O_3, with titanium concentrations of 5–7 wt% TiO_2 (Jaques et al. 1986). For olivine lamproites from the Ellendale field, coarse groundmass micas exhibit decreasing alumina (12 to 6 wt% Al_2O_3) with decreasing Mg# (90 to 65) and Ti concentrations increasing from ~4 to ~10 wt% TiO_2. Fine groundmass micas exhibit decreasing alumina (8 to 1 wt% Al_2O_3) with decreasing Mg# (90 to 60) and variable titanium concentrations of ~1 to ~9 wt% TiO_2 (Jaques et al. 1986). Prairie Creek micas have 11 to 5 wt% Al_2O_3, with 5 to 9 wt% FeO_{tot} and titanium concentrations of 3–8 wt% TiO_2; tetraferriphlogopite rims are also observed with 1–2 wt% Al_2O_3, 3–4.5 wt% TiO_2 and 14–17 wt% FeO_{tot} (Scott Smith and Skinner 1984; Mitchell and Bergman 1991). Tetraferriphlogopite mica has also been documented from olivine lamproites at the American mine, Arkansas (Mitchell 1985), Atri, India (Das et al. 2018) and at Argyle (Jaques et al. 1986). In olivine lamproite, these TFP micas appear as distinct rims (i.e., phlogopite has a distinctive compositional break, and a TFP rim), in comparison to CROLs in which TFP micas are typically part of a continuum of compositions with phlogopite that is zoned to tetraferriphlogopite (Figs. 16, 17).

Olivine chemistry. A significant number of studies have examined olivine compositions in kimberlite, CROL and olivine lamproite. In kimberlites, the key issue is examination and identification of xenocrystic olivine versus magmatic olivine (with the latter collectively including megacrysts, cognate phenocrysts, antecrysts, phenocrysts and microphenocrysts); this is termed the kimberlite "olivine problem" (see Fig. 18). Two quite disparate views are held, namely that all olivine is xenocrystic, excepting the thin rims and rinds (when present) that are interpreted as magmatic overgrowths (e.g., Kamenetsky et al. 2008; Brett et al. 2009). In contrast, Moore et al. (2021) suggest that the majority of olivine in kimberlites is not xenocrystal, but of magmatic origin. A third point of view is that olivine in kimberlite can be both of xenocrystal origin and magmatic (forming at mantle to crustal pressures) origin (e.g., Boyd and Clement 1977; Kjarsgaard et al. 2010; Giuliani 2018; Soltys et al. 2018; Lim et al. 2018; Mitchell et al. 2019; Soltys et al. 2020). In kimberlite, olivine has a continuum of grain sizes (e.g., Field et al. 2009; Moss et al. 2010; Harvey et al. 2013; Moore et al. 2021), with larger grains tending to be rounded, and smaller grains typically subhedral to euhedral (Mitchell 1995; Mitchell et al. 2019). The absence of a 1:1 compositional correlation (e.g., Mg# and Ni, Mn, Ca) between olivine from granular and sheared peridotite xenoliths and kimberlite macrocrystal olivine (with both olivine types sourced from the same kimberlite or kimberlite field), clearly suggest that not all olivine macrocryst cores are derived from disaggregation of mantle peridotite (e.g., Kjarsgaard et al. 2010; Giuliani 2018; Soltys et al. 2020; Moore et al. 2021; see Fig. 18). Specifically, this would include olivine that are not clearly part of the megacryst suite, which have Mg# ~89–78, (e.g., Boyd and Clement 1977; Lim et al. 2018; Giuliani 2018; Moore et al. 2021).

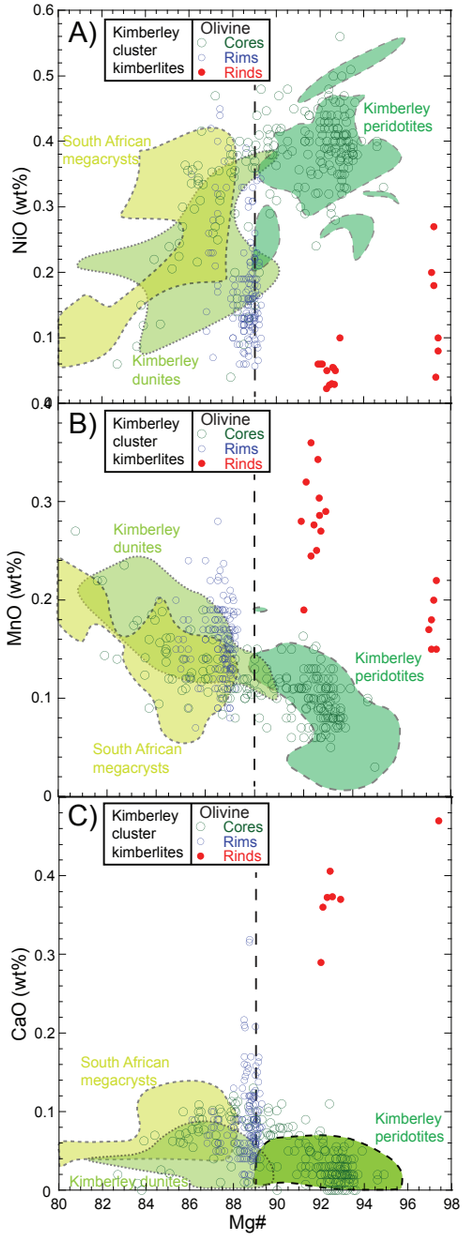

Figure 18. (**A**) Mg# vs NiO (**B**); Mg# vs MnO; (**C**) Mg# vs CaO for Kimberley cluster kimberlite-derived olivine macrocrysts cores, rims and rinds. Composition of olivine from coarse and sheared mantle peridotites, and olivine from dunites (interpreted as magmatic cumulates that are associated with the megacryst suite) from Kimberley cluster kimberlites are shown as fields. The field for southern African olivine megacrysts is also shown. All raw olivine data from Soltys et al. (2020).

Olivine compositions in CROL are remarkably similar to those in kimberlite, with a wide range in modal abundance and grain size, with larger grains often rounded and smaller grains being rounded, subhedral and euhedral (Mitchell 1995; Moore 1998; Howarth and Nembambula 2021). Euhedral and subhedral olivine phenocrysts in CROLs appear to have a more restricted compositional range with Mg# 89–93, as compared to kimberlites with Mg# 85–93 (Mitchell 1995; Mitchell et al. 2019) However, more data for olivine in CROL (and complimentary mantle xenoliths) would be useful to confirm this notion.

Olivine macrocrysts from both the Ellendale, Australia and Prairie Creek, U.S.A. olivine lamproites are interpreted to contain both xenocrystal olivine and phenocrystal olivine (Jaques and Foley 2018; Scott Smith and Skinner 1984). A detailed study of olivine from the Ellendale olivine lamproites (Jaques and Foley 2018) determined that olivine from mantle xenoliths (Mg# 90.1–92.4), larger (>1 mm) olivine macrocryst grains (Mg# 89.7–92.9), and smaller (<1 mm) olivine cores (Mg# 90–93) all have essentially similar Mg#'s, with a subset of phenocryst cores having slightly lower Mg#'s (87–90). However, olivine phenocryst zoning trends (e.g., Ni, Ca, Mn versus Mg#) and rim compositions on all olivine grains indicate that the >1 mm versus <1 mm size break corresponds remarkably well to the xenocrystal olivine and phenocrystal olivine compositional break (Jacques and Foley 2018). The Wajrakarur (India) P4 and P12 olivine lamproites have olivine xenocryts with Mg# ~91–94. However, olivine phenocrysts have lower Mg# of ~89–85 in P4 and ~87–83 in P12 (Shaikh et al. 2018; Sarkar et al. 2021) i.e., they are more evolved as compared to olivine phenocrysts in Ellendale or Prairie Creek olivine lamproites.

Summary of mineral chemistry and the discrimination of kimberlite, CROL and olivine lamproite. The petrography and mineralogy of the three rock types is outlined in Table 1, which details the similarities and differences between them. Some broad generalizations are as follows.

Kimberlites typically have spinel Trend 1 compositions (chromite—magnesian ulvöspinel trend), Importantly however, some kimberlites have spinel Trend 2 compositions (chromite–titanomagnetite trend), as well as spinel compositions that lie intermediate between Trend 1 and Trend 2 (T1–2), or, have higher Mg# than is the "norm" for Trend 1 spinels. Kimberlites also usually have phlogopite micas that exhibit zoning with Al- (and Ba-) enrichment and concomitant Ti- (and Fe-) depletion (the phlogopite-eastonite trend). A second kimberlite mica zoning trend is also known, an Al- and Ti-depletion trend with increasing Fe (i.e., phlogopite to tetraferriphlogopite). Note that kimberlites with atypical spinel or phlogopite mica zoning trends are hosts to diamond mines.

CROLs typically have spinel Trend 2 compositions (chromite–titanomagnetite trend). Phlogopite mica has a characteristic extreme Al- and Ti-depletion with Fe-enrichment (phlogopite to tetraferriphlogopite) trend. A second mica trend has moderate Al-depletion with increasing Fe- and Ti-enrichment. CROL also rarely have spinel compositions intermediate between Trend 1 and Trend 2 (T1–2).

Olivine lamproites are characterized by spinel Trend 2 compositions (chromite–titanomagnetite trend), and phlogopite mica with an Al-depletion and Fe-enrichment trend from phlogopite towards tetraferriphlogopite. The occurrence of tetraferriphlogopite (TFP) in olivine lamproites does not represent a continuous zoning trend from phlogopite, but is discontinuous with a compositional break between Al-poor phlogopite and TFP. Micas in olivine lamproites are Ti-rich as compared to those observed in kimberlites and CROLs.

We note that the compositional trend or trends defined by a single mineral type should not be used in isolation to distinguish one diamond-bearing rock type from another. Compositional trends of spinel and phlogopite, while useful, cannot be construed as diagnostic when considered in isolation (or together), as previously inferred (Mitchell 1986, 1995). We caution that on their own, spinel chemistry trends cannot be used with confidence to distinguish kimberlite (Trend 2) from CROL or olivine lamproite (Trend 2). Phlogopite with Al-depletion and compositional zoning to tetraferriphlogopite is also not diagnostic of kimberlite, or CROL, or olivine lamproite. A sound understanding of the mineralogy is key (Table 1). Spinel and phlogopite discriminant plots should be used along with other criteria (e.g., mineralogy, whole rock geochemistry, isotopic studies, etc.) wherever possible. At present, only an unknown sample with Trend 1 composition spinels and a mica Al-enrichment (phlogopite–eastonite) trend could be construed as a kimberlite.

Any individual or discrete, intrusive or extrusive phase within a given occurrence of kimberlite, CROL or olivine lamproite can have distinctive spinel and phlogopite compositions and zoning trends (e.g., Naidoo et al. 2004; van Straaten et al. 2011). The modal amount of olivine and the relative proportions of xenocrystal olivine to magmatic olivine is exceedingly variable in kimberlite, CROL, and olivine lamproite. Taken together, these observations are very useful for diamond exploration geologists with respect to understanding the geology, and hence furthering understanding of the economic potential of kimberlites, CROLs and olivine lamproites.

Whole rock geochemistry

History of geochemical studies of kimberlite, CROL and olivine lamproite. Kimberlite, the dominant rock type that hosts diamond mines is arguably the most hybridized, diversely altered and xenolith-rich magmatic material to have found their way to Earth's surface. A long history of kimberlite research is only now arriving at a consensus of their definition and classification while their origin remains as contentious as ever—perhaps an indication of the importance of these rocks as geochemical probes of Earth's mantle. This part of the chapter will briefly review the geochemistry of kimberlite, classified on the basis of petrography and mineral chemistry as bonafide kimberlites, and then compare minimally contaminated hypabyssal kimberlite with carbonate-rich olivine lamproite and olivine lamproite. Our aim is to provide the reader with a view of the range of compositions and key geochemical characteristics of the three main magmatic rock types that host diamond deposits. We do not focus on the geochemistry of volcaniclastic (fragmental) examples of these three rock types, except to illustrate their substantive geochemical diversity as compared to minimally contaminated and/or altered hypabyssal samples, and to consider their likely alteration, and mantle and crustal contamination pathways and relationships.

One of the first studies to incorporate whole rock analyses of kimberlites was by Wagner (1914) who applied geochemistry to help distinguish kimberlite from what he thought to be "similar" rocks observed in South Africa, e.g., olivine melilitite. Wagner was perhaps the first author to highlight the lower alumina and alkalis, and higher Mg of what he termed "basaltic" kimberlites compared to these other rock types considered at that time to be "similar", or "related". After a hiatus of research on the topic, the 1970's and early 1980's ushered in new era of whole rock geochemical studies of kimberlites that included significant datasets, e.g. Ilupin and Lutts (1971), Nixon (1973), Gurney and Ebrahim (1973), Fesq et al. (1975), Dawson (1978, 1980) and Clement (1982). In these studies, many of the samples analysed were massive volcaniclastic kimberlite and kimberlite breccia that contained high proportions of entrained crustal and/or mantle xenoliths/xenocrysts. Importantly, these data confirmed the broadly high-Mg and Si-poor geochemical nature of kimberlites determined in earlier studies (e.g., Wagner 1914). The landmark papers by Smith (1983) and Smith et al. (1985) recognized the need for geochemical studies on samples less influenced by crustal input and provided a high-quality dataset for a suite of southern African hypabyssal kimberlites. These studies importantly identified, separated and distinguished Gp Ia (occurring within the Archean nucleus of the craton) and Gp Ib (occurring in the Proterozoic regions of the craton) kimberlites, and Gp II kimberlites (i.e., CROLs) in the Kaapvaal craton. Spriggs (1988) made the first detailed geochemical studies of circum-cratonic kimberlites (from Namibia), focusing on hypabyssal varieties. Taylor et al. (1994) examined whole rock geochemical data from kimberlites from West Africa, making detailed comparison with Kaapvaal kimberlites. This period was followed by a marked proliferation of numerous and noteworthy new geochemical studies, with important contributions by le Roex et al. (2003), Harris et al. (2004), and Becker and le Roex (2006) containing analyses of kimberlites from southern Africa, and by Price et al. (2000) from the Jericho kimberlite, Slave Craton, Canada. Significant bodies of work were also published on the kimberlites of the Lac de Gras field, Slave Craton, Canada (Kjarsgaard et al. 2009; Tappe et al. 2013), West Greenland kimberlites (Tappe et al. 2011), kimberlites from Finland (Dalton 2019) and Na-, Cl-, and CO_2-rich kimberlites from Udachnaya-East, Russia (Kamenetsky et al. 2007a,b).

While the recognition of Group II kimberlite (referred to as CROL here) by Smith (1983) in the Kaapvaal Craton was an immensely significant advance, further studies on these rocks were hindered by the notion that they only occur within southern Africa (Mitchell 1995). However, CROL are now recognized globally (see Fig. 2), with known localities in Finland and adjacent Russia within the Kola composite Craton (e.g., Mahotkin 1998; O'Brien and Tyni 1999; Kargin et al. 2014), in the Man Craton, West Africa (e.g., Skinner et al. 2004; Howarth and Giuliani 2020), in the Bastar Craton, India (e.g., Mainkar and Lehmann 2007; Lehmann et al. 2010; Rao et al. 2011) and in the Rae Craton, Canada (Sarkar et al. 2019). The geochemistry of numerous CROL localities of the Kalahari composite Craton in South Africa, Botswana and Eswatini is well documented (e.g., Wagner 1914; Smith 1983; Smith et al. 1985; Dawson 1987; Fraser and Hawkesworth 1992; Skinner et al. 1994; Tainton and Mckenzie 1994; Becker and le Roex 2006; Coe et al. 2008; Howarth et al. 2011).

Though long recognised (e.g., Cross 1897), the term lamproite was popularised by Niggli (1923). These compositionally unusual rocks with elevated K and Mg contents only became a focus of intense global interest with the discovery of the Tier 1 Argyle diamond mine and the Tier 4 Ellendale 4 and Tier 4 Ellendale 9 diamond mines in western Australia, with all three mines hosted by olivine lamproite (e.g., Jaques et al. 1984, 1986). Several comprehensive studies on olivine lamproites followed soon after (Fraser et al. 1985, 1992; Tainton and McKenzie 1991), in addition to an overview by Mitchel and Bergmann (1991).

The differing rock classification at some specific localities e.g., CROL and also olivine lamproite, or kimberlite and also UML (e.g., West Greenland), remains problematic. The Aries pipe in the Kimberley Block (Australia) is variably interpreted as a kimberlite and also a CROL, compare Edward et al. (1992) with Taylor et al. (1994), or Mitchell (1995), or Downes et al. (2006). The reader is encouraged to read the many papers published on these issues in the extended abstracts (https://ikcabstracts.com /index.php/ikc), and the Proceedings volumes of the International Kimberlite Conference over the last 50 years.

A more recent and comprehensive review of the comparative geochemistry (including major-, trace-element and tracer isotope systematics) of kimberlite, CROL, and olivine lamproite is provided by Pearson et al. (2019). Here, we focus on the most commonly used criteria—major elements—in identifying and characterising these rocks. Major elements have also been used in suggested schemes for evaluating the diamond-potential of kimberlites (e.g., Valsilenko et al. 2012).

Major element database. Numerous examples of kimberlite major element data exist in downloadable databases such as the GEOROC database, which contains >4,500 analyses of rocks reported as kimberlites. We assembled our own kimberlite database using a combination of the GEOROC database and data in the Proceedings of the International Kimberlite Conferences (prior to 2003). This database, with 5,133 major element analyses, labelled as "Kimb–All" in our plots, was assembled to provide an overview on the range of compositions of rocks that have been referred to as kimberlites in the literature, including a number of volcaniclastic kimberlites, kimberlites with large amounts of crustal contamination (e.g., Fulop et al. 2018), or altered kimberlites. We screened this database to eliminate rocks that did not meet the basic petrographic/mineralogical classification of a kimberlite (see below).

To augment the general kimberlite database, we sought to constrain, more accurately, the composition of kimberlite magmatic rocks less affected by significant crustal contamination or alteration. This aim involved the assembly of a much smaller (n = 519) database of kimberlite, referred to here as "Kimb–HK", as the samples are exclusively hypabyssal/coherent. In addition, we assembled and scrutinised similar published datasets and databases for carbonate-rich olivine lamproite (n = 305) and olivine lamproite (n = 306) whole rock analyses. The source references of the data are listed in on-line Appendix A. The databases were constructed using the following guidelines:

i) Confident identification and classification of the rocks based on current or previous petrographic/mineral chemistry and/or tracer isotopic studies studies.

ii) Identification of the rocks as hypabyssal rocks (intrusions) rather than fragmental volcaniclastic rocks.

iii) The data are accompanied by a description of analytical methods with co-analysed reference materials, from a reputable laboratory, or the publication uses methods previously published by that laboratory.

iv) We avoided most rocks from regions where low-T alteration problems are known to be severe (e.g., India) while recognising that there likely are numerous reliable analyses from these regions. Time limits did not permit an extensive investigation of this issue on an individual sample basis.

v) We avoid analyses on rocks that are clearly identified as containing significant crustal contamination, or suites of rocks where this was in fact the objective of the study (e.g., the extensive and well characterized Snap Lake dataset of Fulop et al. 2018).

vi) We avoid rocks containing apparently "excessive" MgO, where instrument calibration or olivine accumulation may have been a major problem.

vii) Unlike in the "Kimb–All" database, in the "Kimb–HK" database we avoided studies where many samples had been analysed from the same kimberlite body (e.g., the extensive studies of Russian kimberlites by Vasilenko et al. 2012) to avoid giving undue weight to particular individual locations.

viii) We screened kimberlites using the Clement Contamination Index (CCI) and the ln (Si/Al) versus ln (Mg/Yb) approach of Dowall (2004) and Kjarsgaard et al. (2009), checking that we did not inadvertently screen-out kimberlites with minimal contamination that may be enriched in K-rich phlogopite, which will drive up the CCI value (Clement 1982). Note that these two screening techniques are not directly applicable to CROL or olivine lamproite, as these approaches have not been rigorously tested on these rock types, which typically have higher CCI values than kimberlites (Fig. 19).

In applying these criteria, we recognize that we may have screened out many "useful" kimberlite, CROL and olivine lamproite analyses, simply because the publications do not contain sufficient information with which to judge the reliability and nature (e.g., hypabyssal versus volcaniclastic kimberlite, degree of alteration) of the data (e.g., Lapin et al. 2007) and or are written in a language not easily accessible to the authors (e.g., Ilupin and Lutts 1971). We partition rocks that were formerly known as "micaceous" kimberlite" (Wagner 1914) or "Group II kimberlites" (Smith 1983; Smith et al. 1985) or orangeites (Wagner 1928; Mitchell 1995) into a category of lamproites referred to as "carbonate-rich olivine lamproites" or CROLs (Pearson et al. 2019), and further investigate the validity of this division. The lamproite database is divided into Mg-rich lamproites that are confidently identified as olivine lamproites, and apply a nominal cut-off requirement of MgO >14 wt% for this category. Note that Jaques and Foley (2018) employed a cut-off at 10 wt% MgO.

Crust–mantle contamination: geochemical diversity of kimberlite, CROL and olivine lamproite. Kimberlites especially are notable for their high load of crust and mantle xenoliths and are one of the few rock-types where "contamination" by both crust and mantle is a serious issue, clouding interpretation. This problem can also be a serious issue with CROLs and olivine lamproites. Quantifying the effects of crustal contamination on kimberlite compositions is key to understanding their geochemistry including parental melt compositions, especially for samples that lack obvious petrographic evidence for contamination (Fig. 19a). Though crustal contamination effects are less severe for some of the incompatible elements that are highly enriched in kimberlites, e.g., Nd and Sr, the effects of this process must still be considered carefully.

A variety of approaches have been developed, with an early popular approach being the "Clement's Contamination Index" (Clement 1982), or CCI, where:

$$CCI = (SiO_2 + Al_2O_3 + Na_2O) / (MgO + 2K_2O)$$

Typically, CCI values < 1 are considered uncontaminated (Clement 1982; Mitchell 1986), an approach taken by Nowicki et al. (2008). However, Clement (1982) reported on apparently uncontaminated kimberlites with CCI values up to 1.5, but these are from phlogopite-rich kimberlites, or from samples that are now recognized as CROLs (Fig. 19b). We have adopted a maximum CCI value of 1.3 in our own kimberlite screening. Although the CCI is widely used,

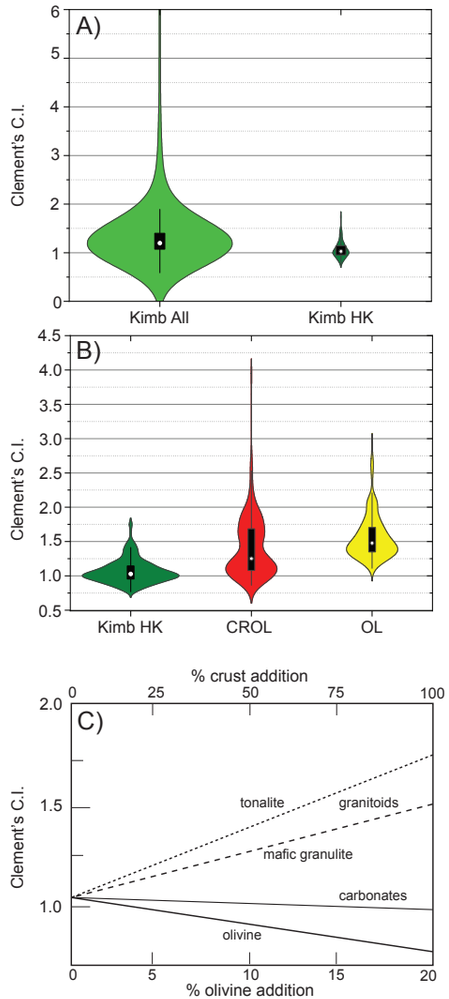

Figure 19. Violin, and box and whisker plots of Clement's Contamination Index (CCI) for: (**A**) Kimb-All and Kimb-HK; note for this plot, the Kimb-HK data was not screened for CCI < 1.3, and; (**B**) Kimb-HK, CROL and olivine lamproite. The box and line plot showing the median (**white circle**) and the interquartile range (50% of the data—the **box, in black**) with the lines representing the upper and lower quartiles of the data; this is combined with a "violin" plot, which is in essence a probability density function of the data. The sources of the data are in the on-line appendix. (**C**) Mass balance for mixing various crustal lithologies and mantle olivine (Mg#92) into a kimberlite with equivalent composition to the Wesselton aphanitic kimberlite (le Roux et al. 2003), as a function of varying CCI. Note the opposing effects of olivine addition versus most crustal lithologies and the insensitivity of this index to carbonate (limestone) contamination. Re-drawn after Dowall (2004).

this approach lacks sensitivity due to the mutually opposing effects of olivine addition from peridotites—a ubiquitous process in kimberlites—and assimilation of typical silicic crust, such as granite (Fig. 19c). Other approaches have suggested that examination of a combination of SiO_2, Al_2O_3, MgO, Pb and HREE can provide more robust screens for crustal contamination;

for example, the application of using Yb, low in "uncontaminated" kimberlites (<0.5 ppm), and typically higher in granitic rocks (~1 ppm) was shown to provide improved sensitivity (le Roex et al. 2003).

There is wide agreement that kimberlites, CROLs and olivine lamproites have incorporated varying proportions of the cratonic lithospheric mantle they have traversed, and that this appropriation of mantle rock is responsible for most of the diamond grade, as >90% of mineral inclusions in diamonds, from most locations, are of lithospheric origin (Stachel and Harris 2008; see Stachel et al. 2022, this volume). Pearson et al. (2019) examined the influence of the local lithospheric mantle composition, and the degree of its incorporation on the bulk composition of kimberlites and suggested there is a strong correlation between the kimberlite Mg/Si ratio and that of entrained lithospheric mantle xenoliths from the same kimberlite or kimberlite field (Fig. 20). This association was strengthened in a follow-up study by Giuliani et al. (2020). These studies demonstrated that incorporation and/or assimilation of orthopyroxene (Mg/Si ~ 0.83) and olivine (Mg/Si ~ 1.64) clearly influences the bulk kimberlite Mg/Si ratio. Kimberlite locations that erupted through olivine-rich, orthopyroxene-poor cratonic mantle, such as Greenland (North Atlantic Craton), have higher Mg/Si than those erupted through the more orthopyroxene-rich cratonic mantle e.g., beneath the Kaapvaal, Siberian and Slave Cratons. Incorporation of lithospheric mantle thus imparts a local flavor to kimberlite compositions (Pilbeam et al. 2013; Pearson et al. 2019; Giuliani et al. 2020), potentially creating differences such as the higher Ti contents of Kaapvaal and Greenland kimberlites relative to Lac de Gras kimberlites (Pearson et al. 2019).

More complex approaches to examine crustal contamination, and combined crustal and mantle contamination were developed by Dowall (2004) and Kjarsgaard et al. (2009), utilising element ratios to combat the "closure effects" inherent in compositional data, an example of which is illustrated in Figure 21 for a suite of hypabyssal kimberlites from Lac de Gras, Slave Craton, Canada. The natural log of Si/Al is a useful screen that is very sensitive to the addition of high Al crustal rocks and neatly divides the Lac de Gras kimberlite sample suite into two distinct groups that are a function of their contamination (Fig. 21). Crustally contaminated rocks that are identified using this measure are also classified as being significantly contaminated on the basis of higher Yb abundances and lower ln Mg/Yb.

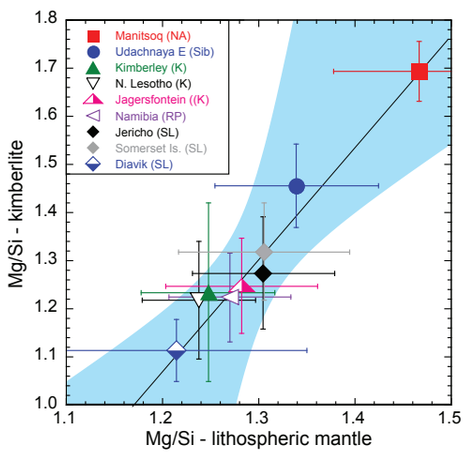

Figure 20. Plot of average molar Mg/Si ratio for kimberlites from nine global localities, versus the molar Mg/Si ratios of coarse peridotite xenoliths from the same kimberlite or kimberlite field. After Pearson et al. (2019), with permission.

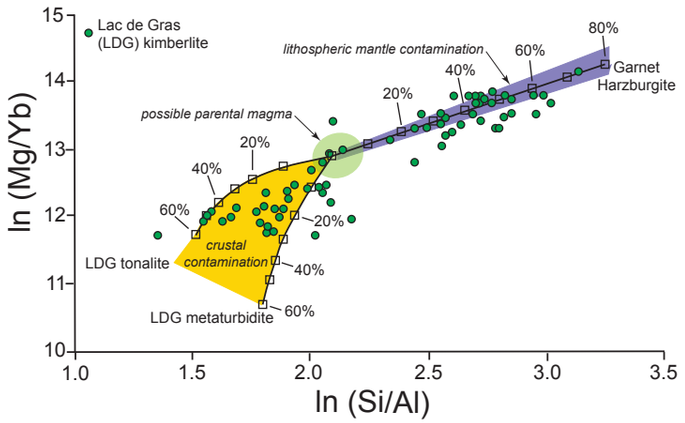

Figure 21. Plot of ln Mg/Yb versus ln Si/Al illustrating the competing effects of crustal contamination versus peridotitic lithospheric mantle assimilation for a "possible parental" Lac de Gras kimberlite magma. Data plotted are the bulk compositions of Lac de Gras hypabyssal kimberlites, unfiltered for the effects of crustal contamination. Endmember metaturbidite and tonalite compositions are from the Lac de Gras area of the central Slave Craton. Kimberlite and crustal whole rock data data are from Kjarsgaard et al. (2009) and Tappe et al. (2013). The garnet harzburgite compositions is a is a typical Slave craton harzburgite.

If, however, we examine the range of CCI values for kimberlites within the two groups of Lac de Gras hypabyssal kimberlites defined from ln Si/Al considerations, they largely overlap in CCI values (Kjarsgaard et al. 2009). Furthermore, a significant number of "non-contaminated" samples, identified on the basis of the ln Si/Al parameter, actually have CCI significantly >1, i.e., they would be flagged as contaminated if we used only this index according to the suggestions of Mitchell (1986) and Nowicki et al. (2008). One reason for this limitation of the CCI is that crustal contamination and peridotite incorporation have mutually opposing effects (see Figs. 19, 21, and also below) that severely limit the sensitivity of this index. On this basis we suggest that the sole use of Clement's C.I. as a screen for identifying crustally contaminated kimberlites be abandoned, or is at least utilized in conjunction with other proposed geochemical screens (e.g., le Roux et al. 2003; Kjarsgaard et al. 2009). The ln Mg/Yb versus ln Si/Al plot (Fig. 21) offers the possibility of visualising the competing effects of crustal assimilation versus peridotite incorporation, and is effective at screening out kimberlites that have experienced significant contamination by continental crust. Nonetheless, the diametrically opposing effects of crust versus mantle incorporation mean that it is likely impossible to guard against small amounts of crustal assimilation in kimberlites apparently free of crustal xenoliths, given the ubiquity of peridotite incorporation. The dilution of Yb by addition of mantle peridotite means that identifying even 5% addition of crust when accompanied by 20% peridotite addition (not an unreasonable mass fraction; e.g., Soltys et al. 2018) remains challenging. Lastly, using parameters such as Si/Al and Yb will not assist in detecting kimberlites containing variable amounts of crustal contamination from platform carbonate sediments, e.g., Udachnaya, Russia, and at Somerset Island, Jericho and Chidliak in Canada. Notwithstanding this limitation, a potentially useful application of the ln Mg/Yb versus ln Si/Al plot (Fig. 21) is that kimberlites with high degrees of lithospheric mantle contamination can be identified—and these may be of interest for their diamond potential.

Key aspects of the geochemistry of kimberlite, CROL and olivine lamproite. Most reviews of kimberlites and kimberlite geochemistry (e.g., Mitchell 1986, 1995) classify these rocks as silica-undersaturated, alkaline, potassic, and MgO- and CO_2-rich rocks. However, Kjarsgaard et al. (2009) and Pearson et al. (2019) noted that, for global kimberlites with minimal crustal contamination they are also H_2O-rich. Furthermore, their relatively low K + Na contents result in them having molar (Na+K)/Al < 1, i.e., they are not alkaline in nature and thus cannot be termed either "sodic" or "potassic" and with K_2O concentrations that are <3 wt%, these rocks certainly cannot be termed "ultrapotassic". In fact, kimberlites typically exhibit K_2O contents similar to mid-ocean ridge basalts (MORB)! In contrast, lamproites (including olivine lamproites and carbonate-rich olivine lamproites) are considered bona-fide alkaline rocks (Mitchell 2020a,b). Herein we utilize a combination of "violin", and box and whiskers statistical plots of the whole rock data to re-examine the similarities and differences between the three main magmatic rock types that host diamond mines, and provide an update on their basic geochemical parameters and ratios.

We start by examining the large, unscreened kimberlite database (Kimb-All; includes fresh and altered samples of both volcaniclastic and hypabyssal kimberlites) and compare this to a hypabyssal kimberlite database (Kimb-HK) to illustrate some of the potential variations in elemental concentration with respect to contamination and alteration (Fig. 22). Wider variations in concentration levels (both higher and lower) for SiO_2 and Al_2O_3 are observed in the Kimb-All data as compared to the Kimb-HK data, with the very high levels of SiO_2 (40–65 wt% SiO_2) and Al_2O_3 (5–18 wt% Al_2O_3) interpreted to result from crustal contamination and/or alteration processes (Figs. 22a,b). In contrast, MgO concentrations are lower in the Kimb-All data as compared to Kimb-HK data, interpreted to result from alteration processes (Figs. 22c, d) and dilution from continental crust. The available and reliable CO_2 data for kimberlites is surprisingly small, with 1487/5133 of the Kim-All samples, while the Kimb-HK data set is improved, with 371 of 519 samples having CO_2 data. Measured CO_2 levels are slightly higher in the Kimb-HK data (median = 5.8 wt%) compared with the Kimb-All data (median value 4.6), perhaps reflecting the more degassed character of the volcaniclastic rocks included in the Kimb-All database. The available and reliable H_2O data for kimberlites is very limited, with 386/5133 of the Kimb-All samples, while the Kimb-HK data set is much improved, with 329 of 519 samples having H_2O data. H_2O levels are similar for both kimberlite categories (6.88 wt% H_2O Kimb-HK versus 6.99 for Kimb-All) (Figs. 22e,f). Molar (Na+K)/Al and K/Al are lower in the Kimb-All data set as compared to the Kimb-HK data, due to a suggested combination of higher Al from crustal contamination, and similar or lower Na and/or K as a result of alteration and de-gassing processes (Figs. 22d, g, h). Based on these observations from comparing the Kimb-All and Kimb-HK data sets, we will subsequently only examine the Kimb-HK data set (screened to CCI values <1.3) for comparative purposes with the CROL and olivine lamproite data sets.

The SiO_2 concentration levels for all three rock types is <52 wt% SiO_2, i.e., they are all basic in composition, and typically, at <45 wt% SiO_2, are ultrabasic in composition (Fig. 23a). TiO_2 concentration levels for all three rock types (Fig. 23b) is quite variable at 0–10 wt% TiO_2, with olivine lamproites typically having higher concentration levels (median 3.1 wt% TiO_2) as compared to kimberlites (median 1.7% TiO_2) and CROLs (median 1.1 % TiO_2). Kimberlites have exceptionally low Al_2O_3 contents (<1–4 wt% Al_2O_3); CROL's and olivine lamproites have similar, but higher concentration levels of ~1–9 wt% Al_2O_3 (Fig. 23c). The highest MgO contents are observed in kimberlites (20–40 wt% MgO, mean 30 wt% MgO); MgO is lower in CROLs and olivine lamproites (mean of 24 and 22 wt% MgO, respectively), but there is quite wide scatter (<10 to >40 wt% MgO) observed in the CROL dataset (Fig. 23d). Sodium contents for all three rock types are <2 wt% Na_2O, notwithstanding a few samples with higher concentrations, which are suggested to be alteration related; kimberlite and CROL are dominated by samples with <0.5 wt% Na_2O, with olivine lamproite exhibiting slightly higher concentrations (Fig. 23e). Many kimberlites have very low Na_2O concentrations, close to or below the instrumental detection limit, often attributed to leaching of Na during alteration, or partitioning of Na into coexisting fluid (e.g., Kamenetsky et al. 2007a,b, 2009; Giuliani et al. 2017; Abersteiner et al. 2017, 2019). Potassium concentrations are lowest in kimberlite (mean ~1 wt% K_2O) and higher in CROL and olivine lamproite, with means of

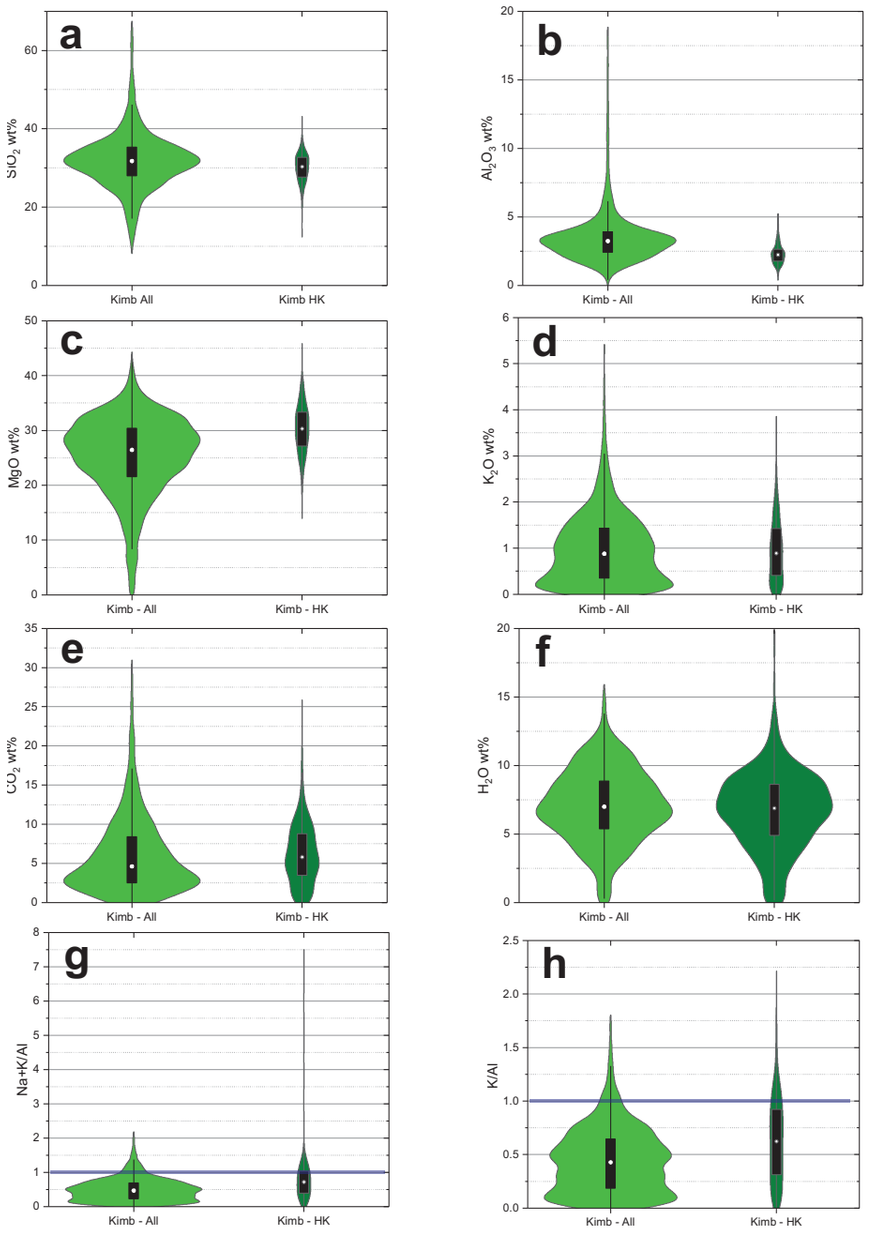

Figure 22. Kimb-All versus Kimb-HK violin plus box plots for (**a**) SiO_2, (**b**) Al_2O_3, (**c**) MgO, (**d**) K_2O, (**e**) CO_2, (**f**) H_2O (**g**) (Na+K)/Al, (**h**) K/Al. The **blue line in (g)** divide alkaline (>1) and subalkaline (<1) samples. The **blue line in (h)** demarcates samples with K/Al > 1 (perpotassic). See text for discussion. The box and line plot showing the median (**white circle**) and the interquartile range (50% of the data—the **box, in black**) with the lines representing the upper and lower quartiles of the data; this is combined with a "violin" plot, which is in essence a probability density function of the data. The sources of the data are in the on-line appendix A.

~2.8 and 3.8 wt% K_2O, respectively (Fig. 23f). Phosphorus concentration levels are similar in kimberlite and CROL (mean of ~0.7 and 0.8 wt% P_2O_5, respectively), but higher in olivine lamproite at ~1.5 wt% P_2O_5 (Fig. 23g).

Kimberlite and CROL have similar CO_2- and H_2O-rich compositions; in comparison, olivine lamproite is typically very CO_2-poor (or absent), with higher H_2O contents (Fig. 23h, i). Moreover, for CROL there is a statistically significant correlation between CaO and CO_2 concentrations (Pearson's $r = 0.87$), indicating that the CO_2 dominantly resides in carbonate (calcite), as is observed in kimberlite (Kjarsgaard et al. 2009). In contrast there is no statistical correlation between CaO and CO_2 for olivine lamproites.

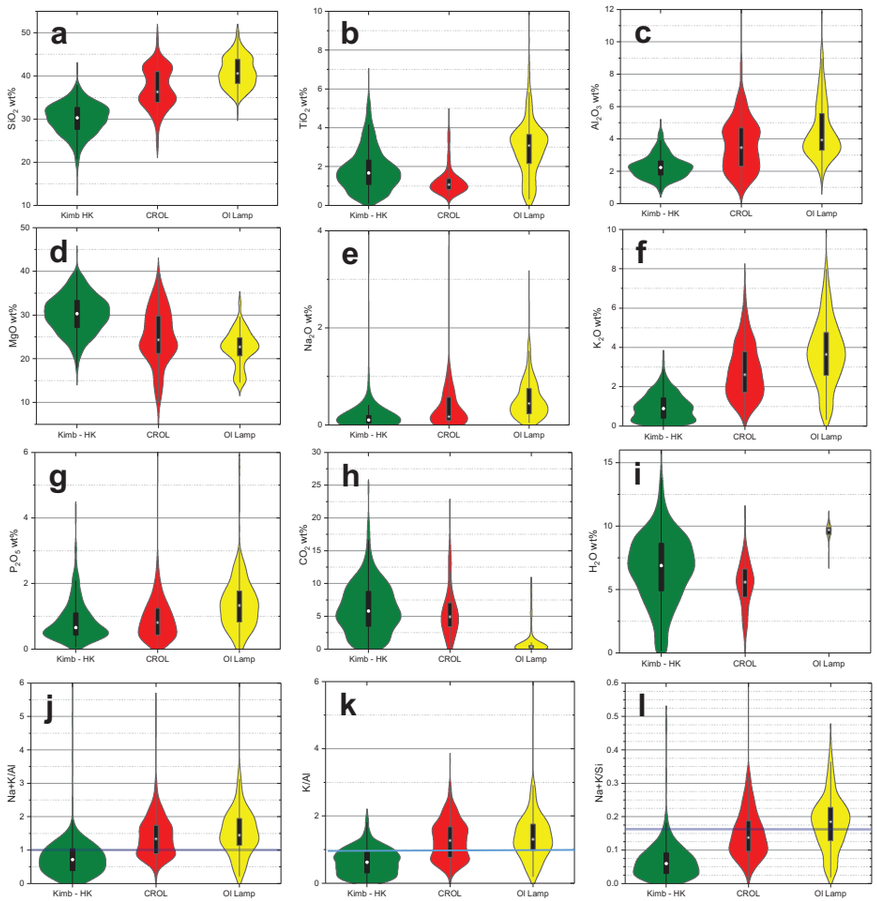

Figure 23. Kimb-HK, CROL, and olivine lamproite violin + box plots for (**a**) SiO_2, (**b**) TiO_2, (**c**) Al_2O_3, (**d**) MgO, (**e**) Na_2O, (**f**) K_2O, (**g**) P_2O_5, (**h**) CO_2, (**i**) H_2O (**j**) (Na+K)/Al, (**k**) K/Al, (**l**) (Na+K)/Si. The **blue lines in (j)** divide alkaline (>1) and subalkaline (<1) samples. The **blue lines in (k)** demarcates samples with K/Al > 1 (perpotassic). The **blue line in (l)** demarcates samples with (Na+K)/Si > 0.1666 that are considered alkaline on the basis of a silica deficiency with respect to alkalis. See text for further discussion. The box and line plot showing the median (**white circle**) and the interquartile range (50% of the data—the **box, in black**) with the lines representing the upper and lower quartiles of the data; this is combined with a "violin" plot, which is in essence a probability density function of the data. The sources of the data are in the on-line appendix A.

Applying the peralkalinity index—molar (Na+K)/Al—clearly illustrates that ~75% of the kimberlite sample suite have values <1, hence kimberlites are not alkaline rocks (Fig. 23j). Because kimberlites are not alkaline, they cannot thus be termed "potassic" even though K/Na is >1. Much of the variation in K/Na for kimberlites may be ascribed to alteration or Na loss to fluids (see references cited above). In contrast >75% of the CROL and olivine lamproites have (Na+K)/Al >1 and are thus alkaline (Fig. 23j), and also potassic, with K > Na. Molar K/Al data for these two rock types is very similar, with ~75% of the CROLs and olivine lamproites in the sample sets being perpotassic with K/Al >1 (Fig. 23k). An additional approach suggested by Mitchell (2020a) is to examine alkalinity by application of the "Shand Index" (molar Na+K:Al:Si = 1:1:6). Shand (1922) stated that "an alkaline rock, then, if names are to mean anything, should be one in which the alkalis are in excess of 1:1:6, either alumina or silica being deficient". Sorenson (1974, p. 6) further noted "this means that contents of alkali feldspar and/or mica do not entitle a rock to be termed alkaline". We have utilized the Shand Index to examine alkali/alumina (i.e., the peralkalinity index; Fig. 23j) and alkali/silica ratios as tests for kimberlite alkalinity and conclude that kimberlites are neither alumina or silica deficient relative to alkalis. This is clearly illustrated by Figure 23l, a plot of (Na+K)/Si, that demonstrates that kimberlites have values less than 1/6 (0.166) and thus cannot be considered alkaline rocks by this criterion. Mitchell (2020a) has stated that crystallization of phlogopite in kimberlite is an expression of their alkaline nature. However, this is manifestly not the case, as per Shand (1922), or Sorenson (1974).

Summary of the geochemistry of kimberlite, CROL and olivine lamproite. From our analysis of the major element composition of the three primary magma types that host diamond deposits, they have some common attributes such as being MgO- and volatile-rich, and ultrabasic (or basic, for a subset of olivine lamproites) in terms of silica contents. Kimberlites can clearly be distinguished from other diamondiferous rocks such as olivine lamproites and their carbonate-rich equivalents, CROL (often referred to as micaceous kimberlite, orangeites, or Group II kimberlite). In contrast to the vast majority of published literature, we re-iterate (Kjarsgaard et al. 2009) that kimberlites, the dominant primary magma type that form diamond mines, cannot be described as alkaline rocks, nor are they potassic. Kimberlites, as sampled at Earth's surface, are better described as silica-poor, ultrabasic rocks (mean MgO ~ 30.2 wt %), that are both CO_2- and H_2O- rich, with relatively low K, Na and Al contents.

PRIMARY DIAMOND MINES

Distribution of primary magmatic-hosted diamond mines

The global distribution of primary magmatic-hosted diamond mines is illustrated in Figure 24. There is a 1:1 correspondence between diamond mines and supercratons. These supercraton regions (Pearson et al. 2021) are "modern" (e.g., utilizing mantle seismic tomography information) outlines of the Earth's cratonic regions, for areas previously termed stable Precambrian cratons in the earlier literature (e.g., Dawson 1980; Janse 1984; Nixon 1995). The age of last major tectonomagmatic disturbance of cratons was originally suggested to be older than 1.5 Ga (Kennedy 1964; Clifford 1966), although Pearson et al. (2021) have revised this age to > ~1 Ga and extended the definition of the craton itself to include the presence of a deep (>150km) lithospheric mantle root. Supercratons are made of two or more composite cratons that are themselves compromised of several cratonic nuclei that are typically Archean in age.

A high proportion of kimberlite-hosted diamond mines lie within Archean cratonic nuclei. Examples include Victor and Renard (Superior Craton), all Slave Craton examples, Kelsey Lake (Wyoming Craton), Mwadui (Tanzanian Craton), Koidu (Man Craton), Mbuji Mayi and Tshibwe (Kasai Craton); all these examples were emplaced through Archean crustal rocks (Fig. 24). However, a number of other kimberlite-hosted diamond mines are associated with

Archean plus Paleoproterozoic crust (and associated mantle lithosphere of the same age span), such as is observed in the Kalahari (e.g., Orapa), Siberian (e.g., Mir, Internationalaya, Udachnaya), and Kola (e.g., Grib, Arkhangelskaya) composite cratons (Fig. 24).

Carbonate-rich olivine lamproites, of quite variable diamond contents, are observed in the Kalahari, Karelian, Indian, Rae-Laurentia and West Greenland cratonic regions (Fig. 2), but CROL-hosted diamond mines are only known from the Kaapvaal Archean nuclei within the Kalahari composite craton (Figs. 2, 25, 26; Table 2). Olivine lamproite-hosted diamond mines (e.g., Argyle, Ellendale 4 and 9, Majghawan), while within supercratons (Figs. 2, 24), all appear to reside in supercraton marginal positions, adjacent to Archean, or Paleo- or Mesoproterozoic terrains.

The majority of magmatic-hosted diamond mines are found in three key areas, the Kalahari (Figs. 24, 25, 26) and the Siberian composite cratons (Figs. 24, 27, 28), and in the Archean Slave Craton (Figs. 24, 29). Important, Tier 1 diamond mines are also found outside these regions, such as the Catoca kimberlite (Angola-South African supercraton) and the Argyle olivine lamproite (Australian supercraton), amongst other significant diamond mines shown on the global maps in Figures 1, 2 and 24. These Tier 1 diamond mines, plus additional key diamond mines and deposits are also shown on the detailed maps that accompany the following section on *Review of Global Secondary Diamond Deposits.*

The Kalahari composite craton provides useful insight to the distribution of the diamond mines with respect to its constituent Archean and Paleoproterozoic terranes (Figs. 25, 26). The Archean Limpopo terrane contains the Tier 1 Venetia mine, the Tier 4 Murowa mine, and the River Ranch deposit; all are kimberlite-hosted. The Paleoproterozoic Magondi fold belt, to the west of the Zimbabwe Archean nuclei, contains the Tier 1 Orapa mine, the Tier 2 Letlhakane mine, and the Tier 4 Karowe and Damtshaa mines. All of these mines are in a restricted geographic area collectively known as the Orapa kimberlite field (Field et al. 2008). The Lerala mine is also within the Magondi belt. Further west of the Magondi belt, the Okwa inlier contains the kimberlite-hosted Ghagoo (Gope-25) mine. The Kaapvaal Archean nucleus, within the Kalahari composite craton, hosts a plethora of kimberlite-hosted diamond mines (Table 2; Figs. 25, 26). These include the Tier 1 Jwaneng and Cullinan mines, the multiple Tier 3 mines that constitute the Kimberly cluster of mines (Kimberley, De Beers, Bultfontein, Dutoitspan, Wesselton), and also multiple Tier 4 (e.g., Koffiefontein, Jagersfontein, Letšeng, Palmietgat, The Oaks) and Tier 5 (e.g., Mothae, Frank Smith) mines. The Kaapvaal Archean nucleus also contains a number of other kimberlite-hosted historic mines and deposits e.g., Leicester, Kamfersdam, Belgravia and Otto's Kopje, for which data are limited or incomplete in terms of diamond grade, rough diamond value, and yearly carats mined.

Within the Archean Kaapvaal nucleus are also a number of important carbonate-rich olivine lamproite hosted diamond mines (Table 2; Fig. 26). These include the Tier 1 Finsch mine, the Tier 3 Marsfontein, Voorspoed and Lace/Crown mines, the Tier 4 Roberts Victor, Helam and Dokolwayo mines, and the Tier 5 Bellsbank fissure mines and Star (Theunissen area) mine. A significant number of additional CROL-hosted historic diamond mines, mainly beneficiated in the late 1800's to early 1900's e.g., Postmas, West End, Peiserton, West Kimberley, Paardeberg (Fig. 26), have no, limited or incomplete data for diamond grade, rough diamond value, and yearly carats mined. A history of mining of the significant diamond deposits in South African within the Kalahari Craton is provided by Wilson et al. (2007a), while Brook (2012) documents the history of the Botswana diamond mines.

The Siberian composite craton contains numerous kimberlites, including a very significant number of important kimberlite-hosted diamond mines (Table 2; Figs. 27, 28). The Daldyn kimberlite field contains the Tier 1 Udachnaya mine, the Tier 2 Zarnitsa mine, and the Dalnayay and Zagadochnaya advanced exploration projects (Table 2; Fig. 28a).

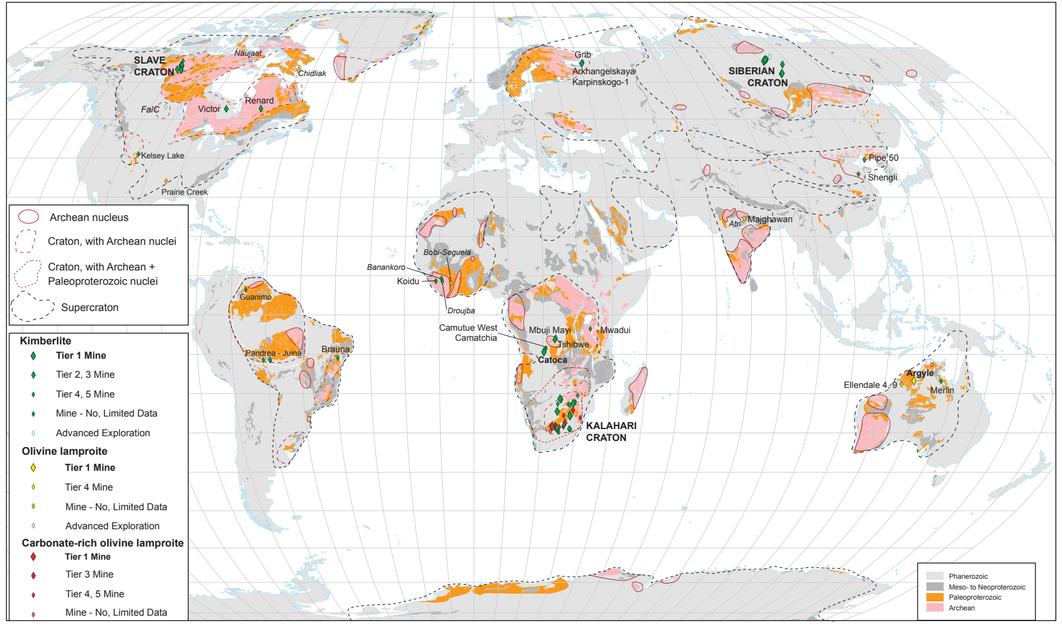

Figure 24. Global diamond mines in primary magmatic source rocks (kimberlite, olivine lamproite, and carbonate-rich olivine lamproite). Advanced exploration projects and former mines with no or limited data are also shown. Tier 1 diamond mines indicated by bold font. Detailed maps of the diamond mines and deposits of the Kalahari Craton, Siberian Craton (southern Yakutia area) and the Slave Craton follow (Figs. 25 to 29). Bedrock geology backdrop from Chorlton (2007); note the dominant bedrock geology is that at the surface i.e., Phanerozoic rocks that overlie Archean or Proterozoic rocks are shown on this map as Phanerozoic. Craton outlines from Pearson et al. (2021). Robinson map projection.

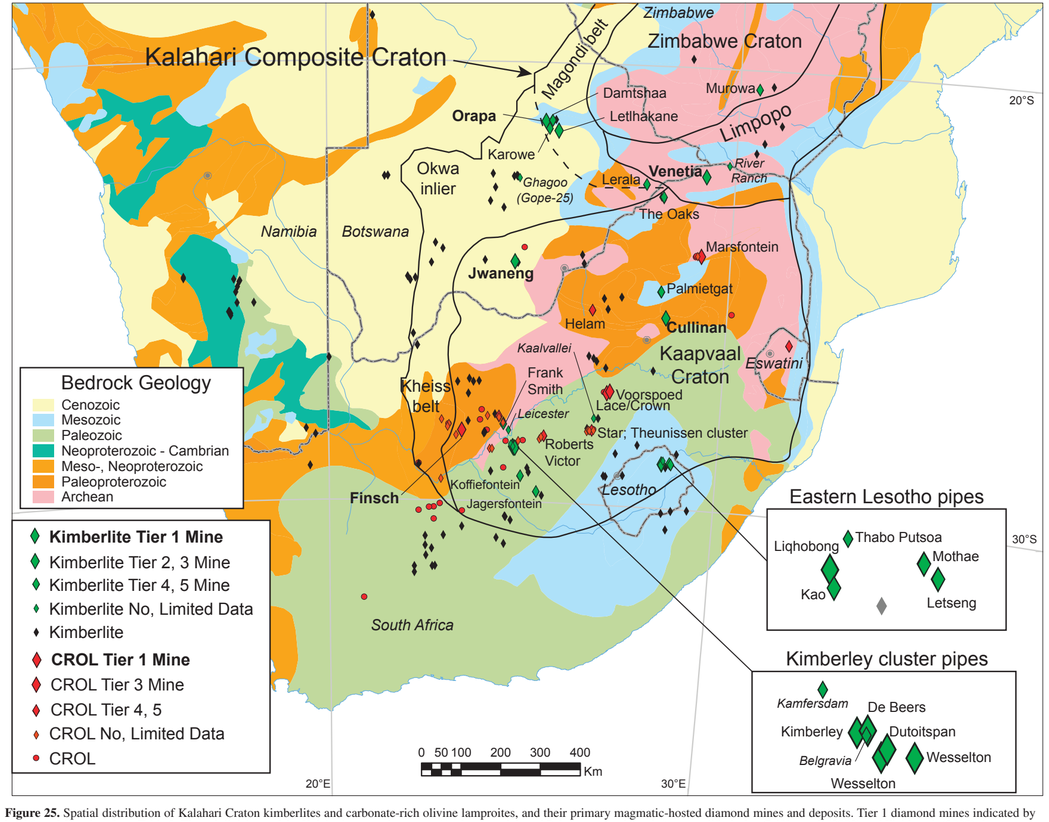

Figure 25. Spatial distribution of Kalahari Craton kimberlites and carbonate-rich olivine lamproites, and their primary magmatic-hosted diamond mines and deposits. Tier 1 diamond mines indicated by bold font. Mine data from Table 2. The subdivisions of the Kalahari composite craton (Archean nuclei, and Paleoproterozoic rocks) are modified after Griffin et al. (2003) and Field et al. (2008). Inset maps show kimberlites, and kimberlite-hosted diamond mines and deposits in the Kimberley and Lesotho kimberlite clusters. Mercator map projection.

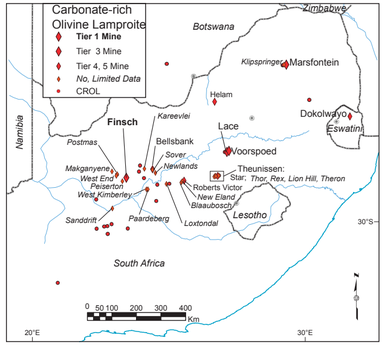

Figure 26. Spatial distribution of carbonate-rich olivine lamproites, and CROL-hosted diamond mines and deposits of the Kaapvaal Craton. Finsch CROL Tier 1 diamond mine indicated by bold font. See text for details. Mercator map projection.

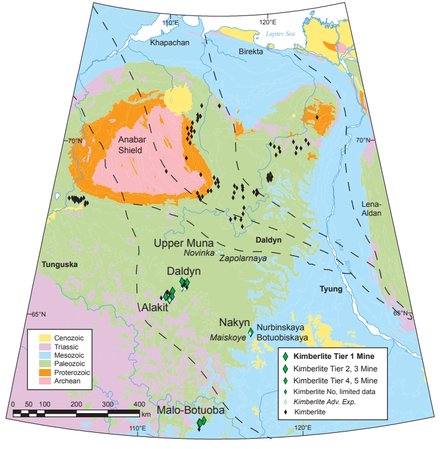

Figure 27. Spatial distribution of Siberian Craton (southern Yakutia) kimberlite-hosted diamond mines, deposits, advanced exploration projects and kimberlites. Tectonic subdivisions after Smelov and Zaitsev (2013). Note that the key kimberlite fields (Daldyn, Alakit-Markha, Nakyn) with diamond mines, as well as the Upper Muna field and its advanced exploration projects all lie in the Tyung domain; the Malo-Botuoba field lies in the Tunguska domain. Mercator map projection.

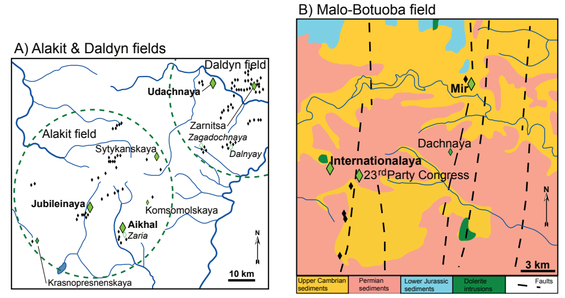

Figure 28. Detail maps of Siberian Craton kimberlites and kimberlite-hosted diamond mines, deposits and advanced exploration projects. Tier 1 diamond mines indicated by bold font. Mine data from Table 2. (**A**) Alakit-Markha and Daldyn kimberlite fields (modified after Ashchepkov ey al. 2015 and Kostrovitsky et al. 2015). (**B**) Malo-Botuoba field (modified after Agashev et al. 2018).

The Alakit-Markha kimberlite field contains the Tier 1 Aikhal and Jubileinaya mines, the Tier 3 Sytykanskaya mine, the Tier 4 Komsomolskaya mine, the Zaria advanced exploration project, and the Krasnopreskenskaya deposit (Table 2; Fig. 28a). The Malo-Botuoba kimberlite field contains the Tier 1 Mir and Internationalaya mines, the Tier 2 23rd Party Congress mine, and the Dachnaya deposit (Table 2; Fig. 28b). The Nakyn kimberlite field contains the Tier 2 Nurbinskaya mine, Tier 3 Botuobiskaya mine, and the Maiskoye advanced exploration project (Table 2; Fig. 27). The Upper Muna kimberlite field contains advanced exploration projects at Novinka and Zapolarnaya, plus at other kimberlites in this area. (Fig. 27).

The Slave Craton, one of the Archean nuclei within the Laurentian supercraton (Figs. 1, 24), contains numerous kimberlites and kimberlite-hosted diamond mines (Table 2; Fig. 29). The Lac de Gras kimberlite field in the central part of the Slave Craton contains two diamond mines, Ekati and Diavik, each comprised of multiple individual mines, as well as advanced exploration projects (Table 2; Fig. 29, inset map). The Diavik mine consists of four Tier 2 Mines (A154 North, A154 South, A418 and A21). The Ekati mine consists of the Tier 2 Koala, Panda, Sable, Fox and Misery mines, the Tier 3 Pigeon and Beartooth mines, and the Tier 4 Koala North and Lynx mines. Advanced exploration projects include the A841, Jay and Leslie kimberlites (Table 2; Fig. 29, inset map). The southeast Slave Craton contains the past producing Snap Lake Mine, and the three Tier 2 Mines (GK5034, Tuzo, Hearne) that constitute the Gahcho Kué mine (Table 2; Fig. 29). To the east of the Gahcho Kué mine area, there is advanced exploration at the Kelvin and Faraday kimberlites (Table 2; Fig. 29). In the north Slave Craton, the Jericho mine was short-lived (<5 years), and limited mine data are available (Fig. 29).

Economic characteristics of global diamond mines

Within a diamond mine, significant grade variations (typically greater than an order of magnitude) are observed between individual intrusive phases and/or extrusive phases and/or resedimented volcaniclastic phases (Clement 1982; Kjarsgaard 2007a). In a diamond mine, this can include kimberlite phase(s) which are of very low grade or very low rough diamond value (and thus very low ore value) and were not mined as ore, such as the "West End" kimberlite in the Kimberley (Big Hole) Mine (Wagner 1914). Furthermore, within an

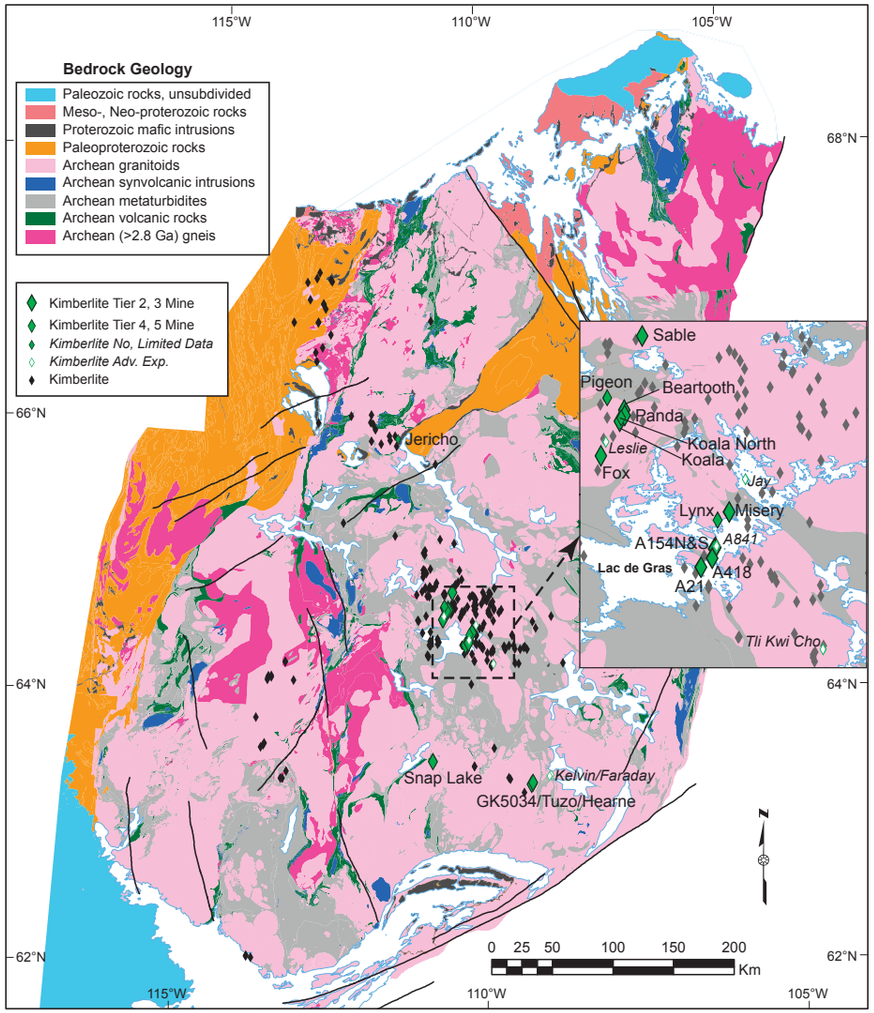

Figure 29. Spatial distribution of Slave Craton kimberlite-hosted diamond mines. Inset map shows mines in the Lac de Gras region of the central Slave Craton. Geology simplified and modified after Stubley and Irwin (2019). Inset map modified after Kjarsgaard et al. (2002).

individual kimberlite phase of a diamond mine, there can also be significant diamond grade variation of more than an order of magnitude. The De Beers kimberlite of the Kimberley cluster of pipes (Fig. 25, inset) provides an excellent example of grade variation between kimberlite phases, and grade variation within a single phase (Clement 1982; Clement et al. 1986; Kjarsgaard 2007a). Hence, the compiled diamond grade data as shown in Table 2 and in Figure 30 is based on interpreted average grades for mined-out deposits, or "head frame" grades for active mines. Also note that many diamond grades in Table 2 are inferred due to a lack of public domain data, or are based on data from exploration or feasibility studies, which may not be a true representation of the run of mine grade due to the smaller size of these preliminary samples. With these caveats in mind, diamond grade for economic diamond

deposits typically ranges from ~0.025 to ~2 carats per tonne (carat/tonne; ct/t), equivalent to 0.005–0.4 ppm by mass (Fig. 30). Less commonly, global diamond mines have grades up to 5 ct/t and rarely (e.g., the exceptional Internationalaya mine) to 9 ct/t, equivalent to 1–2 ppm by mass (Fig. 30). Thus, there is more than two orders of magnitude in diamond grade variation for diamond mines globally, from 0.025 to 9 ct/t, as shown on the log histogram plot of diamond grade in Figure 30. This wide variation in diamond grade is observed for kimberlites, compare Letšeng (Lesotho) with the lowest diamond grade ever mined in a large scale mine, and the very high grade Internationalaya mine (Russia). For olivine lamproites compare the low-grade Ellendale 9 mine with the much higher-grade Argyle mine (both in Australia). For carbonate-rich olivine lamproites, compare the lower grade Voorspoed mine with the higher grade Helam (Swartruggens) mine (both in South Africa).

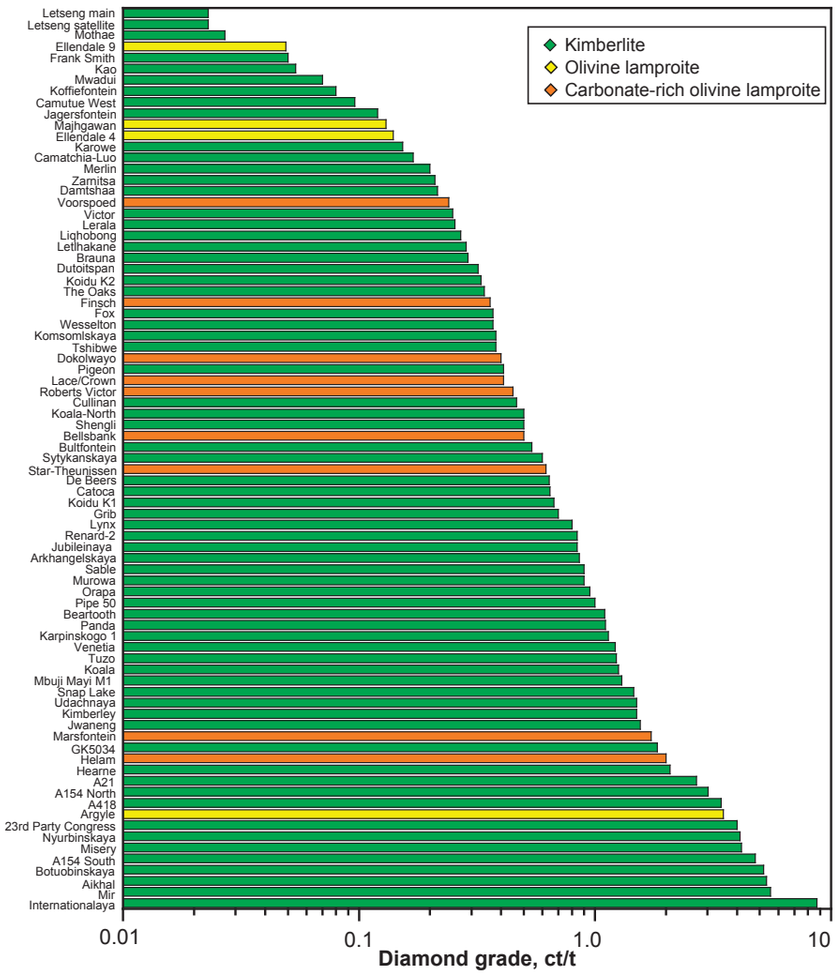

Figure 30. Histogram plot (log scale) illustrating the variation in diamond grade (in carats per tonne; ct/t) for global diamond mines (active and past-producers). Data from Table 2. All primary magmatic hosted diamond mines are color coded by rock type (Kimberlite, CROL, olivine lamproite).

In contrast to the vast majority of commodities (e.g., gold, iron ore, lithium), there is not a single "value" for rough diamonds. Hence, the value of an individual rough diamond can be exceptionally variable, depending upon size (the carat weight), color, and quality. Rough diamonds range from non-gem and near worthless diamonds (boart; <US$1/ct) to exceptional gem quality diamonds (>US$1,000,000/ct). Since a mine typically produces a quite wide range of rough diamonds with respect to value (boart to gem), the average rough diamond value, stated in US$/ct (Fig. 31), is an exceptionally important economic parameter. Note that the caveats previously stated regarding data in Table 2 for diamond grade are also applicable to average rough diamond value; for most active mines, average rough diamond value is considered proprietary data. In this regard, some of the data shown in Table 2 and Figure 31 are probably low, due to use of

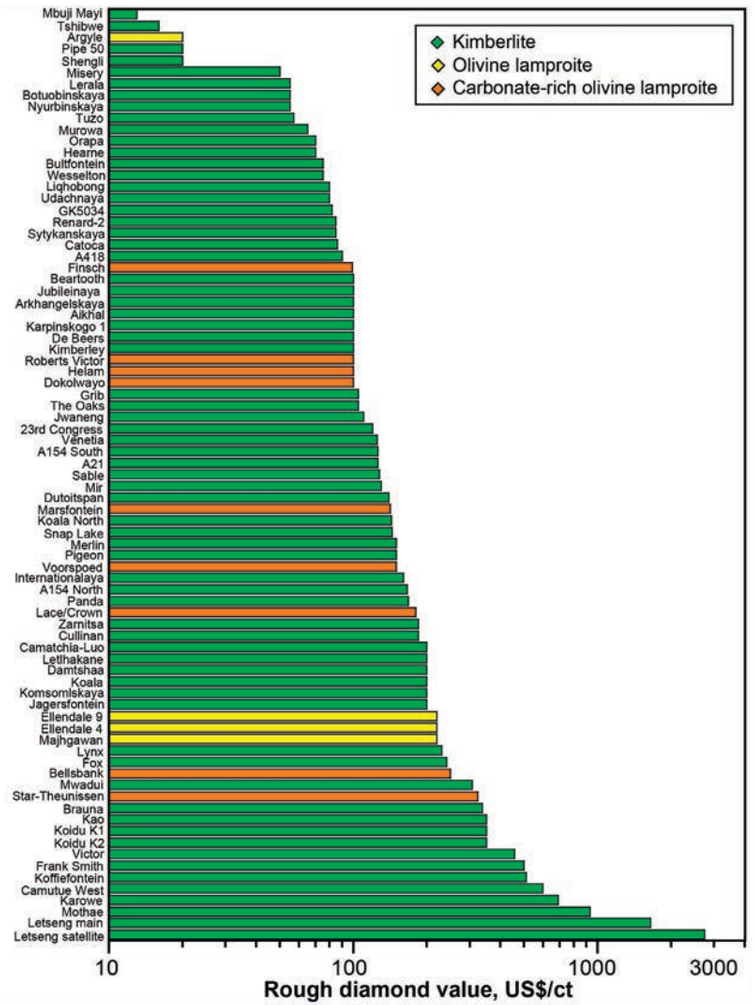

Figure 31. Histogram plot (log scale) illustrating the variation in rough diamond value (in US$ per carat; US$/ct) for global diamond mines (active and past-producers). Data from Table 2. All primary magmatic hosted diamond mines are color coded by rock type (Kimberlite, CROL, olivine lamproite).

exploration or feasibility sampling data. For example, the average value of rough diamonds from the Panda kimberlite (Lac de Gras, Slave Craton, Canada) from the mine feasibility study was US$130/carat, whereas the Panda run of mine rough diamond value increased ~30% to US$168/carat (Kjarsgaard 2007a). This increase can be due to many factors, including lower stone breakage during mining as compared to reverse circulation drilling during exploration sampling, but perhaps more importantly mining typically recovers larger diamonds which can strongly influence average rough diamond values. The more efficient sampling of larger diamonds during mining is due to a statistical under sampling of the larger sieve classes of diamond in exploration or feasibility sampling, even when 3,000 to 10,000 carat parcels of diamond are recovered for evaluation purposes. An additional highly significant problem in comparing average rough diamond values from global mines is the fluctuation in book price over time (years, decades, centuries), due to supply and demand, and general global economic conditions.

The known range for average diamond value from current and past producing mines is quite variable (>2 orders of magnitude), but typically ranges from ~US$13/ct to ~US$300/ct, with exceptional mines having average rough diamond values of ~~US$450/ct to ~US$2,750/ct (Table 2 and in the log histogram plot of rough diamond value in Fig. 31). This wide variation in average rough diamond value for global diamond mines is observed for kimberlites, e.g., compare low value diamonds from Mbuji Mayi or Tshibwe (both in the DRC) and high value diamonds from Karowe (Botswana) or Letšeng (Lesotho) as seen in Figure 31. The variation in average rough diamond value is also observed for olivine lamproites; compare Argyle (lower value diamonds) and Ellendale 4 or 9 (higher value diamonds) mines in Australia Fig. 31). For carbonate-rich olivine lamproites, compare lower value Finsch and higher value Star (Theunissen) average rough diamond values from these two South Africa mines (Fig. 31).

Due to the wide range of diamond grades and rough diamond values observed in individual diamond mines globally, the ore value (Table 2), expressed as US$/t (= grade [ct/t] X rough diamond value [US$/ct]) is a fundamental parameter utilized in assessing the economic potential of a diamond deposit. Global diamond mines have ore values that range from ~US$6/t to ~US$1400/t (log histogram plot, Fig. 32). This wide variation in ore value for global diamond mines is observed for kimberlites, compare the low ore value at Tshibwe (the DRC) with the very high value ore from Internationalaya (Russia). For olivine lamproites, compare lower value Ellendale 9 ore versus higher value ore from Argyle (both in Australia). For carbonate-rich olivine lamproites, compare lower value ore at Finsch with higher value ore at Marsfontein (both in South Africa).

The relationship between diamond grade and rough diamond value is further illustrated on a bivariate log–log plot in Figure 33, which also shows iso-ore value lines. For comparison, the Mbuji Mayi (DRC) and Kao (Lesotho) kimberlites have similar ore values (~17–19 US$/t), but Mbuji Mayi has high diamond grade with low rough diamond value, whereas Kao has low diamond grade, with high rough diamond value (Fig. 33). This general observation regarding the relationship between grade, diamond value and ore value is also applicable to olivine lamproite and carbonate-rich olivine lamproite diamond mines and deposits (Fig. 33).

KIMBERLITE AND LAMPROITE GEOCHRONOLOGY AND THE TEMPORAL DISTRIBUTION OF PRIMARY DIAMOND DEPOSITS

Primary diamond deposits are hosted by kimberlite and a subset of olivine lamproites i.e., olivine lamproite and carbonate-rich olivine lamproite (CROL). Economic diamond-bearing pipes and/or intrusions occur in numerous countries (~15) and typically are found in cratons areas where a relatively thick (>150-km-thick) subcontinental lithospheric mantle is preserved. Globally, the majority of kimberlites and lamproites were emplaced in the last ~25% of Earth

history, with 98% younger than 1.2 Ga (Heaman et al. 2019; this study). There is great interest in understanding whether there is any geodynamic control on enhanced periods of kimberlite and lamproite emplacement and whether temporal windows exist for the formation of these primary magmatic diamond deposits. Recent overviews on the nature of primary diamond deposits in southern Africa (Field et al. 2008; de Wit et al. 2016) showed that kimberlites of economic interest were emplaced over a span of ~1 billion years, with major deposits occurring at approximately 1150 Ma (e.g., Cullinan), 520 Ma (e.g., Venetia), 235 Ma (e.g.,

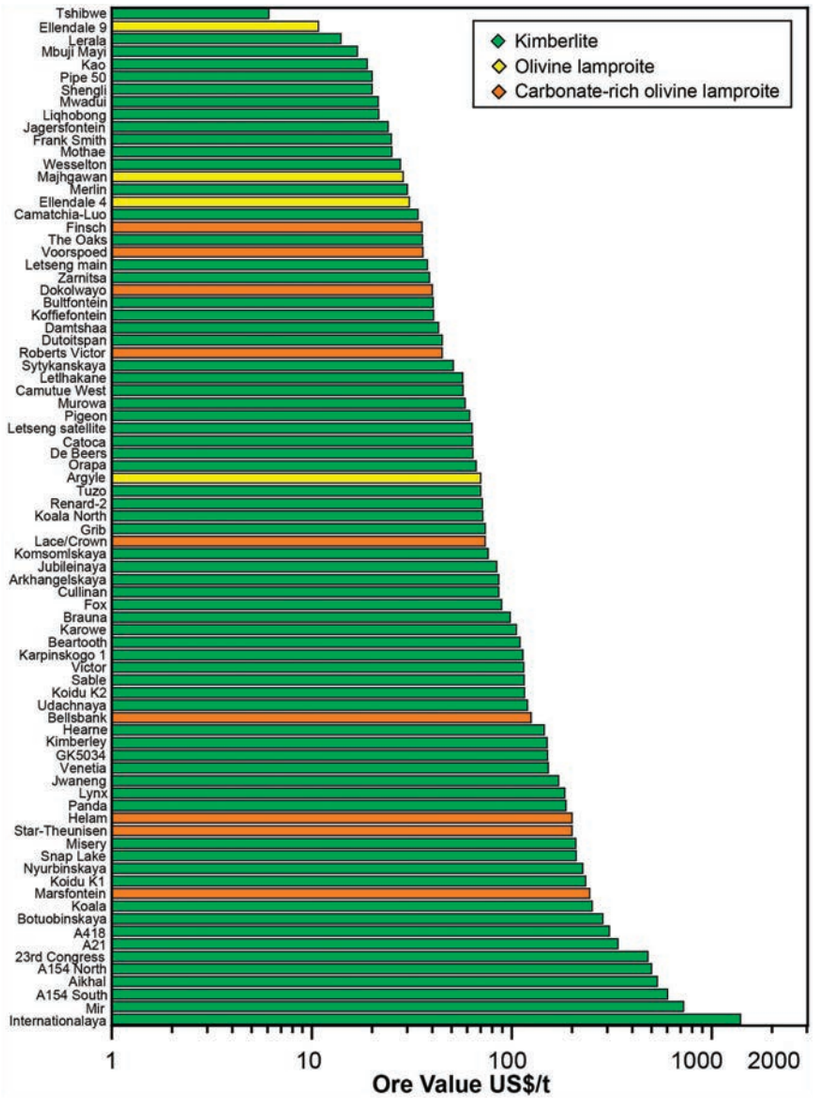

Figure 32. Histogram plot (log scale) illustrating the variation in ore value (in US$ per tonne; US$/t) for global diamond mines (active and past-producers). Data from Table 2. All primary magmatic hosted diamond mines are color coded by rock type (Kimberlite, CROL, olivine lamproite).

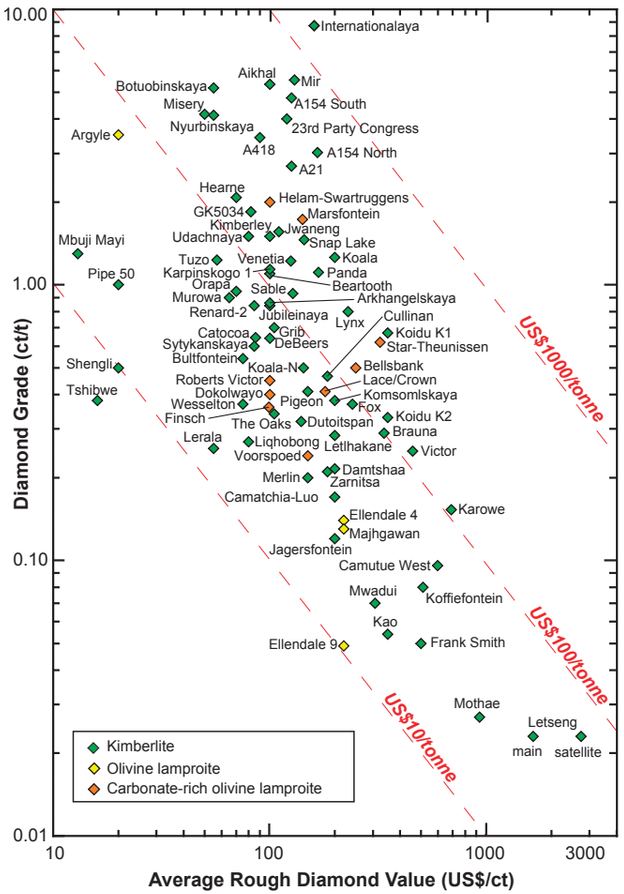

Figure 33. Bivariate log–log plot of diamond grade (ct/t) versus rough diamond value (US$/ct) for global diamond mines (active and past-producers). Data from Table 2. All primary magmatic hosted diamond mines are color coded by rock type (Kimberlite, CROL, olivine lamproite). **Red dashed lines** are iso-ore value lines (US$/t). Note that diamond mines with quite disparate diamond grades and rough diamond values can have very similar ore values; see text for further discussion.

Jwaneng), 95–85 Ma (e.g., Orapa, Kimberley, Letšeng), with CROL of economic interest in the time interval 200–110 Ma (e.g., Dokolwayo, Helam, Voorspoed, Finsch).

In this section we specifically address 1) the importance of applying a higher fidelity screened kimberlite geochronology database, 2) the global age inventory and emplacement history of kimberlites and lamproites, 3) the geochronology of diamond mines and deposits in kimberlite, CROL and olivine lamproite, and 4) the existence of temporal windows that contain a greater proportion of the key economic deposits that have been mined for diamonds. We refer to the "Tier" system of diamond deposits established above (Table 2) that classified the economic value of the various diamond mines that appear as examples in this section.

Veracity of kimberlite and lamproite geochronology

Several kimberlite geochronology databases have been published. Some focus on regions within continents or countries, usually where the majority of known diamond deposits occur e.g., Russia (Smelov and Zaitsev 2013), southern Africa (Jelsma et al. 2004, 2009; Moore et al. 2008; Griffin et al. 2014), and North America (Heaman et al. 2003, 2004). Very few studies have investigated the global pattern of kimberlite emplacement (Heaman et al. 2003, 2019; Tappe et al. 2018a), or the timing of primary magmatic diamond deposit formation. Establishing a robust geochronology database for kimberlites, olivine lamproites and CROLs is challenging because by their nature they are heterogeneous rocks that consist of mixtures of minerals that crystallized from the magma and a plethora of entrained, xenolithic/xenocrystic mantle and crustal material (e.g., Giuliani and Pearson 2019). In some cases, numerous geochronology attempts, by several dating techniques, produced a large range of radiometric dates for a single kimberlite pipe. For example, the Udachnaya East kimberlite has 47 published radiometric dates by four different dating methods yielding a range of dates between 756–326 Ma (most are summarized in Smelov and Zaitsev 2013). In contrast, our approach is different; we use a single Udachnaya East pipe emplacement age of 363.2 ± 1.8 Ma (MSWD = 2.7) based on the agreement of two separate U–Pb perovskite age determinations (Heaman and Mitchell 1995; Kinny et al. 1997). It is certainly possible that there are multiple kimberlite emplacement events within a single pipe that are sufficiently distinct to be resolvable at the precision of current dating methods, as demonstrated for the Renard 2 kimberlite in Quebec in which kimberlite magmatism at this pipe spans ~20 m.y. (Ranger et al. 2018). However, often the large age range reported for a single kimberlite body reflects inclusion of spurious dates that don't accurately record the time of kimberlite emplacement. Spurious dates (too old and too young) can be generated by all geochronology methods and can result from analysing entrained materials, such as crustal or mantle xenocrystic mica or zircon, from a disturbance affecting the dating system that can cause loss or gain of radionuclides (e.g., metamorphism, metasomatism, alteration, weathering), and challenges specific to the analytical methods used, such as incomplete fission track etching (Haggerty et al. 1983) or analyzing mixed mineral fractions. Other limitations with many existing kimberlite geochronology databases, such as 1) many of the dated samples in these databases are not kimberlite—they include dates from "related" and potentially "unrelated" rocks, such as carbonatites, kamafugites, picrites, aillikites, alnöites, melilitites, and various types of lamprophyres, 2) some reported kimberlite dates are inferred, they are not direct determinations but are estimated on the basis of the age of nearby kimberlites that are assumed to be contemporaneous, and 3) the isotopic data for many reported dates are unpublished so the veracity of these cannot be evaluated. We caution against the use of inferred dates because they can be misleading, as many fields contain kimberlites in close proximity that are emplaced over enormous time spans. For example, the central Slave Craton Lac de Gras field (Canada) contains kimberlites erupted over a time span of ~280 m.y. (Sarkar et al. 2015), and in the Siberian craton the Alakit-Markha and Daldyn fields contain kimberlites erupted over 150 m.y. and 200 m.y., respectively.

The kimberlite and lamproite emplacement dates used here are based on a screened geochronology database (Heaman et al. in review) The source references of these dates are listed in on-line Appendix B that contains one date per kimberlite or lamproite, unless there is strong evidence that there are multiple magmatic events with distinct and different age. Where possible, this single date is based on the weighted mean calculation of multiple dating attempts where the determined ages are in agreement within analytical uncertainty. This screened geochronology database of kimberlites and lamproites does not include rock types classified as "related rocks" in previous compilations. The biggest effect by excluding "related rocks" is for Greenland, with 57 emplacement ages that are published (mostly aillikite, ultramafic lamprophyre, and carbonatite) but only seven are kimberlite or lamproite.

Global patterns of kimberlite and lamproite emplacement

Kimberlites and lamproites occur as small intrusions and quite variable but often small volcanic pipes that are often difficult to identify in the field because they are easily weathered, eroded, and/or covered by other deposits. These rock types occur on all continents but their temporal and spatial distribution is uneven. Most known kimberlites pipes and dikes are observed within Archean cratons and it is not surprising that the highest concentration of known kimberlites occur in diamond mining districts where there has been extensive exploration efforts. In this respect, the current global distribution of discovered kimberlites and lamproites, and those for which emplacement dates are available, is biased towards regions with economic diamond deposits. Any kimberlite or lamproite geochronology database will have this inherent bias. Despite this, creating an accurate geochronology database is important for several reasons; it is vital for evaluating the spatio-temporal distribution of kimberlites or lamproites, predicting the location of new clusters/fields, establishing their geodynamic setting, and ultimately understanding their origins. Combining the timing of kimberlite or lamproite magmatism with their diamond tenor enables an evaluation of the possible links between the timing of economic diamond deposits and their geodynamic settings.

A compilation of more than 2350 dates for kimberlites and related rocks was recently summarized in Heaman et al. (2019). Similar to most other compilations, this geochronology database was not filtered, a variety of rock types in addition to kimberlite were included that occur co-spatially with kimberlite clusters/fields. Some kimberlites, such as Udachnaya East discussed above, are over-represented in unfiltered compilations because there is a large number of potentially spurious dates spanning a large age range despite no clear evidence of a protracted emplacement history spanning millions or tens of millions of years. Unfiltered compilations may blur details but can provide a general overview of kimberlite emplacement patterns; the most recent compilation identifies four broad periods of enhanced kimberlite magmatism globally in the last quarter of Earth history at 1,200–1,050 Ma, 600–480 Ma, 400–320 Ma, and 170–50 Ma (Heaman et al. 2019).

Here we have scrutinised the available geochronology data more thoroughly, omitting spurious dates and attempting to avoid over-emphasis on kimberlites with multiple age determinations. We specifically focus on the age distribution of kimberlites, and olivine lamproites and carbonate-rich olivine lamproites, the latter a smaller subset of lamproites (Pearson et al. 2019), because these are the two lamproite sub-types that host economic diamond deposits. Many CROLs reported in this database were previously classified as Group II kimberlites (e.g., Smith 1983). The distribution of dates by continent/country are as follows, with the number of dated occurrences in parentheses; Africa (14 countries; 234), Antarctica (7), Australia (51), Brazil (32), Canada (274), China (2), Finland (14), Greenland (7), India (33), Russia (336), Venezuela (1), and U.S.A. (35).

The total number of compiled dates after screening is 1026; kimberlite (n = 933; 90.9%) and lamproite (n = 93; 9.1%). Despite the uneven abundance of kimberlite and lamproite pipes or intrusions in this database, there is sufficient age data to evaluate whether there are enhanced periods of magmatism and whether there is any overlap in the timing of these magmatic events. We introduce the term epoch to identify globally significant periods of kimberlite magmatism. Epochs are defined here as >30 m.y. periods in Earth history where there is evidence for enhanced kimberlite magmatic activity on a global scale (i.e., in a specific epoch there are occurences in multiple cratons/countries). A kimberlite epoch includes a minimum of 25 known pipes or intrusions and is separated by a >15 m.y. hiatus, or a period of significantly reduced magmatism. We also identify significant temporal periods of kimberlite magmatism that have the potential to become epochs with future geochronology studies on existing, and newly discovered occurrences. For the 93 dated lamproites compiled for this study, we define 6 periods of enhanced lamproite magmatism that each has a minimum of 4 known pipes or intrusions.

Kimberlites. The age distribution of kimberlite magmatism globally is shown in histogram plots (Figs. 34, 35, 36a,b) at increasingly more detailed scale. Greater than 50% of the kimberlite dates are Mesozoic (252–66 Ma) or younger so we highlight their age distribution at the most detailed scale (Figs. 36a,b). A first-order observation from these screened compilation plots is that a larger number of discrete kimberlite epochs are identified compared to the unscreened compilations (e.g., Heaman et al. 2003, 2019; Jelsma et al. 2009; Tappe et al. 2018a). This higher age resolution database emphasizes the value of only reporting high fidelity age determinations (i.e., omitting spurious dates), not over-representing the number of dates reported for a single locality, and being selective about which lithologies are compiled. Although globally it appears that kimberlite magmatism is broadly continuous since ~700 Ma (no substantial emplacement hiatus during this time), eight discrete epochs of enhanced kimberlite magmatism can be discerned from ~1,200–30 Ma, based on frequency distribution plots (Figs. 34, 35). This is a significant increase from the four broad periods of kimberlite/lamproite magmatism based on unfiltered age compilations (e.g., Tappe et al. 2018a; Heaman et al. 2019). These kimberlite epochs with the number of pipes or intrusions per epoch (denoted in parentheses) are:

1) 1,155–1,075 Ma (n = 26)
2) 650–585 Ma (n = 29)
3) 562–505 Ma (n = 29)
4) 440–408 Ma (n = 39)
5) 382–340 Ma (n = 112)
6) 250–214 Ma (n = 69)
7) 197–139 Ma (n = 247)
8) 109–45 Ma (n = 254)

The duration of most kimberlite epochs spans between 30–80 million years. The epochs generally encompass multiple kimberlite fields that individually have emplacement ages spanning <~20–30 m.y. (e.g., Heaman and Kjarsgaard 2000; Heaman et al. 2015). These eight kimberlite epochs capture ~85% of the dated kimberlites. Very young kimberlites with emplacement dates younger than 45 Ma (n = 3), include those in the Kundelungu field, DR Congo (29–33 Ma; Batumike et al. 2008) and the Igwisi Hills volcanoes (Tanzania), that preserve the youngest known pyroclastic rocks and lava flows, with ages of 12,100–6, 000 yr (Brown et al. 2012). There are eight dated kimberlites older than 1,155 Ma, including those in the 1.8–1.6 Ga Kuruman cluster, South Africa (Donnelly et al. 2012), and the 2,128 Ma Turkey

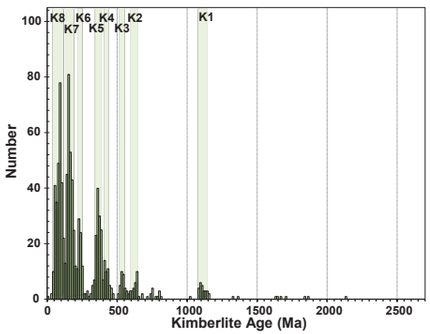

Figure 34. Distribution of kimberlite emplacement dates between 2,500–0 Ma (n = 934). The **green shaded bars** represent global epochs of kimberlite magmatism (K1–K8). Bin width is 10 Ma, 180 bins.

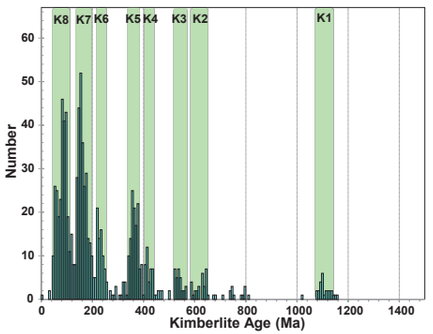

Figure 35. Distribution of kimberlite emplacement dates between 1,200–0 Ma (n = 924) highlighting the 8 identified global epochs (K1–K8) of kimberlite magmatism (**green shaded bars**). Bin width is 7 Ma (larger than the typical 95% confidence limit uncertainty on most kimberlite dates), 180 bins.

Well intrusion, Australia (Jourdan et al. 2012), the latter we consider to be the oldest known kimberlite reliably identified and dated. Thus far, only one kimberlite with sufficient deposit value to be considered economic has been identified that is older than 1.2 Ga, the 1,364 Ma Lerala (Martin's Drift) mine in Botswana.

More than half the kimberlites in the database are Mesozoic or younger and we show a detailed evaluation of the age distribution for these occurrences in Figures 36a,b. Two kimberlite epochs (7 and 8) are currently recognized in this most prolific time of kimberlite magmatism (Fig. 36a). In Figure 36b we show that there is potentially more kimberlite emplacement age structure during the Mesozoic, the light green shaded fields highlighting enhanced sub-periods of magmatism. Epoch 7 (197–139 Ma) can be further subdivided into two significant pulses, at 180–168 Ma and 160–139 Ma. Epoch 8 (109–45 Ma) can be further subdivided into 4 significant pulses at 103–77 Ma, 75–67 Ma, 65–51 Ma and 48–44 Ma (Fig. 36b). A substantial reduction of kimberlite magmatism occurred globally between ~210–180 Ma and ~140–100

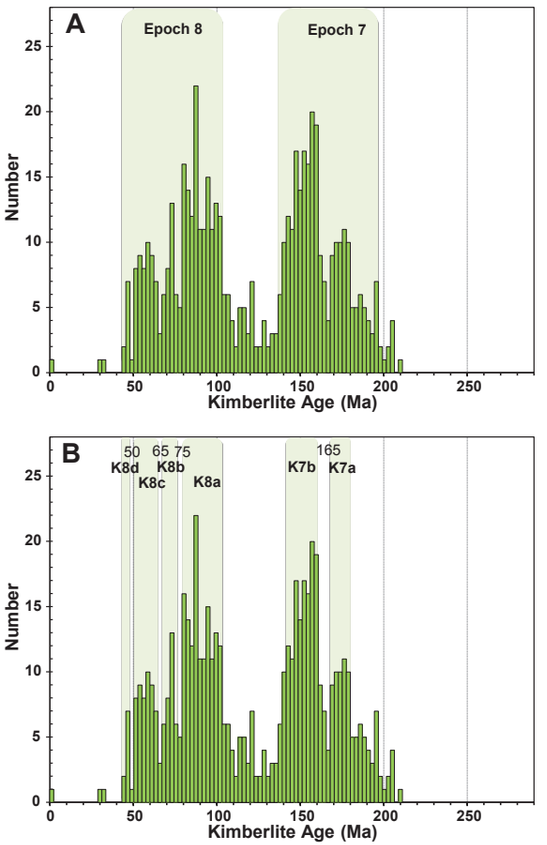

Figure 36. (**A**) Age histogram for Mesozoic and Cenozoic (<210 Ma) kimberlites (n = 553). More than 50% of all dated kimberlites are represented. Shaded green fields (K7 and K8) denote the two youngest kimberlite epochs. Bin width is 2 Ma, 100 bins. (**B**) Detailed evaluation of kimberlite geochronology epochs K7 and K8, identifying up to 6 sub-periods of enhanced magmatism with potential small "time breaks" at ~165, ~125, ~75, ~65, and ~50 Ma. Bin width is 2 Ma, 100 bins.

Ma, in contrast to a greater frequency during earlier Jurassic (180—142 Ma), and subsequent Late Cretaceous (< 100 Ma) times (Figs. 36a,b). High-resolution kimberlite geochronology in the future will reveal whether epochs 7 and 8 can be further refined into additional epochs and whether there are true hiatuses in kimberlite magmatism at ~ 165, 75, 65, and 50 Ma, and lower frequency at 210–180 and 140–100 Ma (Fig. 36b).

Lamproites. Although less abundant than kimberlites, lamproites (dated localities $n = 93$) occur sporadically over the last quarter of Earth history. Unlike kimberlites, a high proportion (~45%) of all lamproite types on Earth are younger than 35 Ma. In this overview we have omitted, and do not discuss a significant number of dated non-diamondiferous lamproite occurrences, such as the leucite lamproites at the Leucite Hills in the U.S.A. ($n = 18$), or the Mediterranean lamproites in Europe ($n = 42$), the latter occurring in a region dominated by Neotectonics far from cratonic regions. Furthermore, in the compilation we have distinguished lamproites (L; $n = 31$), olivine lamproites (OL; $n = 14$) such as the past producing Tier 1 Argyle Mine, and carbonate-rich olivine lamproites (CROL; $n = 48$), such as the Tier 1 Finsch Mine. A high proportion of the lamproites (~65%) occur in three countries/regions, Australia (16), India (11), and southern Africa (33). The oldest lamproites are the Paleoproterozoic 1,719 Ma Por'ya Guba (Russia) and 1,682 Ma Yangare-02 (Australia) intrusions. The youngest is the ~56,000 yr Gaussberg (Antarctica) olivine lamproite. A small number of lamproites are temporally coincident with the kimberlite epochs described above, indicating that a variety of magmas of deep-seated origin can occur in each epoch.

There are six periods where four or more lamproite magmatic events occur (L1 to L6 in Figs. 37a,b):

1) 1,230–1,130 Ma ($n = 10$)
2) 1,080–1,040 Ma ($n = 6$)
3) 550–500 Ma ($n = 5$)
4) 235–200 Ma ($n = 4$)
5) 135–110 Ma ($n = 32$)
6) 22–17 Ma ($n = 14$)

The two youngest time periods of significantly enhanced lamproite magmatism, do not qualify as epochs based on the definition above for kimberlites. Furthermore, two of these periods (L3; 550–500 Ma, and L4; 235–200 Ma) are synchronous with kimberlite epochs K3 and K6, respectively, as described above. However, the two periods of Mesoproterozoic lamproite magmatism do not coincide with Mesoproterozoic kimberlite epoch K1 (Figs. 37a,b). A more detailed histogram of Mesozoic and younger lamproite magmatism is shown in Figure 38, colour coded by country, that highlights the fact that most periods of lamproite magmatism are specific to certain countries/cratons (i.e., most are not global in extent). The 135–110 Ma period (L5 in Fig. 37b) is further subdivided in Figure 38 into two discrete enhanced sub-periods between 135–132 Ma (L5a; $n = 9$; 2 in Russia, 6 CROL in South Africa) and 125–115 Ma (L5b; $n = 20$; all CROL in South Africa). The whole of the 135–110 Ma L5 lamproite period coincides with a lull in global kimberlite magmatism.

The older Mesoproterozoic magmatic period (~1,230–1,130 Ma) is the only lamproite activity that is truly global in extent, with occurrences documented in Australia, Finland, Greenland, India, and Russia (Fig. 39). Some of these lamproites are highly diamondiferous, such as the 1,126 Ma past producing Tier 1 Argyle mine, Australia. A temporally equivalent Mesoproterozoic cluster with CROLs and olivine lamproites occurs in the Karelian craton of Finland and Russia (O'Brien et al. 2007; Phillips et al. 2017; Dalton et al. 2020) and includes the 1,180 Ma Kostomuksha and 1,204 Ma Lentiira intrusions. The younger (1,080–1,040 Ma) Mesoproterozoic lamproite occurrences are all from India (Das et al. 2018). Some of these are diamondiferous, such as the 1,079 Ma Atri deposit and 1,072 Ma Majhgawan mine (Bundelkhand Craton), but have much lower diamond grades than at Argyle. A new finding

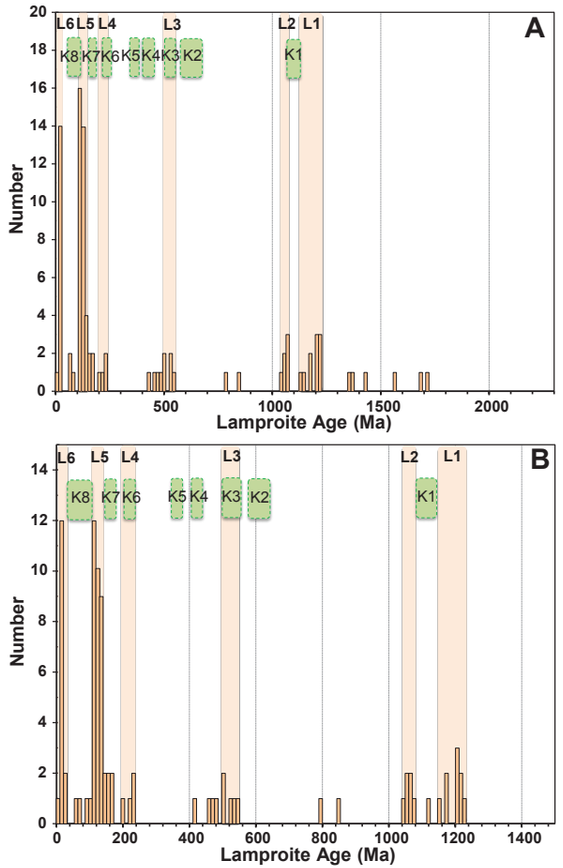

Figure 37. (**A**) Age histogram (2,300–0 Ma) for lamproites ($n = 93$). **Shaded orange fields** denote enhanced periods of magmatism. Kimberlite epochs are denoted by **green fields with green dashed outlines**. Bin width is 16 Ma. Note—lamproite age data does not include Mediterranean lamproites. (**B**) Age histogram (1,500–0 Ma) for lamproites ($n = 87$). **Shaded orange fields** denote enhanced periods of lamproite magmatism. Kimberlite epochs are denoted by **green fields with green dashed outlines**. Bin width is 10 Ma. Lamproite age data do not include Mediterranean lamproites.

from this compilation is the existence of coeval Cambrian kimberlite and lamproite magmatism (Fig. 40). The majority of known Cambrian lamproites occur in the newly discovered Aviat (CROL) and Qilalugaq-Naujaat clusters, northern Rae craton, Canada (Sarkar et al. 2018). One other Cambrian lamproite is reported from Priestly Peak, Antarctica (Black and James 1983).

The youngest period of lamproite magmatism is 22–17 Ma ($n = 14$) and is exclusive to NW Australia. It is curious that there are only three dated olivine lamproites and zero CROLs that are younger than 35 Ma; two of the former localities are in NW Australia, including the two Tier 4 past-producing diamond mines, the 22 Ma Ellendale 4 and 9 pipes. The majority (~65%; 60/93) of dated lamproites are younger than 250 Ma (Fi. 37b). Their most prolific period of emplacement, CROL dominated, was between 135–115 Ma (Fig. 38). Also noteworthy is the conspicuous absence of lamproites from some well-known diamond-producing regions, such as the Slave Craton in Canada.

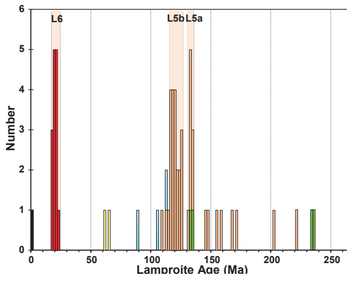

Figure 38. Age histogram of Mesozoic and younger lamproites ($n = 60$). Columns are colour-coded by country: **Gray**-Antarctica, **Red**-Australia, **Yellow**-India, **Blue**-USA, **Orange**-Southern Africa, **Green**-Russia. Enhanced periods of lamproite magmatism denoted by light orange shaded fields. Bin width is 2 Ma.

Summary of global kimberlite and lamproite age distributions

There are two distinct emplacement patterns that describe the timing and distribution of kimberlite and lamproite magmatism. For kimberlites this includes, 1) epochs that are widespread globally and occur in multiple countries/cratons, and 2) epochs that are largely restricted to a specific country or craton. Kimberlites from both of these emplacement patterns are known to contain economic diamond deposits. Using a much smaller geochronology dataset, Heaman et al. (2003) identified four periods of kimberlite magmatism that they considered to be global in extent because contemporaneous kimberlite magmatism was recognized in multiple countries; 60–45 Ma (Canada, Russia, Tanzania), 95–100 Ma (Canada, Russia, South Africa), 140–160 Ma (Canada, Russia, South Africa), and 215–240 Ma (Botswana, Canada, Russia). Based on limited geochronology data available at the time, they also proposed a number of additional potential "global periods" of magmatism, such as a Cambrian kimberlite event recognized in both the Slave and Kaapvaal cratons. Here we propose a slight revision to these conclusions since the few 60–45 Ma age kimberlites previously identified in Russia (e.g., Beta) are ultramafic lamprophyres and not kimberlites senso stricto. Heaman et al. (2003) also identified one period of late Devonian to early Carboniferous kimberlite magmatism (350–370 Ma) that was not global in extent and largely occurred in the Siberian (southern Yakutia) Craton, Russia. These periods of kimberlite magmatism identified previously have a slightly more restricted duration in the current screened compilation, but largely overlap kimberlite epochs 1–5 described here. Lamproite geochronology was not evaluated by Heaman et al. (2003).

The new screened, and hence more objective geochronology database supports the majority of these previous findings but also amplifies our understanding of the number and extent of kimberlite epochs. Ten discrete periods of magmatism are now recognized, eight kimberlite epochs and two periods of enhanced lamproite magmatism. It highlights that some periods of kimberlite magmatism are more prolific and widespread than previously thought. For example, the largely Jurassic epoch 7 kimberlite magmatism (197–139 Ma) was previously recognized in three countries (Canada, Russia and South Africa), but now consists of 248 kimberlites and also 6 lamproites, which have been identified from 12 countries (Angola, Australia, Botswana, Canada, Greenland, Guinea, Lesotho, Russia, Sierra Leone, South Africa, Tanzania, U.S.A.), but are relatively rare or absent in other countries (Brazil, China, and India). Another example of a global kimberlite, and now also a lamproite event, that is more evident from the new data compilation is the late Neoproterozoic to early Cambrian magmatic event (32 intrusions or pipes; Fig. 40) now recognized in 8 countries (Botswana, Canada, Finland, Greenland, Namibia, Russia, South Africa, Zimbabwe).

The geochronology of primary diamond deposit formation

The age of diamond formation in the mantle (Smit et al. 2022, this volume), and the emplacement age of primary magmatic rocks that host diamond deposits emplaced in the crust can differ by billions of years. Diamond formation ages are commonly ancient, as they can reside in the mantle for long periods of time before being entrained in younger kimberlite/lamproite intrusions or pipes. Mesoarchean, Neoarchean and Paleoproterozoic diamonds are known from the Kalahari Craton (Richardson 1986; Richardson et al. 1990, 1999, 2009; summary in Smit et al. 2022, this volume). Mesoarchean diamonds have also been reported from the Slave Craton, Canada. For example, a Re-Os dating study of peridotitic sulfide inclusions in diamond was interpreted to indicate 3.52 Ga growth of diamonds entrained in the Panda kimberlite (Westerlund et al. 2006), whereas the Panda kimberlite pipe that contains the diamonds was emplaced at 53 Ma (Creaser et al. 2004). The processes that form macrodiamonds in the mantle are quite distinct from the processes that form the kimberlite magmas. Diamond formation in the NW Slave craton (e.g., the 173 Ma past-producing Jericho mine) likely occurred during periods of mantle metasomatism related to east-dipping Paleoproterozoic subduction of oceanic crust and the local thermal/metasomatic influence of the 1.27 Ga Mackenzie mantle plume (Heaman et al. 2006; Heaman and Pearson 2010). In contrast, some diamond formation ages correspond to the emplacement age of the magmas that entrained the diamonds and brought them to the surface. Examples include some gem diamonds at Koffiefontein (Pearson et al. 1998), Jwaneng (Gress et al. 2021), Cullinan (Richardson 1986), and fibrous diamonds from a number of localities (Timmerman et al. 2019).

A total of 81 diamond mines (active and past-producers; Table 2), 10 advanced exploration projects and 10 former mines with essentially no diamond production data available, are examined. Of these, 84 are kimberlite and 17 are OL/CROL. Diamond mines and deposits occur in 18 countries; Angola (5), Australia (4), Botswana (8), Brazil (2), Canada (25), China (2), Democratic Republic of Congo (2), Eswatini (1), Guinea (2), India (2), Ivory Coast (1), Lesotho (5), Russia (15), Sierra Leone (2), South Africa (20), Tanzania (1), U.S.A. (2), and Zimbabwe (2). Twelve of these deposits are classified as Tier 1 based on their mined diamond value (to 2019/20) of >13 US$B; Aikhal, Argyle, Catoca, Cullinan, Finsch, Internationalnaya, Jubileinaya, Jwaneng, Mir, Orapa, Udachnaya, and Venetia. Tier 1 deposits occur in most kimberlite epochs except K2 (650–585 Ma) and K7 (197–135 Ma). Two Tier 1 deposits of the same age, 118 Ma Finsch (CROL) and 118 Ma Catoca (kimberlite), do not fall within a proposed kimberlite epoch but do coincide with an enhanced period of lamproite magmatism (L5 = 135–110 Ma), which is prolific in southern Africa. The kimberlites or lamproites for most of these diamonds deposits have accurate emplacement dates, however the age for 13 mines or deposits is unknown (or unpublished) and often inferred based on the age of kimberlites in their vicinity, highlighting the need for additional high-precision geochronology. For example, of the diamond mines listed in Table 2 from Angola, only the 118 Ma Tier 1 Catoca kimberlite has been dated.

The temporal pattern of global diamond deposit formation is similar to the global pattern of kimberlite/lamproite emplacement (Fig. 41). The oldest (1,432 Ma Bobi, Côte d'Ivoire) and youngest (22 Ma Ellendale, Australia) deposits are both hosted in olivine lamproite. There is at least one diamond mine that occurs in each of the eight kimberlite epochs (green-shaded fields in Fig. 41) and the two periods of enhanced lamproite activity that do not overlap any of the kimberlite epochs. The majority of diamond deposits mined so far (51/79; ~65%) are found in kimberlites or lamproites younger than 252 Ma; this is not surprising because the majority of known kimberlites and lamproites are Mesozoic in age.

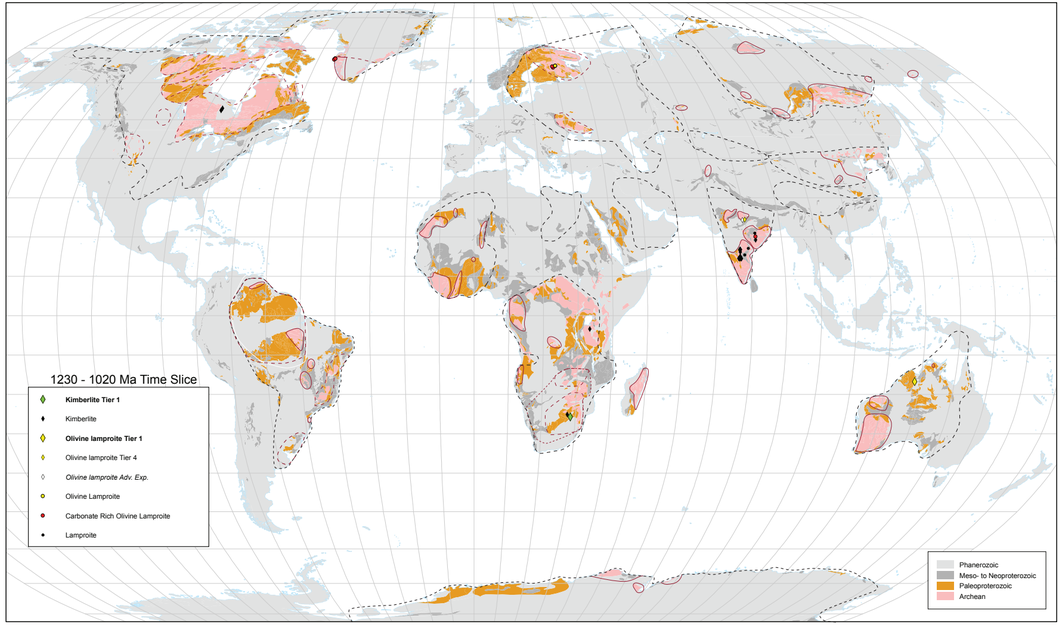

Figure 39. The global distribution of dated kimberlites, olivine lamproites and carbonate rich olivine lamproites during the time interval 1,230–1,020 Ma. **Red solid lines** outline areas of Archean dominated bedrock; **red dashed lines** outline areas of Archean–Paleoproterozoic cratonic regions; **black dashed lines** outline cratonic areas based on mantle geophysics and bedrock > 1 Ga (modified after Pearson et al. 2021). Robinson map projection.

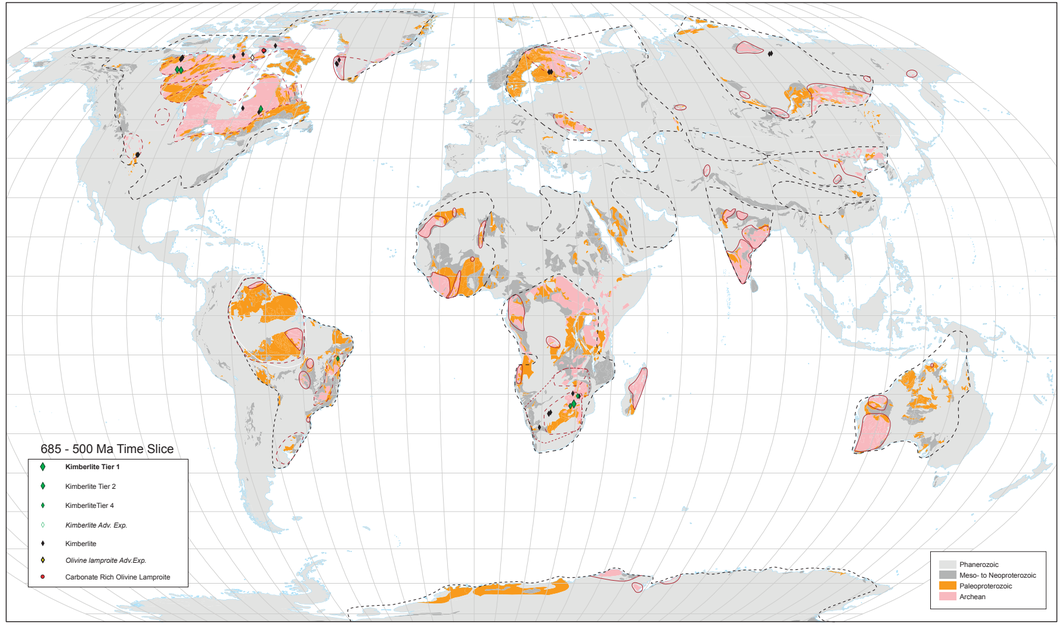

Figure 40. The global distribution of kimberlites, olivine lamproites and carbonate rich olivine lamproites during the time interval 685–500 Ma. **Red solid lines** outline areas of Archean dominated bedrock; **red dashed lines** outline areas of Archean–Paleoproterozoic cratonic regions; **black dashed lines** outline cratonic areas based on mantle geophysics and bedrock > 1 Ga (modified after Pearson et al. 2021). Robinson map projection.

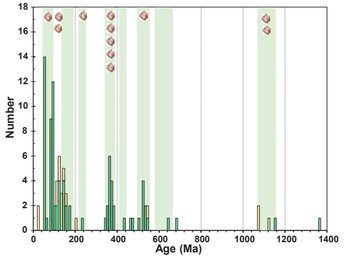

Figure 41. Age histogram (1,400–0 Ma) of worldwide primary diamond mines and deposits (**green** = kimberlite-hosted, **orange** = OL/CROL-hosted); $n = 98$. **Diamond symbols** denote the number of Tier 1 mines in each kimberlite epoch. Bin width is 10 Ma, 120 bins.

From a diamond exploration perspective, it is instructive to know if there are times when diamondiferous kimberlites are more prolific and whether certain kimberlite epochs are more economic than others. A possible reason for this potential variability is that the mantle sources for diamonds may change over time. Local or craton-scale modification of the subcontinental lithospheric mantle (SCLM) can impact the preservation of diamonds. For example, the SCLM beneath Archean cratons is a well-known source of diamonds, but parts of this lithosphere can be chemically modified and/or removed by a variety of processes (Pearson et al. 2021, and references therein), such as metasomatism, thermal erosion during the interaction with one or more mantle plumes (e.g., Liu et al. 2021), or lithosphere delamination. Hence kimberlite or lamproite magmas emplaced prior to lithosphere modification or removal could host economic diamond deposits. Conversely, post-disturbance kimberlite magmatism, such as beneath an area of thinned/hotter lithosphere, is an unlikely source of diamonds, unless the lithosphere subsequently cooled (and thickened) sufficiently to return back into the diamond stability field, as proposed for the Victor Mine, Attawapiskat field, Canada (Smit et al. 2014; Stachel et al. 2018). Griffin et al. (2014) showed that the Sr and Nd isotopic composition of Jurassic and Cretaceous kimberlite magmas erupted into the Kalahari Craton, South Africa become more homogeneous after about 100 Ma, possibly reflecting the removal of ancient metasomatized SCLM at this time, or a temporal switch to more "primitive" deeper magma sources at this time (Woodhead et al. 2019). Both interpretations can explain the paucity of post-100 Ma CROLs, and CROL-hosted diamond deposits in southern Africa.

In a previous study we evaluated whether there is a correlation between the timing of kimberlite emplacement and diamond potential (Heaman et al. 2003) and showed that the majority of economic diamond deposits in various cratons are hosted in kimberlites of different age; Devonian–Carboniferous kimberlites in Russia, Eocene kimberlites in North America, and Cretaceous, Permian and Cambrian kimberlites in southern Africa. Based on this it was concluded that diamond potential is not specifically related to global patterns of kimberlite emplacement. However, in the nearly 20 years since that study there have been numerous new diamondiferous kimberlite discoveries worldwide and more than double the number of kimberlite dates reported, allowing a re-evaluation of this tenet.

Figures 42a,b are plots that show the age of economic diamond deposits in relation to in-situ mined value in US billion dollars (to 2019/20; log scale), and their diamond grade (carat/

tonne), respectively. The deposits are separated into those in kimberlites (green circles) and those in OL/CROLs (orange circles). Also shown for comparison are the 8 epochs of global kimberlite magmatism (light green shaded fields) and 2 distinct enhanced periods of lamproite magmatism (light orange shaded fields) as identified in Figures 34 and 37. Diamond deposits occur in all main epochs of kimberlite, and enhanced periods of lamproite magmatism, but their temporal distribution and diamond grades vary significantly. A first order observation is that there is no correlation between in-situ value and age (Fig. 42a), with Tier 1 (highest value) deposits spanning the range of geological time examined. Using a 1 US$B cut-off, there are a similar number of higher and lower value diamond mines over a 1.2 b.y. time-frame. A second observation from these data is that, apart from Tier 1 Argyle (~18 US$B) and Tier 1 Finsch (~13 US$B), most OL/CROL-hosted deposits are typically lower in mined value (<1 US$B), due to their small size (tonnage), and/or lower diamond grade, and/or lower stone value (see Figs. 5, 30–33).

Two kimberlite epochs (109–45 Ma and 382–340 Ma) contain a substantial endowment (~65%) of known economic primary diamond deposits. As noted in previous studies (Heaman et al. 2003, 2019) some periods of diamondiferous kimberlite are specific to certain cratons. In the 109–45 Ma epoch, 93% (13/14) of the 65–45 Ma diamond mines occur in the Slave craton, Canada, with Mwadui, Tanzania being the exception. For the 110–70 Ma diamond mines, 79% (19/24) occur in the Kalahari Craton, southern Africa (Botswana, Eswatini, Lesotho, South Africa, Zimbabwe). In the 382–340 Ma epoch, all diamond mines are in Russia, with 87% (11/14) in southern Yakutia (Siberian Craton) and 3/14 in the Arkhangelsk area (Kola Craton). However, some diamond-prospective kimberlite epochs occur across multiple cratons; the Neoproterozoic to earliest Cambrian kimberlite-hosted diamond mines are known from both the Slave and Kalahari Cratons. In contrast, there are three kimberlite epochs where economic diamond deposits are scarce, and contain only a small number of diamond mines. There are two mines in the 650–585 Ma epoch, including the 643 Ma Tier 2 Renard 2 (Canada) and the 682 Ma Tier 4, Brauna (Brazil, which is slightly older than epoch K2); one mine in the 440–405 Ma epoch, the Tier 2, 23rd Party Congress (Russia), and; one mine in the 250–210 Ma epoch. However, the latter importantly includes the richest diamond mine worldwide, the 235 Ma Tier 1 Jwaneng kimberlite, Botswana with an in-situ value of 53 US$B.

The majority (10 of 12) of high-value Tier 1 mines (≥13 US$B) are hosted by kimberlite. The exceptions are the 1,126 Ma Tier 1 Argyle olivine lamproite in Australia and the 118 Ma Tier 1 Finsch CROL in South Africa. The number of Tier 1 mines in each kimberlite epoch (shown with diamond symbols in Fig. 41) is as follows; 1,155–1,075 Ma (2; Cullinan, and the Argyle olivine lamproite), 650–585 Ma (0), 562–505 Ma (1; Venetia), 440–408 Ma (0), 382–340 Ma (5), 250–214 Ma (1; Jwaneng), 197–139 Ma (0), and 109–45 Ma (1; Orapa). The high abundance of Tier 1 diamond mines in the 382–340 Ma epoch (i.e., Aikhal, Udachnaya, Jubileinaya, Mir and Internationalaya) is a spatial clustering, related entirely to the Devonian-Carboniferous kimberlites of southern Yakutia, Siberian Craton. As noted above, two Tier 1 mines occur in the 135–110 Ma period of enhanced lamproite magmatism, the 118 Ma Finsch CROL (13.0 US$B), South Africa, and, the 118 Ma Catoca kimberlite (14.7 US$B), Angola.

In Figure 42b there is also no obvious correlation between diamond mine emplacement age and diamond deposit grade (acknowledging that grade can vary widely in a single deposit). Most diamond mines have diamond grades between 0.1 and 1.0 ct/t. Higher grade (>1 ct/t) diamond mines occur in the Mesoproterozoic (1,126 Ma Argyle olivine lamproite, Australia), at Devonian–Carboniferous time in southern Yakutian kimberlites, through to Eocene (56–53 Ma Ekati and Diavik mine kimberlites, Slave Craton, Canada). Mesoproterozoic OL/CROL, of quite variable diamond grades occur in Australia (1,126 Ma Argyle) and India (1,079 Ma Atri and 1,072 Ma Majhagawan).

In Figure 42c we highlight the distribution of diamond deposits by country/region, Canada (red circles), Russia (orange circles), and southern Africa (Botswana, Eswatini,

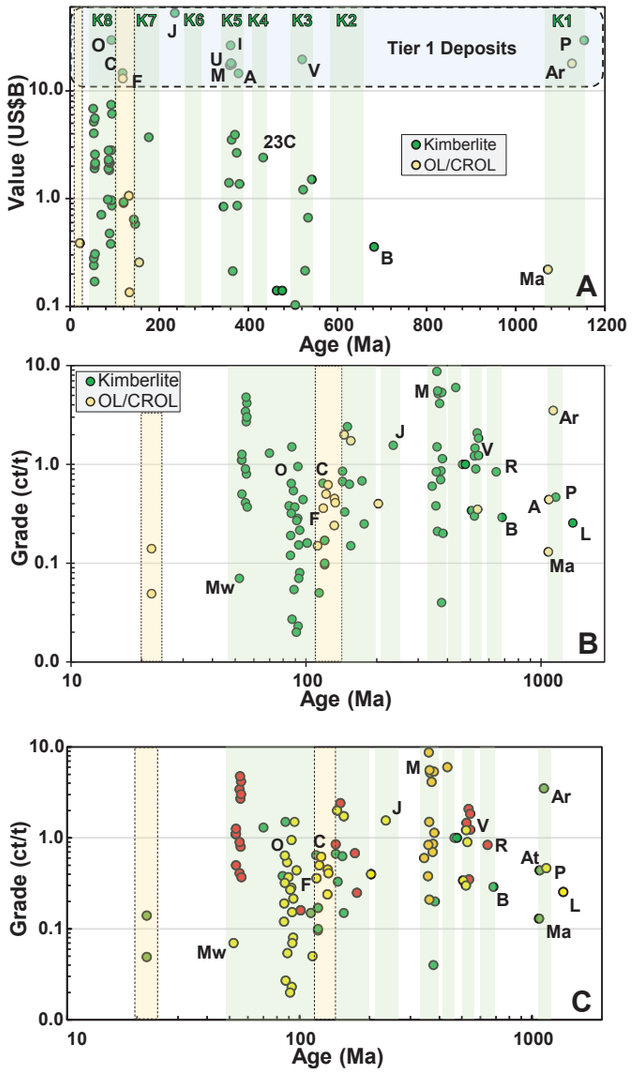

Figure 42. (**A**) Diamondiferous kimberlite and lamproite emplacement age versus diamond mine/deposit in-situ value (US$B log scale). Kimberlites are denoted with **green circles**, lamproites denoted with **orange circles**. Major periods of kimberlite and OL/CROL magmatism shown with **green and orange shaded fields**, respectively. Tier 1 deposits have mine-life values of >13 US$B (**blue shaded field**). (**B**) Diamondiferous kimberlite and lamproite emplacement age versus diamond grade (carat/tonne), log–log plot. (**C**) Diamondiferous kimberlite and lamproite emplacement age versus diamond grade (carat/tonne) highlighting deposit distribution by country: Canada (**red circles**), Russia (**orange circles**), and southern Africa (Botswana, Eswatini, Lesotho, South Africa, Zimbabwe; **yellow circles**), log–log plot. Main kimberlite (**green**) and OL/CROL periods (**orange**) shown as shaded bars. **Green circles** represent other diamond mines/deposits not located in southern Africa, Russia, or Canada. Individual deposits denoted in 42B and 42C as follows: A—Aikhal; Ar—Argyle (Tier 1); B—Brauna (Tier 4); C—Catoca (Tier 1); F—Finsch (Tier 1); J—Jwaneng (Tier 1); M—Mir (Tier 1); Ma—Majhagawan (Tier 4); Mw—Mwadui; O—Orapa (Tier 1); R—Renard (Tier 2); U—Udachnaya; V—Venetia (Tier 1); 23C—23rd Party Congress.

Lesotho, South Africa, Zimbabwe; yellow circles). Note that in the following text, the names of *"Advanced Diamond Exploration Projects"* are shown in *italics*. In some countries the diamond mines occur in specific kimberlite/lamproite epochs. The Majhagawan mine and *Atri advanced exploration project* (India) occur in ~1.1 Ga olivine lamproite. Across Russia (Arkhangelsk and southern Yakutia), >90% (14/15) of the kimberlite diamond mines formed in the 382–340 Ma kimberlite epoch, and most of these (9/15) were emplaced in an even more restricted time period between 356–366 Ma (all in southern Yakutia). In contrast, the Canadian and southern African diamond deposits are distributed between multiple kimberlite epochs. In Canada diamond mines and advanced exploration projects occur during 4 epochs: 56–51 Ma Lac de Gras and 103 Ma *Fort à la Corne* in the 109–45 Ma epoch; 177 Ma Victor, 172 Ma Jericho and 150 Ma *Chidliak* in the 197–139 Ma epoch; 523 Ma Snap Lake, 541 Ma Hearne, 542 Ma GK5034, 542 Ma Tuzo and 546–531 Ma *Qilalugaq-Naujaat* in the 565–505 Ma epoch; 643 Ma Renard 2 in the 650–610 Ma epoch. In southern Africa, diamond deposits formed during six kimberlite epochs and 1 OL/CROL period. Most southern Africa diamond mines occur in Late Cretaceous (<100 Ma) kimberlite pipes (n = 26; ~70%), but importantly include the 250–210 Ma (Jwaneng), 570–520 Ma (Venetia, Murowa, The Oaks, *River Ranch*), and 1155–1075 Ma (Cullinan) mines in kimberlite pipes. In addition, at 180–140 Ma are the Marsfontein and Helam (Swartruggens area) diamond mines in CROL dikes or pipes.

An important new finding in this study is that ~80% of the 32 Cambrian pipes or intrusions worldwide are kimberlite and a relatively high proportion (~25%) are economic (Figure 42a), being either past producers, or are currently mined for diamonds, or are advanced exploration projects. In Canada, this includes Snap Lake, GK5034, Hearne, Tuzo, Qilalugaq-Naujaat, Kelvin, and Faraday, and in southern Africa the Venetia and Murowa mines. These new dating results clearly indicate that economically important Cambrian kimberlites and lamproites are more widespread than previously thought and that this epoch of magmatism is of considerable interest to diamond explorers.

Diamond deposit temporal windows

There are a number of factors that contribute to the generation of primary diamond deposits, including: 1) those that contribute to the formation, preservation and, in some cases, destruction of diamonds in the mantle, and; 2) those that are responsible for entraining and transporting diamonds to the Earth's surface. It is reasoned herein that the nature (magma composition, oxidation state, diamond entrainment capacity, and ascent rate), location (depth of magma generation, ascent path relative to diamond-rich mantle regions) and timing of kimberlite magmatism are key factors in forming primary diamond deposits. For example, if certain periods of kimberlite magmatism are corrosive to diamonds or they don't ascend through diamond-enriched mantle then such magmas would be barren of diamonds. Regarding the importance of kimberlite timing, in mantle sections where diamond formation is young and close in age to periods of broadly synchronous kimberlite formation (e.g., Koffiefontein), older kimberlites in the field cannot entrain diamonds that have not yet formed. In some locations mantle processes occurring after diamond formation, such as metasomatism, delamination, or thermal perturbations, could destroy or modify the quality of diamonds. For example, some diamond deposits have a high abundance of diamonds with graphite coatings that could form during subsequent mantle metasomatism. This could explain why, in certain fields where kimberlite magmatism occurs periodically over a long period of time, diamond mines occur in specific kimberlite epochs.

Below we focus on three examples of diamond deposit temporal windows that occur in some of the most productive primary magmatic sourced diamond mining areas on Earth, the Cretaceous Kalahari Craton deposits in southern Africa (Botswana, Eswatini, Lesotho, South Africa, Zimbabwe), the Devonian-Carboniferous Siberian Craton deposits in Yakutia, Russia (plus temporally equivalent kimberlite-hosted deposits in the Kola Craton), and the Paleocene (Eocene) central Slave Craton deposits in the Northwest Territories, Canada.

Kalahari Craton, southern Africa. The majority of diamond mines (n = 33) in southern Africa (Botswana, Eswatini, Lesotho, South Africa, Zimbabwe) are associated with Mesozoic age kimberlites and CROLs. A summary of the timing of this Mesozoic kimberlite (green) and OL/CROL (orange) magmatism is shown in Figure 43 (bin size is ~4 m.y.). Also shown in Figure 43 is the timing of economic diamond deposits (denoted by diamond symbols). There are two dominant periods of magmatism (135–105 Ma and 95–70 Ma) and both contain important diamond producers/past producers (20 and 13 mines, respectively). In the time period between 150–100 Ma, ~65% (33/50) of the dated localities in southern Africa are CROL. The majority of CROL magmatism (135–115 Ma) overlaps with but is generally older than southern Africa kimberlite magmatism (55–120 Ma). Two peaks in CROL magmatism can be discerned in Figure 43, the main peak is between 125–113 Ma containing the notable Tier 1 Finsch mine and a narrow secondary peak between 135–132 Ma (n = 7; Blaaubosch, Besterskraal, Lace/Crown, Roberts Victor, Saltpetrepan, Stieniesrus-Rex Mine, and Voorspoed). Economic diamond deposits occur in both periods of CROL magmatism.

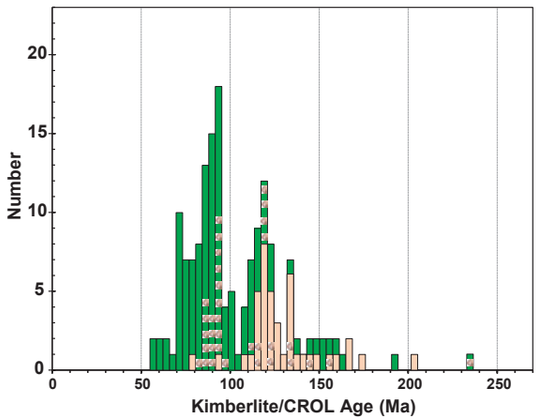

Figure 43. Histogram of Mesozoic and Cenozoic kimberlite (**green**) and CROL (**orange**) emplacement ages from southern Africa (Botswana, Eswatini, Lesotho, South Africa, Zimbabwe). Emplacement age of primary magmatic diamond deposits are shown with a diamond symbol. Bin width = 3.5 Ma.

A more detailed summary of the emplacement ages for Late Cretaceous (100–70 Ma) southern Africa kimberlites is shown in Figure 44. The producing/past producing diamond mines are labelled. A significant proportion (36%; 16/44) of kimberlite-hosted diamond mines in southern Africa occur within a narrow (~10 m.y.) time window between ~95–86 Ma in the Late Cretaceous.

Siberian and Kola Cratons, Russia. A very high proportion of diamond mines in Russia are observed in Paleozoic age kimberlites (Fig. 45). These kimberlites are colour coded to distinguish those that occur in the Arkhangelsk field (dark green circles) in the Kola Craton, from those that occur in the southern Yakutia kimberlite fields of the Siberian Craton (white and light green circles). The Yakutia kimberlites are further distinguished, to identify those that occur within kimberlite fields (Alakit, Daldyn, Nakyn, Malo-Botuobiya) where there is active diamond mining (light green circles), in contrast to kimberlite in fields with no active diamond mines (white circles). The locality names of the kimberlite diamond mines are also labelled. Diamond mines occur in Paleozoic kimberlites that have a large range in emplacement age (~90 m.y.). The oldest Paleozoic diamond mine is the 433 Ma 23rd Party Congress kimberlite, the youngest is the 344 Ma Sytykanskaya kimberlite. However, the most striking feature of this plot is that 60%

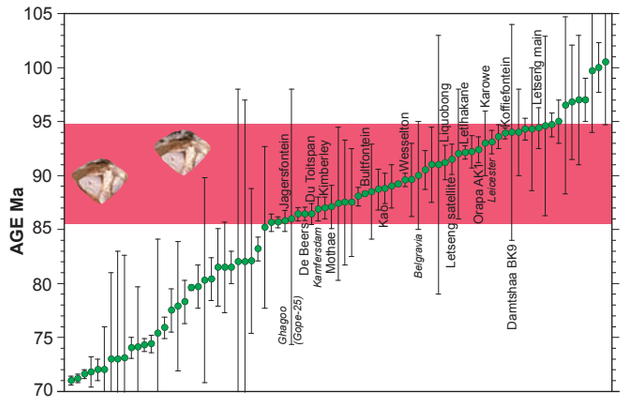

Figure 44. Compilation of kimberlite emplacement dates in southern Africa within the age range of 100–70 Ma. The 17 Cretaceous age diamond mines are denoted by name; all are within the narrow (~10 m.y.) temporal window between 95–85 Ma.

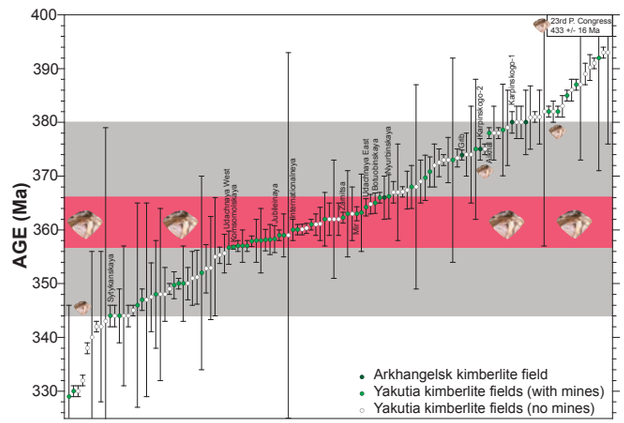

Figure 45. Age distribution of Paleozoic kimberlites in Russia. The kimberlites are subdivided into those from the Arkhangelskaya (**dark green**) and southern Yakutia (**white and light green circles**) kimberlite fields. Yakutian kimberlites that occur within fields that host diamond mines and deposits are denoted with **light green circles**. Individual diamond mines are identified. The **red shaded region** denotes the proposed temporal window for 75% of the Yakutian diamond mines (9 of the 12), except the Aikhal, Sytykanskaya and 23rd Party Congress mines. The broader 380–344 Ma timespan encompasses 14 of the 15 Russian diamond mines.

(9/15) of Russian kimberlite-hosted diamond mines were emplaced within the narrow (~10 m.y.) period between 366–356 Ma (red shaded field), and 14/15 Russian diamond mines (Yakutia and Arkhangelsk regions) over ~45 m.y. within the time span 380–344 Ma (grey shaded field). As noted previously, this group of Paleozoic kimberlites is exceptional, with five Tier-1 diamond mines, more than within any other epoch, or within a single craton.

Central Slave Craton, Canada. The Lac de Gras kimberlite field in the central Slave Craton, Canada consists of more than 250 kimberlites, 53 of which have well-established emplacement dates (Fig. 46). An Eocene diamond mine window for the Lac de Gras field, of 52–56 Ma (~50–58 Ma including age uncertainties) based on seven kimberlites from the Ekati and Diavik

mines was first reported on by Kjarsgaard et al. (2002). The occurrence of dated diamond-bearing kimberlites in this field was further delineated by Sarkar et al. (2015; ~45–55 Ma) and Heaman et al. (2019; ~45–56 Ma). In this study we specifically re-investigate the age pattern of the kimberlite diamond mines. The ages of Lac de Gras kimberlites are shown in Figure 46. In this evaluation, the ten dated kimberlite-hosted diamond mines in the Lac de Gras field (Fig. 46) have a very narrow (3 m.y.) emplacement period between 56–53 Ma (51–61 Ma with age uncertainties), despite the fact that there is an extended period (~280 m.y.) of kimberlite magmatism in this field, with one kimberlite, the Eddie pipe, being as old as ~325 Ma (Sarkar et al. 2015) and the youngest at ~45 Ma (the Aaron kimberlite; Heaman et al. 2004). Furthermore, of all the 56–53 Ma dated kimberlites in the Lac de Gras field, a high proportion (10/15) contain economic diamond deposits and support the contention that diamond deposit temporal windows are real and significant.

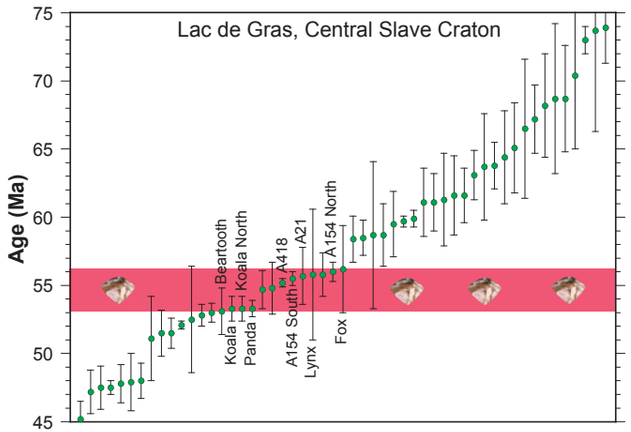

Figure 46. Compilation of Eocene-Cretaceous kimberlite emplacement ages from the Lac de Gras kimberlite field, central Slave Craton, NT, Canada. Ten of the thirteen kimberlite mines/deposits listed in Table 2 have precise emplacement dates and their pipe names are denoted. The **red band** highlights a remarkably short temporal diamond window (56–53 Ma) for this field. It should be noted that a 325 Ma kimberlite also exists in this field, that is not economic.

The examples outlined above demonstrate that a high proportion of diamond mines in arguably the most productive diamond-mining regions on the planet (Russia, southern Africa, Canada) are in kimberlites that were emplaced within extremely narrow temporal windows (≤10 m.y.), within restricted geographic areas. It is noteworthy that these three temporal windows are specific to each craton/country (366–356 Ma, 95–86 Ma, 56–53 Ma, respectively).

Origins of kimberlite diamond deposit temporal windows

The various kimberlite provinces and fields that have detailed geochronology available, as examined above, make a strong case that kimberlites erupting within specific time windows are more likely to be of higher economic value than others. There are clear exceptions, such as Jwaneng, but in fields where many kimberlites have been dated, a case for temporal clustering can be made. The time windows for all or the majority of economic kimberlites vary from ~ 10 m.y. for Yakutia and for the Kalahari Craton, to ~3 m.y. for the Lac de Gras field. This relationship has made kimberlite geochronology a critical part of diamond exploration in some regions. The cause of the apparent correlation between kimberlite age and the likelihood of economic viability, i.e., diamond deposit temporal windows, is unknown.

In many respects, this apparent temporal relationship runs contrary to "conventional wisdom" that diamondiferous kimberlites represent a random event with respect to kimberlite sampling of un-related diamond source rocks in the mantle (e.g., Gurney et al. 2005).

In order to better understand the origin of diamond deposit temporal windows it is important to have a clear understanding of the abundance, distribution, and origin of the diamonds recovered in these deposits together with salient features of the kimberlite magmas that transport the diamonds to the surface; such as their depth of formation, ascent pathway through the mantle and crust, and carrying capacity for transporting mantle material. Some insight into the origin of diamonds can be gleaned from the nature of their mineral inclusions, although only a fraction of mined diamonds contains such inclusions (Stachel et al. 2022, this volume). Previous diamond mineral inclusion studies (Stachel and Harris 2008) have shown that diamonds occur throughout the Earth's mantle below the diamond–carbon stability transition at > ~140 km depth. Certain diamonds (~8%) originate from ultra-deep mantle sources (e.g., >410 km depth in the transition zone or lower mantle; Stachel et al. 2000; Tappert et al. 2005; Pearson et al. 2014; Walter et al. 2022, this volume) based on the preservation of unusual mineral inclusions that are only stable at great depths in the mantle (e.g., majorite, jeffbenite, ringwoodite). If a large inventory of super-deep diamonds exists in the transition zone or lower mantle, then they will only be sampled by kimberlite magmas that form at equally great depths, unless mantle convection acts as an intermediary, somehow bringing these diamonds to asthenospheric depths, or to the base of the lithosphere.

Accepting the former assertion of a deep source region, one end-member explanation for a temporal restriction in diamond deposits is that the Tier 1 diamond mines are in kimberlites that have these very deep mantle sources and have entrained a large cargo of super-deep plus lithospheric diamonds. However, few diamond mines listed in Table 2 are known to contain super-deep diamonds (exceptions include Argyle, Cullinan, Diavik, Ekati, Jagersfontein, Karowe, and Letšeng). Unless there are a large number of undetected super-deep diamonds occurring in mines that formed during a distinct kimberlite diamond mine temporal window, we conclude that there is no correlation between very deep kimberlite magma formation and the formation of diamond deposit temporal windows. A possible association between depth of kimberlite magma generation and the economic value of a deposit is the presence of very large, highly valuable Type II diamonds, which only occur in kimberlites, but not in olivine lamproite- or CROL-hosted diamond mines. It is possible that Rayleigh–Taylor instabilities at a deep Earth boundary layer, such as the lower mantle / upper mantle boundary, or the core / mantle boundary may produce short temporal bursts of kimberlite magmatism that are capable of transporting these deeply derived, very high value diamonds that make some low-grade deposits (e.g., Letšeng, Lesotho), economically viable. However, such a hypothesis would have to invoke different depths of origin for other kimberlites of similar or different age, that did not contain these high value gems.

Because diamond inclusion studies indicate that most inclusion-bearing diamonds (92%) originate from relatively shallow (140–250 km depth) SCLM lithologies, primarily peridotite and eclogite (Stachel and Harris 2008), other explanations must be sought for the temporal window association of diamond deposits. The oldest diamonds (>2.7 Ga) typically occur in harzburgite lithologies whereas eclogitic and lherzolitic diamonds are typically younger than 2.7 Ga and are predominantly of Proterozoic age (Shirey et al. 2013; Smit et al. 2022, this volume). There is a growing list of deposits (Cullinan, Koffiefontein, Damtshaa, Finsch, Jwaneng, Orapa, Letlhakane, Venetia, Mir, 23rd Party Congress) with diamonds that formed during multiple distinct diamond forming events, often spanning a large time-frame (>2 billion years; see Smit et al. 2022, this volume for summary). An important feature of some diamond deposits listed in Table 2 is that there are multiple discrete periods of diamond formation at a single mine (Smith et al. 1991; Pearson et al. 1998; Richardson et al. 2004; Koornneef et al. 2017). In an innovative study of diamonds recovered from the 363 Ma Mir kimberlite, part of the Siberian Paleozoic diamond deposit temporal window, it was shown that sulphide inclusions

extracted from diamond core and rim growth zones yield distinct Re–Os dates of 2.1 and 1.0 Ga, respectively (Wiggers de Vries et al. 2013). The 92 Ma Orapa and Letlhakane mines both recover diamonds that formed at distinct time periods (Timmerman et al. 2017; Gress et al. 2021). In fact, it seems that the more diamonds that are dated from a given deposit, the higher the likelihood of finding multiple generations of diamond growth in the underlying mantle lithosphere that was subsequently sampled by the kimberlite. These diamond growth events can often be linked to large-scale (global) mantle processes, such as the formation of Large Igneous Provinces, periods of continental rifting, and enhanced periods of oceanic lithosphere subduction. We conclude that a pre-requisite for the formation of economic primary diamond deposits is the existence of mantle regions that are rich in diamonds, produced by multiple diamond forming events, which are subsequently sampled by passing kimberlite/lamproite magmas during their ascent. However, there is no obvious connection between the generation of diamond mineralization in the mantle and the formation of diamond deposit temporal windows, since some of the Tier 1 deposits (e.g., Orapa) that contain multiple diamond growth ages occur within a temporal window, and some (e.g., Jwaneng, Catoca) do not occur in a diamond deposit temporal window.

Another possible explanation of why certain temporal periods of kimberlite magma formation could be more favourable to containing diamond deposits is that magma generation occurred at sufficient depth within the diamond stability field (>140 km) and the source region was relatively spatially focused. During ascent these magmas passed through a diamond-rich region in the mantle and were successful at entraining a large cargo of mantle material from this region. As the magmas continued to ascend through to the crust they followed local structures, forming dikes, sills and pipes at the surface. This can be described as the common magma source hypothesis for synchronous diamond deposit formation. If correct, one prediction of this hypothesis is that the diamond mines or deposits in kimberlites (or lamproites) should have similar ages, geochemistry, and radiogenic isotopic compositions that reflect the nature of their common source. Although there are some published Lac de Gras kimberlite Sr–Nd–Hf isotopic data (Dowall 2004; Tappe et al. 2013; Woodhead et al. 2019; Tovey et al. 2021), there are insufficient radiogenic isotope data for the Eocene age kimberlite diamond mines in the Lac de Gras field, NT, Canada (those listed in Table 2) at present to test this hypothesis. However, in southern Africa, radiogenic isotope studies of the Cretaceous age kimberlite-hosted diamond mines (Woodhead et al. 2009; Griffin et al. 2014) indicate two possible sources for these kimberlite magmas based on their perovskite initial strontium isotope compositions; a lower $^{87}Sr/^{86}Sr_i$ group (0.7032–0.7036; Kao, Letšeng, Liquobong, Lethlakane, Orapa) and a higher $^{87}Sr/^{86}Sr_i$ group (0.7039–0.7046; Jagersfontein, De Beers, Dutoitspan, Matsoku, Wesselton, Koffiefontein). These perovskite Sr isotope results either point to two different kimberlite magma sources, or there is a single magma source ($^{87}Sr/^{86}Sr_i$ ~0.7032) that was variably contaminated with more radiogenic lithosphere. We conclude that a single magma hypothesis could explain the existence of some diamond formation temporal windows, but that more research is required.

REVIEW OF GLOBAL SECONDARY DIAMOND DEPOSITS

Background

Secondary diamond deposits are formed by a range of sedimentary and diagenetic processes that operate under different climatic and geomorphological conditions of which the fluvial and marine environments have shown to have been the most effective. Placers specifically are accumulations of valuable minerals (e.g., diamond) formed by gravity separation during sedimentary processes. Diamond has a specific gravity higher than most common minerals (SG = 3.52) and hence, much like any other heavy mineral, there is sufficient density contrast to separate it from the worthless gangue (non-ore) minerals, and also most rock types. Only if the deposit is winnowed in this way can the minerals be concentrated to economic levels. The importance of trap-sites and other ingredients required to develop alluvial deposits has been covered in contributions such as Sutherland (1982), Muggeridge (1995), Marshall and Baxter-Brown (1995) and Jacob et al. (1999).

Diamond is also the hardest mineral (hardness of 10) and is therefore tough, but it can break along fractures by interparticle collision. Hence diamonds do break during transport especially those that are weakened by fractures and inclusions, and as a result the percentage of durable "cleaner" and superior quality stones increases during sedimentary cycle(s). Diamonds are also resistant to chemical weathering and can therefore be concentrated during diagenesis and/or pedogenesis of the host material when this is broken down and removed.

To assess a complete source-to-sink model, a robust understanding of stratigraphy, geomorphology and climatic conditions is required. Identification of hiatal periods when there is neither erosion nor sedimentation, is crucial in the stratigraphic record. New technologies have been applied to improve the source-to-sink resolution such as, single grain geochronology, cosmogenic dating, low-temperature thermochronological estimates for long-term erosion rates, off-shore seismic studies to quantify sediment fluxes from the catchment areas (sources) to off-shore basins (sinks). Finally, uplift and exhumation events, critical in the development of secondary deposits, and timing thereof are now integrated with landscape evolution and depositional models. Not many source-to-sink systems are complete and we may only see part of the journey of diamonds that have been eroded out of kimberlites or lamproites to their final resting place.

Three categories of placer deposits have been recognized: *retained* (such as in the kimberlite craters, or deposits associated with, but external to kimberlites; diamonds trapped in karst sediments, or in older intra-cratonic sediments); *transient* (diamond-bearing sediment accumulations along dispersal routes or within the active drainage basin); and *terminal* placers (at the terminal end of the transport system usually along basin margins subjected to marine reworking processes) (Bluck et al. 2005).

Archean

South Africa (Gauteng Province): Witwatersrand supergroup—Transient/terminal placer (Mesoarchean). The oldest reported alluvial diamonds are from the conglomerates of the Witwatersrand Supergroup gold placer (Fig. 47) where several hundred carats were recovered from the Turffontein Subgroup (previously the Elsburg Series) of the Central Rand Group, particularly on the West Rand, but some also from the East Rand (Raal 1969). Single zircon U/Pb dating results show that sedimentation in the basin occurred between 3,074 and 2,714 Ma, a period of some 360 m.y. (Robb and Robb 1998). The Elsburg Reef is between 2,894 Ma and 2,780 Ma in age, and the diamonds from here are between 1 and 2 ct in size with one 8 ct reported stone (Young 1914). However, Smart et al. (2016) suggest that diamonds were also recovered from the base of the Witwatersrand Supergroup (West Rand Group) deposited between 3.1 and 2.9 Ga.

Deposition in the Witwatersrand basin commenced in a shallow marine environment, forming the lower West Rand Group. During the subsequent Central Rand Group regression stage (Tucker et al. 2016), sedimentation occurred on coalescing lobes on extensive braid deltas or alluvial fans that spread along the margins of the basin with typical braided stream processes (Minter and Leon 1991). Since there is evidence of localized marine incursions, fluvial deposits may in part have been upgraded by marine reworking (Tucker et al. 2016). The headwaters of the rivers, based on paleocurrent analysis along the northern margin of the basin, were to the north and northwest. Diamonds have been described ranging from cadmium-yellow to yellow-green and dark green (Williams 1932). The color is only skin deep and is due to radiation damage from the uranium that is present in the same conglomerates (Raal 1969). Raal (1969) also mentioned that most of the Wits diamonds are Type I, and Denny (1897) described most of them as rhombic dodecahedra.

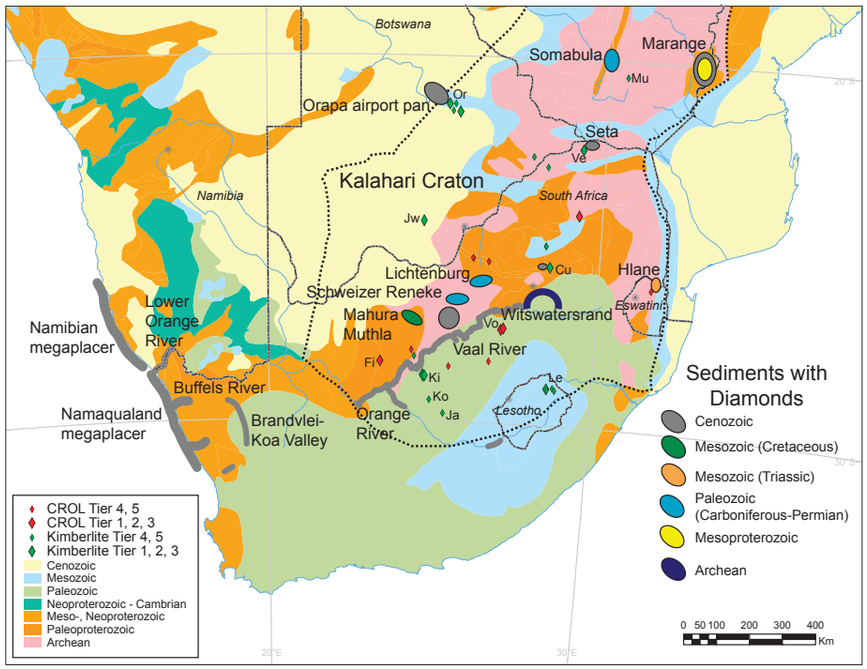

Figure 47. Southern Africa placer deposits, as labeled on the map (Marange, Somabula, Lichtenburg/Ventersdorp, Schweizer Reneke, Vaal River, Orange River, Brandvlei/Koa valley, Lower Orange River, Buffels River, Namaqualand megaplacer, Namibian megaplacer, Mahura Muthla, Witwatersrand, Hlane, Orapa Airport pan and Seta). Primary magmatic kimberlite and CROL mines/deposits as follows: Mu, Murowa; Or, Orapa; Ve, Venetia; Jw, Jwaneng; Cu, Cullinan; Vo, Voorspoed; Fi, Finsch; Ki, Kimberley pipes; Ko, Koffiefontein; Ja, Jagersfontein; Le, Letšeng. Mercator map projection.

Canada (Nunavut): Tree River area—Terminal placer (Mesoarchean). Three diamonds have recently been recovered from a Mesoarchean gold-bearing conglomerate (2.96 Ga) on the northern part of the Slave Craton (Fig. 48) in the Tree River area (Timmerman et al. 2020). These quartz-pebble conglomerates are at the base of the Central Slave Cover Group and have been interpreted as continental margin deposits followed by a marine transgression (Haugaard et al. 2021). This indicates that diamonds were released from deeply derived volcanic rocks and concentrated in Archean marine settings not only in South Africa but also in Canada.

Canada (Ontario): Wawa area—Retained and transient/terminal placers (Neoarchean). It has been shown that erosion rates of the central shield areas in Canada have generally been low (Flowers et al. 2006). Cretaceous fluvial networks in northern Canada drained eastwards to Hudson Bay and the Labrador Sea (MacMillan 1973), however, minimal uplift of the shield areas since the Eocene prevented the development of extensive alluvial deposits in Canada. Further, any weathered material would have been eroded and transported by the Quaternary Laurentide ice sheet from the Canadian shield towards the south where diamonds have been found in glacial till in parts of the United States, such as Wisconsin and Indiana (Kjarsgaard and Levinson 2002).

There is however one reported Canadian paleo-placer in the Wawa area on the Superior Craton (Fig. 48). This is spatially associated with a diamondiferous matrix- and clast-supported volcaniclastic breccias of the Catfish assemblage within the Archean Michipicoten Greenstone Belt. This crudely bedded and poorly-sorted volcaniclastic unit is a "retained"

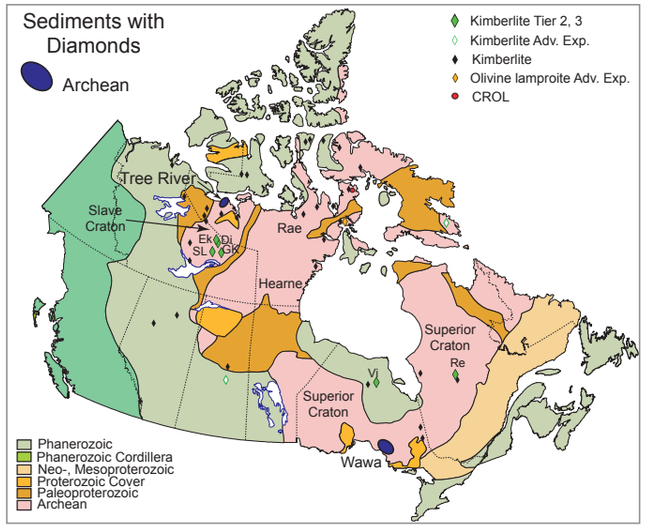

Figure 48. Canada placer deposits, as labeled on the map (Tree River and Wawa). Primary magmatic kimberlite and CROL mines/deposits as follows: Ek, Ekati; Di, Diavik, SL, Snap Lake; GK, Gahcho Kué; Vi, Victor; Re, Renard.

placer that has been interpreted as debris flows (Lefebvre et al. 2003). The breccias and associated lamprophyric dikes, both diamond-bearing, resulted possibly from a subduction-related Archean eruption (Lefebvre et al. 2003; Stachel et al. 2006), and both have been dated at between 2,744 Ma and 2,618 (Kopylova et al. 2010).

Unconformably overlying these volcanic rocks, but still part of the Michipicoten Greenstone Belt, are the Leadbetter Conglomerates (Wendland et al. 2012). These 2,701–2,697 Ma (Miller et al. 2012) conglomerates are dominated by debris flows at the base, followed by channel bars and lags representing a braided fluvial system on a sub-aerial alluvial fan which was terminated by a marine transgression. The best concentration of the diamonds is associated with braid-plain deposition and occurs in the middle of the upward-fining sequence (Wendland et al. 2012). The forecasted grades of the latter range from 0.11 to 0.29 ct/t (Ryder et al. 2008). However, based on diamond studies, the stones from the conglomerates seem to have a different source compared to those from the volcaniclastic rocks and dikes (Kopylova et al. 2010). Wendland et al. (2012) suggest that the main reason for the existence of this placer is its proximity to a primary source(s) and not through hydrodynamic concentration of diamonds from a distal source.

Proterozoic

Brazil (Amapá State): Vila Nova—Retained placer? (Paleoproterozoic). Diamonds in Brazil were discovered on the banks of the Jequitinhonha River in 1725 near the village of Arraial do Tijuco (later renamed Diamantina) Minas Gerais State, while artisanal miners were searching for alluvial gold. Brazil has produced close to 50 Mct since the discovery of its first diamond and most of these have been derived from conglomerates (Romaria, Minas Gerais State), glacial (paleo-diamictite) rocks (Tibagi, Parana), metasedimentary rocks (Diamantina, Minas Gerais State and Chapada, Bahia State) and recent alluvials. However, diamonds have only been mined successfully out of the Espinhaço Supergroup (Mesoproterozoic) and the Capacete Formation of the Late Cretaceous Mata da Corda Group (palaeo-placers; Pereira et al. 2017). The rest have come from Quaternary deposits.

The oldest known occurrence of diamonds in Brazil are the Palaeoproterozoic Vila Nova Group metavolcanic-sedimentary rocks (Fig. 49) located in the central southeast part of the Amapá State (Spier and Ferreira Filho 1999). Mafic and ultramafic rocks are covered by this volcanic–sedimentary sequence and both are metamorphosed to upper amphibolite facies. Diamond-bearing fine- and coarse-grained clastic meta-sediments including the meta-conglomerates have been dated at 2,264 Ma and suggested to represent a Palaeoproterozoic greenstone belt broadly comparable to the Guyana Shield greenstone belts (Spier and Ferreira 1999). The Vila Nova occurrences are also contemporaneous with the Birrimian meta-sediments of West Africa (Tompkins and Gonzaga 1989).

Brazil (Roraima State) and Guyana: Roraima Supergroup—Transient fluvial placer (Paleoproterozoic). Late Palaeoproterozoic diamonds have been associated with the Roraima Supergroup which forms a continuous area of chemically mature sedimentary rocks (orthoquartzite, quartz arenite and polymictic conglomerate) that can be traced over large tracks of the Guiana Shield in parts of Venezuela, Brazil and Guyana (Fig. 49), with outliers in Suriname (Grubb and McCallum 1991). This thick sequence of relatively flat-lying unaltered Precambrian clastic sediments was deposited unconformably on the underlying basement complex roughly between 1.95 and 1.78 Ga (Reis et al. 2017). No diamonds have been reported coming directly from the Roraima units, but almost all alluvial deposits, whether terrace or recent river gravels that have been exploited for diamonds, are associated with the rivers that flow across the basal Arai Formation of the Roraima Group (Meyer and McCallum 1993). Fleischer (1998) believes that the diamonds are restricted to lithologies of the middle member of the Roraima Group. The sediments of the Arai Formation have been interpreted as braided fluvial facies with paleo-terraces (Reis et al. 2017). Interestingly the diamonds from Boa Vista (Roraima State) show almost no sign of abrasion and have similar green spots that are also found on the diamonds from the Guaniamo kimberlite sills (Fig. 49) and it has been suggested that the Boa Vista diamonds have been derived from a nearby kimberlite source (Tappert et al. 2006).

Phanerozoic-aged uplift of the Guyana Shield combined with climatic fluctuations has eroded and upgraded these siliciclastic rocks into colluvial-type deposits proximal to exposed outcrop of the Roraima rocks (Watkins 2009). These and two Pleistocene terraces with braided river type alluvium and a Holocene age gravel-rich valley fill in the surrounding rivers have all been mined (Grubb and McCallum 1998). The grade and diamond quality improve in successively younger terraces and are best in the recent channel fills. The diamonds are either gem or near gem with only 10% boart (Meyer and McCallum 1993), and Grubb and McCallum (1998) report up to 65% gem-quality in the recent alluvium. The main sources of sediments of the Roriama Group were rocks of Trans-Amazonian age showing common sources from the greenstone belts in the northernmost portion of Guyana and Venezuela, with paleo-flow direction coming from the north and northeast (Reis et al. 2017). Reid (1974) has suggested that the diamonds were derived from Proterozoic kimberlites in West Africa (Ivory Coast, Ghana or Liberia).

Diamonds in Guyana were discovered in 1890, with most of the deposits occurring within 25 km of the Roraima escarpment in recent fluvial sediments of the Puruni and Mazaruni valleys, with the highest grades at the bedrock contact. In more distal cases they are associated with the Cenozoic White Sand Series, which are thought to be derived from the erosion of the Roraima sediments. Some 60% of the diamonds are gem quality and the average size range is between 10 and 15 stones/carat (st/ct) (Guyana Office for Investment 2019). It is estimated that Guyana has produced some 10 Mct since discovery.

Diamonds in Venezuela came from many localities scattered over the Guyana Highlands of the Bolívar province, but mainly below the steep rises of the highlands. Many of these alluvial deposits occur in tributaries of the Orinoco River, such as the Paragua, Caroni and Cuyon, as terraces and recent gravels in channels in the navigable parts of the rivers, which were exploited by mechanical dredges.

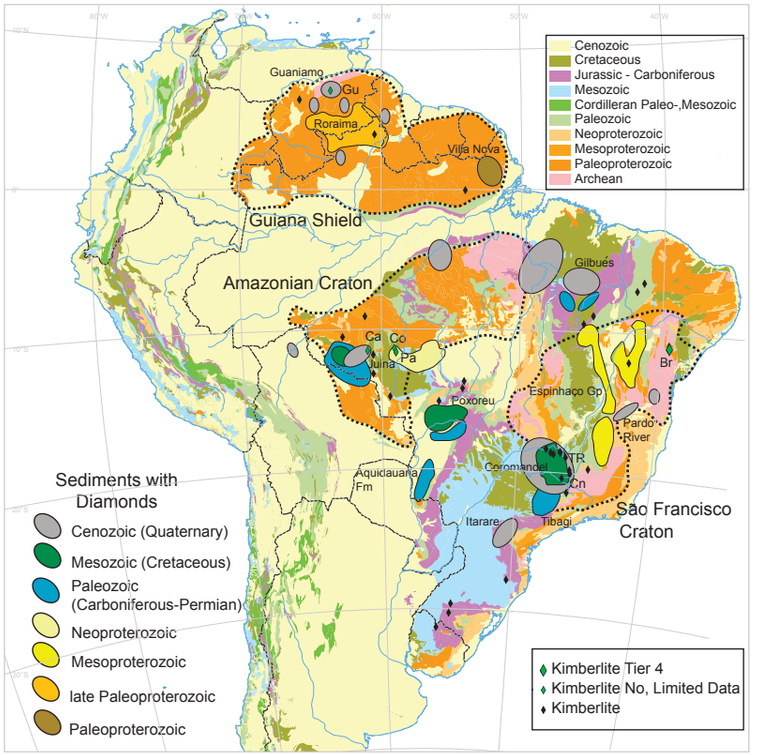

Figure 49. South America placer deposits, as labeled on the map (Villa Nova, Roraima, Espinhaço Group, Tibagi, Itarare, Coromandel, Poxoreu, Guaniamo, Aquidauana Formation, Juína, Gilbués, Pardo River). Primary magmatic kimberlite mines/deposits as follows: Gu, Guaniamo; Br, Brauna; Ca, Carolina; Co, Collier; Pa, Pandrea; Br, Brauna; TR, Tres Ranchos; Cn Canastra. **Black dotted lines** outline the Shield/Cratons, as labeled. Mercator map projection.

Brazil (Minas Gerais, Bahia States): Espinhaço Supergroup—Transient fluvial/glacial placer (Mesoproterozoic). Diamonds have been mined from the Mesoproterozoic meta-conglomerates and breccias of the Espinhaço Supergroup (Minas Gerais and Bahia States) that stretches as a north-south belt across the São Francisco Craton (Fig. 49). Diamonds occur in two formations. Firstly, in the Sopa-Brumadinho Formation (Diamantina Group; Fig. 50) around the town of Diamantina in central Minas Gerais State that has a minimum age of 1,715 Ma (Pedreira and de Waele 2008). Secondly, to the north in the Chapada Diamantina area in Bahia State, diamonds are found in the slightly younger Tombador (Figs. 51, 52) and Moto do Chapéu Formations that are both part of the Chapada Diamantina Group, which has a maximum age of 1,515 Ma (Pedreira and de Weale 2008). It is here that significant amounts of carbonado are also found, especially close to the town of Lençois (Fig. 52).

In the Diamantina area the meta-conglomerates have been variably interpreted as alluvial fans, glaciofluvial sediments, coastal marine facies, and breccias associated with debris flows in a tidal flat environment (Chaves et al. 2001), or as possible volcanic breccias (Fleischer 1998). The meta-conglomerates have grades between 0.04 and 0.08 ct/m³ and some 5 Mct have been estimated to have been produced from the Diamantina district alone (Karfunkel et al. 1994). The diamonds are generally small, well-sorted in the 0.6 to 0.9 ct/st range and of good quality (Chaves and Uhlein 1991), which suggests periods of reworking and upgrading.

Figure 50. Poorly sorted breccias of the Sopa-Brumadinho Formation, at Campo Sampio west of Diamantina, Brazil.

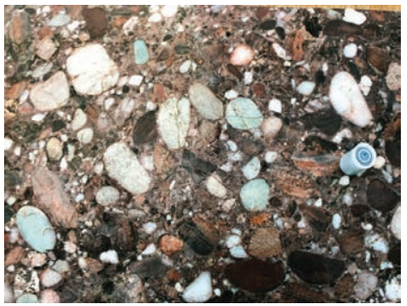

Figure 51. Conglomerates of the Tombador Formation near Lencois, Brazil.

Figure 52. Diamonds from the Tombador conglomerates, Brazil. Note the presence of carbonado (black).

Some have green and brown surface colors. Diamonds from the Bahia State area are colorless, brown and grey. There are no kimberlitic indicator minerals in these rocks and no primary sources have yet been linked to these diamonds. Sources could be unknown, eroded or buried distal kimberlites located in the São Francisco Craton. Another idea is a proximal source located within the confines of the diamondiferous Proterozoic sedimentary basin (Battilani et al. 2007). Recently it has been shown that metamorphosed igneous rocks intruded into the lower Tombador Formation, and these contain microdiamonds. Erosion and reworking of these intrusive rocks could be the source of diamonds which tend to be concentrated in the upper levels of the Tombador and Moto do Chapéu Formations (Battilani et al. 2007).

The drainage basin of the Jequitinhonha River (Minas Gerais State), which rises in the Espinhaço Mountains, was responsible for most of Brazil's historic diamond production, and these were mainly derived from weathering of the Mesoproterozoic Espinhaço Supergroup. Grades in the recent alluvium in this river were up to 0.6 ct/m³ of mainly gem quality diamonds (Dupont 1991). Mining was initially mainly by hand although later junior companies introduced dredges to mine the river gravels.

Zimbabwe (Mutare/Chimanimani Districts): Chiadzwa (Marange)—Terminal placer (Mesoproterozoic). Diamonds were discovered in outcropping Mesoproterozoic conglomerate in the Marange area of eastern Zimbabwe in 2001 (Fig. 47). These basal sediments of the Umkondo Group (>1.11 Ga) comprise thin (10 cm–2m) compositionally mature, quartz pebble and cobble conglomerates (Fig. 53). The deposit represents a craton margin, basin edge deposit of the Umkondo Foreland Basin fed by an easterly directed drainage from the Zimbabwe Craton by comparatively small rivers (Ward et al. 2013). Gravel and sand, including diamond, were introduced to the Umkondo Basin shoreline at Chiadzwa in the east (the Makodzi anomaly), where considerable reworking and concentration took place

by wave action and tidal energy variations during an initial transgression of the basin (Zhou 2015). In the absence of longshore drift, diamond concentration falls sharply over a short distance from north to south (Ward et al. 2013). It produced extremely coarse (5 to 7 carat stones), but poor-quality diamonds that become finer-grained further eastwards into the basin where at Chimanimani the average size is between 0.5–1 ct/st (Ward et al. 2013). Diamond quality improves from the Makodzi area towards the east into the Umkondo Foreland Basin. Furthermore, the high degree of abrasion displayed by many of the diamonds is a reflection of the reworking processes which also contributed to the higher grades. Another unique feature of the Marange diamonds is the brownish to black coating indicative of radiation damage and as a result it is estimated that only some 10% are of gem quality (Fig. 54).

Erosion of these Mesoproterozoic conglomerates has also produced diamondiferous Quaternary alluvium comprised of surface lag, talus (scree slope), sheetwash and ephemeral riverine sediments and these have been the primary mining targets. Together, these conglomerates and recent sediments have reportedly produced ~65 Mct to date, although in reality it is estimated that this could be as much as ~100 Mct (de Wit et al. 2016).

Figure 53. Metaproterozoic conglomerates from the basal Umkondo Group at Marange, eastern Zimbabwe. Note the well rounded quartz clasts dominate the pebble population.

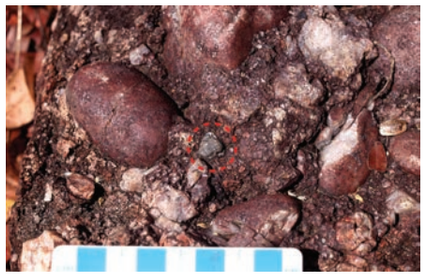

Figure 54. Poor quality but large diamond present in the Marange conglomerates, eastern Zimbabwe (photo courtesy J.D. Ward).

India (Andhra Pradesh State): Banganapalle—Terminal placer (Meso-, Neoproterozoic). India and Indonesia are historically the first countries where diamonds were found, with the Krishna River (described later) having produced some of the world's famous diamonds. There are two main areas with palaeoplacers in India, the Banganapalle conglomerates that are associated with the Dharwar Craton in the south, and the Panna diamond belt on the northern margin of the Vindhyan Basin on the Bundelkhand Craton central-north (Fig. 55), supplemented by Quaternary diamondiferous gravels.

The late Meso- to early Neoproterozic Banganapalle Formation occurs at the base of the Kurnool Group and can be followed for 225 km in the Cuddapah Basin (Bertram 2010). The thin quartzitic conglomerate beds vary in thickness from 0.01 to 3 m, are flat lying and have been interpreted as a beach gravel developed during a transgressive phase (Fareeduddin and Mitchell 2012). The average grade is between 2–3 ct/100t with some 75% gem quality diamonds (Joy et al. 2012). Diamonds from these conglomerates are distinct from those derived from the alluvials of the Krishna River; they have no radiation damage nor any abrasion features on their surfaces and are believed to have been derived from proximal source(s) (Ravi et al. 2012). The proximal occurring Chelima lamproites, of 1,370–1,287 Ma age (Joy et al. 2012), are now believed to be the source for the diamonds in this terminal placer, since the mineral chemistry of mantle minerals in the conglomerates eliminates kimberlites occurring to the SW as its potential source (Joy et al. 2012). Also, Type IIa diamonds, which occur among the Krishna River diamonds, are not seen in the Banganapalle conglomerates.

India (Madhya Pradesh State): Panna diamond belt—Retained/terminal placer (Meso-, Neoproterozoic). In the Panna belt (Fig. 55) diamond-bearing conglomerates occur in the Meso- to Neoproterozoic Vindhyan Supergroup. Sedimentation of the upper part of this supergroup, the Rewa Group, started around 1,100 Ma and continued until 650 Ma (Ray 2006) and include the diamondiferous Itwa (Lower Rewa Group), and Jhiri and Gahadra (both Upper Rewa Group) conglomerates, which are separated by shale horizons. The lower Itwa conglomerates are poorly sorted and have up to boulder size sub-rounded to sub-angular clasts that are dominated by footwall lithologies, in a sandy matrix. Its thickness varies from 0.05 to 2 m (Soni et al. 2002). Diamond grades of as high as 27.9 ct/100 t have been recorded and there is also a high percentage of gem quality diamonds (Fareeduddin and Mitchell 2012). These deposits formed during uplift resulting in high gradient rivers that accelerate erosion and rapid incision bringing into the basin poorly-sorted coarse-grained sediments enriched in diamonds that were reworked out of pre-incision erosion surfaces or retained placers (Gupta et al. 2003). The diamondiferous Jhiri conglomerate (Fig. 56), a terminal placer which is between 0.02 to 0.70 m thick with isolated channels, form banket sheets of clast- and matrix-supported lenses. It is well-sorted and composed of well-rounded pebble size clasts and these lenses have been interpreted as shoreline lags (Gupta et al. 2003). The Gahadra conglomerate, containing well-rounded pebbles composed mainly of local sandstone (Soni et al. 2002; Rau 2007), are reported to have grades of up to 28 ct/100t (Fareeduddin and Mitchell 2012). Based on evaluation work done by Geological Survey of India, some 22.8 Mt of indicated resource has been established for the Jhiri and Itwa conglomerates (Rau et al. 2012). The local 1,040 Ma old Majhgawan (average grade 14 cpht) and Hinota diamond-bearing olivine lamproites, are interpreted as the likely sources of the diamonds in these conglomerates (Fareeduddin and Mitchell 2012).

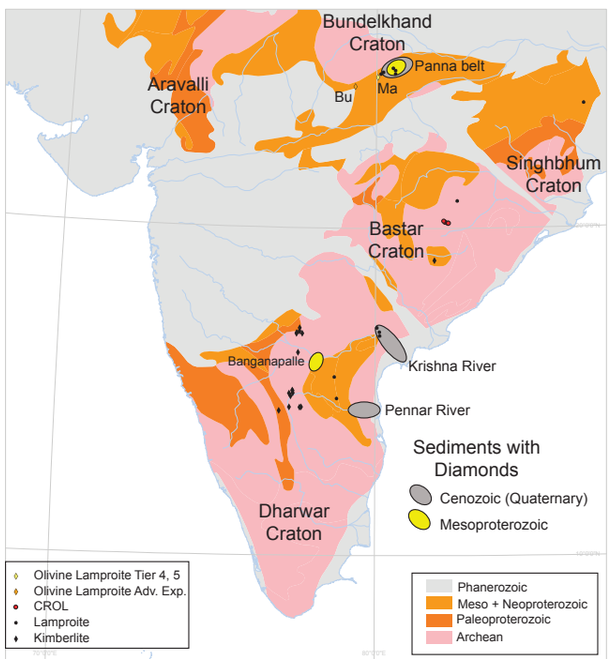

Figure 55. India placer deposits, as labeled on the map (Banganapalle, Panna Belt, Krishna and Pennar Rivers). Primary magmatic olivine lamproite mines/deposits as follows: Ma, Majhgawan; Bu, Bunder (Atri). Mercator map projection.

Diamonds released by erosion of these Proterozoic conglomerates are mined in recent gravels of the Baghain and Ranj Rivers. The former is the most important, with gravels returning grades of up to 26 ct/100t (Fareeduddin and Mitchell 2012), and has a Proven Diamond Resource of 1.1 Mct (Rau et al. 2012). Gravels along the Ranj and other tributaries have yielded considerably lower grades. Remnants of lateritic gravel, which occur as a thin deflation layer on the Baghain plateau often trapped in joints, have been mined by artisanal miners with variable success.

Figure 56. Diamonds in fine-grained Jhiri conglomerates from the Vindhyan Supergroup in the Panna Belt, northern India.

Paleozoic

Russia: Urals—Reworked terminal placer (Lower–Middle–Upper Devonian). The occurrence of alluvial diamonds along the western edge of the middle and northern Ural Mountains has been known since 1829. The diamonds are found in two main areas; near Perm in the middle and northern Ural Mountains (Fig. 57) where diamonds occur in the Lower Devonian (Emsian stage) Takaty Formation (Laiginhas et al. 2009), and in the Timan areas further north (Fig. 57) where diamonds are derived from the basal conglomerates of the Middle Devonian Travyanka, and Upper Devonian Nadezhda and Kumushka Formations (Konstantinovskii 2003). Sources for these Devonian placer diamonds are not known but Sobolev et al. (2019) noted, based on the chemical composition of certain diamond inclusions as well as the high eclogitic/peridotitic inclusion ratios, that the Ural diamonds show striking similarities to those from the northeast Siberian placers (except for their carbon isotope compositions), and in part to those from the Arkhangelsk kimberlite province to the west/northwest. However, the eruption age of its primary magmatic source rocks, based on $^{40}Ar/^{39}Ar$ dating of clinopyroxene inclusions in some Urals diamonds is 472 Ma (Laiginhas et al. 2009), which is older than the *ca.* 380—374 Ma Lomonosov and Grib diamond mines in the Arkhangelsk kimberlite province and precludes them as a source.

Ural Mountain diamonds are concentrated in 1 to 5 m thick basal conglomerates, composed of alluvial sediment, that were partially reworked within a coastal-marine zone. The diamonds, mainly rounded dodecahedra, were thus concentrated in terminal placers along a shoreline on an eastern active margin of the East European Craton during the Devonian (Laiginhas et al. 2009). Only rare pyrope garnets are associated with these conglomerates. Erosion and reworking of these Devonian sediments have produced numerous Quaternary transient placers in the form of terraces and recent river gravels preserved in Mesozoic–Cenozoic karst depressions, which have been mined. The diamonds, many of which have green and brown spots, are well-sorted, and also abraded (Konstantinovskii 2003).

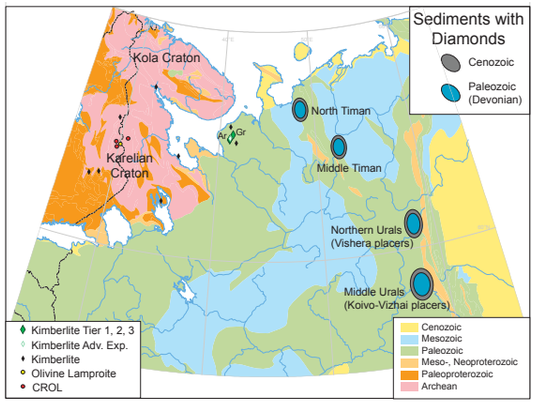

Figure 57. Western Russia (East European Platform) placer deposits, as labeled on the map (Northern Timan placers, Middle Timan placers, Northern Urals—Vishera placers Middle Urals/Perm—Koivo/Vizhai placers). Primary magmatic kimberlite mines/deposits as follows: Gr, Grib; Ar, Arkhangelskaya. Mercator map projection.

Russia (Republic of Sakha): central Siberian Shield—Retained placers (Carboniferous and Permian). There are some 1,070 kimberlites known in Yakutia in 15 Palaeozoic and Mesozoic fields. Of these 195 kimberlites occur in the central Siberian Craton and are predominantly Palaeozoic in age, which include most of the economic kimberlites such as Mir and Udachnaya. Some 875 kimberlites occur in the northern Siberian Craton (Anabar-Olenek subprovince) almost 200 km north of Udachnaya, and are almost barren or at best are weakly diamondiferous (Sobolev et al. 2018). Many of these Triassic and Jurassic–Cretaceous kimberlites are eroded; they have been described as hypabyssal kimberlite (Sun et al. 2014; Sobolev et al. 2018).

There are two types of placer deposits on the Siberian platform. Retained placers which are closely associated with the known kimberlite mines in the central Siberian Craton, and transient placers found in the north that are associated with the Anabar-Olenek drainage basins (also referred to as the Anabar, Lower Olenek and Lena alluvial deposits, discussed under the *Cenozoic* section).

Poorly-sorted retained placers, close to the kimberlite mines/deposits (Fig. 58, Mir, Nyurbinskaya, Botuobinskaya, Udachnaya, Verkne-Munskoye), occur as Lower and Middle Carboniferous, Lower Permian and in Triassic–Jurassic proximal alluvials fans. These have an abundance of coarse kimberlitic minerals which supports a proximal source (Kedrova et al. 2022; Konstantinovskii 2003).

The Vostochnaya (Fig. 59) and Solur retained placers are two spatially adjacent alluvial paleo-placers of Upper Palaeozoic and Mesozoic age, respectively, some 25 km northwest of the Mir mine, between the Irelyakh and Chuonalyr Rivers. The poorly sorted sediments are described as clayey conglomerates and fine breccias interpreted as alluvial fan deposits which were controlled by repeated tectonic movement along faults resulting in the formation and burial of these placers (Konstantinovskii 2003). The Carboniferous (Serpukhovian stage) Vostochanaya deposit stretches over 5 km and is on average 0.7 m thick (Petrov et al. 2016). The Lower Jurassic Solur deposit has an average thickness of 2.4 m and is mainly made up of pebbly conglomerate with interbedded sands, siltstones, clays and coals (Micon International Co Ltd 2016). The grades of the Vostochnaya deposit is on average much higher than that of the Solur deposit.

The Vodorazdelnye Galechniki deposit is a buried retained alluvial placer close to the Mir mine under some 2 m of waste, and sourced diamonds from both the Mir and Sputnik

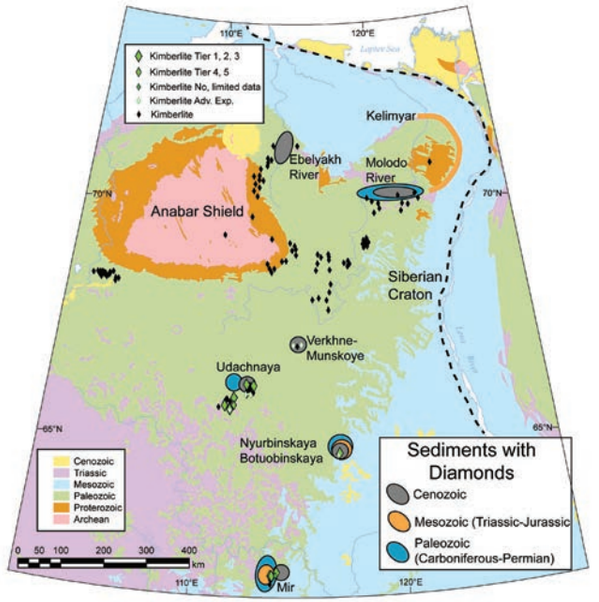

Figure 58. Russia (Siberia) placer deposits, as labeled on the map (Ebelyakh River, Molodo River, Kelimyar, Mir, Udachnaya, Verkhne-Munskoye, Nyurbinskaya-Botuobinskaya). Mercator map projection.

Figure 59. Section of Carboniferous Vostochanaya retained placer near the Mir diamond mine in central Siberia, Russia (photo courtesy J.D. Bristow).

kimberlites. It is a Late Triassic proximal alluvial fan that was upgraded by marine processes at the interface of the fan (Konstantinovskii 2003). The diamonds, which are concentrated in the basal gravel, show no sign of wear (Afanasiev and Pokhilenko 2013).

Zimbabwe (Gweru District): Somabula—Residual placer (Permo-Carboniferous). Diamonds were first reported in Zimbabwe in 1903 (Moore and Moore 2006) and came from deflated glaciofluvial conglomerates at Somabula in central Zimbabwe (Fig. 47). The linear, southeast–northwest aligned Somabula Karoo outlier, preserved on Archean basement, has a discontinuous basal diamond-bearing gravel overlain by Upper Karoo sediments (Moore et al. 2009). The basal braided river system gravel was interpreted as a lag deposit formed by fluvial winnowing of former Permian tillites before the Upper Karoo sediments were deposited. The paleo-current and isopach evidence indicate that the flow of the Somabula River was to the northwest and Moore et al. (2009) suggested that the ca. 520 Ma Murowa kimberlites to the south might be the source for these diamonds. It is estimated that this deposit has produced close to 20,000 ct with the largest stone a 50 ct boart (Moore et al. 2006).

South Africa (North West Province): Lichtenburg/Ventersdorp area—Residual placer (Permo-Carboniferous). Diamond-bearing gravels of the Lichtenburg-Ventersdorp area of the North West Province in South Africa (Fig. 47) are associated with sinuous North–South orientated "runs" that occur exclusively on a flat erosional surface comprised almost entirely of Transvaal dolomites. Some of the coarse-grained gravels (texturally diamictites) that make up the runs, occur within sinkholes directly or indirectly linked to the runs. The gravels have been mined since 1926 and have produced some 12 Mct of diamonds. The runs are narrow, elongated, positive ridges that meander across the dolomite surface. They are up to 30 km long, between 80 and 300 m wide and up to 20 m high (Fig. 60) New data, including field evidence, geomorphological studies, age-dating of diamond inclusions and zircons, indicate that the runs are Permian paleo-eskers deposits that formed during final deglaciation of the Dwyka continental ice sheet, rather than post-Gondwana drainage deposits linked to southward flowing late Cenozoic river systems, as has previously been assumed (de Wit 2016).

Figure 60. Permo-Carboniferous and diamond-bearing sinuous eskers on the Transvaal dolomites near Lichtenburg, South Africa.

Brazil (Mato Grosso do Sul State): Paranaíba and Parana Basins—Transient glacial placer (Permo–Carboniferous). The Carboniferous glacial outwash plains of the Aquidauana Formation (Mato Grosso do Sul State; Fig. 49) and the fluvio-deltaic facies of the Poti Formation (Piauí State) further north, are related to the Carboniferous glaciation of the Paranaíba Basin, and have been reported to contain diamonds (Tompkins and Gonzaga 1989). In addition, mineralized parts of recent drainages in the Parana Basin are intimately associated with glaciofluvial conglomerates and reworked tillites of the Itararé Group. It has

been suggested that the glacial centres were located in southern Africa (Dos Santos et al. 1996), and based on glacial groove direction, pebble orientations, and paleocurrent patterns, that these glaciogenic deposits (and hence their diamonds) are interpreted to be derived from the Kaapvaal Craton (Perdoncini and Soares 1999).

Australia (South Australia State): Springfield Basin—Transient glacial placer (Permo-Carboniferous). Within the Springfield Basin (Fig. 61) diamonds occur exclusively in basal conglomerate, which are most likely glaciofluvial sedimentary rocks of Permo–Carboniferous age, and that in part were subsequently reworked into younger sediments (Tappert et al. 2009). Many of the diamonds from the younger sediments resemble those derived from the nearby Jurassic kimberlites at Eurelia. However, the diamonds found in gold mining operations SE of Adelaide in the Echunga area are abraded and have green and brown radiation spots, and Tappert et al. (2008) suggested that these placer diamonds and the "older" diamonds from the Springfield Basin were transported to south Australia by Permo-Carboniferous glaciers from the eastern part of Antarctica.

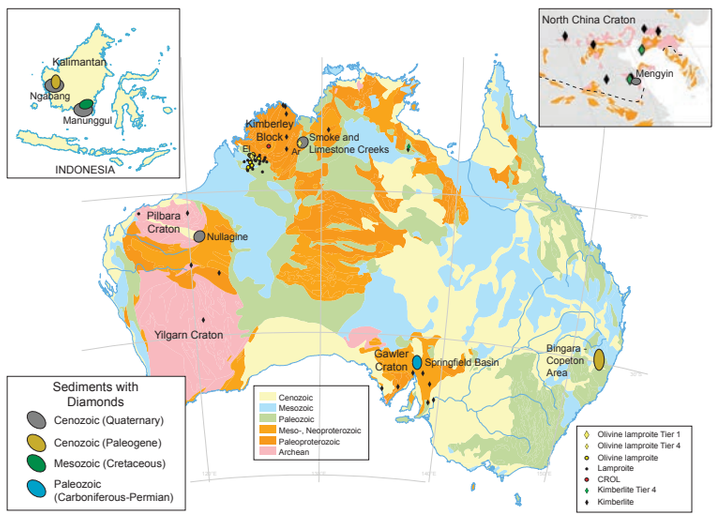

Figure 61. Australia placer deposits as labeled on the map (Springfield Basin, Bingara-Copeton, Smoke and Limestone Creeks; Nullagine). Primary magmatic olivine lamproite mines/deposits as follows: Ar, Argyle; El, Ellendale. Mercator map projection. Indonesia placer deposits as labeled on the **top left inset** map (Ngabang, Manunggul); China placer deposit (Mengyin) as labeled on the **top right inset** map.

South Africa (North West Province): Schweizer-Reneke area—Terminal placer (Permian). Diamondiferous gravels in the Schweizer-Reneke area, south of Lichtenburg (Fig. 47), have been subdivided into a derived gravel unit and four younger alluvial units (Marshall 1990). The derived unit is the oldest and formed as a result of the landscape lowering by weathering and deflation. These gravels are preserved as remnants on a pre-Karoo surface and have often been referred to as "Rooikoppie" gravels (de Wit et al. 2000). Recent research has shown that these deflated gravels may be closely linked to the Permian paleo-shoreline of the Ecca Group, which has reworked some of the diamondiferous glacial sediments of the Dwyka Group (Ward et al. in prep) that can be linked to the residual placers of the Lichtenburg/ Ventersdorp area (de Wit 2016). The younger alluvial units occur at respective lower elevations towards the Vaal River and have reworked the Permian paleo-placers. Some 2.5 Mct have been recovered from this area, with diamond values much higher than those from Lichtenburg and Ventersdorp (de Wit 2016).

Mesozoic

Eswatini (Lubombo Region): Hlane—Transient fluvial placer (Upper Triassic). In northeast Eswatini (formerly Swaziland), diamonds were discovered in Upper Triassic grits and conglomerates (Elliot Formation) at Hlane (Fig. 47). These sediments represent erosionally based, clast-supported channel-fills and host a well-sorted population with 95% of the diamonds that fall in the 0.5 to 2 mm fraction (Turner and Minter 1985). This transient placer formed as a result of a single phase of tectonic uplift and denudation accompanied by climatic change (Turner and Minter 1985). Sedimentological studies of these grits led directly to the discovery of the primary source, the Dokolwayo (Hawthorne et al. 1982) carbonate-rich olivine lamproite.

Russia (Republic of Sakha): Kelimyar River region, northern Siberian Shield—Terminal marine placers (Upper Triassic and Jurassic). Diamond placers were discovered on the northern Siberian platform in 1965. Several types have been identified: terminal near-shore marine placers of Triassic and Jurassic ages, early Jurassic deltaic deposits and Neogene to Quaternary transient alluvial deposits (Prokopchuk 1972). The mineralized Upper Triassic basal conglomerates, which were found to host diamonds and kimberlitic indicator minerals, represent a Mesozoic terminal placer (Grakhanov et al. 2010, 2015; Sobolev et al. 2013; Nikolenko et al. 2018). These Triassic (Rhaetian Stage) basal marine shoreline facies of between 0.1 to 1 m thick, can be traced from the lower reaches of the Lena River (reference section along the Kelimyar River) westwards along the Laptev Sea as it wraps around the Anabar and Olenek blocks (Fig. 58). These sediments formed during transgressions across paleo-surfaces that represent major breaks in sedimentation after the Middle Devonian uplift of the Anabar and Olenek blocks.

Detrital zircons from these sediments returned an age range of 245–230 Ma. Comparable aged zircons are also found in the Jurassic marine rocks (Grakhanov et al. 2015) and in the Cenozoic Ebelyakh River (Fig. 58) placer (Sobolev 2018), which illustrates the level of reworking towards younger formations. These ages are also similar to the weakly diamondiferous local Triassic kimberlites (Davis et al. 1980; Smelov and Zaitsev 2013).

The coastal and deltaic placers are generally lenticular in shape with low diamond concentration (Prokopchuk 1972). The Upper Triassic deposits are thought to represent an entire second-order transgressive–regressive cycle (Egorov and Mørk 2000) while the Lower Jurassic deposits rest on an erosion surface above these formations (Ilyina and Egorov 2008). These Upper Triassic sediments have indicator minerals derived from the Triassic kimberlite bodies, but no indicator minerals derived from the Palaeozoic kimberlite-hosted diamond mines much further to the south (Grakhanov et al. 2010).

Cretaceous

Indonesia (Kalimantan Barat, Kalimantan Selatan Provinces)—Transient fluvial placer (Upper Cretaceous–Lower Paleogene). Diamonds were found in west Kalimantan (Barat) around 600 AD associated with the Landak and Kapuas Rivers near Ngabang (Fig. 61, inset map). Much later, in the 1600's, diamonds were recovered from the Martapura drainage basin in the southeast (Selatan) at Cempaka, along the Apukan, Riam Kanan and Riam Kiwa rivers (Fig. 61, inset map). Other small occurrences of diamonds have been reported from the more central part of Kalimantan. In total just under 2 Mct have been produced and at its peak the annual production for the island was between 20,000 and 30,000 ct of generally small (average of 0.3 ct/st) but gem-quality diamonds (Spencer et al. 1988). The largest diamond recorded is a 166.8 ct stone from southeast Kalimantan.

In the southeast, diamonds occur in clastic rocks of the Upper Cretaceous to Lower Paleogene Manunggul Formation (Fig. 62) that crop out in the Meratus Mountains, and in Pleistocene fanglomerates and alluvial fans or sheet wash sediments. Diamonds also occur in Holocene alluvials (Fig. 63) and recent alluvium and river terraces (White et al. 2016), but in the more distal areas around Cempaka, a large part of this region is covered by swamps.

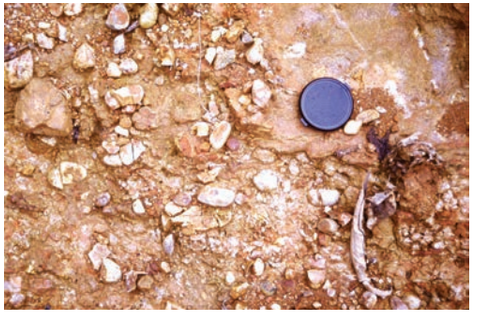

Figure 62. Cretaceous Manunggul conglomerates in southeast Kalimantan, Indonesia

Figure 63. Younger Holocene gravels being concentrated using wooden cone-shaped "pans', around Cempaka, Indonesia.

The Manunggul Formation is believed to be the source for the Cempaka diamonds. Continuous uplift of the Meratus ophiolite and erosion of the Manunggul conglomerates was the source of the diamonds to the younger sediments. Although the Manunggul Formation has been mined, grades in the Pleistocene fanglomerates and the alluvial gravels of the younger paleochannels were higher as a result of reworking processes. Interestingly Spencer et al. (1998) noted that the upper gravels proved to have higher grades than the basal gravels. Around Ngabang in the west of Kalimantan, diamonds occur in Eocene stream channels, and in derived recent stream beds that drain exposed areas of these ancient stream channels, usually near the flanks of uplands (Spencer et al. 1998).

White et al. (2016) recognized two groups of Cempaka diamonds, based on the study of the heavy mineral suite from the Cempaka alluvial deposit. One group, supported by evidence of long-distance transport and/or multiple recycled stages, indicates that these were either already present in Borneo at least by the Early Cretaceous and were reworked several times, or they were transported from NW Australia to Borneo before it rifted from Gondwana in the Late Jurassic. A second, more proximal sourced group was interpreted to have come from local diamondiferous diatremes emplaced during the Neogene tectonic events (White et al. 2016). Smith et al. (2009), based on the abrasion features and the surface occurrence of radiation damage brown and green spots on many of the diamonds, concluded that the diamonds have gone through multiple cycles of fluvial transportation. This is supported by Kueter et al. (2016) who, based on zircon provenance and diamond morphologies, indicate that the great majority of the Kalimantan and other SE Asia diamonds have northern Australian source(s).

South Africa (Northern Cape Province): Mahura Muthla—Transient placer (Upper Cretaceous). Remnants of diamond-bearing fluvial gravels of Cretaceous age have been preserved on the dolomites of the Ghaap Plateau, northwest of Kimberley (Fig. 47). This north-westerly orientated paleo-channel was directly linked to the Kalahari River drainage basin that drained the northern part of the Northern Cape and southern Botswana via the paleo-Molopo and lower Orange River. By the Early Cenozoic the latter had captured the Vaal and the upper and middle Orange Rivers that had previously been part of the Karoo River during the Cretaceous. The gravels, which are highly calcretized, have yielded over 3,500 carats, the largest diamond was an 8 ct stone; these diamonds were probably sourced from some of the carbonate-rich olivine lamproites known from the Ghaap Plateau to the south and southeast (de Wit et al. 2009).

Angola/DRC (Lunda Norte/Kasai Provinces): Calonda/Kwango Formations—Retained placer (Upper Cretaceous). In Angola, with the exception of the recent alluvial diamond deposits around the Cretaceous diamond-bearing kimberlites, all diamond placers (Fig. 64) are directly related to the presence of the Upper Cretaceous Calonda Formation in northern Angola (Pereira et al. 2003) and the equivalent Upper Kwango Group in southern DRC (Roberts et al. 2015). Many of the diamond-bearing kimberlites in northeast Angola have been dated at between 113 and 145 Ma, including Catoca at 118 Ma (Robles-Cruz et al. 2012). A group of older, low-grade, Triassic kimberlites on the west side of the Kasai Craton are the sources for small-scale diamond operations in recent stream sediments in the Lubia area (Jelsma et al. 2013).

The Cretaceous period of kimberlite emplacement is followed by a phase of subsidence of the Congo Basin from 110 to 60 Ma (Linol et al. 2015) which triggered the deposition of the Upper Kwango Group, also referred to as C3 and C4 (Calonda Formation) of Late Cretaceous age (Roberts et al. 2015). This formation, which is highly weathered, consists of a series of sandstones and conglomerates (Fig. 65), and locally contains diamonds. The basal gravels are generally upward-fining with siliceous resistant and non-resistant clasts up to boulder-size.

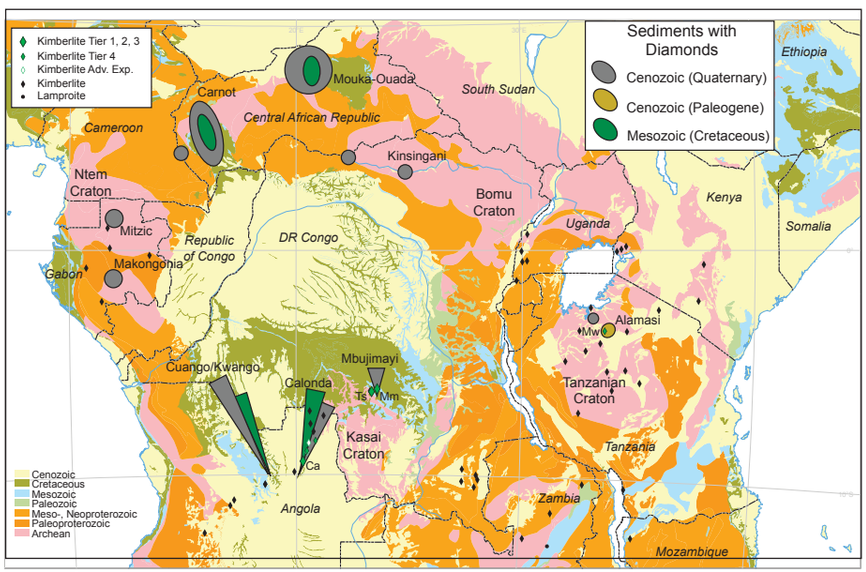

Figure 64. Central Africa placer deposits as labeled on the map (Mouka-Ouadda, Carnot, Mitzic, Makongonio, Cuango/Kwango River, Calonda, Mbujimayi, Alamasi, Kinsangani). Primary magmatic kimberlite mines/deposits as follows: Ca, Catoca; Ts, Tschibwe; Mm, Mbuji Mayi, Mw, Mwadui. Mercator map projection.

The thickness can be up to 250 m in structurally controlled grabens, but in the diamondiferous areas the thickness is generally less than 50 m.

In Angola the basal conglomerates of the Calonda Formation represent the first cycle of diamond capture after release from the proximal kimberlites. This diamondiferous formation occurs in channels and runs from the Lucapa area in a broad subsided part of the western Kasai Craton towards the northeast to cover the region of the Luachimo (Longatshimo) and Chicapa (Tshikapa) Rivers (Ambroise 1991). This northward orientated Cretaceous river system entered the DRC south of Tshikapa. The diamonds here are generally smaller and believed to have been derived from the erosion of the Angolan kimberlites and Calonda sediments, but some economically viable deposits still exist up to 600 km from source (Sutherland 1982). Reworking of the intensely chemically weathered Calonda sediments has resulted in upgraded younger Miocene, Plio–Pleistocene and recent deposits on floodplains, terraces (with an elevation of 1 to 40 m above the present river level) and slope eluvium (directly derived from Calonda conglomerates), but particularly in the Late Quaternary alluvial deposits (Spaggiari and de Wit 2021). The Cenozoic onset of erosion of the Calonda, which has been recorded by younger alluvial deposits, is closely linked to the Oligocene (30 to 35 Ma) and post-Pliocene uplifts of the Angolan Highlands (White et al. 2009). These uplifts initiated alluvial cycles that have upgraded the diamonds to a higher percentage of gem quality stones. The alluvial deposits in the Tshikapa triangle have produced over 90 Mct and are part of the largest diamond megaplacer in central Africa, stretching from Lucapa in northeast Angola to Tshikapa in the southern DRC that has contributed in excess of 200 Mct (de Wit et al. 2016).

Brazil (Minas Gerais State): Capacete, Coromandel area—Retained placer (Upper Cretaceous). Fernandes et al. (2014) have shown that the basal polymictic conglomerates of the Upper Cretaceous Capacete Formation, uppermost in the Mata da Corda Group, contain diamonds (Fig. 49). Diamonds were mined from lithified conglomerates at the Romaria mine (western Minas Gerais State) on the northeastern side of the Paraná Basin in a tributary of the Bagagem River at Água Suja (Svisero et al. 2017). The Tauá conglomerate, which contains the diamonds (Fleischer 1998), forms the base of the Upper Cretaceous Uberaba Formation, which is an equivalent to the Capacete Formation conglomerates. These conglomerates have been interpreted as a debris flow or alluvial fan deposit consisting of materials from surrounding Neoproterozoic meta-sediments (Araxá Group) and Lower Cretaceous Botucatu sandstone and basalt (Areado Group) (Pereira et al. 2017). The diamonds are concentrated in a 6 m thick conglomerate deposit which has grades of 0.05 to 0.12 ct/m³ (Pereira et al. 2017). The diamond suite is dominated by rhombododecahedral shapes. They are generally colorless with 70% gem quality (Svisero et al. 2017) and are similar to diamonds from the proximal Cretaceous diamondiferous Três Ranchos cluster kimberlites (99–81 Ma) (Pereira et al. 2017).

The source of these alluvial diamonds, however, has been debated. Some suggest that erosion of the many local kimberlites released diamonds to be incorporated into the Capacete conglomerates (Karfunkel et al. 2014) and were subsequently distributed throughout the Coromandel region (Fernandes et al. 2014). Others propose that the diamonds have been transported by ice from the São Francisco Craton by Neoproterozoic (Jequitái, Ibiá glaciations) and Paleozoic (Santa-Fé de Minas tillites) glacial events (Tomkins and Gonzaga 1989, Gonzaga et al. 1994). Read et al. (2004) on the other hand, based on stratigraphic relationships and mantle-derived indicator mineral suites, advocate that the thickness of the underlying lithospheric mantle of the Quiricó Basin and surrounding areas of the Coromandel thinned dramatically during the onset of the Upper Cretaceous Mata da Corda Group. The Mata de Corda Group sediments covered the Lower Cretaceous kimberlites, which were emplaced when the mantle was still cool enough to form and preserve diamond to be transported by kimberlites to the surface.

Fernandes et al. (2014) interpreted the basal Capacete conglomerates as being deposited by alluvial fans and braided rivers as a result of local Late Cretaceous uplift. These probably

formed the main diamond source rock in the Santo Antônio do Bonito, Santo Inácio and Douradinho river alluviums. The possibility that the Neoproterozoic and Palaeozoic diamictites as well as the Cretaceous kimberlites, have all contributed to the mix at certain localities has not been excluded (Fernandes et al. 2014). However, most of the mined alluvial deposits are of Late Cenozoic age and mainly from terraces and floodplain gravels.

Brazil (Mato Grosso State): Poxoréu—Retained placer (Upper Cretaceous). Rivers such as the Coité, São João, Poxoréu and Pomba in the northwestern part of the Paraná Basin (Fig. 49) have been producing diamonds since the 1930s with grades up to 0.05 ct/m³ and with some 27% being gem-quality (Souza 1991). All these diamonds are recovered from sedimentary rocks of the Upper Cretaceous Bauru Group (Uberaba Formation), which is associated with a half graben (Svisero 1995; Souza 1991). Diamonds are also recovered in various outliers of residual gravel on the high plateaus to the W and NW of Poxoréu (Fleischer 1998), which are thought to be related to conglomerates of the same formation (Weska 1996). Although the Capacete and Uberaba Formations are time equivalents, Quintão et al. (2017) have shown that the diamonds from the Uberaba Formation are not related to those from the Romaria mine in the Capacete conglomerates.

Cenozoic

Tanzania (Shinyanga Region): Alamasi—Retained "epiclastic" placer (Paleogene). The first diamonds found in Tanzania were from alluvial gravels at Mabuki in 1917, which were mined from 1925 onwards, and led to the discovery of Tanzania's first kimberlite, the Mabuki pipe. The Mwadui mine (Fig. 64), the world's largest kimberlite-hosted diamond mine, was found thereafter and mining here initially concentrated on surficial deposits adjacent to and over the pipe. This residual placer of eluvial gravels is mainly lag deposits that resulted from the weathering of the tuff ring surrounding the pipe and the uppermost deposits within the kimberlite crater. Limited down wasting resulted in tremendous increase of the diamond grades in these lag deposits, particularly adjacent to the pipe—the Alamasi deposit (Fig. 66). A regional geomorphological study suggested that very little erosion had occurred since the eruption of the kimberlite at 52 Ma (Stiefenhofer and Farrow 2004), and hence there has been limited dispersion of diamonds and indicator minerals <1 km away from the pipe (Edwards and Howkins 1966). Field (2010) makes the point that these deposits are technically not "alluvials" as there has not been any recognizable fluvial transport and are therefore explained as Eocene residual remnants of proximal reworked eluvial material.

Australia (New South Wales State): Bingara and Copeton—Transient placer (Paleogene). There are two main areas of alluvial mining in Australia; one along the east coast and the other associated with the Argyle olivine lamproite in the Kimberley Block of northwest Australia (Fig. 61). Some small occurrences of alluvial diamonds occur in southern Australia as described earlier.

Alluvial diamonds are found in eastern Australia from Queensland in the north to Tasmania in the south, but have only been mined in the New South Wales area (since 1867). Historical production from the Bingara and Copeton areas (Fig. 61) up to 1973 was 34,000 and 167,000 carats, respectively; the total production for these two areas has been estimated to be 500,000 carats (Davies et al. 1999). The average stone size in Bingara is 0.2 ct and the largest reported stone 2.6 ct; the Copeton area has an average stone size of 0.25 ct with the largest stone being a 12 ct piece of boart (MacNevin 1977).

The diamonds occur in upper Cenozoic gravels, sands and silts that are beneath Miocene basalts. The gravels occur in channels preserved as remnants of a palaeo-river system. Reconstruction of the palaeo-drainage system in the Bathurst region suggest that the general flow direction was towards the north, from the late Mesozoic and through to the Cenozoic (Cham 1998). In some areas the basal planar cross-bedded conglomerates, interpreted as

Figure 65. Calonda Formation gravels of Cretaceous age at Chitotolo, Angola. Note the weathered and "bleached" state of the locally derived clasts.

Figure 66. Poorly sorted and coarse-grained conglomerates at the outer edge of the Mwadui kimberlite, Tanzania.

lateral accreting channels and typically associated with fluvial processes, has been the target for the miners. In other areas, such as the Craddocks claim, breccias are overlain by upward-coarsening sandstone beds and are believed to be associated with a sequence of volcaniclastic rocks into which the diamonds were incorporated, in processes resembling debris flows or even via primary volcaniclastic processes (Fig. 67). Pillow lavas, basalt-filled valleys, intercalated sediments between basalt flows and almost "tuffaceous" textures in the fluvial sediments all indicate that volcanic activity interrupted the fluvial system transporting the diamonds.

The diamonds can be grouped into two distinct populations. One group, similar to those found in kimberlites and lamproites, has abrasion features and radiation damage

Figure 67. Poorly-sorted diamondiferous breccias overlain by volcaniclastic rocks in the Callas Hill audit, near Bingara, southeast Australia.

suggesting that they represent diamonds recycled from older sedimentary deposits. These could have been transported northwards by Permian glaciers that affected most of southern Australia and derived from primary source(s) as far afield as Antarctica (Davies et al. 2002). This interpretation is supported by inclusion studies that suggest these diamonds are associated with ~340 Ma magmatism (Burgess et al. 1998). The second group, characterized by unusual heavy C isotope compositions and Ca-rich eclogitic inclusions (Sobolev et al. 1984), has been linked to a young subduction model (Davies et al. 1999). There are no typical diamond indicator minerals associated with these sediments.

South Africa (North West, Northern Cape Provinces): Orange–Vaal River terraces—Transient placers (Paleogene to Quaternary). The Vaal–Orange River system (Fig. 47) is the main route along which the diamonds have been transported from the Kaapvaal Craton to the southwest African coast. There were two main ancestral rivers, flowing westwards since break up of west Gondwana: the Kalahari River, with its lower part following the present Lower Orange River and the Molopo River out of Botswana, and; the Karoo River that drained most of the Vaal and middle and upper Orange Rivers before it entered the Atlantic Ocean much further to the south than currently (de Wit 1999). River capture by the end of the Cretaceous resulted in the present-day Orange–Vaal drainage configuration. This interpretation is supported by diamond inclusion geochronology studies which suggests that many of the diamonds along the west coast of South Africa (Namaqualand) are sourced from kimberlites or carbonate-rich olivine lamproites with eruption ages of between 115 and 300 Ma via the Karoo River (Phillips and Harris 2018). Using the same techniques, Phillips et al. (2009) were able to show that most of the diamonds along the west coast of Namibia, north of the Orange River mouth, are derived from younger (<90 Ma) kimberlites and also older carbonate-rich olivine lamproites, and were transported to the coast by the present Orange–Vaal River configuration. Longshore drift has carried diamond populations from both of these rivers northwards along the coast.

Examples of retained placers in this system include the diamond deposit on Nooitgedacht close to Kimberley with diamonds from the Kimberley mines (Fig. 47), before it became incorporated into transient Vaal River placers (de Wit 2004), as well as deposits adjacent to some of the Lesotho kimberlites, such as the Letšeng diamond mine (Fig. 47).

The oldest (Eocene) Orange River deposit (Bluck et al. 2005) has a low grade (<0.5 ct/100t) and low average stone size (<0.4 ct). The Oligocene pre-Proto Orange River terrace deposits have grades up to 35 ct/100t and an average stone size of 2 ct, these are followed by the Miocene Proto Orange River terraces with grades of 1 to 5 ct/100t and average stones sizes of 1 to 2 carats, and then by the Meso Orange terraces (Plio-Pleistocene; Figs. 68, 69) with low

Figure 68. Coarse-grained Plio–Pleistocene gravels along the Vaal River at Gong Gong near Barkly West, South Africa. Note imbrication of the oversize boulders.

Figure 69. Gravels being mined in the town of Windsorton along the Vaal River, north of Kimberley, South Africa.

grades <0.5 ct/100t. This suggests that there was an early entry of fine diamonds in the Eocene, followed by the main flush in the pre-Proto time and since then a declining diamond grade; however, big stones are associated with the younger terraces (Bluck et al. 2005).

Terraces along the middle Orange River, where terrace elevation varies from some 270 m (Late Cretaceous?) to some 20 m (Pliocene) above the river, have a quite notable large diamond population, with several +200 ct stones and at least 22 +100 ct stones recovered (De Meillon 2019; Norton et al. 2007). This area produces a mixture of diamonds sourced from the Cretaceous kimberlite in Lesotho (e.g., Letšeng), the Free State and Northern Cape Province (Kimberley, Koffiefontein, Jagersfontein, Finsch etc.), Permo-Carboniferous sources, as well as the reworked deposits in the Northwest Province and the Witwatersrand basin. In addition to the terrace stratigraphy along the Vaal and Orange Rivers, there are large areas within the river valleys covered by what is termed "Rooikoppie" or derived gravel. These are thin but chemically mature deflation deposits from older alluvial gravel or tillite units, consisting mainly of well-rounded and often polished siliceous pebbles in a loose red colored sand that are often highly profitable (Marshall 2004).

The economic sections of the upper Orange are restricted to residual placers next to the Lesotho kimberlites. From Lesotho to Hopetown the Orange River flows over horizontally bedded sandstones and shales of the Karoo Supergroup with only Jurassic dolerite dikes as potential trap-sites and these are not conducive to development of economic placers (Fig. 47). Only from Hopetown to Prieska, where the river cuts through the Dwyka tillites at the base of the Karoo, diamonds are trapped in the coarse gravel fabrics developed as a result of the breakdown of the tillites such that viable deposits are formed (de Wit 1996). From Prieska to Noordoewer there are only a few isolated and small remnant alluvial deposits, but the final 270 km stretch of the lower Orange River from Noordoewer to the mouth at Alexander Bay (Fig. 70) is where the lower Orange River economic deposits occur.

Figure 70. The Orange River and its delta, with aggressive wave action and long-shore drift transporting diamonds northwards. Looking northwards along Namibia shoreline.

Some of the large-scale trap-sites that have formed are splay deposits were the river exits narrow gorges, cut into bedrock, and develops coarse grained terraced fans. This is seen along the Vaal (e.g., Windsorton, Barkly West) and the Orange Rivers (de Wit 1996). These are often controlled by faults or due to changes in basement lithologies. Trap-sites on a smaller scale are coarse cobble-boulder size basal gravels close or on bedrock, with the development of scour pools, push bars and bedrock highs where turbulence created by boundary conditions at these fixed bedrock sites, are conducive for stable growth of gravel that retains the concentrated diamonds (Jacob et al. 1999).

South Africa/Namibia (Northern Cape Province/Karas Region): West Coast—Terminal placers (Paleogene to Quaternary). Epeirogenic uplift of southern Africa in the Cretaceous (de Wit 2007) has been the driving force in the development of the alluvial placers along the Orange River but also the creation of the spectacular marine deposits along the coast of southwest Africa (Figs. 47, 70). The diamonds in this terminal marine setting are hosted in fluvial, marine, deflation and aeolian placer types with temporal ranges from at least the end of the Cretaceous to the modern day. This large deposit, which stretches over 1,500 km from the Namaqualand coast of South Africa northwards to the Skeleton Coast of Namibia (Hallam 1964; Corbett 1996; de Wit 1996; Bluck et al. 2005), is separated into two distinct terminal placers, defined as the Namaqualand and Namibian megaplacers (Bluck et al. 2005), which from their initial discovery until 2019, have produced 53 and 112 Mct, respectively. The bulk of the diamonds were derived from the Namibian deposits along the Sperrgebiet coast, including almost 16 Mct from unique deflation and aeolian deposits (de Wit et al. 2016).

Offshore mining in this area was pioneered by a Texas oilman, Sammy Collins in the early 1960s but it was only in the 1970s that the significant deposits in water depths of 120–140 m were discovered. These deposits consist of mostly thin accumulations of coarse clastic submerged beach gravel, overlying an Eocene and Cretaceous clay footwall (de Wit et al. 2016). Following a long period of prospecting and technical development, mining of these marine deposits started in earnest in the early 1990s, and approximately 25 Mct have been recovered from the offshore areas. The greatest remaining potential along the West Coast is located in these deposits, with indicated/measured and inferred resources at 12.3 and 70.6 Mct and grades of 0.08 and 0.07 ct/m² respectively for the midwater and marine placers combined (Anglo American Ore reserves and mineral resources report 2019).

Russia (Republic of Sakha): Ebelyakh (Anabar River basin), northern Siberian Platform—Transient fluvial placers (Neogene to Quaternary). Although diamonds are present in the Mesozoic terminal placers (see above), these are uneconomic to mine and act only as a source to the viable Quaternary transient alluvial placers that are associated with tributaries of the Anabar River (Fig. 58). These occur towards the northeastern edge of the Siberian platform, east of the Archean Anabar shield, west of the Palaeoproterozoic Olenek uplift and some 450 km north-northeast of the Udachnaya and Zarnitsa mines. These alluvials are lenticular shaped deposits following valley profiles and are enriched in areas where they directly erode the older diamond bearing coastal and deltaic deposits. Other placers in northern Siberia, are found along the Molodo River (Fig. 58), a tributary of the Lena River, some 500 km northeast of the Udachnaya and Zarnitsa mines. This region is considered to be one of the world's largest secondary diamond fields (Micon 2016); combined these transient alluvial deposits have produced between 4.8 and 5.2 Mct/year between 2014 and 2016 with resource grades of between 0.77 to 1.33 ct/t (Alrosa 2017).

The Ebelyakh placer is underlain by Paleozoic and Mesozoic sediments and has a cover of unconsolidated Cenozoic sediments. Much of this placer is diamondiferous, mainly as the results of transgressive-regressive cycles (Ilyina and Egorov 2008). Paleo-weathering surfaces developed at various stratigraphic levels during periods of regression from the end of the Carboniferous to the Neogene, concentrating diamonds as a result of chemical and physical deflation. Reworked remnants of these diamond-bearing weathering surfaces and older sediments form the economic Neogene to Quaternary age transient diamond placers along several tributaries of the Anabar River, such as the Ebelyakh River. The Ebelyakh River deposits cover 83 km from its confluence with the Anabar River and is on average some 80 m wide, and include deposits along different branches of the Ebalyakh River. All the alluvial formations, the riverbed, the floodplain deposits and terraces, as well as the reworked weathering crusts in the river valley are diamond bearing.

The next major tributary to the Anabar River is the Maiat River some 25 km to the north, whose economic alluvial deposits occur mainly in branches in its upper reaches. Between the Ebelyakh and Maiat rivers is the Billiakh River and associated alluvial deposits. The Ebelyakh, Maiat and Billiakh rivers are right tributaries of the Anabar River, draining areas to the east. Other placers occur on left tributaries to the Anabar and include the Khara Mas stream, almost opposite the Billiakh River, and the Bolshaya Kuonamka (B-K) River some 20 km south of and opposite to the Ebelyakh River. The B-K River drains near-shore marine deposits of Meso-, and Neoproterozoic (Ediacaran) and early Cambrian age that are intruded by barren or low-grade Triassic and Jurassic kimberlites. Over 95% of the B-K reserves are comprised of Quaternary upper and lower floodplain (river placer) deposits, the rest being contained in three terraces that are of lower volume—but higher grades. The diamonds from the latter deposits are mainly colorless and significantly abraded (Afanas'ev et al. 2009). Indicator minerals derived from Upper Palaeozoic sediments also occur in these younger sediments (Grakhanov et al 2010), emphasizing the importance of the process of reworking and upgrading of older marine deposits to form the transient placer diamond deposits. This is also illustrated by placer gold recovered from some of these rivers, which has likewise been derived from the reworking of older sequences (Gerasimov 2019). By comparing diamonds from Palaeozoic, Mesozoic and Quaternary alluvial deposits, which are dominated (>85%) by eclogitic stones (Shatsky et al. 2019), and Triassic kimberlites of the same district, it was found that these kimberlites have only contributed to a part of the Anabar placer diamond population (Sobolev et al. 1999). Since the diamonds from the northern placer deposits are different to those from the southern Yakutian Palaeozoic kimberlite-hosted diamond mines (Grakhanov et al. 2010; Sobolev et al. 2018), the source(s) of these diamonds is still not known (Olev 1973; Sobolev et al. 1999).

Australia (Western Australia State): Smoke and Limestone Creeks of Argyle—Retained placers (Neogene to Quaternary). The discovery of diamonds in Smoke Creek in Western Australia (Fig. 61) led directly to the AK1 Argyle olivine lamproite pipe (Rayner et al. 2018; Smith et al. 2018), which occurs within the Halls Creek mobile belt, east of the Kimberley Craton (Shigley et al. 2001). Alluvial diamond deposits occur along Smoke Creek and Limestone Creek and these retained placers developed because of the proximity to a high-grade primary source (average grade 3 ct/t) that is part of a major positive topographic feature, with streams flowing to the north (Smoke Creek) and to the south (Limestone Creek). Local Devonian-aged conglomerates provided coarse clasts to the alluvial fabric necessary to concentrate diamonds, and finally the older alluvial terraces were upgraded by chemical deflation during periods of laterization.

Both creeks have been mined extensively and a total of 44.3 Mct and 6.8 Mct have been mined out of Smoke Creek and Limestone Creek, respectively (B. Janse pers. comm. 2020). Smoke Creek is mineralized over its entire length from the Argyle lamproite pipe to where it enters Lake Argyle, a distance of some 35 km (Fig. 71). The creek has three terrace levels according to elevation and the difference in the proximal reach between the oldest and youngest terraces is roughly 10 m. Pits dug in the 1 to 2 m thick oldest terrace show typical coarsening-upwards sequences indicative of an alluvial braidplain or alluvial fan system with gravel bars that have well-developed bar-top pavements. The grade of the older terrace was on average 3 to 4 ct/t reaching up to 15 ct/t in more proximal sites. The younger terraces are texturally less mature and become sandier downstream suggesting an increase in aggradation with distance. This is reflected in the reduced grades of between 1 to 2 ct/t.

The Limestone Creek alluvials have a very similar stratigraphy with three terraces, possibly from Pliocene or even Miocene age through to the Late Pleistocene for the youngest terrace, above the Holocene present-day river deposits. The oldest terrace deposit has been interpreted as a veneer of residual lag gravel on limestone where karstification of the carbonates in the form of sinkholes contributed to its preservation. Both Limestone and Smoke creeks are comparatively minor low-energy alluvial systems but with increased sediment transport capabilities during the wet season.

Figure 71. Aerial view looking south, of Argyle mine (Australia) in the gap of the Ragged Range hills with Smoke Creek draining to the north. Note the terraces levels in the valley.

Russia (Republic of Sakha): Molodo River, northeast Siberian platform—Transient fluvial placers (Quaternary). The Molodo placer is on a tributary to the Lena River south of the Olenek high (Fig. 58). Diamonds are mined from Quaternary alluvial sediments in the midstream section of the Molodo. The river has cut through Permian coal, Lower Triassic volcanics and Jurassic sandy-silty strata and the bedrock substrate is weathered Lower to Middle Cambrian carbonates and siliciclastics. The economic part of the deposit is in the present river bed gravels and in the five terraces of the lower and upper floodplain which are Pleistocene in age. Almost 40% of the diamond reserves are held in the upper floodplain and another 48% in the recent alluvium (Micon 2016). A high concentration of diamonds was also found near the mouth of the Bulkur River, a left tributary of Lena River and to the north of the Molodo River.

Siberia (Republic of Sakha): Mir, Udachnaya, Nyurbinskaya and Botuobinskaya alluvials, central Siberian Craton—Retained placers (Quaternary). There are two recent and proximal retained placers close to the Mir kimberlite, associated with the Irelyakh River (Fig. 58). These are sandy to pebbly river and floodplain gravels that include four associated terraces which are up to 6.4 m thick and covered by some 2 m of overburden. These have been mined by open pit methods. The Gornoye placer, 26 km southeast of Mir, features river gravels that stretch for almost 6 km, with a width of between 150 and 1,650 m along the Irelyakh and Malaya Botuobiya rivers. Both have been dredged and generally produce good quality diamonds.

Other retained secondary deposits that are also proximal and intimately related to the primary kimberlite sources include the Kluch Piropovy (av. grade 0.55 ct/m³) and Zakonturnaya placers (grade from 0 to 1.24 ct/m³) on the Piropovy stream that has eroded kimberlite and diamonds from the Udachnaya mine (Fig. 58) to produce proximal clay-rich flood deposits. The scattered Verkhne-Munskoye retained placers (Fig. 58) formed from weathering and erosion of the five diamondiferous kimberlites (including the Zapolarny and Magnitny kimberlites) of the upper Muna field, some 160 km northeast of the Udachnaya mine. The Nyurbinskaya and Botuobinskaya placers (Fig. 58), are gravels that are adjacent to, or partially overly the kimberlite-hosted diamond mines with the same names (Micon 2016). Although the diamond grade in all these examples drops off quickly away from the primary source, a 214.6 ct stone was recovered from the Nyurbinskaya placer close to the pipe (Alrosa press release 2016).

Venezuela (Bolivar State): Guaniamo—Transient fluvial placers (Quaternary). In 1969 newly discovered deposits at Guaniamo in Venezuela (Fig. 49) resulted in a large increase in diamond production from alluvial terraces and recent river sediments in that country, particularly from the Cuchivero River in the Orinoco River Basin. Initially it was thought that

the diamonds had been derived from the Roraima sediments. However, in 1982 the Guaniamo kimberlites sills and dikes were found in the Venezuelan portion of the Guyana Shield (Baxter-Brown and Baker 1991; Meyer and McCallum 1993). These were dated at 712 Ma (Kaminsky et al. 2004) and clearly indicated that Guaniamo kimberlite and Roraima diamond populations are not related. This also suggests that the Palaeoproterozoic primary sources that supplied diamonds to the base of the Roraima Supergroup might still exist. Venezuela is estimated to have produced some 16 Mct by 2010 of which some 14.5 Mct have likely come out of alluvial deposits (B. Janse pers. comm. 2020).

Brazil (Paraná State): Tibagi and Itararé—Transient reworked placers (Quaternary). Although diamonds occur in many stratigraphic sequences, in most instances it is only the reworking of the weathering products that are upgraded sufficiently to permit economic exploitation. Hence there are many areas in Brazil that are, or have been, mined from Late Cenozoic terraces, floodplains and present river channels. Much of the terrace development along the major rivers in the Paraná Basin is Quaternary in age (Oliveira et al. 2019).

Tibagi and Itararé are the most important diamondiferous sites of the eastern Paraná Basin (Fig. 49) and occur in high and low terraces and in active stream sediments of the Tibagi, Cinzas, Peixe and Verde Rivers. These deposits, which have grades of up to 0.62 ct/m³, were originally discovered by gold prospectors. The diamonds are generally small with an average stone size of between 0.1 to 0.3 ct/st but of high value (90% gem quality; Liccardo and Chieregati 2013). No kimberlites have ever been found in the region and there are no kimberlite indicators associated with these placers. The alluvial diamonds are spatially associated with the glacial-marine and glaciofluvial facies deposits of the Permo–Carboniferous Itararé Group (Liccardo and Chieragti 2013); mineralized parts of recent drainages are often located over the glaciofluvial conglomerates of the Itararé Group.

Brazil (Minas Gerais State): Coromandel area—Transient placer (Quaternary). The Coromandel area and specifically the Alto Paranaíba province (Fig. 49) of the southern São Francisco River basin (Minas Gerais State), is occupied by the Quiricó basin, which is underlain by Neoproterozoic Bambuí Group sediments and contains Lower (Areado Group) and Upper (Mata da Corda Group) Cretaceous sediments and volcaniclastics (Read et al. 2004). Rivers draining this area are a major source area for large high-value diamonds (Karfunkel et al. 2014), such as the 726.6 ct Presidente Vargas, 455 ct Darci Vargas and 400.7 ct Coromandel from the northward draining Santo Antônio do Bonito River, and the 262 ct Star of the South from the Bagagem River. High value diamonds are also found east of the head waters of the Santo Antônio do Bonito River, in the upper and north-eastward flowing Abaeté drainage basin (Read et al. 2004), which has produced a 452 ct stone.

Although the source of the diamonds has been discussed previously, the large diamonds could also have been transported from the São Francisco Craton by two glacial events: the Neoproterozoic Jequitaí, and Cambrian Santa-Fé glaciations (Tompkins and Gonzaga 1989; Gonzaga et al. 1994), although no diamonds have so far been recovered from these glacial sediments and the primary sources of the large diamonds have never been found.

Brazil (Mato Grosso State): Juína—Transient placer (Quaternary). This area is associated with the southern Amazonian Craton where the alluvium of the Juína Mirim, Vinte e Um de Abril and Cinta Larga rivers have been producing diamonds that are likely derived from Cretaceous sediments of the Parecis Basin. In the 1970-80's the rich Juina placer deposits in Mato Grosso State (Fig. 49) produced up to 5-6 million carats annually (Kaminsky et al. 2009), with diamond grades varying from 7 (Cinta Larga River basin) to 0.6 ct/m³ (Juína Mirim River Basin) (Tremblay 2005), and the major producers had mined some 40 Mct by 2014. Although some of the stones proved to be superdeep diamonds (sub-lithospheric) and mainly Type IIa stones (e.g., Harte et al. 1999; Kaminsky et al. 2009), most diamonds are of industrial quality (85%). The biggest diamond found was 452 ct and at least 15 plus 100 ct stones have

been reported with eight over 200 ct (Nannini et al. 2017). In 2006 a group of diamondiferous kimberlitic pipes (Pandrea 1 to 7) were found at the head of a drainage system and some 30 km upstream from the alluvial placers. Diamonds from these kimberlites and the placer deposits proved to be from the same population, which suggests that these kimberlites were probably the source for most of the alluvial diamonds. The kimberlites are Late Cretaceous, Cenomanian/Turonian in age (*ca.* 100–90 Ma), and although the basal conglomerates of the younger sedimentary Cretaceous Parecis Formation contain diamonds, they are not economic. Only the recent river alluvial material at Juína, that has been upgraded from the primary sources via the Upper Cretaceous conglomerates, are mined economically.

Brazil (Piauí, Mato Grosso, Bahia states): other deposits—Mainly transient placers (Quaternary). Diamonds, generally small but good quality, were discovered in 1946 southwest of Gilbués (Piauí State; Fig. 49) along the Riachão stream, an area known for significant historical alluvial diamond production (Junior Mining Network, May 2017). Gravels were mined from the river alluvium and terrace deposits, and it was subsequently the area where the first kimberlite, Redondão, was found in Brazil (Svisero et al. 1977). It has been suggested that the diamonds have been derived from the Lower Palaeozoic (Poti Formation), Upper Palaeozoic (Santa Fé Group, Piaui Formation; Gomes et al. 1972), and/or Cretaceous sediments (Fleischer 1998). This area seems to be off-craton and judging from the generally small sizes but good quality of diamonds, these deposits are likely to have been reworked from older sediments and not related to the nearby Cretaceous kimberlites.

Other deposits include Arenapolis (Mato Grosso State) where alluvials have been mined in Quaternary sediments associated with the headwaters of the Paraguay River and where the diamonds were interpreted to be derived from the Cretaceous conglomerates of the Parecis Formation. This is supported by the high degree of abrasion of these stones (Tappert et al. 2006).

Diamonds were found in recent alluvial sediments in the Lower Pardo River Basin (Bahia State), between the São Francisco and Jequitinhonha rivers (Fig. 49) and some 60 km inland from the coast, and it is estimated that some 980,000 ct were recovered between 1881 and 1890 (Pan American Union 1907, p. 582). Since the rivers cut through the Salobro Formation, a sequence of Lower Cambrian meta-conglomerates and pebbly meta-greywackes, it has been assumed to have been the source of the diamonds. However, no diamonds were ever found in the Salobro Formation and it is therefore more likely that these diamonds had ultimately been derived from the older Espinhaço Supergroup.

India (Andhra Pradesh State): Krishna and Pennar Rivers—Transient placer (Quaternary). In India diamonds were discovered over four thousand years ago. The country has produced some of the world's famous diamonds, such as the Koh-i-noor (1st cut 186 ct), Nizamz (440 ct), Great Moghul (787 ct), Hope (115 ct when purchased in 1666 by Jean Baptiste Tavenier, now 45.52 ct and on display in the Smithonian), Regent (410 ct) and others, all from the Krishna River alluvials (Ravi et al. 2013).

The Quaternary gravels along the Krishna and Pennar Rivers (Fig. 55) have long been known to be a source of gem quality diamonds. The greatest intensity of mining was along a 60 km stretch of the Krishna River between Kollur and Paritala, where diamond bearing gravel is some 30 cm thick. Old workings are also present along the banks of the Pennar River in the area south of the Krishna River. The Krishna diamonds have an average weight of 0.83 ct and nearly 40% of the stones are over 0.5 ct (Ravi et al. 2012). The alluvial diamonds display abrasion features such as percussion marks as well as radiation damage (green and brown spots) suggesting that there has been recycling through older sediments (Ravi et al. 2012). Furthermore, small diamonds have been reported from terminal beach placers of the Krishna–Godavari delta region, but are not considered to be of economic value (Subrahmanyam et al. 2005).

Angola/DRC (Malanje/Kwango Provinces): Cuango/Kwango River—Transient placer (Quaternary). Diamonds are associated with alluvial sediments within the Cuango/Kwango River over a distance of some 700 km (Fig. 64). This river and its tributaries tap into diamondiferous kimberlites and Calonda Formation sediments in its headwaters, to develop very rich deposits in floodplain, terraces and recent river gravels. The maximum age for the Kwango terraces is between 0.3 and 0.5 Ma (de Wit and Thorose 2015). The highest diamond concentrations were found where the river cut the basement, forming rich deposits that have been exposed in river diversions at Luzamba, Cafunfo and Luremo in Angola; in the 1980s these areas were producing some 100,000 ct/month. There is a significant decrease in stone size in the Cuango Valley, from an average stone size of 1.9 ct (Modern Mining, March 2017) in the small Caculio tributary in the upper reaches, to less than 10 st/ct in typical terrace and river deposits along the middle and lower reaches of the Kwango River along the border with the DRC (de Wit and Thorose 2015).

Central African Republic (Mambéré-Kadéï, Lobaye and Haute-Koko Prefectures): Carnot and Mouka-Oudda Formations—Transient placers (Quaternary). Diamonds from the Central African Republic (CAR) are exclusively derived from alluvial deposits (Fig. 64). To date, the country has produced some 25 Mct, of which ~75% are gem quality (Censier 1996). The alluvial deposits show an obvious spatial relationship with two horizontally-bedded Mesozoic fluvial formations: the Mouka-Ouadda Formation in the northeast (Haute-Koko) and the Carnot Formation in the west of the country (Mambéré-Kadéï, Lobaye). Flow directions of these Late Cretaceous palaeodrainage systems are to the north into basins of the Central African Rift system. These two formations unconformably overly Palaeozoic tillites and glaciofluvial deposits on an outwash plain (Censier 1996).

Most of the diamonds have been mined out of recent alluvial sediments that occur in streams on basement proximal to the Mesozoic formations and in streams flowing over these formations. The following alluvial placer deposit types are present: alluvial flat or floodplain, channel deposits and low and high terrace deposits (Chirico et al. 2010). The most prospective alluvial deposits occur on hard basement with fixed trap-sites such as scours, sluits, waterfalls and rapids, but always in proximity of the Mesozoic formations. The terraces may be lateritized, especially if it they are covered by colluvium. One restricted digging operation, in the northeast and upstream from the village of N'Zako, comprises a major, 60–80 m thick, benched, red excavation, and is known for its larger stones (Fig. 72). This digging regularly produces +50 ct stones and Bardet (1974) reports a +300 ct diamond from this deposit.

Figure 72. Diggings at N'zako where some of the largest diamonds have been produced in the Central African Republic.

There are no kimberlite indicator minerals reported from any of the CAR alluvial deposits, but the heavy mineral suite of the diamondiferous gravels and the Mesozoic sandstones are very similar (Censier 1996), suggesting that the Late Cretaceous formations are the source of the diamonds (Censier 1996). Because the clasts in the conglomerates of the Mesozoic formations are believed to have been derived from the Palaeozoic tillites, it is possible that the diamonds could also have been reworked out of the latter. Since the transport direction for both the Mesozoic fluvial as well as the Palaeozoic glaciofluvial systems was from the south, it is reasonable to suggest that the source(s) are located in the northern DRC although the Proterozoic metasediments overlying much of the CAR basement have also been highlighted as a possible, but more unlikely source rock (Chirico et al. 2010).

Diamonds have been produced north of Kisangani in the DRC (Fig. 64) mainly from recent alluvium and are of a similar population to those from the CAR. Most of the diamonds are rhombododecahedral (Censier and Toureng 1995), with a high proportion of the diamonds showing percussion marks, edge abrasions, network patterns and general surface corrosion (Harris 1985).

Sierra Leone (Eastern Province): Kono and Tongo—Retained/Transient placers (Quaternary). The pre-2008 production of diamonds in West Africa was mainly from alluvial sources, but in Sierra Leone the Koidu kimberlite-hosted diamond mine came on stream in 2012 and this increased significantly diamond output. There are two main alluvial mining areas in eastern Sierra Leone, Kono, close to the Koidu kimberlites, and Tongo, near the Tongo kimberlite dikes (Fig. 73). These areas are associated with recent sediments of the Sewa and Moa rivers, respectively. The Kono area in particular is known for the recovery of some very large stones such as the 969.8 ct Star of Sierra Leone, a 770 ct stone and the 709.5 ct Peace Diamond. In some potholes from the Sewa River, extremely high grades of over 1,000 ct/t have been achieved (Marshall et al. 2013). Diamond production from the Tongo area has been exclusively from alluvial sources with relatively high grades and high-quality stones, though in general the stone size at Tongo is smaller with no reported occurrence of +100 ct stones. The alluvials are present in river channels, flood plains and terraces as part of a Late Pleistocene to recent laterally migrating channels with isolated bedrock trapsites often associated with cross-cutting dikes.

The Mano River (Fig. 73) further east has also been targeted for alluvial mining, but it is a less prolific producer. Since the Cretaceous, diamonds have been transported along the Sewa, Moa and Mano Rivers to coastal areas, a distance of some 200 km. These Atlantic-directed rivers were rejuvenated as a result the subsiding continental margin that uplifted watershed areas (Sutherland 1982) following rifting at about 185 Ma.

Liberia (Lofa County): Mano, Lofa and Yambasi rivers—Transient placers (Quaternary). Production in Liberia of around 0.4 Mct/a, has been exclusively from alluvial sources and primarily from the west of the country close to the border with Sierra Leone in the Mano, Lofa and Yambasi River basins (Fig. 73). The alluvial deposits are similar to those in other parts of West and Central Africa and occur in high- and low-level terrace gravels, alluvial river flats and deep plunge pools within the active rivers and in the current river bed. Large gem-quality diamonds up to 170 ct as well as industrial diamonds have been recovered in diggings in west Liberia (Gunn et al. 2018). At Camp Alpha in the northwest, diamonds exceeding 300 ct have been found in alluvial gravels (S. Haggerty pers. comm. 2014).

Ivory Coast (Woroba, Vallée du Bandama Districts): Séguéla and Tortiya—Retained placers (Quaternary). Diamond production in the Ivory Coast, which has amounted to some 8.5 Mct, has mainly been from the alluvial fields at Tortiya in the north-central part of the country, and at Séguéla some 150 km to the southwest (Fig. 73). At Séguéla there are meta-

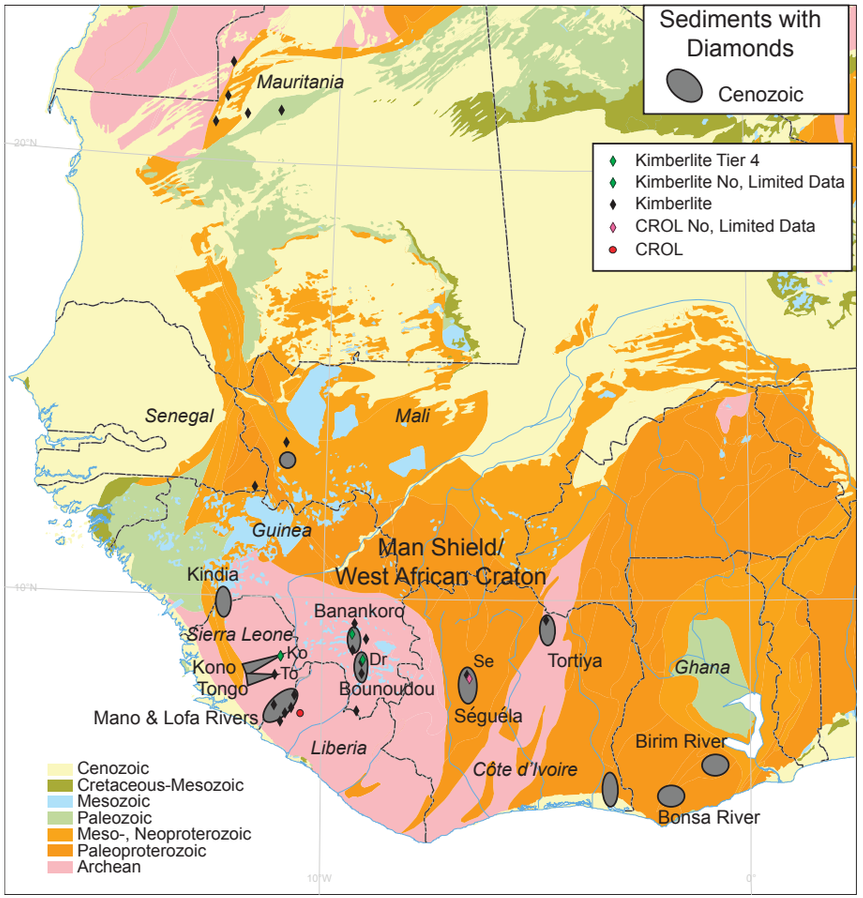

Figure 73. West Africa placer deposits as labeled on the map (Kono, Tongo, Mano and Lofa Rivers, Tortiya, Séguéla, Banankoro, Bounoudou, Kindia, Birim River, Bonsa River). Primary magmatic kimberlite and CROL mines/deposits as follows: Ko, Koidu; To, Tongo; Dr, Droujba; Se, Séguéla.

kimberlite (or metamorphosed carbonate-rich olivine lamproite) dikes dated at between 1,145 and 1,429 Ma (Bardet 1974), but exploitation here is restricted to small-scale mining of the associated recent colluvial and alluvial sediments proximal to these dikes. Diamonds are small, some 4 to 5 st/ct, and only one third is gem-quality.

The diamonds at Tortiya along the Bou River are sourced from a Proterozoic meta-volcanic-sedimentary complex trending NNE. Bardet (1974) believes the diamonds occur in conglomerates of the Birimian Supergroup and these were probably introduced during sedimentation at ~2.3 Ga, prior the Eburnian Orogeny (Milesi et al. 1992). After the break-up of Gondwana, the only major erosional events that would have affected Tortiya are sea level and climatic changes associated with Quaternary glaciations. The bulk of the diamonds, which are generally small and typically between 0.2–2.5 mm in size, occur in Quaternary colluvial deposits that are less than 10 m thick. These were formed by the weathering, erosion, and re-concentration of earlier deposits (Teeuw 2002) and the highest grades are found towards the base of what appears to be ferruginized mudflows.

Guinea (Kankan, Nzèrékoré, Kindia Regions): Banankoro, Bounoudou, Kindia areas—Retained and transient placers (Quaternary). In Guinea all of the ~20 Mct diamond production to date has come from alluvial deposits. There are four known kimberlite clusters in Guinea, all located in the southeast of the country and all have associated alluvial diamond fields (Figs. 73, 74). The most prolific of these is the Banankoro cluster where over 20 pipes and dikes were found in the 1950s. This area has seen extensive alluvial mining since the 1930's and has produced the most diamonds, including some large stones from the large scale commercial alluvial mining at the Aredor Mine at Kérouané along the Baoulé River in the 1990's to mid-2000's. Here the grades range from 5 to 9 ct/100t, and a resource of almost 1 Mct was declared (de Wit et al. 2016). Terraces west of the main mining area, which are between 20 and 30 m above the present river level, are extensively lateritised and fine-grained, with a granular- to pebble-size basal gravel. Both the retained placers, in the form of eluvial-alluvial deposits close to primary sources (and associated with small tributaries), and the transient alluvial placers that represent reworked gravels with rich deposits in flats and lower terraces of the larger rivers, are present (Chirico et al. 2012).

Figure 74. Chemically mature conglomerates at Kindia, Guinea, with well-rounded predominately siliceous clasts.

The watersheds of the Atlantic and Niger directed drainages had a major influence in the dispersal, size and quality of the alluvial deposits. The topography of rivers of the northeast directed Niger River Basin, such as the Baoulé, have a more mature relief with broad valleys and well-developed terraces. Limited down cutting has retained the diamonds close to its sources and little reworking has resulted in low to moderate diamond concentration in the main trunk rivers (Chirico et al. 2012). The Atlantic-directed drainages have been rejuvenated and the main concentration occurs in the large channels reworked out of older terraces (Sutherland 1993).

Some 70 km to the southeast of Banakoro alluvial mining has occurred in the Bounoudou region. For many years this was the largest diamond producing area of Guinea. Extremely high grades of up to 2.60 ct/t have been recorded next to the Droujba kimberlite, although grades of 0.25 ct/t are more common. A resource of 1.5 Mct at a value of 30 US$/ct (2016 prices) was established for the flats of this part of the Diani River basin (de Wit et al. 2016).

Diamonds have also been mined on a small scale in western Guinea in the Kindia and Forécariab areas. One-meter thick gravels occupy paleochannels and low terraces along the Atlantic-draining Konkouré River. These are structurally controlled and clearly follow bedrock fractures. These deposits are located on the edge of Palaeozoic Bove Basin. The bedrock varies from Late Archean and Proterozoic gneisses to Ordovician sandstones and conglomerates, but

since no kimberlitic minerals are associated with these gravels it has been suggested they have been reworked from white conglomeratic sandstone and diamictite of the Ordovician Pita Group.

Ghana (Eastern and Western Regions): Birim and Bonsa Rivers—Transient placers (Quaternary). Diamonds in Ghana are concentrated in two main areas, one near the Birim River close to Akwatia and another field in the Bonsa River further the southwest, referred to as the Birim and Bonsa diamond fields (Fig. 73). These are exclusively alluvial deposits and no diamond bearing kimberlites have been found in this part of West Africa. However, diamonds have been recovered from actinolite—tremolite schists that have been interpreted as "syn-eruptive volcaniclastic mega-turbidites derived from a diamond-bearing komatiite" similar to some of the diamond bearing rocks that have been described in French Guiana in South America (Canales 2005). Field evidence suggests that these komatiitic rocks are coeval with the meta-sediments indicating an age of 2,155 –2,085 Ma for the diamond bearing schists.

The concentration of the recent alluvial deposits is the result of the extensive weathering of these Proterozoic diamond-bearing phyllites, and subsequent redistribution into the local river systems. However, these diamond-bearing phyllites and schists are not mined. The regolith of weathered bedrock on the interfluve areas is covered by a laterite crust and erosion of these have supplied diamonds to the river terraces and floodplain gravels. Eroded quartz veins have provided large amounts of gravel clasts, that with bedrock traps (e.g., the sudden widening of the channel), are important constituents that help to retain the diamonds in the trap. Grades within these alluvial deposits are highest for the river flats, decreasing in the lower and higher terraces respectively, from 43, to 24 to 16 ct/100t for the Birim deposits, and from 27, to 14 to 7 ct/100t for the Bonsa deposits (Chirico et al. 2010).

The diamonds are in general small with average stone sizes of 0.033 ct/st for Birim and 0.025 ct/st for Bonsa and both fields have a high percentage (~35% and ~45%, respectively) of industrial diamonds (Chirico et al. 2010). Most of the diamonds are macles and dodecahedral crystals, and abrasion features appear more prominent on those from Bonsa area.

It is estimated that of the 120 Mct that have been mined in Ghana, 108 Mct are from the Birim area and 12 Mct from Bonsa, with 89 Mct and 2.6 Mct of diamonds still remaining in the Birim and Bonsa fields, respectively (de Wit et al. 2016). However, due to the patchy nature and lower grades of the remaining deposits, most of these would not be economically viable except as a by-product of gold dredging operations in the Bonsa region, and as artisanal operations in both areas.

Finally, isolated and less significant diamondiferous sediments have been reported from Gabon (Fig. 64), Mali (Fig. 73), China (Figs. 61, 75), and in California (associated with alluvial

Figure 75. Lower Cenozoic, upwards-coarsening diamond-bearing gravels at Mengyin, Shandong, China

gold recovery). Alluvial diamonds in Mali are not associated with the Kéniéba kimberlites, which have been shown to be barren.

Summary of economic diamond placers

This review has highlighted a few critical components for the development of economic placers. Most important is probably some form of epeirogenic uplift (e.g., Espinhaço range, Roraima basin, southern Africa, Anabar, West Africa etc.) to initiate erosion, transport and concentration of heavy minerals. The presence of retained placers in these areas of uplift would add a dimension of reworking and upgrading which is illustrated by the concentration of placers in the more recent transport systems during the Cenozoic. Hence recycling produces large diamond placers, such as the Roraima (Brazil) and Ebelyakh (Russia) deposits, but reworking in terminal settings, where there is upgrading of transient placers by marine processes, produces the largest diamond placers such as the Namibian, Namaqualand and Marange deposits. In a Gondwana context it is interesting to note how many diamonds are linked to having been distributed by the Permo-Carboniferous glaciation affecting deposits in Africa, Brazil and Australia.

ACKNOWLEDGEMENTS

This chapter is dedicated to Professor Peter H. Nixon who, since discovering the Letšeng la Terae deposit in 1957 has made a lifetime of important contributions to our field, inspiring many along the way. We thank the volume editors for the patience with us during the compilation of this chapter. Nick Pokhilenko and Sergie Kostrovitsy kindly granted permission to use images from their book for Figures 10 and 11b. Murray Rayner and Stephen Moss kindly provided images used for Figures 8 and 11a, respectively, and permission to reproduce them. Evelina Wieleba's GIS expertise in producing the global and craton/country scale maps is greatly appreciated. We thank reviewers George Read and Volker Lorenz for tackling a rather lengthy manuscript, as well as additional reviews specifically on the mineralogy and geochemistry section by Andrea Giuliani, and on the secondary diamond deposit section by Tania Marshall. Thomas Stachel and Stephan Kurszlaukis provided highly useful commentary and information on the volcanology section. BAK acknowledges funding from the GSC and the Geomapping for Energy and Minerals (GEM) program.

REFERENCES

Abersteiner A, Golovin A, Chayka I, Kamenetsky VS, Goemann K, Ehrig K, Rodemann T (2022) Carbon compounds in west Kimberley diamondiferous lamproites (Australia): Insights from melt and fluid inclusions. Gond Res (accepted)

Abersteiner A, Kamenetsky VS, Goemann K, Giuliani A, Howarth GH, Castillo-Oliver M, Thompson J, Kamenetsky M, Cherry A (2019) Composition and emplacement of the Benfontein kimberlite sill complex (Kimberley, South Africa): Textural, petrographic and melt inclusion constraints. Lithos 324:297–314

Afanas'ev VP, Zinchuk NN, Logvinova AM (2009) Distribution of placer diamonds related to Precambrian sources. Geol Ore Deposits 51:675–683

Afanasiev VP, Pokhilenko NP (2013) Wear of diamonds: An experimental study and field evidence. *In:*Proceedings of the 10th International Kimberlite Conference, DG Pearson, HS Grutter, JW Harris, BA Kjarsgaard, H O'Brien, NVC Rao, S Sparks (eds)1:317–321

ALROSA (2017) IR-release: Q4 and FY 2016 Operational Overview, 30 January 2017

Ambroise M (1991) Geology of the NE Angolan kimberlite region. 5th International Kimberlite Conference, Extended Abstracts, 6–9

Apter DB, Harper FJ, Wyatt BA, Smith BHS (1984) The geology of the Mayeng kimberlite sill complex, South Africa. *In:*Kimberlites and Related Rocks, Proceedings of the Third International Kimberlite Conference. Kornprobst J (ed) Elsevier Science Publishers, Clermont Ferrand, France 1:43–57

Armstrong JP, Wilson M, Barnett RL, Nowicki T, Kjarsgaard BA (2004) Mineralogy of primary carbonate-bearing hypabyssal kimberlite, Lac de Gras, Slave Province, Northwest Territories, Canada. Lithos 76:415–433

Ashchepkov I, Logvinova AM, Reimers LF, Ntaflos T, Spetsius ZV, Vladykin NV, Downes H, Yudin DS, Travin AV, Makovchuk IV, Palesskiy VS, Khmel'nikova OS (2015) The Sytykanskaya kimberlite pipe: Evidence from deep-seated xenoliths and xenocrysts for the evolution of the mantle beneath Alakit, Yakutia, Russia. Geosci Front 6:687–714

Atkinson WJ (1989) Diamond exploration philosophy, practice, and promises: a review *In:*Kimberlites and Related Rocks, Proceedings from the Fourth International Kimberlite Conference. Ross J (ed) GSA Spec Publ 14, Blackwell, Perth, Australia 2:1075–1107

Atkinson WJ, Hughes FE, Smith CB (1984) A review of the kimberlitic rocks of Western Australia. *In:* Kimberlites and Related Rocks, Proceedings of the Third International Kimberlite Conference. Vol 1. Kornprobst J, (ed) Elsevier Science Publishers, Clermont Ferrand, France, p 195–224

Balfour I (1987) Famous Diamonds. William Collins & Co., London

Bardet MG (1974) Geologie du Diamant. Gisements de Diamant d'Afrique. Memoire 83, Vol 2, B.R.G.M., Paris

Bartlett PJ (1998) Premier Mine. 7th International Kimberlite Conference, Large Mines Field Excursion, University of Cape Town, South Africa, p 39–49

Battilani GA, Gomes NS, Guerra WJ (2007) The occurrence of microdiamonds in Mesoproterozoic Chapada Diamantina intrusive rocks—Bahia/ Brazil. Anais da Academia Brasileira de Ciências 79: 321–332

Batumike JM, Griffin WL, Belousova EA, Pearson NJ, O'Reilly SY, Shee, SR (2008) LAM-ICPMS U–Pb dating of kimberlitic perovskite: Eocene–Oligocene kimberlites from the Kundelungu Plateau, D.R. Congo. Earth Planet Sci Lett 267, 609–619

Baxter-Brown R, Baker NR (1991) Discover of diamond deposits in the Quebrada Grande catchment Venezuela. International Kimberlite Conference, Extended Abstracts, v5

Becker M, Le Roex AP (2006) Geochemistry of South African on- and off-craton, Group I and Group II kimberlites: Petrogenesis and source region evolution. J Petrol 47:673–703

Bergman SC (1987) Lamproites and other potassium-rich igneous rocks: a review of their occurrence, mineralogy and geochemistry. *In:* Alkaline Igneous Rocks. Vol 30. Fitton JG, Upton BGJ, (eds) Geol Soc London, Spec Publ, p 103–190

Bertram CN (2010) Sedimentology, Age and Stable Isotope Evolution of the Kurnool Group, Cuddapah Basin. BSc(Hons) thesis (unpubl.), University of Adelaide, Australia

Black LP, James PR (1983) Geological history of the Napier Complex of Enderby Land. Antarctic Earth Science, International Symposium 4, RL Oliver et al. (ed) Canberra, Austral Acad Sci, p 11–15

Bluck BJ, Ward JD, de Wit MCJ (2005) Diamond mega-placers: southern Africa and the Kaapvaal craton in a global context. *In:*Mineral Deposits and Earth Evolution. I McDonald et al. (eds) Geol Soc London, Spec Publ 248:213–245

Bolivar SL (1984) An overview of the Prairie Creek intrusion, Arkansas. AIME Fall Meeting, October 1984, Preprint 84–346

Boxer GL, Lorenz V, Smith CB (1989) The geology and volcanology of the Argyle (AK1) lamproite diatreme, Western Australia. *In:* Kimberlites and Related Rocks, Proceedings from the Fourth International Kimberlite Conference. Ross J (ed) GSA Spec Publ 14, Blackwell, Perth, Australia, 1:140–152

Boyd F, Clement C (1977) Compositional zoning of olivines in kimberlite from the De Beers Mine, Kimberley, South Africa. International Kimberlite Conference Extended Abstracts 2:39–41

Boyd F, Nixon P (1973) Origin of the discrete nodules in the kimberlites of northern Lesotho. *In:* International Kimberlite Conference: Extended Abstracts 1:51–54

Brett RC, Russell JK, Moss S (2009) Origin of olivine in kimberlite: Phenocryst or impostor? Lithos 112:201–212

Brook MC (2012) Botswana's Diamonds. Longpack Co Ltd, China

Brown RJ, Manya S, Buisman I, Fontana G, Field M, MacNiocaill C, Sparks RSJ, Stuart FM (2012) Eruption of kimberlite magmas: physical volcanology, geomorphology and age of the youngest kimberlitic volcanoes known on earth (the Upper Pleistocene/Holocene Igwisi Hills volcanoes, Tanzania) Bull Volcanol 74:1621–1643

Burgess R, Phillips D, Harris JW, Robinson DN (1998) Antarctic diamonds in South-eastern Australia? Hints from $^{40}Ar/^{39}Ar$ Laser probe dating of clinopyroxene inclusions from Copeton diamonds. Extended Abstract 7th Int. Kimberlite Conference, Cape Town, South Africa

Bussweiler Y, Stone RS, Pearson DG, Luth RW, Stachel T, Kjarsgaard BA, Menzies A (2016) The evolution of calcite-bearing kimberlites by melt-rock reaction: evidence from polymineralic inclusions within clinopyroxene and garnet megacrysts from Lac de Gras kimberlites, Canada. Contrib Mineral Petrol 171:1–25

Bussweiler Y, Pearson DG, Stachel T, Kjarsgaard BA (2018) Cr-rich megacrysts of clinopyroxene and garnet from Lac de Gras Kimberlites, Slave Craton, Canada—Implications for the origin of clinopyroxene and garnet in cratonic lherzolites. Mineral Petrol 112 Suppl 2:S583–S596

Büttner R, Dellino P, La Volpe L, Lorenz,V, Zimanowski B (2002) Thermo-hydraulic explosions in phreatomagmatic eruptions as evidenced by the comparison between pyroclasts and products from Molten Fuel Coolant Interaction experiments. J Geophys Res Solid Earth 107(B11):2277

Carmichael IS (1967) The mineralogy and petrology of the volcanic rocks from the Leucite Hills, Wyoming. Contrib Mineral Petrol 15:24–66

Caro G, Kopylova MG, Creaser RA (2004) The hypabyssal 5034 kimberlite of the Gahcho Kue cluster, southeastern Slave craton, Northwest Territories, Canada: a granite-contaminated Group-I kimberlite. Can Mineral 42:183–207

Cas R, Porritt L, Pittari A, Hayman P (2008a) A new approach to kimberlite facies ten-ninology using a revised general approach to the nomenclature of all volcanic rocks and deposits: Descriptive to genetic. J Volcanol Geotherm Res 174:226–240
Cas RAF, Hayman P, Pittari A, Porritt L (2008b) Some major problems with existing models and terminology associated with kimberlite pipes from a volcanological perspective, and some suggestions. J Volcanol Geotherm Res 174:209–225
Cas RAF, Porritt L, Pittari A, Hayman PC (2009) A practical guide to terminology for kimberlite facies: A systematic progression from descriptive to genetic, including a pocket guide. Lithos 112:183–190
Cham RA (1998) Palaeodrainage and its significance to mineral exploration in the Bathurst region, NSW. Cooperative Research Centre for Landscape Evolution and Mineral Exploration, Monograph 3, p 38–54
Chaves MLCS, Uhlein A (1991) Depósitos diamantiferos da região do Alto/Médio Rio Jequitinhonha, Minas Gerais. *In:* Principals Depósitos Minerais do Brasil, DNPM and CPRM, Brasilia. Vol. IV, p 117–138
Chirico PG, Barthélémy F, Ngbokoto FA (2010) Alluvial Diamond Resource Potential and Production Capacity Assessment of the Central African Republic. US Geol Surv Scientific Investigations Report 2010–5043
Chirico PG, Malpeli KC, Van Bockstael M, Diaby M, Cissé K, Amadou Diallo T, Sano M (2012) Alluvial Diamond Resource Potential and Production Capacity Assessment of Guinea. US Geol Surv Scientific Investigations Report 2012–5256
Chorlton L (2007) Generalized geology of the world: bedrock geology and major faults in GIS format. Geol Surv Can Open File 5259
Clement CR (1982) A comparative geological study of some major kimberlite pipes in the Northern Cape and Orange Free State. Ph.D. thesis, University of Cape Town, Cape Town, South Africa
Clement CR, Skinner EMW (1979) A textural-genetic classification of kimberlite rocks. Kimberlite Symposium II, Cambridge, U.K., Extended Abstracts
Clement CR, Skinner EMW (1985) A textural-genetic classification of kimberlites. Trans Geol Soc S Afr 88:403–409
Clement CR, Dawson JB, Geringer GJ, Gurney JJ, Hawthorne JB, Krol L, Kleinjan L, van Zyl AA (1973) Guide for the first field excursion. 1st International Kimberlite Conference, University of Cape Town, South Africa
Clement CR, Skinner EMW, Scott Smith BH (1984) Kimberlite redefined. J Geol 92:223–228
Clement CR, Harris JW, Robinson DN, Hawthorne JB (1986) The De Beers kimberlite pipe—a historic South African diamond mine. *In:*Mineral Resources of Southern Africa. Anhaeusser CR, Maske S (eds) Geol Soc S Afr, Johannesburg, p 2193–2214
Clifford TN (1966) Tectono-metallogenetic units and metallogenetic provinces of Africa. Earth Planet Sci Lett 1:421–434
Coe N, Le Roex A, Gurney J, Pearson DG, Nowell G (2008) Petrogenesis of the Swartruggens and Star Group II kimberlite dyke swarms, South Africa: constraints from whole rock geochemistry. Contrib Mineral Petrol 156:627–652
Corbett IB (1996) A review of diamondiferous marine deposits of western southern Africa. Afr Geosci Rev 3:157–174
Creaser RA, Grutter H, Carlson J, Crawford B (2004) Macrocrystal phlogopite Rb-Sr dates for the Ekati property kimberlites, Slave Province, Canada: evidence for multiple intrusive episodes in the Paleocene and Eocene. Lithos 76:399–414
Cross CW (1897) The igneous rocks of the Leucite Hills and Pilot Butte, Wyoming. Am J Sci 4:115–141
Dalton H, Giuliani A, O'Brien H, Phillips D, Hergt J, Maas R (2019) Petrogenesis of a hybrid cluster of evolved kimberlites and ultramafic lamprophyres in the Kuusamo area, Finland. J Petrol 60:2025-
Dalton H, Giuliani A, Phillips D, Hergt J, Maas R, Matchan E, Woodhead J, O'Brien H (2020) A comparison of geochronological methods commonly applied to kimberlites and related rocks: three case studies from Finland. Chem Geol 558:119899
Das H, Kobussen AF, Webb KJ, Phillips D, Maas R, Soltys A, Rayner MJ, Howell D (2018) The Bunder Diamond Project, India: Geology, geochemistry, and age of the Saptarshi lamproite Pipes. *In:* Geoscience and Exploration of the Argyle, Bunder, Diavik, and Murowa Diamond Deposits. Davy AT, Smith CB, Helmstaedt HH, Jaques AL, Gurney JJ (Eds.) Allen Press Inc., Kansas, p 201–222
Davies RM, O'Reilly SY, Griffin WL (1999) Growth Structures and nitrogen characteristics of Group B alluvial diamonds from Bingara and Wellington, Eastern Australia. *In:* Proc 7th International Kimberlite Conference. JJ Gurney, JL Gurney, MD Pascoe, SH Richardson (eds) Cape Town, South Africa 1:156–163
Davies RM, O'Reilly SY, Griffin WL (2002) Multiple origins of alluvial diamonds from New South Wales, Australia. Econ Geol 97:109–123
Dawson JB (1967) A review of the geology of kimberlite. *In:*Ultramafic and Related Rocks. Wyllie PJ (ed) Wiley, New York, p 241–251
Dawson JB (1980) Kimberlites and Their Xenoliths. Springer, Berlin
Dawson JB (1987) The kimberlite clan: relationship with olivine and leucite lamproites, and inferences for upper mantle metasomatism. *In:* Alkaline Igneous Rocks. Fitton JG, Upton BGJ, (eds) Geol Soc London, Spec Publ 30, London, p 95–101
Dawson JB (1994) Quaternary kimberlitic volcanism on the Tanzania craton. Contrib Mineral Petrol 116:473–485
De Beers (2014) Diamond exploration. The Insight Report, p 46–49
de Wit MCJ (1996) The distribution and stratigraphy of inland alluvial diamond deposits in South Africa. Afr Geosci Rev 3:175–189

de Wit MCJ (2004) The diamondiferous sediments on the farm Nooitgedacht (66), Kimberley, South Africa. S Afr J Geol 107:477–488
de Wit MJ (2007) The Kalahari Epeirogeny and climate change: differentiating cause and effect from core to space. Inkaba yeAfrica Spec Vol. S Afr J Geol 110:367–392
de Wit MCJ (2016) Early Permian diamond-bearing proximal eskers in the Lichtenburg/Ventersdorp area of the North West Province, South Africa. S Afr J Geol 119:585–606
de Wit MCJ, Marshall TR, Partidge TC (2000) Fluvial deposits and drainage evolution. *In:* The Cenozoic of Southern Africa. TC Partridge, RR Maud (eds) Oxford Monographs on Geology and Geophysics 40:55–72
de Wit MCJ, Thorose E (2015) Diamond-bearing gravels along the Lower Kwango River DRC. Ch 16 *In:*Geology and Resource Potential of the Congo Basin, Regional Geology Reviews. MJ de Wit et al. (eds) Springer, Berlin, p 341–360
de Wit MCJ, Bhebhe Z, Davidson J, Haggerty SE, Hundt P, Jacob J, Lynn M, Marshall T, Skinner C, Smithson K, Stiefenhofer J, Robert M, Revitt A, Spaggiari R, Ward J (2016) Overview of diamond resources in Africa. Episodes 39:199–238
de Wit MCJ, Ward JD, Bamford MK, Roberts MJ (2009) The significance of the cretaceous diamondiferous gravel deposit at Mahura Muthla, northern cape province, South Africa. S Afr J Geol 112:89–108
Dobrzhinetskaya LF, O'Bannon EF III, Sumino H (2022) Non-cratonic diamonds from UHP metamorphic terranes, ophiolites and volcanic sources. Rev Mineral Geochem 88:191–256
Donnelly CL, Griffin WL, Yang J-H, O'Reilly SY, Li Q-L, Pearson NJ, Li X-H (2012) In situ U–Pb dating and Sr–Nd isotopic analysis of perovskite: constraints on the age and petrogenesis of the Kuruman Kimberlite Province, Kaapvaal Craton, South Africa. J Petrol 53:2497–2522
Dos Santos PR, Rocha-Campos AC, Canuto JR (1996) Patterns of late Palaeozoic deglaciation in the Paraná Basin, Brazil. Palaeogeogr Palaeoclimatol Palaeoecol 125:165–184
Dowall DP (2004) Elemental and Isotopic Geochemistry of Kimberlites from the Lac de Gras field, Northwest Territories, Canada. Ph.D. thesis, Durham University
Downes PJ, Wartho JA, Griffin BJ (2006) Magmatic evolution and ascent history of the Aries micaceous kimberlite, Central Kimberley Basin, Western Australia: Evidence from zoned phlogopite phenocrysts, and UV laser Ar-40/Ar-39 analysis of phlogopite–biotite. J Petrol 47:1751–1783
Eccles DR, Heaman LM, Luth RW, Creaser RA (2004) Petrogenesis of the Late Cretaceous northern Alberta kimberlite province. Lithos 76:435–459
Edwards CB, Howkins JB (1966) Kimberlites in Tanganyika with special reference to the Mwadui occurrence. Econ Geol 61:537–554
Edward D, Rock NMS, Taylor WR, Griffin BJ, Ramsay RR (1992) Mineralogy and petrology of the Aries diamondiferous kimberlite pipe. J Petrol 3:1157–1191
Eggler DH, McCallum ME, Smith CB (1979) Megacryst Assemblages in kimberlites from northern Colorado and southern Wyoming: Petrology, geothermometry–barometry, and areal distribution. *In:* The Second International Kimberlite Conference. Boyd FR, Meyer HOA (eds) Am Geophys Union, Santa Fe, USA 2:213–226
Ekkerd J, Stiefenhofer J, Field M, Lawless P (2003) The geology of Finsch mine, Northern Cape Province, South Africa. International Kimberlite Conference: Extended Abstracts, Vol 8
Erlich EI, Hausel WD (2002) Diamond Deposits: Origin, Exploration, and History of Discovery. Society for Mining Metallurgy and Exploration Inc
Fernandes AF, Karfunkel J, Hoover DB, Sgarbi PBdA, Sgarbi GNC, Oliveira GD, de Souza Pereira Gomes JC, Kambrock K (2014) The Basal Conglomerate of the Capacete Formation (Mata da Corda Group) and its Relation to Diamond Distributions in Coromandel, Minas Gerais State, Brazil. Braz J Geol 44:91–103
Fesq HW, Bibby DM, Erasmus CS, Kable EJD, Sellschop JPF (1975) A comparative trace element study of diamonds from Premier, Finsch and Jagerfontein mines, South Africa. *In:* Proceedings of the First International Kimberlite Conference, Phys Chem Earth, Vol 9. Ahrens LH, Dawson JB, Duncan AR, Erlank AJ (eds) Pergamon Press, Cape Town South Africa, p 817–836
Field M (2010) An assessment of the diamond potential of the Itilima property, Tanzania. Report prepared for Midlands Minerals Inc, Diakim Consulting Ltd
Field M, Scott Smith BH (1999) Contrasting geology and near-surface emplacement of kimberlite pipes in Southern Africa and Canada. *In:* The JB Dawson Volume, Proceedings of the VIIth International Kimberlite Conference. Gurney JJ, Gurney JL, Pascoe MD, Richardson SH (eds) Reed Roof Design, Cape Town, p 214–237
Field M, Steifenhofer J (2006) Orapa as a Type 1 kimberlite pipe. 8th International Kimberlite Conference, Kimberlite Emplacement Workshop, Extended Abstracts, Saskatoon, Canada
Field M, Gibson JG, Wilkes TA, Gababotse J, Khutjwe P (1997) The geology of the Orapa A/K1 kimberlite Botswana: further insight into the emplacement of kimberlite pipes. *In:* Kimberlites, Related Rocks and Mantle Xenoliths, Proceedings of the Sixth International Kimberlite Conference. Vol 1. Dobretsov NL, Mitchell RH (eds) Russ Geol Geophys Vol 38, Novosibirsk, Russia, p 24–39
Field M, Stiefenhofer J, Robey J, Kurszlaukis S (2008) Kimberlite-hosted diamond deposits of southern Africa: A review. Ore Geol Rev 34:33–75

Field M, Gernon TM, Mock A, Walters A, Sparks RSJ, Jerram DA (2009) Variations of olivine abundance and grain size in the Snap Lake kimberlite intrusion, Northwest Territories, Canada: A possible proxy for diamonds. Lithos 112:23–35
Fieremans C (1953) Geologie en geochemie der Diamantvelden van Belgisch-Congo. Technisch-Wetenschappelijk Tijdschrift, Jaargang 22, no 4–5, 1–16. Forminière 1956. Ouvrage publié par la Société Internationale Forestière et Minière du Congo a l'occassion du 50e anniversaire de sa création. Édition M L Cuypers, Bruxelles, 15 juin 1956
Fisher RV (1961) Proposed classification of volcaniclastic sediments and rocks. Geol Soc Am Bull 72:1409–1414
Fisher RV (1966) Rocks composed of volcanic fragments and their classification. Earth Sci Rev 1:287–298
Fleischer R (1998) A rift model for the sedimentary diamond deposits of Brazil. Mineralium Deposita 33:238–254
Flowers RM, Bowring SA, Reiners PW (2006) Low long-term erosion rates and extreme continental stability documented by ancient (U–Th)/He dates. Geology 34:925–928
Foley SF, Yaxley GM, Kjarsgaard BA (2019) Kimberlites from source to surface: insights from experiments. Elements: 15:393–398
Fraser KJ, Hawkesworth CJ (1992) The petrogenesis of Group-2 ultrapotassic kimberlites from Finsch Mine, South-Africa. Lithos 28:327–345
Fraser KJ, Hawkesworth CJ, Erlank AJ, Mitchell RH, Scott Smith BH (1985) Sr, Nd and Pb isotope and minor element geochemistry of lamproites and kimberlites. Earth Planet Sci Lett 76:57–70
Fulop A, Kurszlaukis S (2016) Monogenetic v. polygenetic kimberlite volcanism: in-depth examination of the Tango Extension Super Structure, Attawapiskat kimberlite field, Ontario, Canada. *In:*Monogenetic Volcanism. Nemeth K, Carrasco-Nunez G, Aranda-Gomez JJ, Smith IEM (eds) Geol Soc London, Spec Publ 446:205–224
Fulop A, Kopylova M, Kurszlaukis S, Hilchie L, Ellemers P, Squibb C (2018) Petrography of Snap Lake Kimberlite Dyke (Northwest Territories, Canada) and its interaction with country rock granitoids. J Petrol 59:2493–2518
Gaudet M, Kopylova M, Muntener C, Zhuk V, Nathwani C (2018) Geology of the Renard 65 kimberlite pipe, Québec, Canada. Mineral Petrol 112:433–445
Gerasimov B (2019) Typomorphism of fine placer gold and potential primary sources of the Anabar mineral subprovince (North-eastern Siberian Platform) IOP Conf Ser Earth Environ Sci 362:012039
Gernon TM, Fontana G, Field M, Sparks RSJ, Brown RJ, Mac Niocaill C (2009) Pyroclastic flow deposits from a kimberlite eruption: The Orapa South Crater, Botswana. Lithos 112:566–578
Giuliani A (2018) Insights into kimberlite petrogenesis and mantle metasomatism from a review of the compositional zoning of olivine in kimberlites worldwide. Lithos 312:322–342
Giuliani A, Pearson DG (2019) Kimberlites: from deep earth to diamond mines. Elements 15:377–380
Giuliani A, Phillips D, Kamenetsky VS, Fiorentini ML, Farquhar J, Kendrick MA (2014) Stable isotope (C, O, S) compositions of volatile-rich minerals in kimberlites: a review. Chem Geol 374:61–83
Giuliani A, Soltys A, Phillips D, Kamenetsky VS, Maas R, Goemann K, Woodhead JD, Drysdale RN, Griffin WL (2017) The final stages of kimberlite petrogenesis: petrography, mineral chemistry, melt inclusions and Sr–CO isotope geochemistry of the Bultfontein kimberlite (Kimberley, South Africa) Chem Geol 455:342–356
Gomes HA, Silva EFA, Quinh JS, Lopes JI (1972) Projecto Gilbués, Relatório Final, Vol 3 CPRM-DNPM, Recife
Gonzaga GM, Teixeira NA, Gaspar JC (1994) The origin of diamonds in western Minas Gerais, Brazil. Mineralium Deposita 29:414–421
Grakhanov SA, Malanin YuA, Pavlov VI, Afanas'ev VP, Pokhilenko NP, Gerasimchuk AV, Lipashova AN (2010) Rhaetian diamond placers in Siberia. Russ Geol Geophys 51:127–135
Grakhanov SA, Zinchuk NN, Sobolev NV (2015) The age of predictable primary diamond sources in the northeastern Siberian Platform. Dokl Earth Sci 465:1297–1301
Gress MU, Pearson DG, Chinn IL, Thomassot, E, Davies, GR (2021) Mesozoic to Paleoproterozoic diamond growth beneath Botswana recorded by Re–Os ages from individual eclogitic and websteritic inclusions. Lithos 388–389:106058
Griffin WL, O'Reill SY, Natapov LM, Ryan CG (2003) The evolution of lithospheric mantle beneath the Kalahari Craton and its margins. Lithos 71:215–251
Griffin WL, Batumike JM, Greau, Y, Pearson NJ, Shee SR, O'Reilly, SY (2014) Emplacement ages and sources of kimberlites and related rocks in southern Africa: U–Pb ages and Sr–Nd isotopes of groundmass perovskite. Contrib Mineral Petrol 168:10–32
Grubb MD, McCallum ME (1991) Genesis of diamond placers on the Guiana Shield, South America. Fifth International Kimberlite Conference, Brazil. Extended Abstracts, p 151–153
Gunn AG, Dorbor JK, Mankelow JM, Lusty PAJ, Deady EA, Shaw RA, Goodenough KM (2018) A review of the mineral potential of Liberia. Ore Geol Rev 101:413–431
Gupta S, Jain KC, Srivastava VC, Mehrotra (2003) Depositional environment and tectonism during the sedimentation of the Semri and Kaimur Groups of rocks, Vindhyan Basin. J Pal Soc India 48:181–190
Gurney JJ, Ebrahim S (1973) Chemical composition of Lesotho kimberlites. *In:* Lesotho Kimberlites. Nixon PH (ed) Maseru National Development Board, Maseru, p 280–284
Gurney JJ, Kirkley MB (1996) Kimberlite dyke mining in South Africa. Afr Geosci Rev 3:191–201
Gurney JJ, Helmstaedt HH, le Roex AP, Nowicki TE, Richardson SH, Westerlund, KJ (2005) Diamonds: crustal distribution and formation processes in time and space and an integrated deposit model. Econ Geol 100:143–177

Haggerty S (1976) Oxide minerals. Rev Mineral 3:6–88
Haggerty SE, Raber, E, Naeser, CW (1983) Fission track dating of kimberlitic zircons. Earth Planet Sci Lett 63:41–50
Hallam CD (1964) The geology of the coastal diamond deposits of southern Africa. *In:* The Geology of Some Ore Deposits in Southern Africa. SH Haughton (ed) Geol Soc S Afr 2:671–728
Hanson EK, Moore JM, Robey J, Bordy EM, Marsh JS (2006) Re-estimation of erosion levels in Group I and II kimberlites between Lesotho, Kimberley and Victoria West, South Africa. 8th International Kimberlite Conference, Kimberlite Emplacement Workshop, Saskatoon, Canada, Extended Abstracts
Hanson EK, Moore JM, Bordy EM, Marsh JS, Howarth G, Robey JVA (2009) Cretaceous erosion in central South Africa: evidence from upper-crystal xenoliths in kimberlite diatremes. S Afr J Geol 112:125–140
Harlow GE (1998) The Nature of Diamonds. Cambridge University Press, Cambridge
Harris JW, Smit KV, Fedortchouk Y, Moore M (2022) Morphology of monocrystalline diamond and its inclusions. Rev Mineral Geochem 88:119–166
Harris M, le Roex A, Class C (2004) Geochemistry of the Uintjiesberg kimberlite, South Africa: petrogenesis of an off-craton, group I, kimberlite. Lithos 74:149–165
Harris PG (1984) Kimberlite volcanism. *In:* Kimberlite Occurrence and Origin: A Basis for Conceptual Models in Exploration. Glover JE, Harris PG (eds) Uni West Aust Spec Publ 8:125–142
Harvey S, Kjarsgaard B, McClintock M, Shimell M, Fourie L, Du Plessis P, Read G (2009) Geology and evaluation strategy of the Star and Orion South kimberlites, Fort a la Corne, Canada. Lithos 112:47–60
Haugaard R, Waterton P, Ootes L, Pearson DG, Luo Y, Konhauser K (2021) Detrital chromites reveal Slave cratons missing komatiite. Geology 49:1079–1083
Hawthorne B (1975) Model of a kimberlite pipe. Phys Chem Earth 9:1–15
Hawthorne JB, Carrington AJ, Clement CR, Skinner EMW (1982) Geology of the Dokolwayo kimberlite and associated palaeo-alluvial diamond deposits. *In:*Kimberlites, Diatremes, and Diamonds: Their Geology, Petrology, and Geochemistry. HOA Meyer, FR Boyd (eds) Am Geophys Union, Washington, DC
Heaman LM, Mitchell RH (1995) Constraints on the emplacement age of Yakutian province kimberlites from U–Pb perovskite dating. 6th International Kimberlite Conference, Novosibirsk, Russia, 6IKC Extended Abstract, p 233
Heaman LM, Kjarsgaard BA (2000) Timing of eastern North American kimberlite magmatism: continental extension of the Great Meteor hotspot track? Earth Planet Sci Lett 178:253–268
Heaman LM, Pearson, DG (2010) Nature and evolution of the Slave Subcontinental Lithospheric Mantle. Lithoprobe Synthesis Volume II—Parameters, Processes and the Evolution of a Continent. Can J Earth Sci 47:369–388
Heaman LM, Kjarsgaard BA, Creaser RA (2003) The timing of kimberlite magmatism in North America: implications for global kimberlite genesis and diamond exploration. Lithos 71:153–184
Heaman LM, Kjarsgaard BA, Creaser RA (2004) The temporal evolution of north American kimberlites. Lithos 76:377–397
Heaman LM, Creaser RA, Cookenboo HO, Chacko T (2006) Multi-stage modification of the Northern Slave mantle lithosphere: evidence from zircon-and diamond-bearing eclogite xenoliths entrained in Jericho kimberlite, Canada. J Petrol 47:821–858
Heaman LM, Pell J, Grütter HS, Creaser RA (2015) U–Pb geochronology and Sr/Nd isotope compositions of groundmass perovskite from the newly discovered Jurassic Chidliak kimberlite field, Baffin Island, Canada. Earth Planet Sci Lett 415:183–199
Heaman LM, Phillips, D, Pearson DG (2019) Dating kimberlites: methods and emplacement patterns through time. Elements 15:399–404
Howarth GH, Büttner SH (2019) New constraints on archetypal South African kimberlite petrogenesis from quenched glass-rich melt inclusions in olivine megacrysts. Gondwana Res 68:116–126
Howarth GH, Giuliani A (2020) Contrasting types of micaceous kimberlite-lamproite magmatism from the Man Craton (West Africa): New insights from petrography and mineral chemistry. Lithos 362:19
Howarth GH, Nembambula T (2021) Petrogenesis of Kaapvaal lamproites (aka orangeites) constrained by the composition of olivine and similarities with kimberlites and other diamondiferous lamproites. Lithos 406:106499
Howarth GH, Michael E, Skinner W, Prevec SA (2011) Petrology of the hypabyssal kimberlite of the Kroonstad group II kimberlite (orangeite) cluster, South Africa: Evolution of the magma within the cluster. Lithos 125:795–808
Hutchison MT, Frei D (2009) Kimberlite and related rocks from Garnet Lake, West Greenland, including their mantle constituents, diamond occurrence, age and provenance. Lithos 112:318–333
Ilupin IP, Lutts BG (1971) The geochemical composition of kimberlite and questions on the origin of kimberlite magma. Sovietskaya Geologiya 6:61–73
Ilyina N, Egorov AY (2008) Upper Triassic of northern Middle Siberia: stratigraphy and paynology. Polar Res 27:372–392
Irvine TN (1965) Chromian spinel as a petrogenetic indicator: Part 1. Theory. Can J Earth Sci 2:648–672
Janse AJA (1984) Kimberlites—where and when. *In:* Kimberlite Occurrence and Origin: A basis for conceptual models in exploration, Glover JE and Harris PG (eds), Uni West Aust Spec Pub 8: 19–62
Janse AJA (1993) The aims and economic parameters of diamond exploration. *In:*Diamonds: Exploration, Sampling and Evaluation. Sheahan P, Chater A (eds) Short Course Proceedings, Prospectors and Developers Association of Canada, Toronto, p 173–184

Janse AJA (1995) A history of diamond sources in Africa: Part I. Gems Gemol 31:228–255
Janse AJA (1996) A history of diamonds in Africa: Part II. Gems Gemol 32:2–30
Janse AJA (2007) Global rough diamond production since 1870. Gems Gemol 43:98–119
Jaques AL, Foley SF (2018) Insights into the petrogenesis of the West Kimberley lamproites from trace elements in olivine. Mineral Petrol 112:519–537
Jaques AL, Lewis JD, Smith CB (1986) The kimberlites and lamproites of Western Australia. Geol Surv West Austral, Perth
Jaques AL, Lewis JD, Smith CB, Gregory GP, Ferguson J, Chappell BW, McCulloch MT (1984) The diamond-bearing ultrapotassic (lamproitic) rocks of the west Kimberley region, Western Australia. *In:*Kimberlites and Related Rocks, Proceedings of the Third International Kimberlite Conference. Vol 1. Kornprobst J (ed) Elsevier Science Publishers, Clermont Ferrand, France, p 225–254
Jacob DE, Mikhail S (2022) Polycrystalline diamonds from kimberlites: Snapshots of rapid and episodic diamond formation in the lithospheric mantle. Rev Mineral Geochem 88:167–190
Jacob RJ, Bluck BJ, Ward JD (1999) Tertiary-age diamondiferous fluvial deposits of the Lower Orange River Valley, southwestern Africa. Econ Geol 94:749–758
Jelsma HA, de Wit MJ, Thiart, C, Dirks, PHGM, Viola, G, Basson IJ, Anckar E (2004) Preferential distribution along transcontinental corridors of kimberlites and related rocks of Southern Africa. S Afr J Geol 107:301–324
Jelsma H, Barnett W, Richards S, Lister G (2009) Tectonic setting of kimberlites. Lithos 112:155–165
Jourdan F, Thern E, Wilde SA, Frewer L (2012) $^{40}Ar/^{39}Ar$ dating of unusual minerals (tourmaline, K-richterite, yimengite, wadeite and priderite) and applicability to the geological record. EGU Conference Abstract
Joy S, Jelsma HA, Preston RF, Kota S (2012) Geology and diamond provenance of the Proterozoic Banganapalle conglomerates, Kurnool Group, India. *In:*Palaeoproterozoic of India. Mazumder R, Saha D (eds) Geol Soc London Spec Publ 365:197–218
Kaminsky FV, Sablukov SA, Sablukova LI, Channer D (2004) Neoproterozoic "anomalous" kimberlites of Guaniamo, Venezuela: mica kimberlites of "isotopic transitional" type. Lithos 76:565–590
Kaminsky FV, Khachatryan GK, Andreazza P, Araujo D, Griffin WL (2009) Super-deep diamonds from kimberlites in the Juina area, Mato Grosso State, Brazil. *In:* Proc. 9th International Kimberlite conference. SF Foley, S Aulbach, GP Brey, HS Grütter, HE Höfer, DE Jacob, V Lorenz, T Stachel, AB Woodland (eds) Lithos 112S: 833–842
Kamenetsky VS, Kamenetsky MB, Sharygin VV, Golovin V (2007a) Carbonate-chloride enrichment in fresh kimberlites of the Udachnaya-East pipe, Siberia: A clue to physical properties of kimberlite magmas? Geophys Res Lett 34:101029
Kamenetsky VS, Kamenetsky MB, Sharygin VV, Faure KA, Golovin V (2007b) Chloride and carbonate immiscible liquids at the closure of the kimberlite magma evolution (Udachnaya-East kimberlite, Siberia) Chem Geol 237:384–400
Kamenetsky VS, Kamenetsky MB, Sobolev AV, Golovin AV, Demouchy S, Faure K, Sharygin VV, Kuzmin DV (2008) Olivine in the Udachnaya-East kimberlite (Yakutia, Russia): Types, compositions and origins. J Petrol 49:823–839
Karfunkel J, Chaves MLSC, Svisero DP, Meyer HOA (1994) Diamonds from Minas Gerais, Brazil: an update on sources, origin and production. Int Geol Rev 36:1019–1032
Karfunkel J, Hoover D, Fernandes AF, Sgarbi GNC, Kambrock K, Oliveira GD (2014) Diamonds from the Coromandel area, west Minas Gerais State, Brazil: an update and new data on surface sources and origin. Braz J Geol 44:325–338
Kargin AV, Nosova AA, Larionova YO, Kononova VA, Borisovsky SE, Koval'chuk EV, Griboedova IG (2014) Mesoproterozoic orangeites (Kimberlites II) of West Karelia: Mineralogy, geochemistry, and Sr–Nd isotope composition. Petrology 22:151–183
Kedrova TV, Bogush IN, Zinchuk NW, Bhardukhinov LD, Lipashova AN, Saltykova VP (2022) Diamond placers of the Nakyn kimberlite field. Russ Geol Geophys 63:245–254
Kennedy W (1964) The structural differentiation of Africa in the Pan-African (± 500 m.y.) tectonic episode. 8th Annual Report of the Research Institute of African Geology, University Leeds, p 48–49
Kilham J, Field M, Steifenhofer J (1998) Orapa and Lethlakane Mines. *In:*7th International Kimberlite Conference, Large Mines Field Excursion, University of Cape Town, South Africa, p 11–21
Kirkley MB, Gurney JJ, Levinson A (1992) Age, origin and emplacement of diamonds: A review of scientific advances in the last decade. CIM Bull 85:48–57
Kjarsgaard, BA (2003) Volcanology of kimberlite. *In:*Diamonds Short Course Notes. Tosdal R (ed) Cordilleran Round-Up, Vancouver BC, January 29–30
Kjarsgaard BA (2007a) Kimberlite diamond deposits. *In:*Mineral Deposits of Canada: A Synthesis of Major Deposit-Types, District Metallogeny, the Evolution of Geological Provinces, and Exploration Methods. Vol Special Publication No. 5. Goodfellow WD (ed) Geological Association of Canada, Ottawa, p 245–272
Kjarsgaard BA (2007b) Kimberlite pipe models: Significance for exploration. *In:*Proceedings of Exploration 2007. Milkereit B (ed) PDAC, Toronto p 667–677
Kjarsgaard BA, Levinson AL (2002) Diamonds in Canada. Gems Gemol 38:208–238
Kjarsgaard BA, Wilkinson L, Armstrong J (2002) Geology, Lac de Gras Kimberlite Field, Central Slave Province, Northwest Territories—Nunavut. Geol Surv Can Open File 3228, 1:250,00 scale, with descriptive notes and figures

Kjarsgaard BA, Leckie DA, Zonneveld JP (2007) Discussion of "Geology and diamond distribution of the 140/141 kimberlite, Fort a la Corne, central Saskatchewan, Canada", by A Berryman BH Scott Smith and BC Jellicoe. Lithos 97:422–428
Kjarsgaard BA, Pearson DG, Tappe S, Nowell GM, Dowall DP (2009) Geochemistry of hypabyssal kimberlites from Lac de Gras, Canada: Comparisons to a global database and applications to the parent magma problem. Lithos 112:236–248
Kjarsgaard BA, Pearson DG, Malarkey J (2010) The kimberlite olivine phenocryst/macrocryst/xenocryst problem, re-visited. GeoCanada 2010, Calgary, May 2010
Kjarsgaard BA, Januszczak N, Stiefenhofer J (2019) Diamond exploration and resource evaluation of kimberlites. Elements 15:411–416
Kinny PD, Griffin BJ, Heaman LM, Brakhfogel FF, Spetsius ZV (1997) SHRIMP U–Pb ages of perovskite from Yakutian kimberlites. Russ Geol Geophys 38:97–105
Konstantinovskii AA (2003) Epochs of diamond placer formation in the Precambrian and Phanerozoic. Lithol Min Res 38:530–546
Koornneef JM, Gress MU, Chinn IL, Jelsma HA, Harris JW, Davies, GR (2017) Archaean and Proterozoic diamond growth from contrasting styles of large-scale magmatism. Nat Commun 8:648
Kopylova M, Bruce L, Ryder J (2010) Diamonds in an Archaean greenstone belt: diamond suites in unconventional rocks of Wawa, northern Ontario (Canada) Geophys Res Abstracts 12:EGU2010-6835
Kostrovitsky ZV, Spetsius DA, Fon-der-Flaas GS, Suvorova LF, Bogush IN (2015) Atlas of Primary diamond deposits of Yakutian kimberlite province. Pokhilenko NP (ed), Scientific Council of NIGP ALROSA, Mirny
Kruger K, Maphane K (2017) Orapa, Lethlakane and Damtshaa Mines field guide. *In:* Desert Gems Botswana's Major Mines, 11th International Kimberlite Conference Field Guide, Gabarone, Botswana
Kueter N, Soesilo J, Fedortchouk Y, Nestola F, Belluco L, Juliana Troch J, Wälle M, Guillong M, Von Quadt A, Driesner T (2016) Tracing the depositional history of Kalimantan diamonds by zircon provenance and diamond morphology studies. Lithos 265:159–176
Kurszlaukis S, Lorenz V (2008) Fornation of "Tuffisitic Kimberlites" by phreatomagmatic processes. J Volcanol Geoth Res 174:68–80
Kurszlaukis S, Büttner R, Zimanowski B, Lorenz V (1998) On the first experimental phreatomagmatic explosion of a kimberlite melt. J Volcanol Geotherm Res 80:323–326
Kurszlaukis S, Mahotkin I, Rotman AY, Kolesnikov GV, Makovchuk IV (2009) Syn- and post-eruptive volcanic processes in the Yubileinaya kimberlite pipe, Yakutia, Russia, and implications for the emplacement of South African-style kimberlite pipes. Lithos 112:579–591
Laiginhas F, Pearson DG, Phillips D, Burgess R, Harris JW (2009) Re–Os and $^{40}Ar/^{39}Ar$ istopoe measurements of inclusions in alluvial diamonds from the Ural mountains: constrains on diamond genesis and eruption ages. Lithos 112S:714–723
Lapin AV, Tolstov AV, Vasilenko VB (2007) Petrogeochemical characteristics of the kimberlites from the Middle Markha region with application to the problem of the geochemical heterogeneity of kimberlites. Geochem Int 45:1197–1209
le Roex AP, Bell DR, Davis P (2003) Petrogenesis of Group I Kimberlites from Kimberley, South Africa: Evidence from Bulk-rock Geochemistry. J Petrol 44:2261–2286
Leckie DA, Kjarsgaard BA, Bloch J, McIntyre D, McNeil D, Stasiuk L, Heaman L (1997) Emplacement and reworking of Cretaceous, diamond-bearing, crater facies kimberlite of central Saskatchewan, Canada. Geol Soc Am Bull 109:1000–1020
Lefebvre N, Kopylova M, Kivi K, Barnett R (2003) Diamondiferous volcaniclastic debris flows of Wawa, Ontario, Canada. 8th International Kimberlite Conference, Long abstracts, FLA 0289, 5 pp
Lehmannn B, Burgess R, Frei D, Belyatsky B, Mainkar D, Rao NVC, Heaman LM (2010) Diamondiferous kimberlites in central India synchronous with Deccan flood basalts. Earth Planet Sci Lett 290:142–149
Lewis HC (1888) The matrix of diamond. Geol Mag 5:129–131
Liccardo A, Chieregati LA (2013) A extração de diamantes na história geológica e mineral no Paraná. Boletim de geociências paranaense 70:166–179
Lim E, Giuliani A, Phillips D, Goemann K (2018) Origin of complex zoning in olivine from diverse, diamondiferous kimberlites and tectonic settings: Ekati (Canada), Alto Paranaiba (Brazil) and Kaalvallei (South Africa) Mineral Petrol 112:539–554
Linol B, de Wit MJ, Barton E, Guillocheau F, de Wit MCJ, Colin JP (2015) Facies analyses, chronostratigraphy and paleo-environmental reconstructions of Jurassic to Cretaceous Sequences of the Congo Basin. Ch 8 *In:*Geology and Resource Potential of the Congo Basin, Regional Geology Reviews. MJ de Wit et al. (eds) Springer-Verlag, p 135–161
Liu J, Pearson DG, Wang LH, Mather KA, Kjarsgaard BA, Schaeffer AJ, Irvine GJ, Kopylova MG, Armstrong JP (2021) Plume-driven re-cratonisation of deep continental lithospheric mantle. Nature 592:732–736
Lorenz V (1975) Formation of phreatomagmatic maar-diatreme volcanoes and its relevance to kimberlite diatremes. *In:* Proceedings of the First International Kimberlite Conference, Phys Chem Earth, Vol 9. Ahrens LH, Dawson JB, Duncan AR, Erlank AJ (eds) Pergamon Press, Cape Town, South Africa, p 17–27
Lorenz V (1987) Phreatomagmatism and its relevance. Chem Geol 68:149–156
Lorenz V, Kurszlaukis S (2007) Root zone processes in the phreatomagmatic pipe emplacement model and consequences for the evolution of maar-diatreme volcanoes. J Volcanol Geotherm Res 159:4–32
MacNevin AA (1977) Diamonds in New South Wales. Geol Surv NS Wales, Mineral Resources No. 42

Mahotkin IL (1998) Petrology of the Group 2 kimberlite–olivine lamproite (K2L) series from the Kostomksha area, Karelia, NW Russia. 7th International Kimberlite Conference, Cape Town, South Africa, p 529–531
Mahotkin IL, Skinner EMW (1998) Kimberlites from the Archangelsk region—a rock type transitional between kimberlites, melnoites and lamproites. 7th International Kimberlite Conference, Cape Town, South Africa, p 532–534
Mainkar D, Lehmannn B (2007) The diamondiferous Behradih kimberlite pipe, Mainpur kimberlite field, Chhattisgarh, India: Reconnaissance petrography and geochemistry. J Geol Soc India 69:547–552
Mainkar D, Lehmannn B, Haggerty SE (2004) The crater-facies kimberlite system of Tokapal, Bastar district, Chhattisgarh, India. Lithos 76:201–217
Mannard GW (1962) The Singida Kimberlite Pipes. PhD thesis, McGill University, Montreal, Canada
Marshall T (1990) The Nature, Origin and Evolution of the Diamondiferous Gravels of the South Western Transvaal. Ph.D thesis (unpubl.), University of the Witwatersrand, Johannesburg
Marshall T (2004) Rooikoppie deposits in South Africa. Rough Diamond Rev 6:21–25
Marshall TR, Baxter-Brown R (1995) Basic principles of alluvial diamond exploration. J Geochem Explor 53:277–272
Marshall TR, Ward JD, de Wit MCJ (2013) African Alluvial diamond deposits. Presentation Diamond Course Oct. 2013, University of Pretoria
McClintock M, Ross PS, White JDL (2009) The importance of the transport system in shaping the growth and form of kimberlite volcanoes. Lithos 112:465–472
McPhie J, Doyle M, Allen RL (1993) Volcanic Textures. University of Tasmania
Meyer de Stadelhofen C (1963) Les breches kimberlitiques du Territoire de Bakwanga (Congo) Arch Sci Geneve 16:8–143
Meyer HOA, McCallum ME (1993) Diamonds and their sources in the Venezuelan portion of the Guyana Shield. Econ Geol 88:989–998
Micon International Co Ltd (2016) Alrosa Group of companies: Independent expert report on the reserves and resources of the diamond assets (JORC Code), Russian Federation
Milesi JP, Ledru P, Feybesse JL, Dommanget A, Marcoux E (1992) Early Proterozoic ore deposits and tectonics of the Birimian orogenic belt, West Africa. Precambrian Res 58:305–344
Miller CE, Kopylova MG, Ryder J (2012) Vanished diamondiferous cratonic root beneath the southern Superior province: evidence from diamond inclusions in the Wawa meta conglomerate. Contrib Mineral Petrol 164:697–714
Mitchell R (1984) Mineralogy and origin of carbonate-rich segregations in a composite kimberlite sill. Neues Jahrb Mineral Abh 150:185–197
Mitchell R (1985) A review of the mineralogy of lamproites. Trans Geol Soc S Afr 88:411–437
Mitchell RH (1986) Kimberlites: Mineralogy, Geochemistry, and Petrology. Plenum Press, New York
Mitchell RH (1995) Kimberlites, Orangeites and Related Rocks. Plenum Press, New York
Mitchell RH (2013) Paragenesis and oxygen isotopic studies of serpentine in kimberlite. Paragenesis and oxygen isotopic studies of serpentine in kimberlite. *In:*Proceedings of the 10th International Kimberlite Conference, Vol 1, Pearson DG, et al. (eds) Springer, p 1–12
Mitchell RH (2020a) Potassic Alkaline Rocks: Leucitites, Lamproites, and Kimberlites. Encycl Geol, 2nd edition
Mitchell RH (2020b) Igneous Rock Associations 26. Lamproites, Exotic Potassic Alkaline Rocks: A Review of their Nomenclature, Characterization and Origins. Geosci Can 47:119–142
Mitchell RH, Bergman SC (1991) Petrology of Lamproites. Springer
Mitchell RH, Skinner EMW, Scott Smith BH (2009) Tuffisitic kimberlite from the Wesselton Mine, South Africa: Mineralogical characteristics relevant to their formation. Lithos 112 S1:452–464
Mitchell RH, Scott Smith BH, Skinner EMW (2012) Mineralogy of magmaclasts and interclast matrices of Kimberley-type pyroclastic kimberlites from Kao, Letseng-la-Terae, Lethlakane and Premier kimberlite pipes, southern Africa. International Kimberlite Conference Extended Abstracts 10:10IKC-094
Mitchell RH, Giuliani A, O'Brien H (2019) What is a kimberlite? Petrology and mineralogy of hypabyssal kimberlites. Elements 15:381–386
Mmualefe MK (2017) Jwaneng diamond mine, Botswana: History, geology and mining. *In:* Desert Gems, Botswana's Major Mines, 11th International Kimberlite Conference Field Guide, Gabarone, Botswana, p 1–31
Moore R, Gurney J (1991) Garnet megacrysts from Group II kimberlites in southern Africa. International Kimberlite Conference: Extended Abstracts 5, p 298–300
Moore A, Moore J (2006) A glacial ancestry for the Somabula diamond-bearing alluvial deposit, Central Zimbabwe. S Afr J Geol 109:625–636
Moore A, Costin G, Proyer A (2021) Cognate versus xenocrystic olivines in kimberlites–A review. Earth Sci Rev 221:103771
Moore A, Blenkinsop T, Cotterill F (2008) Controls on post-Gondwana alkaline volcanism in Southern Africa. Earth Planet Sci Lett 268:151–164
Moore AE, Cotterill FPD, Broderick T, Plower D (2009) Landscape evolution in Zimbabwe from the Permian to present with implications for kimberlite prospecting. S Afr J Geol 112:65–88
Moss S, Russell JK, Brett RC, Andrews GDM (2009) Spatial and temporal evolution of kimberlite magma at A154N, Diavik, Northwest Territories, Canada. Lithos 112 S1:541–552
Moss S, Russell JK, Smith BHS, Brett RC (2010) Olivine crystal size distributions in kimberlite. Am Mineral 95:527–536

Moss S, Webb, K, Hetman, C, Manyumbu A (2013) Geology of the K1 and K2 kimberlite pipes at Murowa, Zimbabwe. *In:*Proc 10th International Kimberlite Conference, J Geol Soc India, Spec Issue 2, p 35–50
Moss S, Porritt L, Pollock K, Fomradas G, Stubley M, Eichenberg D, Cutts J (2018) Geology, mineral chemistry, and structure of the kimberlites at diavik diamond mine: indicators of cluster-scale cross-fertilization, mantle provenance, and pipe morphology. *In:*Geoscience and Exploration of the Argyle, Bunder, Diavik and Murowa diamond deposits. Davy AT, Smith CB, Helmstaedt H, Jaques AL, Gurney JJ (eds) Soc Econ Geol Spec Publ 20, p 287–318
Muggeridge MT (1995) Pathfinder sampling techniques for locating primary sources of diamond: Recovery of indicator minerals, diamonds and geochemical signatures. J Geochem Explor 53:183–204
Naidoo P, Stiefenhofer J, Field M, Dobbe R (2004) Recent advances in the geology of Koffiefontein Mine, Free State Province, South Africa. Lithos 76:161–182
Nannini F, Neto IC, Silveira FV, Cunha LM, de Oliveira RG, Weska RK (2017) Áreas kimberlíticas e diamantíferas do estado do Mato Grosso. Projeto diamante Brasil, Serviço Geológico do Brasil—CPRM, Série Pedras Preciosas, No 12
Nielsen TF, Sand KK (2008) The Majuagaa kimberlite dike, Maniitsoq region, West Greenland: constraints on an Mg-rich silicocarbonatitic melt composition from groundmass mineralogy and bulk compositions. Can Mineral 46:1043–1061
Nielsen TFD, Jensen SM, Secher K, Sand KK (2009) Distribution of kimberlite and aillikite in the Diamond Province of southern West Greenland: A regional perspective based on groundmass mineral chemistry and bulk compositions. Lithos 112:358–371
Niggli P (1923) Gesteins und Mineralprovinzen: Verlag Gebrüder Borntraegar, Berlin
Nikolenko EI, Logvinova AM, Izokh AE, Afanasiev VP, Oleynikov OB, Biller Aya. (2018) Polyphase inclusions in chrome spinels from Upper Triassic gravelites from the northeastern part of the Siberian Platform. Dokl Earth Sci 480:656–660
Nixon PH (1973) Lesotho Kimberlites. Lesotho National Development Corporation, Maseru, Lesotho
Nixon PH (1987) Mantle Xenoliths. John Wiley & Sons, Chichester
Nixon PH (1995) The morphology and nature of primary diamondiferous occurrences. J Geochem Explor 53:41–71
Norton G, Bristow J, van Wyk H (2007) Alluvial deposits and diamonds of the Lower Vaal and Middle Orange River, northern Cape Province RSA (2007) S Afr Inst Min Metal Diamonds—Source to Use. Extended Abstracts
Nowicki T (2014) On the value of geology in kimberlite evaluation: are we oversampling? Kimberley Diamond Symposium and Trade Show, Kimberley, September 11–13, Proc Geol Soc S Afr
O'Brien H, Tyni M (1999) Mineralogy and geochemistry of kimberlites and related rocks from Finland. *In:* Proc 7th International Kimberlite Conference, Gurney JJ, Gurney JL, Pascoe MD, Richardson SH (eds) Red Roof Design, Cape Town, p 625–636
O'Brien H, Phillips D, Spencer R (2007) Isotopic ages of Lentiira–Kuhmo–Kostomuksha olivine lamproite–Group II kimberlites. Bull Geol Soc Finland 79:203–215
Oliveira SC, Pupim FN, Stevaux JC, Assine ML (2019) Luminescence chronology of terrace development in the Upper Paraná River, southeast Brazil. Front Earth Sci 7:200
Pan American Union (1907) Monthly International Bureau of the American Republics, Jan—Jun, Washington, 14
Pasteris JD (1982) Representation of compositions in complex titanian spinels and application to the De Beers kimberlite. Am Mineral 67:244–250
Pasteris JD (1983) Spinel zonation in the De Beers kimberlite, South Africa: possible role of phlogopite. Can Mineral 21:41–58
Pearson D, Wittig N (2014) The formation and evolution of cratonic mantle lithosphere: Evidence from mantle xenoliths. Ch 3.6 *In:* Treatise on Geochemistry. Carlson RW (ed) Elsevier, p 255–292
Pearson DG, Shirey SB, Harris JW, Carlson, RW (1998) Sulphide inclusions in diamonds from the Koffiefontein kimberlite, S. Africa: constraints on diamond ages and mantle Re–Os systematics. Earth Planet Sci Lett 160:311–326
Pearson DG, Canil D, Shirey SB (2003) Mantle samples included in volcanic rocks: xenoliths and diamonds. *In:* Treatise on Geochemistry. Carlson RW (ed) Elsevier. The mantle and core 2:171–276
Pearson DG, Brenker FE, Nestola F, McNeill J, Nasdala L, Hutchison MT, Matveev S, Mather K, Silversmit G, Schmitz S, Vekemans B (2014) Hydrous mantle transition zone indicated by ringwoodite included in diamond. Nature 507:221–224
Pearson D, Liu J, Smith C, Mather K, Krebs M, Bulanova G, Kobussen A (2018) Characteristics and origin of the mantle root beneath the Murowa diamond mine: Implications for craton and diamond formation. *In:* Geoscience and Exploration of the Argyle, Bunder, Diavik and Murowa Diamond Deposits. Vol 20. Spec Publ Soc Econ Geol, p 403–424
Pearson DG, Woodhead J, Janney PE (2019) Kimberlites as geochemical probes of earth's mantle. Elements 15:387–392
Pearson DG, Scott JM, Liu J, Schaeffer A, Wang LH, van Hunen J, Szilas K, Chacko T, Kelemen PB (2021) Deep continental roots and cratons. Nature 596:199–210
Pedreira AJ, de Waele B (2008) Contemporaneous evolution of the Paleoproterozoic–Mesoproterozoic sedimentary basins of the São Francisco-Congo Craton. *In:*West Gondwana Pre-Cenozoic Correlations Across the Southern Atlantic Region. Pankhurst RJ et al. (eds) Geol Soc London Spec Publ 294:33–48

Perdoncini LC, Soares PC (1999) O diamante na bacia do rio Santa Rosa, Tibagi (pr) Revista Brasileira de Geociências 29:299–306
Pereira E, Rodrigues J, Reis B (2003) Synopsis of Luanda geology, NE Angola: Implications for diamond exploration. Comun Inst Geol e Mineiro 90:189–212
Pereira RS, Fuck RA, França OS, Leite AA (2017) Evidence of young, proximal and primary (YPP) diamond source occurring in alluviums in the Santo Antônio do Bonito, Santo Inácio and Douradinho rivers in Coromandel region, Minas Gerais. Braz J Geol 47:383–401
Petrov OV, Morozov AF, Shatov VV, Molchanov AV, Terekhov AV, Lukyanova LI, Artem'ev DS, Belova VN, Khalenev VO (2016) Russia, *In:* Mineral Resources in the Arctic. Geol Surv Norway Spec Publ Ch 9, p 374–482
Pervov VA, Somov SV, Korshunov AV, Dulapchii EV, Felix JT (2011) The Catoca kimberlite pipe, Republic of Angola: A Paleovolcanological model. Geol Ore Dep 53:295–308
Phillips D, Harris JW (2009) Diamond provenance studies from $^{40}Ar/^{39}Ar$ dating of clinopyroxene inclusions: An example from the west coast of Namibia. Lithos 112S:793–805
Phillips D, Zhong D, Matchan EL Maas R, Farr H, O'Brien H, Giuliani A (2017) A Comparison of Geochronology Methods Applied to Kimberlites and Related Rocks from the Karelian Craton, Finland. 11th International Kimberlite Conference, Botswana, Extended Abstract, 11IKC-4880
Phillips D, Harris JW, de Wit MCJ, Matchan EL (2018) Provenance history of detrital diamond deposits, West Coast of Namaqualand, South Africa. Mineral Petrol 112:S259–S273
Pilbeam L, Nielsen T, Waight T (2013) Digestion fractional crystallization (DFC): an important process in the genesis of kimberlites. Evidence from olivine in the Majuagaa kimberlite, southern West Greenland. J Petrol 54:1399–1425
Pivin M, Femenias O, Demaiffe D (2009) Metasomatic mantle origin for Mbuji-Mayi and Kundelungu garnet and clinopyroxene megacrysts (Democratic Republic of Congo) Lithos 112:951–960,
Porritt LA, Russell JK, McLean H, Fomradas G, Eichenberg D (2013) A Phreatomagmatic kimberlite: The A418 kimberlite pipe, Northwest Territories, Canada. *In:* Proc 10th International Kimberlite Conference, J Geol Soc India, Spec Issue 2:97–107
Price S, Russell J, Kopylova M (2000) Primitive magma from the Jericho Pipe, NWT, Canada: constraints on primary kimberlite melt chemistry. J Petrol 41:789–808
Prokopchuk BI (1972) Zoning in the distribution of diamond placers on old platforms. Dokl Akad Nauk SSSR 212:100–103
Quintão DA, Caxito FdA, Karfunkel J, Vieira FR, Seer HJ, de Moraes LC, Ribeiro LCB, Pendrosa-Soares AC (2017) Geochemistry and sedimentary provenance of the Upper Cretaceous Uberaba Formation (Southeastern Triângulo Mineiro MG, Brazil). Braz J Geol 47:159–182
Raal FA (1969) A study of some gold mine diamonds. Am Mineral 54:292–296
Ranger I, Heaman LM, Pearson DG, Muntener C, Zhuk V (2018) Punctuated, long-lived emplacement history of the Renard 2 kimberlite, Canada, revealed by new high precision U–Pb groundmass perovskite dating. Mineral Petrol 112:639–651
Rao NVC, Lehmannn B, Mainkar D, Belyatsky B (2011) Petrogenesis of the end-Cretaceous diamondiferous Behradih orangeite pipe: implication for mantle plume–lithosphere interaction in the Bastar craton, Central India. Contrib Mineral Petrol 161:721–74
Rau TK (2007) Panna diamond Belt, Madhya Pradesh—A critical review. J Geol Soc India 69:513–521
Rau TK, Wadhwa R, Mishra V, Fareeduddin (2012) Field guide to central Indian lamproite field. Guidebook prepared for the 10th International Kimberlite Conference 12016 Feb 2012
Ravi S, Sufija MV, Patel SC, Sheikh JM, Sridhar M, Kaminsky FV, Khachatryan GK, Nayak SS, Bhaskara Rao KS (2012) Diamond potential of the Eastern Dharwar Craton, India: their physical and infrared characteristics. Short Abstract 10th International Kimberlite Conference, p 282–283
Ravi S, Sufija MV, Patel SC, Sheikh JM, Sridhar M, Kaminsky FV, Khachatryan GK, Nayak SS, Bhaskara Rao KS (2013) Diamond potential of the Eastern Dharwar Craton, Southern India, and a reconnaissance study of physical and infrared characteristics of the diamonds. *In:*Proceedings of the 10th International Kimberlite Conference, DG Pearson, HS Grutter, JW Harris, BA Kjarsgaard, HO'Brien, NV Chalapathi Rao, S Sparks (eds) 1:335–348
Ray JS (2006) Age of the Vindhyan Supergroup: A review of recent findings. J Earth System Sci 115:149–160
Rayner MJ, Moss SW, Jaques AL, Lorenz V, Boxer GL, Smith CB, Webb K (2017) New insights into volcanic processes and diamond grades from deep mining at Argyle. IKC extended abstracts 11
Rayner MJ, Moss SW, Lorenz V, Jaques AL, Boxer GL, Smith CB, Webb K (2018a) New insights into volcanic processes from deep mining of the southern diatreme within the Argyle lamproite pipe, Western Australia. Mineral Petrol 112:351–363
Rayner MJ, Jaques A, Boxer G, Smith C, Lorenz V, Moss SW, Webb K, Ford D (2018b) The geology of the Argyle (AK1) diamond deposit, Western Australia. *In:* Geoscience and Exploration of the Argyle, Bunder, Diavik, and Murowa Diamond Deposits. Society of Economic Geologists
Read GH, Janse AJA (2009) Diamonds: Exploration, mines and marketing. Lithos 112:1–9
Reid AR (1974) Proposed origin of Guianan diamonds. Geology 2:67–68

Reid AM, Donaldson CH, Dawson JB, Brown RW (1975) The Igwisi Hills extrusive "kimberlites". *In:* Proceedings of the First International Kimberlite Conference, Phys Chem Earth, Vol 9. Ahrens LH, Dawson JB, Duncan AR, Erlank AJ, (eds) Pergamon Press, Cape Town, South Africa, p 199–218
Reis NJ, Nadeau S, Fraga LM, Betiollo LM, Faraco MTL, Reece J, Lachhman D, Ault R (2017) Stratigraphy of the Roraima Supergroup along the Brazil–Guyana border in the Guiana shield, Northern Amazonian Craton—Results of the Brazil–Guyana Geology and Geodiversity Mapping Project. Braz J Geol 47:43–57
Richardson, SH (1986) Latter-day origin of diamonds of eclogitic paragenesis. Nature 322:623–626
Richardson SH, Erlank AJ, Harris JW, Hart SR (1990) Eclogitic diamonds of Proterozoic age from Cretaceous kimberlites. Nature 346:54–56
Richardson SH, Chinn IL, Harris, JW (1999) Age and origin of eclogitic diamonds from the Jwaneng Kimberlite, Botswana. Proc 7th International Kimberlite Conference 2:709–713
Richardson SH, Shirey SB, Harris, JW (2004) Episodic diamond genesis at Jwaneng, Botswana, and implications for Kaapvaal Craton evolution. Lithos 77:143–154
Richardson SH, Poml, P, Shirey SB, Harris, JW (2009) Age and origin of peridotitic diamonds from Venetia, Limpopo Belt, Kaapvaal-Zimbabwe craton. Lithos 112:785–792
Robles-Cruz SE, Escayola M, Jackson S, Galí S, Pervov V, Watangua M, Gonçalves A, Melgarejo JC (2012) U–Pb SHRIMP geochronology of zircon from the Catoca kimberlite, Angola: Implications for diamond exploration. Chem Geol 310–311:137–147
Roberts EM, Jelsma H, Hegna (2015) Mesozoic sedimentary cover sequences of the Congo Basin in the Kasai Region, Democratic Republic of Congo. Ch 9 *In:*Geology and Resource Potential of the Congo Basin, Regional Geology Reviews, MJ de Wit et al. (eds) Springer-Verlag, p 163–191
Rock NM (1988) Lamprophyres. Springer
Roeder P, Schulze D (2008) Crystallization of groundmass spinel in kimberlite. J Petrol 49:1473–1495
Roffey S, Rayner MJ, Davy AT, Platell RW (2018) Evaluation of the AK1 diamond deposit, Western Australia. *In:* Geoscience and Exploration of the Argyle, Bunder, Diavik and Murowa Diamond Deposits. Davy AT, Smith CB, Helmstaedt H, Jaques AL, Gurney JG (eds) Soc Econ Geol Spec Publ 20, p 65–88
Rozova YV, Frantsesson EV, Pleshakov AP, Botova MM, Filipova LP (1982) High iron chrome spinels in kimberlites of Yakutia. Int Geol Rev 24:1417–1425
Sampson DH (1953) The volcanic hills of Igwisi. Rec Geol Surv Tanganika 3:47–53
Sarkar C, Heaman LM, Pearson DG (2015) Duration and periodicity of kimberlite volcanic activity in the Lac de Gras kimberlite field, Canada and some recommendations for kimberlite geochronology. Lithos 218–219:155–166
Sarkar C, Kjarsgaard BA, Pearson DG, Heaman LM, Locock A, Armstrong JP (2018) Geochronology, classification and mantle source characteristics of kimberlites and related rocks from the Rae Craton, Melville Peninsula, Nunavut, Canada. Mineral Petrol 112:653–672
Sarkar S, Giuliani A, Ghosh S, Phillips D (2021) Petrogenesis of coeval lamproites and kimberlites from the Wajrakarur field, Southern India: New insights from olivine compositions. Lithos 406:106524
Schmid R (1981) Descriptive nomenclature and classification of pyroclastic deposits and fragments: Recommendations of the IUGS Subcommission on the Systematics of Igneous Rocks. Geology 9:41–43
Schulze DJ (1987) Megacrysts from alkalic volcanic rocks. *In:* Mantle Xenoliths. Nixon PH (ed) John Wiley & Sons Ltd., Chichester, p 433–451
Scott BH (1979) Petrogenesis of kimberlites and associated potassic lamprophyres from central West Greenland. *In:* The Second International Kimberlite Conference. Vol 1. Boyd FR, Meyer HOA (eds) Am Geophys Union, Santa Fe, USA, p 190–205
Scott BH (1981) Kimberlite and lamproite dykes from Holsteinborg, Greenland. Medd Gronland Geosci 4:3–24
Scott Smith BH (2006) Canadian kimberlites: geological characteristics relevant to emplacement. 8th International Kimberlite Conference, Kimberlite Emplacement Workshop, Saskatoon, Canada, Extended Abstracts
Scott Smith BH (2008) Canadian kimberlites: geological characteristics relevant to emplacement. J Volc Geotherm Res 174:9–19
Scott Smith BH, Skinner EMW (1984) A new look at Prairie Creek, Arkansas. *In:*Kimberlites 1: Kimberlites and related rocks. Kornprobst J (ed) Elsevier, Amsterdam, p 255–283
Scott Smith BH, Danchin RV, Harris JW, Stracke KJ (1984) Kimberlites near Orroroo, South Australia. *In:* Kimberlites and Related Rocks, Proceedings of the Third International Kimberlite Conference. Kornprobst J (ed) Elsevier Science Publishers, Clermont Ferrand, France, 1:121–142
Scott Smith BH, Skinner EMW, Loney PE (1989) The Kapamba lamproites of the Luangwa Valley, Eastern Zambia. *In:* Kimberlites and Related Rocks, Proceedings from the Fourth International Kimberlite Conference. Ross J (ed) GSA Spec Publ No.14, Blackwell, Perth, Australia, 1:189–205
Scott Smith BH, Nowicki TE, Russell JK, Webb KJ, Mitchell RH, Hetman CM, Harder M, Skinner EMW, Robey JVA (2013) Kimberlite Terminology and Classification. *In:* Proceedings of the 10th International Kimberlite Conference, Pearson DG, et al. (eds) Spec Pub J Geol Soc India 2:1–17
Scott Smith BH, Nowicki TE, Russell JK, Webb K, Mitchell RH, Hetman C, Robey JVA (2018) A Glossary of Kimberlite and Related Terms. Scott Smith Petrology Incorporated, North Vancouver

Shaikh AM, Kumar SP, Patel SC, Thakur SS, Ravi S, Behera D (2018) The P3 kimberlite and P4 lamproite, Wajrakarur kimberlite field, India: mineralogy, and major and minor element compositions of olivines as records of their phenocrystic vs xenocrystic origin. Mineral Petrol 112:609–624
Shand SJ (1922) The problem of the alkaline rocks. Proc Geol Soc S Afr 25:xix–xxxii
Shatsky V, Zedgenizov D, Ragozin A, Kalinina V (2019) Silicate melt inclusions in diamonds of eclogite parageneis from placers on the northeastern Siberian craton. Minerals 9:412
Shigley JE, Chapman J, Ellison RK (2001) Discovery and mining of the Argyle diamond deposit, Australia. Gems Gemol 37:26–41
Shirey SB, Cartigny P, Frost DJ, Keshav S, Nestola F, Nimis P, Pearson DG, Sobolev NV, Walter MJ (2013) Diamonds and the geology of mantle carbon. Rev Mineral Geochem 75:355–421
Skinner EMW (1989) Contrasting Group I and Group II kimberlite petrology: towards a genetic model for kimberlites. *In:*Kimberlites and Related Rocks, Proceedings from the Fourth International Kimberlite Conference. Ross J (ed) GSA Spec Publ 14, Blackwell, Perth, Australia, 1:528–544
Skinner EMW, Viljoen KS, Clark TC, Smith CB (1994) The petrography, tectonic setting and emplacement ages of kimberlites in the southwestern border region of the Kaapvaal craton, Prieska area. *In:* Proceedings of the 5th International Kimberlite Conference, CPRM, Brazil. Meyer HOA, Leonardos OH (eds) 1:80–97
Skinner E, Marsh JS (2004) Distinct kimberlite pipe classes with contrasting eruption processes. Lithos 76:183–200
Skinner EMW, Apter DB, Morelli C, Smithson NK (2004) Kimberlites of the Man Craton, West Africa. Lithos 76:233–260
Smart KA, Tappe S, Stern RA, Webb SJ, Ashwal LD (2016) Early Archaean tectonics and mantle redox recorded in Witwatersrand diamonds. Nat Geosci 9:255–259
Smelov AP, Zaitsev AI (2013) The age and localization of kimberlite magmatism in the Yakutian Kimberlite Province: Constraints from isotope geochronology—An overview. *In:* Proceedings of 10th International Kimberlite Conference, DG Pearson et al. (eds.) Spec Issue J Geol Soc India 1:225–234
Smit KV, Pearson DG, Stachel, T, Seller, M (2014) Peridotites from Attawapiskat, Canada: Mesoproterozoic reworking of Palaeoarchaean lithospheric mantle beneath the Northern Superior superterrane. J Petrol 55:1829–1863
Smit KV, Timmerman S, Aulbach S, Shirey SB, Richardson SH, Phillips D, Pearson DG (2022) Geochronology of diamonds. Rev Mineral Geochem 88:567–636
Smith C (1983) Pb, Sr and Nd isotopic evidence for sources of southern African Cretaceous kimberlites. Nature 304:51–54
Smith CB, Lorenz V (1989) Volcanology of the Ellendale lamproite pipes, Western Australia. *In:* Kimberlites and Related Rocks, Proceedings from the Fourth International Kimberlite Conference. Ross J (ed) GSA Spec Publ 14, Blackwell, Perth, Australia, 1:505–520
Smith C, Gurney J, Ebrahim N, Skinner E, Clement C (1985) Geochemical character of southern African kimberlites: a new approach based on isotopic constraints. Trans Geol Soc S Afr 88:267–280
Smith C, Gurney JJ, Harris JW, Otter ML, Kirkley MB, Jagoutz, E (1991) Neodymium and strontium isotope systematics of eclogite and websterite paragenesis inclusions from single diamonds, Finsch and Kimberley Pool, RSA. Geochim Cosmochim Acta 55:2579–2590
Smith CB, Bulanova GP, Kohn SC, Milledge HJ, Hall AE, Griffin BJ, Pearson DG (2009) Nature and genesis of Kalimantan diamonds. Lithos 112S:822–832
Smith CB, Atkinson WJ, Tyler EW, Hall AE, Macdonald I (2018) The discovery of the Argyle pipe, western Australia: The world's first lamproite hosted diamond mine. *In:* Geoscience and exploration of the Argyle, Bunder, Diavik and Murowa diamond deposits. Vol 20. AT Davy CB Smith, H Helmstaedt, AL Jaques, JJ Gurney (eds) Soc Econ Geol, p 49–64
Sobolev NV (1977) Deep-seated inclusions in kimberlites and the problem of the composition of the upper mantle. (Translated from the Russian edition 1974) Am Geophys Union, Washington
Sobolev NV, Yefimova ES, Lavrent'yev YG, Sobolev VSD (1984) Dominant calcsilicate association of crystalline inclusions in placer diamonds from southeastern Australia. Dokl Akad Nauk SSSR 274:172 5
Sobolev NV, Yefimova ES, Koptil VI (1999) Mineral inclusions in Diamonds in the Northeast of the Yakutian Diamondiferous Province. *In:* JJ Gurney, JL Gurney, MD Pascoe, SH Richardson (eds) Proceedings 7th International Kimberlite Conference, Cape Town 2: 816–822
Sobolev NV, Logvinova AM, Nikolenko EI, Lobanov SS (2013) Mineralogical criteria for the diamond potential of Upper Triassic placers of the northeastern margin of the Siberian Platform. Russ Geol Geophys 54:903–916
Sobolev NV, Sobolev AV, Tomilenko AA, Kovyazin SV, Batanova VG, Kuz'min DV (eds) (2015) Paragenesis and complex zoning of olivine macrocrysts from unaltered kimberlites of teh Udachnaya-East pipe,Yakutia: relationship with the kimberlite formation conditions and evolution. Russ Geol Geophys 56:260–279
Sobolev NV, Sobolev AV, Tomilenko AA, Kuz'min DV, Grakhanov SA, Batanova VG, Logvinova AM, Bul'bak TA, Kostrovitskii SA, Yakovlev DA, Fedorova EN, Anastasenko GF, Nikolenko EI, Tolstov AV, Reutskii VN (2018) Prospects of search for diamondiferous kimberlites in the northeastern Siberian Platform. Russ Geol Geophys 59:1365–1379

Sobolev NV, Logvinova AM, Tomilenko AA, Wirth R, Bul'bak TA, Luk'yanova Li, Fedorova EN, Reutsky VN, Efimova ES (2019) Mineral and fluid inclusions in diamonds from the Urals placers, Russia: Evidence for solid molecular N_2 and hydrocarbons in fluid inclusions. Geochim Cosmochim Acta 266:197–219
Soltys A, Giuliani A, Phillips D (2018) A new approach to reconstructing the composition and evolution of kimberlite melts: a case study of the archetypal Bultfontein kimberlite (Kimberley, South Africa). Lithos 304:1–15
Soltys A, Giuliani A, Phillips D, Kamenetsky VS (2020) Kimberlite metasomatism of the lithosphere and the evolution of olivine in carbonate-rich melts—evidence from the Kimberley kimberlites (South Africa) J Petrol 61:egaa062
Soni MK, Jha DK, Rao TK, Mukul Tiwari (2002) Proterozoic diamondiferous placers, Panna diamond belt M.P. (2002) International Conference on Diamond and Gemstones, Raipur, India. Extended abstracts, p 19–21
Sorenson H (1974) Introduction. *In:*The Alkaline Rocks, Sorenson H (ed) Wiley, New York, p 1–15
Sparks RSJ (2013) Kimberlite volcanism. Annu Rev Earth Planet Sci 41:497–528
Sparks RSJ, Baker L, Brown RJ, Field M, Schumacher J, Stripp G, Walters A (2006) Dynamical constraints on kimberlite volcanism. J Volcanol Geotherm Res 155:18–48
Spencer LK, Dikinis SD, Keller PC, Kane RE (1988) The Diamond deposits of Kalimantan, Borneo. Gems Gemol 24:67–80
Spier CA, Ferreira Filho CF (1999) Geologia, estratigrafia e depósitos minerais do projeto Vila Nova, escudo das Guianas, Amapá, Brasil. Revista Brasileira de Geociências 29:173–178
Spriggs A (1988) An Isotopic and Geochemical Study of Kimberlites and Associated Alkaline Rocks from Southern Namibia. PhD Dissertation, University of Leeds, UK
Stachel T, Harris JW (2008) The origin of cratonic diamonds—Constraints from mineral inclusions. Ore Geol Rev 34:5–32
Stachel T, Lorenz V, Smith CB, Jaques AL (1994) Evolution of four individual lamproite pipes, Ellendale volcanics field (Western Australia) *In:*Kimberlites, Related Rocks and Mantle Xenoltihs: Proceedings of the Fifth International Kimberlite Conference. Vol 1. Meyer HOA, Leonardos OH (eds) CPRM, Araxa, Brazil, p 177–194
Stachel, T, Harris JW, Brey GP, Joswig W (2000) Kankan diamonds: lower mantle inclusion parageneses. Contrib Mineral Petrol 140:16–27
Stachel T, Banas A, Aulbach S, Smit KV, Wescott P, Chinn IL, Kong J (2018) Victor Mine: Neoproterozoic lherzolitic diamonds from a thermally modified cratonic root. Mineral Petrol 112S:311–324
Stachel T, Aulbach S, Harris JW (2022) Mineral inclusions in lithospheric diamonds. Rev Mineral Geochem 88:307–392
Stanley JR, Flowers RM, Bell DR (2015) Erosion patterns and mantle sources of topographic change across the southern African Plateau derived from shallow and deep records of kimberlites. Geochem Geophys Geosyst 16:3235–3256
Stiefenhofer J, Farrow DJ (2004) Geology of the Mwadui kimberlite, Shinyanga district, Tanzania. Lithos 76:139–160
Stubley MP, Irwin D (2019) Bedrock geology of the Slave Craton, Northwest Territories and Nunavut. Northwest Territories Geological Survey, Open File Report 2019–01
Subrahmanyam AV, Anil Kumar V, Deshmukh RD, Viswanathn G (2005) Discovery of microdiamonds in beachplacers of east coast, Andhra Pradesh, India Curr Sci 88:1227–1228
Sun J, Liu C-Z, Tappe S, Kostrovitsky SI, Wu F-Y, Yakovlev D, Yang Y-H, Yang J-H (2014) Repeated kimberlite magmatism beneath Yakutia and its relationship to Siberian flood volcanism: insights from ins situ U–Pb and Sr–Nd perovskite isotope analysis. Earth Planet Sci Lett 404:283–295
Sutherland DG (1982) The transport and sorting of diamonds by fluvial and marine processes. Econ Geol 77:1613–1620
Sutherland DG (1993) Drainage Basin evolution in southeast Guinea and the development of diamondiferous placer deposits. Econ Geol 88:44–54
Svisero DP, Meyer HOA, Tsai HM (1977) Kimberlite minerals from Vargem (Minas Gerais) and Redondão (Piauí) diatremes, Brazil: and garnet lherzolite xenolith from Redondão diatreme. Revista Brasileira de Geosciências, 7:1–13
Svisero DP, Shigley JE, Weldon R (2017) Brazilion Diamonds: a historical and recent perspective. Gems Gemol 53:2–33
Tainton KM (1992) The Petrogenesis of Group-2 Kimberlites and Lamproites from the Northern Cape Province, South Africa. University of Cambridge
Tainton KM, Browning P (1991) The Group-2-kimberlite–lamproite connection: Some constraints from the Barkly–West District, Northern Cape Province, South Africa. International Kimberlite Conference, Extended Abstracts, v5
Tainton KM, McKenzie D (1994) The generation of kimberlites, lamproites, and their source rocks. J Petrol 35:787–817
Tappe S, Foley SF, Jenner GA and Kjarsgaard BA (2005) Integrating ultramafic lamprophyre into the IUGS classification of igneous rocks: Rationale and implications. J Petrol 46:1893–1900
Tappe S, Pearson DG, Kjarsgaard BA, Nowell G, Dowall D (2013) Mantle transition zone input to kimberlite magmatism near a subduction zone: origin of anomalous Nd–Hf isotope systematics at Lac de Gras. Earth Planet Sci Lett 371–372:235–251
Tappe S, Smart K, Torsvik T, Massuyeau M, de Wit M (2018) Geodynamics of kimberlites on a cooling Earth: Clues to plate tectonic evolution and deep volatile cycles. Earth Planet Sci Lett 484:1–14
Tappert R, Stachel T, Harris JW, Muehlenbachs K, Ludwig T, Brey GP (2005) Diamonds from Jagersfontein (South Africa): Messengers from the sublithospheric mantle. Contrib Mineral Petrol 150:505–522
Tappert R, Stachel T, Harris JW, Muehlenbachs K, Brey GP (2006) Placer diamonds from Brazil: Indicators of the composition of the earth's mantle and the distance to their kimberlitic sources. Econ Geol 101:453–470
Tappert R, Foden J, Muehlenbachs K, Stachel T, Goryniuk M, Wills K (2008) The diamonds of South Australia. 9th International Kimberlite Conference, Extended abstract, 9IKC-A-00209

Tappert R, Foden J, Stachel T, Muehlenbachs K, Tappert M, Wills K (2009) The diamonds of south Australia. Lithos 112S:806–821
Taylor WR, Kingdom L (1999) Mineralogy of the Jagersfontein kimberlite—An unusual Group I micaceous kimberlite—and a comment on the robustness of the mineralogical definition of "Orangite". *In:* Proceedings of the Seventh International Kimberlite Conference. Gurney JJ, Gurney JL, Pascoe MD, Richardson SH (eds) Red Roof Design, Cape Town, South Africa 2:861–866
Taylor WR, Tompkins LA, Haggerty SE (1994) Comparative geochemistry of West-African Kimberlites —Evidence for a micaceous kimberlite endmember of sublithospheric origin. Geochim Cosmochim Acta 58:4017–4037
Teeuw RM (2002) Regolith and diamond deposits around Tortiya, Ivory Coast, West Africa. Catena 49:111–127
Thy P, Stecher O, Korstgard JA (1987) Mineral chemistry and crystallization sequences in kimberlite and lamproite dikes from the Sisimiut area, central West Greenland. Lithos 20:391–417
Timmerman S, Koornneef JM, Chinn IL, Davies GR (2017) Dated eclogitic diamond growth zones reveal variable recycling of crustal carbon through time. Earth Planet Sci Lett 463:178–188
Timmerman S, Yeow H, Honda M, Howell D, Jaques AL, Krebs MY, Woodland S, Pearson DG, Ávila JN, Ireland TR (2019) U–Th/he systematics of fluid-rich "fibrous" diamonds–evidence for pre-and syn-kimberlite eruption ages. Chem Geol 515:22–36
Timmerman S, Nestola F, Stachel T, Reimink JR, Ielpi A, Jackson V, Pearson G, Banas A, Stern RA, Vezinet A, Mircea C (2020) Diamond-bearing metasediments point to thick, cool lithospheric root established by Measoarchean beneath parts of the Slave Craton. AGU Fall Meeting, Abstract paper 732477
Tompkins LA, Gonzaga GM (1989) Diamonds in Brazil and a proposed model for the origin and distribution of diamonds in the Coromandel Region, Minas Gerais, Brazil. Econ Geol 84:591–602
Tovey M, Giuliani A, Phillips D, Moss S (2020) Controls on the explosive emplacement of diamondiferous kimberlites: New insights from hypabyssal and pyroclastic units in the Diavik mine, Canada. Lithos 360:105410
Tovey M, Giuliani A, Phillips, D, Pearson DG, Sarkar C, Nowicki T, Carlson J (2021) The spatial and temporal evolution of primitive melt compositions within the Lac de Gras kimberlite field, Canada: Source evolution vs lithospheric mantle assimilation. Lithos 392–393:106142
Tremblay M (1956) Geology of the Williamson Diamond Mine, Mwadui, Tanzania. PhD thesis, McGill University, Montreal, Canada
Turner BR, Minter WEL (1985) Diamond-bearing upper Karoo fluvial sediments in NE Swaziland. J Geol Soc London 142:765–776
van Straaten BI, Kopylova M, Russell J, Smith BS (2011) A rare occurrence of a crater-filling clastogenic extrusive coherent kimberlite, Victor Northwest (Ontario, Canada). Bull Volcanol 73:1047–1062
Vasilenko V, Kuznetsova L, Tolstov A, Minin V (2012) Evaluating the diamondiferous potential of unaltered kimberlites by the population models of their composition. Geochem Int 50:988–1006
Vespermann D, Schminke H-U (2000) Scoria cones and tuff rings. *In:*Encyclopedia of Volcanoes. Sigurdsson H, Houghton B, Rymer H, Stix J, McNutt S (Eds), Academic Press, New York, p 653–697
Wagner PA (1914) The diamond fields of southern Africa. The Transvaal Leader, Johannesburg
Wagner PA (1928) The evidence of kimberlite pipes on the constitution of the outer part of the Earth. S Afr J Sci 25:127–148
Walter MJ, Thomson AR, Smith EM (2022) Geochemistry of silicate and oxide inclusions in sublithospheric diamonds. Rev Mineral Geochem 88:393–450
Ward JD, de Wit MCJ, Revitt AW, Abson JP (2013) Geological and economic aspects of the Proterozoic Umkondo Group Diamond placer near Marange, Zimbabwe. Abstract, Geoforum, Johannesburg
Ward JD, de Wit MCJ, de Jager P (in prep) Placers of the Southern Alluvial Diamond Field, North West Province: a case for Palaeozoic marine influence in the "Rooikoppie Gravels"
Watkins JM (2009) Diamonds in South America. Presentation PROEXPLO Congress Lima, Peru
Webb K, Stiefenhofer J, Field M (2003) Overview of the geology and emplacement of the Jwaneng DK2 kimberlite, southern Botswana. 8th International Kimberlite Conference Extended Abstracts
Wendland C, Fralick P, Hollings P (2012) Diamondiferous, Neoarchean fan-delta deposits, western Superior Province, Canada: sedimentology and provenance. Precambrian Res 196:46–60
Westerlund KJ, Shirey SB, Richardson SH, Carlson RW, Gurney JJ, Harris JW (2006) A subduction wedge origin for Paleoarchean peridotitic diamonds and harzburgites from the Panda Kimberlite, Slave Craton; evidence from Re–Os isotope systematics. Contrib Mineral Petrol 152:275–294
White JD, Ross P-S (2011) Maar-diatreme volcanoes: A review. J Volcanol Geotherm Res 201:1–29
White N, Al-Hajri Y, Fishwick S (2009) Scales of transient convective support beneath West Africa. Geology 37:883–886
White LT, Graham I, Tanner D, Hall R, Armstrong RA, Yaxley G, Barron L, Spencer L, van Leeuwen TM (2016) The provenance of Borneo's enigmatic alluvial diamonds: A case study from Cempaka, SE Kalimantan. Gondwana Res 38:251–272
Wiggers de Vries DF, Pearson DG, Bulanova GP, Smelov AP, Pavlushin AD, Davies GR (2013) Re–Os dating of sulphide inclusions zonally distributed in single Yakutian diamonds: Evidence for multiple episodes of Proterozoic formation and protracted timescales of diamond growth. Geochim Cosmochim Acta 120:363–394

Wilson MGC, McKenna N, Lynn MD (2007a) The Occurrence of Diamonds in South Africa. Council for Geoscience, Pretoria
Wilson MR, Kjarsgaard BA, Taylor BE (2007b) Stable isotopic composition of magmatic and deuteric carbonate phases in hypabyssal kimberlite, Lac de Gras field, Northwest Territories, Canada. Chem Geol 242:435–454
Wood CA (1980) Morphometric evolution of cinder cones. J Volcanol Geotherm Res 7:387–413
Woodhead J, Hergt J, Phillips D, Paton C (2009) African kimberlites revisited: in situ Sr–isotope analysis of groundmass perovskite. Lithos 112:311–317
Woodhead J, Hergt J, Giuliani A, Maas R, Phillips D, Pearson DG, Nowell GM (2019) Kimberlites reveal 2 billion years of evolution of a deep isolated mantle reservoir. Nature 573:578–581
Zhou T (2015) Geology, regional diamond exploration and diamond provenance of the Proterozoic diamondiferous Umkondo conglomerates, Umkondo group, Eastern Zimbabwe. MSc thesis (unpubl), Rhodes University, Grahamstown, South Africa
Zimanowski B, Frohlich G, Lorenz V (1991) Quantitative experiments on phreatomagmatic explosions. J Volcanol Geotherm Res 48:341–358
Zimanowski B, Büttner R, Dellino P, White JDL, Wohletz KH (2015) Magma–water interaction and phreatomagmatic fragmentation. *In:*Encyclopedia of Volcanoes. Sigurdsson H, Houghton B, Rymer H, Stix J, McNutt S (Eds), Academic Press, New York, p 473–484
Zonneveld J-P, Kjarsgaard BA, Harvey SE, Heaman LM, McNeil DH, Marcia KY (2004) Sedimentologic and stratigraphic constraints on emplacement of the Star Kimberlite, east-central Saskatchewan. Lithos 76:115–138